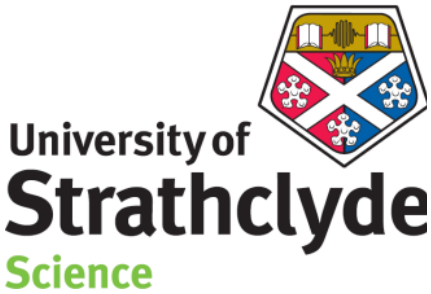

FORENSIC TOXICOLOGY OF GAMMA HYDROXYBUTYRATE (GHB) METABOLISM

By

SAMAR ADNAN ALZEER

A thesis presented in fulfilment of the degree of
Doctor of Philosophy

University of Strathclyde
Strathclyde Institute of Pharmacy and Biomedical Sciences

2011

This thesis is the result of author's original research. It has been composed by the author and has not been previously submitted for the examination which has lead to the award of a degree.

'The copyright of this thesis belongs to the author under the terms of the United Kingdom Copyright Acts as qualified by University of Strathclyde Regulation 3.50. Due acknowledgment must always be made of the use of any material contained in, or derived from, this thesis.

Signed Date

ACKNOWLEDGEMENTS

It is pleasure to thank the many people who made this thesis possible.

First of all, I would like to express my sincere gratitude to my supervisor Dr Elizabeth Ellis for her continuous guidance, support and encouragement throughout my studies. I will always remember her sense of humour, kindness and caring during these years under her supervision.

I am grateful to Dr Dave Watson, my second supervisor, for his expert assistance with the GC/MS machine. I remember also Dr Eve Lutz for her valuable ideas. Thanks to Ms Patricia Keating, technician in the Chemistry department, for her help and time.

I take the opportunity to thank Dr Fiona Wylie, University of Glasgow, for introducing me to hair analysis, and all the volunteers who donated hair samples.

I would like also to thank my colleagues in the lab, past and present for their friendship and cooperation and especially for making the lab an enjoyable place to work.

I am indebted to the University of Damascus in Syria for the financial support without which I will not have been able to undergo such study. I hope my work will benefit my country in some way.

Finally, yet importantly, I express my deepest gratitude to my parents for their love, faithful support, sacrifice, continuous encouragement and understanding. To them I dedicate this thesis.

TABLE OF CONTENTS

LIST OF FIGURES

LIST OF TABLES

LIST OF ABBREVIATIONS

%	percent
μg	micro gram
μl	micro litre
μM	micro molar
AKR	Aldo-Keto Reductase
ALDH	Aldehyde dehydrogenase
ATCC	American Type Culture Collection
BSTFA	N,O-bis(trimethylsilyl)trifluoroacetamide
cAMP	cyclic adenosine monophosphate
cDNA	complementary DNA
CNS	Central Nervous System
Da	Dalton
DFSA	Drug facilitated sexual assault
DMEM	Dulbecco's Modified Eagle's Medium
DMSO	dimethyl sulfoxide
DNA	Deoxyribonucleic acid
DTT	dithiothreitol

EDTA	ethylenediaminetetraacetic acid
FBS	Fetal Bovine Serum
g	grams
GAPDH	glyceraldehyde 3-phosphate dehydrogenase
GABA	γ-aminobutyric acid
GC/MS	Gas Chromatography/Mass Spectrometry
GHB	γ- hydroxybutyrate
HOT	Hydroxyacid oxoacid transhydrogenase
H2O2	hydrogen peroxide
HepG2	human hepatocellular carcinoma cell line
IPTG	isopropyl D-thiogalactoside
KDa	Kilo Dalton
LB	Lysogeny broth
LOD	Limit of Detection
LOQ	Limit of Quantification
M	Molar
min	minute(s)
ml	milli litre(s)

mM	milli molar
mRNA	messenger RNA
MTT	3-(4,5-Dimethylthiazol-2-yl)-2,5-diphenyltetrazolium bromide
NAD	Nicotinamide Adenine Dinucleotide
NADP	Nicotinamide Adenine Dinucleotide Phosphate
NADPH	reduced form of Nicotinamide Adenine Dinucleotide Phosphate
nm	nanometres
nM	nanomolar
°C	degree Celsius
OD	optical density
PBS	phosphate buffer saline
PCR	polymerase Chain Reaction
p-NBA	p-nitrobenzaldehyde
RNA	Ribonucleic acid
RT-PCR	quantitative Real Time Polymerase Chain Reaction
rpm	revolutions per minute

SDS	Sodium Dodecyl Sulphate
SEM	Standard Error of the Mean
SH-SY5Y	human neuroblastoma cell line
SIM	Selected Ion Monitoring
siRNA	small interfering RNA
SSA	succinic semialdehyde
SSADH	succinic semialdehyde dehydrogenase
TEMED	N, N, N',N'-tetramethylethylenediamine
Tris	tris(hydroxymethyl)methylamine
UV	Ultraviolet

ABSTRACT

Gamma hydroxybutyrate (GHB) is a notorious drug of abuse that has been taken as a recreational drug and as a date-rape drug. GHB metabolism raises difficulties in forensic analysis since the drug is rapidly metabolised and cleared from the body and therefore, its window of detection in body fluids is limited to few hours after ingestion. In addition, the endogenous source of GHB interferes with drug analysis in toxic cases. The present study was undertaken with the aim of defining the role of two enzymes in the catabolic pathway of GHB, and to investigate endogenous GHB in hair, an alternative biological sample in which the window of detection is extended to several weeks. The first enzyme, hydroxyacid oxoacid transhydrogenase (HOT), was expressed and purified as a recombinant protein and its transhydrogenase and dehydrogenase activities were assayed. HOT was capable of oxidizing micromolar concentrations of GHB in a transhydrogenase reaction using α-ketoglutarate as a co-substrate, but it does not show any dehydrogenase activity with GHB. The second enzyme aldehyde reductase (AKR1A1) was knocked down in 1321N1 (human astrocytoma) and HepG2 (human hepatoma) cell lines and the ability of the transfected cells to metabolize endogenous and exogenous GHB was examined. AKR1A1 takes part in exogenous GHB breakdown, especially in HepG2 cells, but it does not participate in endogenous GHB biosynthesis and breakdown. Finally, the sensitivity of endogenous GHB levels in hair to certain epidemiological factors was examined in hair samples from GHB-free volunteers. In conclusions, the study shows that *in vitro*, AKR1A1 is responsible for oxidizing high concentrations of GHB, while HOT works on much lower levels of GHB. Furthermore, disposition of GHB in hair does not appear to be influenced by gender, age, and lifestyle habits.

CHAPTER ONE

GENERAL INTRODUCTION

1 INTRODUCTION

Drugs of abuse can be defined as drugs that are used for a reason other than for what they were designed. Such drugs could have valuable therapeutic purposes but they also possess properties that lead to their misuse. The misuse is often associated with a harmful consequence, meaning that most of these drugs are controlled by law (King *et al.*, 2008). Drugs of abuse are either self-administrated deliberately to produce an euphoric effect, or are given to another individual in order to commit an offence, or both.

Euphoric drugs include a wide range of illicit substances commonly used for recreational purposes. Among those are methylenedioxymethamphetamine (MDMA), amphetamine, cannabis, cocaine, and gamma hydroxybutyric acid (GHB).

Drug Facilitated Sexual Assault (DFSA) drugs are compounds that are utilized to control the will of a person in order to facilitate the perpetration of a sexual offense. These drugs are also known as "date-rape" drugs. The most commonly abused drugs in this group are GHB, ketamine and flunitrazepam (Rohypnol).

As observed, GHB is used for euphoric purposes, but it is widely known as a date-rape drug. Intriguingly, GHB is also produced endogenously, and has a role in the central nervous system. These properties make GHB quite a unique drug, and are the reason why it was chosen as a topic for research.

1.1 Synopsis of GHB:

GHB is a four carbon fatty acid that was synthesized in 1960 by the French scientist Laborit in order to produce an analogue to gamma amino butyric acid (GABA), the main inhibitory neurotransmitter in the brain (Laborit, 1964). GHB is structurally similar to GABA, having a hydroxyl group on the fourth carbon instead of the nitrogen group in GABA (Figure 1.1 A). It was hoped that the new compound would have a hypnotic action and would be able to cross the blood brain barrier in order to serve as an assistant analgesic in small surgical operations. GHB fulfilled these requirements, and had additional advantages such as its low toxicity, and the lack of ventilatory depression that is observed with some other anesthetics.

Shortly after its synthesis, it was discovered that GHB occurs naturally in the brain, and is derived from GABA (Bessman and Fishbein, 1963, Roth and Giarman, 1970). This attracted increasing attention to this molecule and its role in the central nervous system. Many evidence has suggested that GHB itself may serve as a neurotransmitter or neuromodulator (Maitre, 1997). GHB serves also as a pro-drug of GABA (Vayer *et al.*, 1985a, Gobaille *et al.*, 1999)

Another therapeutic application emerged for GHB after several studies demonstrated that GHB is beneficial in the management of narcolepsy, a rare sleeping disorder that is characterized by excessive day sleeping and cataleptic attacks (Broughton and Mamelak, 1979).

A

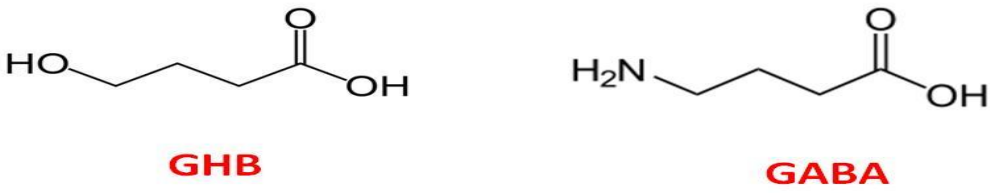

B

Figure 1.1: Gamma hydroxybutyric acid (GHB). **A)** Chemical structures of GHB and its precursor gamma amino butyric acid (GABA). **B)** The sodium salt of GHB was manufactured by *Jazz Pharmaceuticals* under the trade name Xyrem® (In Canada, Xyrem is distributed by *Valeant Pharmaceuticals International* http://www.valeantcanada.com/html/xyremr.html)

Introducing GHB at two high doses (around 4 g) at bed time decreased the occurrence and strength of cataplexy and enhanced the wakefulness at daytime (Mamelak, 2009). The use of GHB for narcoleptic patients was approved by the FDA in 2002 with restricted distribution to patients due to incidents associated with the abuse of this drug (Fuller and Hornfeldt, 2003). The sodium salt of the drug is distributed by Jazz Pharmaceuticals under the trade name Xyrem® (Figure 1.1 B).

Furthermore, GHB was found to be useful in the management of alcohol withdrawal. It reduces alcohol consumption by decreasing alcohol craving in addicted individuals, and it relieved withdrawal symptoms such as anxiety and tremor (Addolorato *et al.*, 1999, Nimmerrichter *et al.*, 2002). GHB also helped patients to keep abstinent (Addolorato *et al.*, 1996). The mechanism for that is not totally clear but it has been proposed that GHB substitutes for alcohol and imitates its actions in the central nervous system (Gessa *et al.*, 2000). The drug was approved in Italy and Austria and was sold by *Laboratorio Farmaceutico C.T* under the trade name Alcover® (Beghè and Campanini, 2000).

The Cochrane Library published a systematic review of the role of GHB in treating alcoholism (Leone *et al.*, 2010) where 13 randomized controlled trials (RCT) were evaluated while 22 studies were excluded for methodological reasons or for not fulfilling the criteria in this review. The study concluded that there was evidence to suggest that GHB at a dose of 50 mg/kg/day is effective to treat alcohol withdrawal syndrome and to prevent relapse. Nevertheless, side effects were reported as the dose increased to 100 mg/kg/day, most commonly vertigo and dizziness.

1.2 GHB abuse

Different ways of abusing the drug have appeared, turning GHB from a possible treatment for many illnesses to a notorious drug that is banned in most countries. The effect of GHB varies significantly depending on the administrated dose as shown in Table (1.1).

Single dose (oral)	Effect
10 mg/kg	Relaxation, euphoria, sedation, short-term amnesia
20-30 mg/kg	Sleep and drowsiness
50-60 mg/kg	Unconsciousness
60-100 mg/kg	Respiratory depression, coma, myoclonic seizures

Table 1.1: Dose-effect relationship of GHB. GHB manifests different effects depending on the administrated dose (Kam and Yoong, 1998, Bernasconi *et al.*, 1999, Wong *et al.*, 2004, Madea and Musshoff, 2009)

1.2.1 GHB abuse as an anabolic drug

The capacity of GHB to increase growth hormone (GH) release (Donjacour *et al.*, 2011) was the reason behind the popularity of the drug as an anabolic supplement in health clubs and among body builders in the 1980s. Although the mechanism of GH release by GHB is not fully elucidated, it was hypothesized

that GH is released during slow-wave sleep induced by GHB, most observed in the first two hours after sleep onset (Van Cauter *et al.*, 1997). Another study suggested that this action is mediated by cholinergic receptors as GH release was completely suppressed in healthy and Parkinsonian subjects when they were pretreated with pirenzepine, a cholinergic antagonist, before administrating GHB (Volpi *et al.*, 2000)

The FDA altered the status of GHB to a prescribed-only drug in 1990 after reports of intoxication (Center for Disease Control, 1990, Chin et al., 1992), but this did not prevent the continuing misuse of the drug.

1.2.2 GHB abuse as a recreational drug

Shortly after the ban of its selling over the counter, GHB gained a reputation among clubs attendees as a club drug or recreational drug, because low doses of GHB produce an euphoric feeling, relaxation, and socialization (Rodgers *et al.*, 2004, Andresen *et al.*, 2008). Illicit preparations of GHB were obtainable under different street names ("Liquid Ecstasy", "Georgia Home Boy", "Soap", etc) (Nicholson and Balster, 2001). Since the consumption of GHB in many of these cases is usually defined by tea-spoon, the exact dose taken was not exactly known. This resulted in several reports of overdoses and death related cases (Ingels *et al.*, 2000, Knudsen *et al.*, 2010, Zvosec *et al.*, 2011). The recreational use of GHB is often accompanied by the consumption of alcohol, which intensifies its CNS inhibiting effects and increases the risk of respiratory depression and coma.

Subsequently, GHB was classified as a controlled substance in most countries; it was classified as schedule C under the Misuse of Drugs Act in the UK in 2003, while in the USA it was categorized as schedule I in 2000, but as schedule III for the therapeutic drug Xyrem® (Wood *et al.*, 2008)

To overcome these restrictions, users turned to two precursors of GHB: gamma butyrolactone (GBL), and 1, 4 butanediol (1,4 BD). GBL and 1,4 BD are used in industrial solvents and until recently, they were legal in most countries. The two compounds are quickly converted in the body to GHB by enzymatic reactions (Figure 1.2): GBL is hydrolyzed by lactonase (Roth and Giarman, 1965), and 1,4 BD is converted by the stepwise actions of alcohol dehydrogenase and aldehyde dehydrogenase (Roth and Giarman, 1968, Maxwell and Roth, 1972). Moreover, GBL can be hydrolyzed *in vitro* by the addition of sodium hydroxide to produce illicit GHB. Therefore, GBL was added to the list of controlled substances in the UK in 2009.

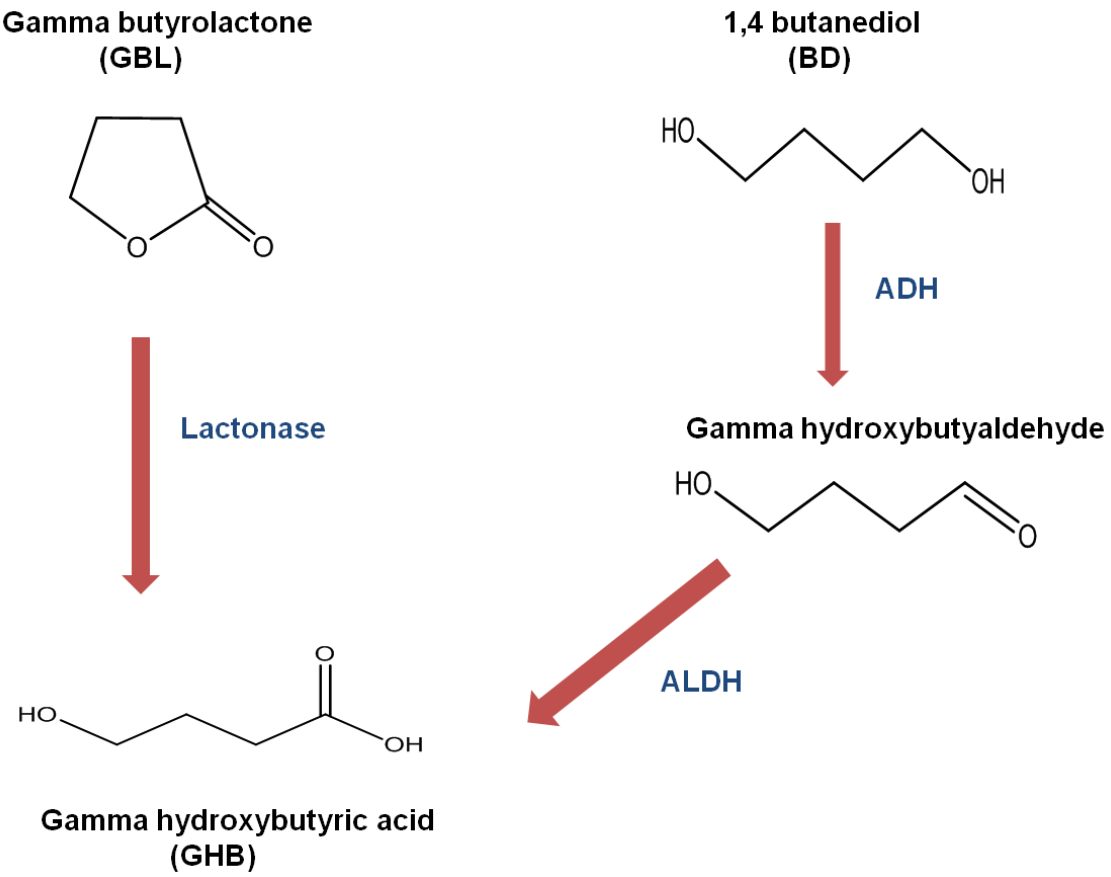

Figure 1.2: Conversion of GBL and 1,4 BD to GHB. GBL and 1,4 BD are rapidly converted in the body to GHB. GBL is transformed to GHB by the action of peripheral lactonase, and 1,4 BD is converted by alcohol dehydrogenase (ADH), and aldehyde dehydrogenase (ALDH)

1.2.3 GHB as a drug-facilitated sexual assault (DFSA)

The notoriety associated with GHB came after the widespread use of drug to render female victims vulnerable to sexual assault. There were numerous reports of employing GHB for committing an offence (Stillwell, 2002, Varela *et al.*, 2004, Anderson *et al.*, 2006). Since GHB is a colourless, odourless and flavourless compound (slightly salty when used as its sodium salt), it goes unnoticed when spiked in to a drink. GHB is described as a "fast in, fast out" drug: it is rapidly absorbed, reaching its plasma peak in 20-45 minutes (Brenneisen *et al.*, 2004) and therefore, manifesting its sedative effects in a short period of time. It is then metabolized and eliminated from the blood circulation in 6 to 8 hours and from the urine in 12 hours (Palatini *et al.*, 1993)

Given that GHB causes amnesia and hallucinations, reporting GHB-related incidents to the police is often delayed, which hinders its detection in the body and consequently obstructs the legal progression of the case.

1.2.4 GHB dependency

Persistent use of GHB leads to develop dependency. This can happen when consuming GHB several times daily for a few months. However, in one case, a woman developed a craving after consuming 3 ounces of GHB every 3 hours for 7 days (Perez *et al.*, 2006). If stopped abruptly, a withdrawal syndrome

occurs within hours (van Noorden et al., 2009). Symptoms include tremors, insomnia, anxiety, hypertension, delirium, confusion and seizures (Galloway *et al.*, 1997). There are several reported cases of the withdrawal of GHB and its analogues GBL and 1,4 butanediol (Mahr et al., 2001, Wojtowicz et al., 2008, LeTourneau et al., 2008).

Treatment against dependency usually includes benzodiazepines at high doses because they are selective $GABA_A$ agonists so they improve GABA activity (Schneir *et al.*, 2001). Pentobarbital, another $GABA_A$ agonist, was beneficial in treating some cases (Sivilotti *et al.*, 2001); and baclofen , a $GABA_B$ agonist, was effective in the management of withdrawal symptoms (LeTourneau et al., 2008)

1.3 Pharmacology of GHB

1.3.1 Pharmacodynamics

Exogenous GHB crosses the blood brain barrier by a carrier-mediated mechanism, mainly by the monocarboxylate transporter (MCT) family (Bhattacharya and Boje, 2004). In the brain, GHB acts at two dose-dependent receptors: the GHB receptor and the $GABA_B$ receptor

1.3.1.1 GHB Receptor

At low concentrations and at endogenous levels, GHB binds to a specific receptor with high affinity. In rat and human brain, an isoform of GHB receptor has a K_d of 30-580 nM (Benavides *et al.*, 1982a, Snead and Liu, 1984). These specific receptors are located mainly in the presynaptic neurons of cortex and hippocampus (Kemmel *et al.*, 2006) and not on glia (Maitre.,1997). Although peripheral organs such as liver, kidney and the gastrointestinal tract express abundant amount of endogenous GHB (Nelson *et al.*, 1981, Tedeschi *et al.*, 2003), the receptors are absent from these organs (Snead and Liu, 1984, Andriamampandry *et al.*, 2003)

GHB receptors are thought to be linked to a G-protein (Snead, 2000, Andriamampandry *et al.*, 2003) , and binding lowers adenylyl cyclase activity which leads to a reduction in cAMP. However, some other studies did not observe this link (Castelli *et al.*, 2003, Odagaki and Yamauchi, 2004). An *in vitro* study was carried out on a neurohybridoma cell line (NCB-20) showed that binding of GHB to the receptor stimulated the entering of Ca^{2+} via T-type calcium channels when the membrane is at resting potential. This leads to hyperpolarisation of the cell membrane by activating potassium channels (Kemmel *et al.*, 2003). Nanomolar levels of GHB were able to trigger cAMP response while micromolar concentrations activate calcium signaling (Coune *et al.*, 2010).

A specific antagonist for the GHB receptor was identified and synthesized (Maitre *et al.*, 1990), and named NCS-382 (Figure 1.3A). This compound was shown to possess both anti-sedative and anti-cataleptic effects (Schmidt *et al.*, 1991). Later, GHB receptor was cloned from both rat and human brain (Andriamampandry *et al.*, 2003, Andriamampandry *et al.*, 2007), and showed different characteristics and sensitivity to NCS-382.

1.3.1.2 $GABA_B$ receptor

The $GABA_B$ receptor is also a G-protein coupled receptor that is negatively coupled to adenylyl cyclase (Kaupmann *et al.*, 1997, Odagaki *et al.*, 2000). It was initially identified in the peripheral nervous system (Bowery and Hudson, 1979), but has been demonstrated to be present through the CNS (Andrade *et al.*, 1986, Becher *et al.*, 2001). It consists of two subunits: $GABA_{B1}$ and $GABA_{B2}$ (Jones *et al.*, 1998, Kaupmann *et al.*, 1998). Activation of the $GABA_B$ receptors provokes multiple effects on presynaptic and postsynaptic neurons. In contrast to GHB receptor, activation inhibits calcium influx in presynaptic neurons, but similar to GHB receptor it reduces cAMP levels. It also causes postsynaptic neuronal hyperpolarization (Sakaba and Neher, 2003).

Although GABA is the main activator of $GABA_B$ receptor, relatively high levels of GHB can activate the receptors, indicating that GHB is a weak agonist of $GABA_B$ receptors (Lingenhoehl *et al.*, 1999). It was initially thought that GHB acted only via the $GABA_B$ receptors but gathering evidences indicated that separate GHB receptors exist (see previous section). GHB binding to the high

affinity receptors in rat brain have been shown to not compete with baclofen (Figure 1.3 B) which is a well known agonist of $GABA_B$ receptor (Benavides *et al.*, 1982a),while GHB antagonist NCS-382 has no affinity for the $GABA_B$ receptor (Wu *et al.*, 2004).

It is believed that GHB symptoms in overdoses and toxicity cases result from its interaction with $GABA_B$ receptors. *In vivo* studies in mice showed that the $GABA_B$ receptor mediates the sedative/hypnotic effect of GHB at a dose of 1g/kg (Carai *et al.*, 2001), as well as EEG activity and sleep at a dose of 300 mg/kg of GBL (Vienne *et al.*, 2010). In addition, $GABA_{B(1)^-}$ deficient mice did not show hypolocomotion, hypothermia, or delta wave sleep (Kaupmann *et al.*, 2003). Although *in vivo* GHB might trigger $GABA_B$ receptor either directly or indirectly by its conversion to GABA, no correlation was observed between GABA concentrations and sedative/hypnotic effect after administrating high doses of GHB to rats (Felmlee *et al.*, 2010)

A

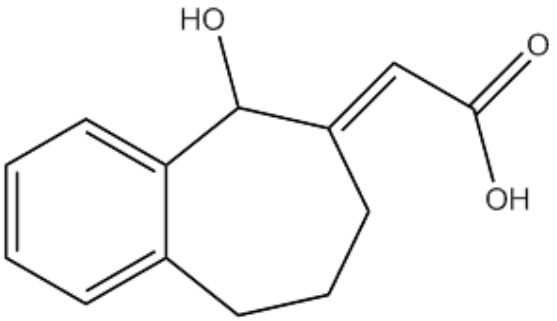

B

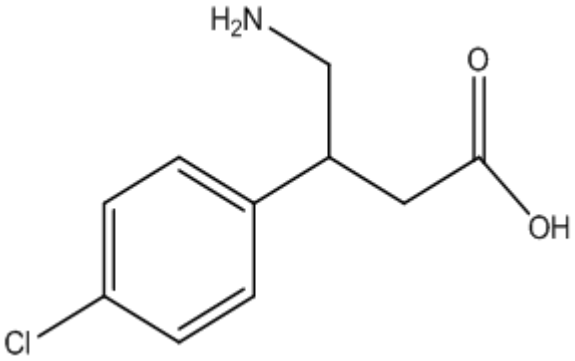

Figure 1.3: Chemical structures of NCS-382 and baclofen. **A)** NCS-382 is the sodium salt of 6,7,8,9-tetrahydro-5-(H)-benzocycloheptene-5-ol-4-ylideneacetic acid. It is a specific antagonist of GHB receptor. **B)** Baclofen [4-amino-3-(4-chlorophenyl) butanoic acid] is an agonist for $GABA_B$ receptor

1.3.2 GHB role in the central nervous system

1.3.2.1 Endogenous GHB as a neurotransmitter or a neuromodulator

GHB has been proposed to be a neurotransmitter because of its structure similarity to GABA and to its storage, up take and release systems in the neuron. (Vayer *et al.*, 1987)

GHB meets many criteria that support this hypothesis: first, it is a CNS depressant that is produced from GABA and accumulates in cerebral neurons (Maitre, 1997); second, the release of GHB from neurons is Ca^{2+} dependent (Maitre *et al.*, 1983) and this is a necessary condition for a neurotransmitter; third, there is a sodium dependent uptake system for GHB in brain which ends its synaptic effects (Benavides *et al.*, 1982b); finally, the presence of two GHB binding sites in CNS as described above.

1.3.2.2 Interaction of GHB with other neuromodulators

GABA and glutamate

GHB influences the presynaptic release of glutamate and GABA. Doses of GHB between 250 μM and 1.5 mM significantly decreased the presynaptic basal release of GABA and the calcium dependent K^+ evoked release of glutamate and GABA in rat ventrobasel nucleus of the thalamus (Banerjee and Snead, 1995). Similar results were obtained in rat cerebral cortex where GHB reduced

basal GABA and K^+ evoked GABA release but did not affect glutamate release, and this was correlated in time with absent seizures (Hu *et al.*, 2000). Taken together, the results suggest that GHB mediation of neurotransmitter release is responsible for absent seizures induced by GHB.

Gathering evidence indicates that GHB effect is mediated by its binding to $GABA_B$ receptors which regulate Ca^{2+} influx through voltage-gated Ca^{2+} channels (Sakaba and Neher, 2003) (Figure 1.4), as millimolar concentrations of GHB were required to achieve maximal effects, and these effects were mimicked by baclofen and blocked by $GABA_B$ receptor selective antagonists (Banerjee and Snead, 1995, Hu *et al.*, 2000, Jensen and Mody, 2001, Gervasi *et al.*, 2003).

Some studies have reported a GHB-receptor- mediated effect of GABA release in rat hippocampus and substantia nigra based on GHB inhibitory effects in the presence of $GABA_B$ selective antagonists, and on the ability of NCS-382 to block these effects (Cammalleri *et al.*, 2002, Brancucci *et al.*, 2004b, Brancucci *et al.*, 2004a). However, these studies did not test whether the $GABA_B$ receptor was fully blocked at the antagonist concentrations used, and non-specific effects were reported for NCS-382 in the thalamus and the hippocampus (King *et al.*, 1997, Gervasi *et al.*, 2003).

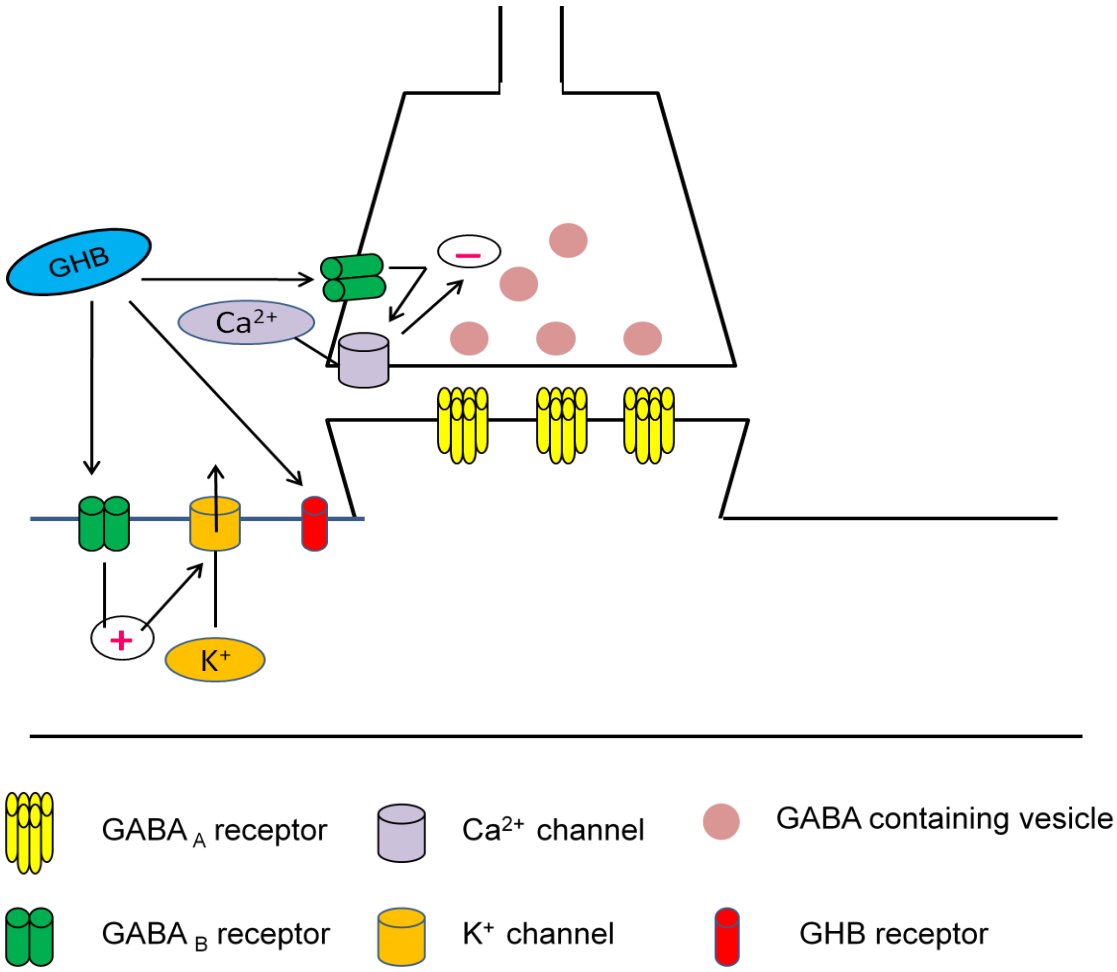

Figure 1.4: GHB activation of GHB and GABA$_B$ receptor. Presynaptically, GHB prevents GABA release by inhibiting Ca^{2+} influx via voltage gated Ca^{2+} channels. Postsynaptically, activation of GABA$_B$ receptors leads to the opening of K^+ channels and consequently the neurons are hyperpolarized. Adapted from (Drasbek *et al.*, 2006).

Dopamine

GHB has an influence on multiple neuromodulatory systems in the central nervous system (CNS). In particular, GHB expresses dual action on the dopaminergic system, where low doses of GHB stimulate dopamine release, while high doses inhibit dopamine release in the mesolimbic dopamine system (Cruz *et al.*, 2004). As most drugs of abuse including ethanol increase dopamine release in the mesolimbic dopamine system (Pierce and Kumaresan, 2006), the effect of GHB on the dopamine system is important to explain its anti-craving effects, and also to explain the addictive characteristic of GHB.

Serotonin

GHB interacts with the serotonergic system, inducing the accumulation of tryptophan and enhancing serotonin turnover in rat brain (Gobaille *et al.*, 2002). In patients suffering from SSADH-deficiency, an inherited decease illustrated by the excessive accumulation of GHB, a correlation was established between GHB and serotonin levels (Gibson *et al.*, 2003). Serotonin is involved in the regulation of sleep, appetite and mood, so it may mediate the behavioral and pharmacological effects of GHB.

Acetylcholine

In vivo study in rats has demonstrated a dose-dependent reduction in extracellular acetylcholine levels in the hippocampus following GHB administration. This effect was mimicked by baclofen and was blocked by a $GABA_B$ antagonist, indicating that it is mediated by the $GABA_B$ receptor (Nava *et al.*, 2001). Given that increasing hippocampal acetylcholine levels in amnesic rodent models improved the memory/learning performance (Roland *et al.*, 2008), it was hypothesized that the interaction of GHB with the cholinergic system is responsible for the amnesic state observed with GHB.

Physostigmine, an acetyl cholinesterase inhibitor, was proposed for the treatment of GHB toxicity by revesving the anaesthetic effect of GHB (Yates and Viera, 2000), however, this use is controversial because it was only applied on a limited number of patients, and because of the adverse effect produced by physostigmine (Bania and Chu, 2005)

1.3.3 Pharmacokinetics of GHB:

1.3.3.1 Absorption and distribution

GHB is usually administrated orally in the form of capsules, solution, or as powder dissolved easily in water, and it is quickly absorbed from the gastrointestinal track. Oral bioavailability was determined in rat to be dose-dependent, ranging from 62% to 94% (Lettieri and Fung, 1979) and absorption

appears to be capacity-limited, meaning that plasma peak concentration (C_{max}) is dose-independent (Ferrara *et al.*, 1992) .

In healthy individuals taking an oral solution of 25 mg/kg of sodium GHB (~ 1.5 to 2 g), plasma peak concentration occurred between 20-45 minutes (t_{max}) (Brenneisen *et al.*, 2004, Palatini *et al.*, 1993). These parameters were similar in alcohol-dependent patients (Ferrara *et al.*, 1992). When dosing higher amounts of GHB (4.5 g) as sodium oxybate solution, t_{max} was extended to 1 hour after ingestion (Borgen *et al.*, 2003).

In narcoleptic patients, GHB absorption was observed for a single and chronic usage (Borgen *et al.*, 2004). Plasma peak concentration occurred at 52 minutes after a single dose, and at 43 minutes after a chronic dose.

Food considerably alters the absorption of GHB by reducing the plasma peak concentration (C_{max}) and extending the required time to reach it (t_{max}) (Borgen *et al.*, 2003), therefore, reducing the bioavailability of the drug.

GHB distributes quickly into the tissues following a two compartment model with a small apparent volume of distribution and a fast distribution phase (Van Sassenbroeck *et al.*, 2001). It does not bind to plasma proteins regardless of the dose (Morris *et al.*, 2005), and it easily moves through the blood-brain barrier (Bhattacharya and Boje, 2004).

1.3.3.2 Metabolism and elimination

GHB is subject to first pass metabolism in the liver and goes through different enzymatic reactions. GHB is converted to succinic semialdehyde (SSA) then to succinate which enters the TCA cycle and turns into carbon dioxide and water (Doherty *et al.*, 1975). Radioactive studies in rat showed that around 0.5 to 2% of GHB is converted to GABA in certain regions of the brain after 160 minutes of administration, and radioactive glutamate and glycine were detected as well. (Gobaille *et al.*, 1999). The intermediate in these two reactions is succinic semialdehyde (SSA). Evidence has also been shown for β-oxidation metabolism of GHB to acetyl-CoA, which also enters the TCA cycle (Brown *et al.*, 1987) (Figure 1.5).

GHB is rapidly cleared from the blood stream, having a terminal plasma elimination half–life of 20-30 min (Palatini *et al.*, 1993, Borgen *et al.*, 2003, Brenneisen *et al.*, 2004). A small percentage of GHB is recovered unchanged in the urine (less than 5%) one hour after consumption (Brenneisen *et al.*, 2004). The rate of GHB elimination was demonstrated to be dose independent at high doses (zero order) (Van Sassenbroeck *et al.*, 2001).

Co administration of monocarboxylate transporter (MCT) substrates like L-lactate or pyruvate with GHB increased its renal and total clearance and decreased its plasma concentrations in the rat (Morris *et al.*, 2005). This is because of the competition of these substrates and GHB over the transporter.

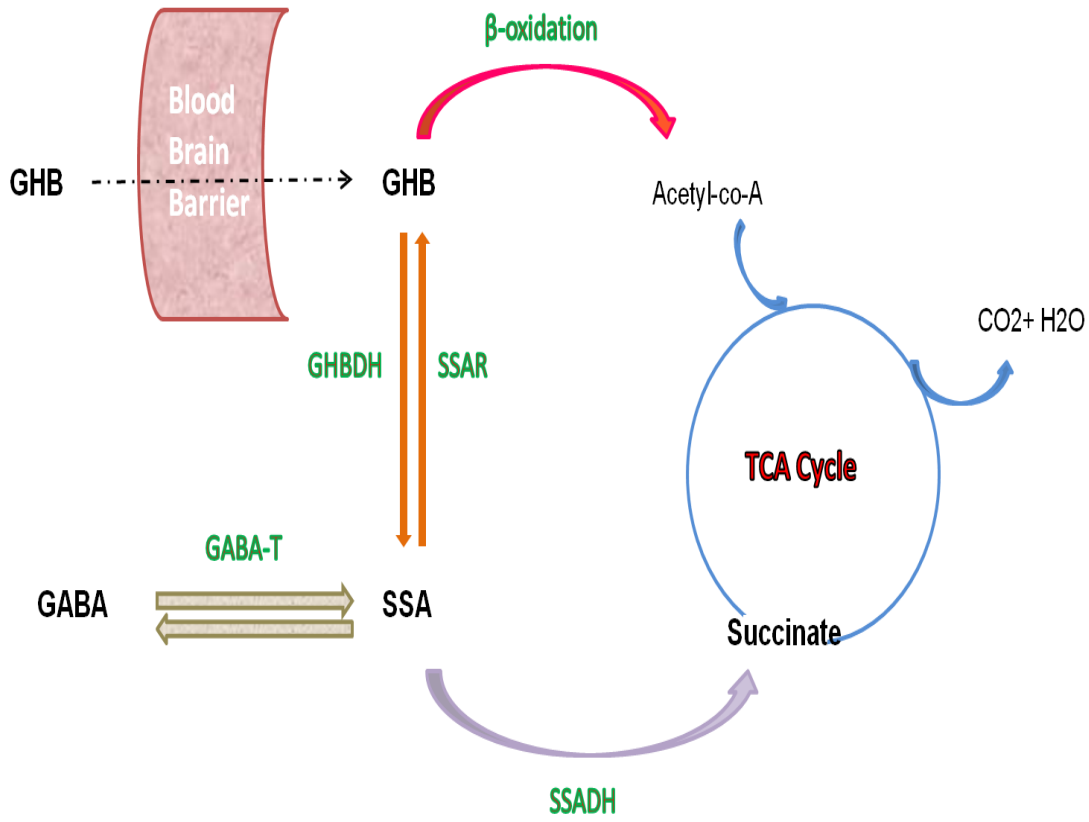

Figure 1.5: Overview of GHB metabolism. GHB is transported through the blood–brain barrier into the cell, where it is oxidized by GHB-dehydrogenase (GHBDH) to SSA. SSA is further oxidized to succinate to enter the TCA cycle and the final product is carbon dioxide and water. A small amount of SSA is converted to GABA by GABA-transaminase (GABA-T). There is evidence that GHB can undergo β-oxidation to enter the Krebs cycle as Acetyl-co-A.

1.4 The endogenous GHB metabolic pathway

Since the detection of endogenous GHB in the mammalian body (Bessman and Fishbein, 1963, Roth and Giarman, 1970, Nelson *et al.*, 1981), considerable efforts have been made to clarify its route of synthesis, and to determine the enzymes involved in its metabolic pathway.

1.4.1 GHB biosynthesis

GABA is the predominant precursor for GHB in the brain. Earlier studies showed that GABA-transaminase (GABA-T) converts GABA to succinic semialdehyde (SSA) (Bessman *et al.*, 1953) and that the latter product is oxidized to succinate by succinic semialdehyde dehydrogenase (Albers and Salvador, 1958). Later it was demonstrated that SSA can also be reduced to form GHB (Fishbein and Bessman, 1964). Therefore GHB is produced from GABA via the chronological actions of GABA-T and succinic semialdehyde reductase (Anderson *et al.*, 1977). However, the largest fraction of SSA is oxidized to succinate, while the reductive route is less than 0.1% of GABA (Gold and Roth, 1977).

1.4.1.1 GABA- transaminase (GABA-T)

GABA-T is one of the three key enzymes in the GABA shunt along with glutamic acid decarboxylase (GAD) and succinic semialdehyde dehydrogenase (SSADH). It is a dimeric enzyme located in the mitochondria (Reijnierse *et al.*, 1975), and is responsible for the reversible conversion of GABA and α-ketoglutarate to SSA and glutamate using pyridoxal-5'-phosphate (PLP) as a cofactor (Figure 1.6) (Maitre *et al.*, 1975). The human protein has a molecular weight of 53 KDa, and a 96-98% similarity to pig protein (De Biase *et al.*, 1995). The gene encoding GABA-T is named ABAT and is expressed in various tissues including liver, pancreas, kidney and brain (De Biase *et al.*, 1995)

In epileptic patients , GABA-T activity in platelets is significantly higher than control subjects , and the uptake of GABA is defective (Rainesalo *et al.*, 2003). Therefore, selective inhibitors for GABA-T such as Vigabatrin can be used in the treatment of epilepsy (Choi and Silverman, 2002)

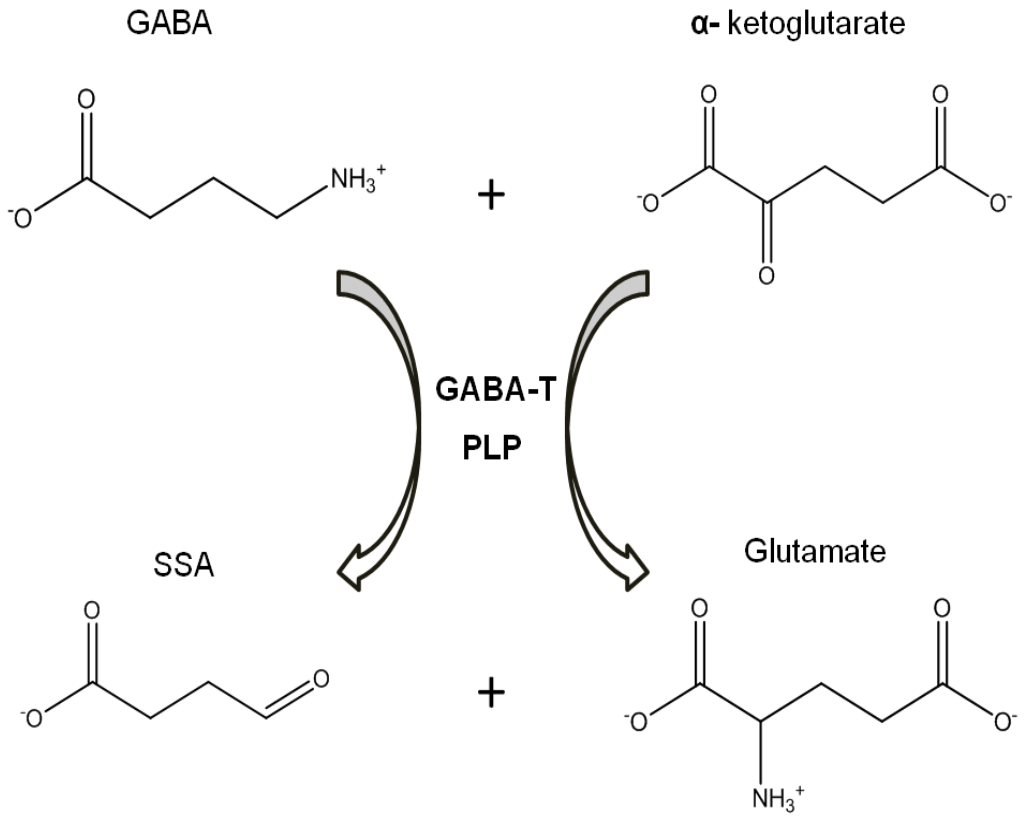

Figure 1.6: The transaminase reaction of GABA and α-ketoglutarate: GABA-T catalyzes the reversible conversion of GABA to SSA in the mitochondria using α-ketoglutarate as a nitrogen acceptor. The reaction is dependent on the presence of pyridoxal-5′-phosphate (PLP). The final products are SSA and glutamate which is a precursor of GABA.

1.4.1.2 Succinic semialdehyde reductase (SSAR)

Although earlier studies proposed that lactate dehydrogenase is the enzyme responsible for reducing SSA to GHB in mammalian brain (Fishbein and Bessman, 1964), separation of SSAR enzymes from rat brain cytosol confirmed that they are not identical to lactate dehydrogenase (Tabakoff and von Wartburg, 1975). These enzymes aren't inhibited by pyrazole (a major inhibitor for alcohol dehydrogenase) and sodium oxalate (a major inhibitor for lactate dehydrogenase), and their chromatographic characteristics were different from alcohol dehydrogenase. The preferred cofactor was NADPH with a lower activity with NADH.

Later studies demonstrated the existence of two NADPH-dependent SSAR in human reducing SSA to GHB (Cash *et al.*, 1979). It is now clear that the two enzymes, aldehyde reductase (AKR1A1) and aflatoxin B1 aldehyde reductase (AKR7A2), belong to the aldo-keto reductase superfamily (AKR).

The aldo-keto reductase superfamily (AKRs)

The aldo-keto reductase superfamily represents a group of NADP(H)-dependent oxidoreductases that are responsible for the conversion of aldehydes and ketones to their related alcohols (Bohren *et al.*, 1989). The enzymes share a TIM-barrel motif (triosphosphate isomerase) or $(\alpha/\beta)_8$ (Figure 1.7) which is important for enzyme activity (Jez *et al.*, 1997a). The group is divided to 15

families and it is widely distributed in nature and found in all plants, mammals and microorganisms. They differ in their substrate selectivity and tissue distribution so a definite physiological role for AKRs or for a subfamily cannot be allocated.

The nomenclature of the group consists of the root (AKR), an Arabic number assigning the family, a latter stands for the subfamily, and an Arabic number represents the unique protein sequence. Classification of the group is based on sequence identities where families share a 40% similarity and subfamilies share a 60% similarity in their gene sequences (Jez *et al.*, 1997b).

To date, 15 bona fide AKRs belonging to families 1, 6 and 7 have been reported in humans. They are AKR1A1 (aldehyde reductase), AKR1B1 ,AKR1B10 and AKR1B15 (aldose reductases), AKR1C1, AKR1C12 , AKR1C3 and AKR1C4 (hydroxysteroid dehydrogenases), AKR1D1 (Δ4-3-ketosteroid-5-β-reductase), AKR1E2 (testis-specific protein) AKR6A3, AKR6A5, and AKR6A9 (voltage-gated potassium β proteins), and AKR7A2 and AKR7A3 (aflatoxin reductases) (Barski *et al.*, 2008). These AKRs widely differ in their substrate selectivity and tissue distribution, and specific physiological roles cannot be allocated to a subfamily of AKRs.

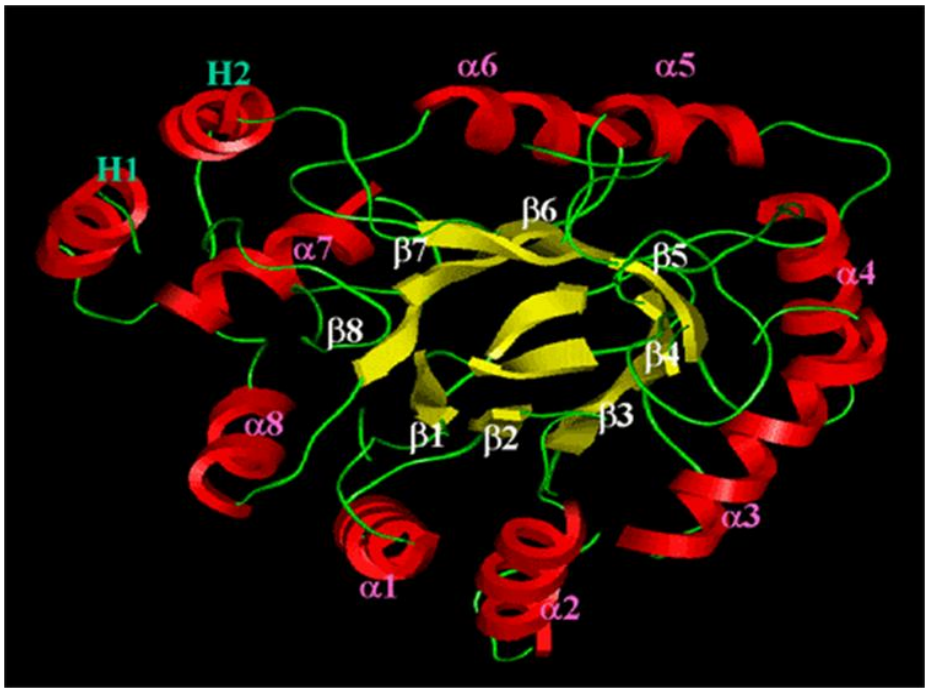

Figure 1.7: The $(\alpha/\beta)_8$ motif for aldo-keto reductase (AKRs). Aldo-keto reductases share a TIM-barrel motif (triosphosphate isomerase) which consists of 8 alpha-helix and 8 beta sheets (courtesy to the AKR superfamily website http://www.med.upenn.edu/akr/)

1.4.1.2.1 Aldehyde reductase (AKR1A1)

Aldehyde reductase belongs to the first family in the AKRs group and it was one of the first characterized AKR enzymes. It is a cytosolic enzyme that exhibits wide substrate activity with a preference for negatively-charged groups, and the best substrates are D-glucuronate and p-nitrobenzaldehyde (Branlant and Biellmann, 1980). AKR1A1 is widely expressed in most tissues with high levels observed in liver and kidney, moderate levels in cerebrum, small intestine and testis, and low levels in lung, prostate and spleen (O'Connor et al., 1999). However, the only biological function for this enzyme has been demonstrated in the ascorbic acid biosynthetic pathway in mice as AKR1A1 catalyzes the reduction of D-glucuronate to L-gulonate which is converted to L-gulonolactone and subsequently to L-ascorbic acid (Gabbay *et al.*, 2010).

The involvement of AKR1A1 in the metabolic pathway of GHB was of interest as SSA is also a substrate of AKR1A1 with a K_m of 650 μM in human brain (Cash *et al.*, 1979) and 130 μM in rat brain (Rivett *et al.*, 1981). The enzyme was named the high K_m aldehyde reductase to distinguish it from the second enzyme that has a lower K_m for SSA. It was shown to be a monomeric enzyme of ~35 KDa (Wermuth *et al.*, 1977) and is sensitive to anticonvulsant drugs such as barbiturates (Cash *et al.*, 1979). Further investigation revealed the ability of this enzyme to work in the opposite direction and oxidize GHB to SSA (Vayer *et al.*, 1985b). The K_m for GHB was much higher (10 mM), but when coupling the enzyme to GABA-T, the K_m was reduced to 175 μM.

1.4.1.2.2 Aflatoxin B1 aldehyde reductase (AKR7A2)

AKR7A2 belongs to the seventh family of the AKR superfamily. It is a dimeric protein that was revealed to be identical to aflatoxin B1 aldehyde reductase (Schaller *et al.*, 1999). AKR7A2 is highly expressed in kidney, pancreas and small intestine, and to a lower extent in liver and heart, while its lowest levels were observed in brain, lung and colon (Ireland *et al.*, 1998). The subcellular localization of AKR7A2 is still in question: although AKR7A2 was considered a cytosolic enzyme in early research, a Golgi-targeting sequence was discovered at the N-terminus (Kelly *et al.*, 2002). In the neuroblastoma cell line SHSY5Y, AKR7A2 was localized in the mitochondria of the cells (Keenan *et al.*, 2006)

AKR7A2 has a high degree of specificity for SSA with K_m of 20 μM (O'Connor et al., 1999) and is not responsive to anticonvulsant drugs (Cash *et al.*, 1979). Given that the administration of these drugs stimulated the accumulation of GHB in brain (Snead *et al.*, 1980), this illustrates a significant role of AKR7A2 in endogenous GHB synthesis in contrast to AKR1A1 which is inhibited by these drugs. Using knock-out techniques, the enzyme was shown to be the major SSA reductase in the neuroblastoma cell line, but silencing the enzyme did not affect the activity in the opposite direction (Lyon *et al.*, 2007). Nevertheless, it has been employed as GHB-dehydrogenase in an enzymatic assay to detect GHB in spiked drinks (Bendinskas *et al.*, 2011).

1.4.1.3 Endogenous synthesis of GHB from 1,4 butanediol (1,4 BD) and gamma butyrolactone (GBL)

The natural occurrence of GHB in peripheral tissues such as liver and kidney, and the high expression levels of GHB catabolic enzymes in these tissues indicate the presence of an alternative synthetic route of GHB other than its formation from GABA. Evidence was provided that GHB is a metabolite of 1,4 butanediol (1,4 BD) (Roth and Giarman, 1968), and that 1,4 BD is an endogenous metabolite in mammalian tissues such as rat brain and liver and human brain (Barker *et al.*, 1985). Taken together, 1,4 butanediol seems to serve as precursor of GHB *in vivo*.

The conversion of 1,4 BD to GHB is thought to occur via two NAD-dependent enzymes: alcohol dehydrogenase (ADH) and aldehyde dehydrogenase (ALDH) (Bessman and McCabe, 1972, Snead et al., 1989, Vayer et al., 1987). *In vitro* studies in human liver showed that this conversion is blocked by ethanol and ADH inhibitors (at high concentrations) such as 4-methylpyrazole and fomepizole and to a less extent by the ALDH inhibitor disulfiram. (Lenz *et al.*, 2011). However, conversion of 1,4 BD to GHB in brain was insensitive to pyrazole and ethanol, indicating a different enzymatic pathway for 1,4 BD to GHB conversion arise in the brain (Snead *et al.*, 1989). The liver conversion was accelerated in a dose-dependent manner in the presence of acetyl aldehyde (Lenz *et al.*, 2011)

A study in SH-SY5Y cell lines has indicated that the efficiency of the 1,4 butanediol GHB pathway is increased when the GHB synthesis pathway from GABA is blocked (Lyon *et al.*, 2007). A possible explanation is the existence of specific threshold for GHB in the cell. Once the GHB concentration declines below the threshold, the cell responds in a substitute way to make GHB.

Although gamma butyrolactone (GBL) is also a natural product in rat brain at 10% concentrations of GHB (Snead *et al.*, 1989), the enzyme converting GBL to GHB (Lactonase) is absent in brain tissues (Snead and Gibson, 2005), and GBL itself was shown to be biologically inactive (Roth *et al.*, 1966, Snead, 1991). Given that GBL occurs in certain dietary products such as wine (Vose *et al.*, 2001), it seems that only exogenous GBL is converted to GHB by lactonase which is present in blood and liver (Roth and Giarman, 1965), then the resultant GHB crosses the blood-brain barrier and exhibits its neurological effects.

1.4.2 GHB catabolism

GHB catabolism is an important process to control endogenous GHB levels. GHB is oxidized to SSA and there are at least two enzymes that have been shown to catalyze this reaction; a NADP dependent aldehyde reductase which was named GHB-dehydrogenase (Kaufman *et al.*, 1979) and a hydroxyacid oxoacid transhydrogenase (HOT) (Kaufman *et al.*, 1988b, Kaufman *et al.*, 1988a). SSA is further oxidized to succinate via the action of succinic semialdehyde dehydrogenase (SSADH) to enter the TCA cycle (Doherty *et al.*, 1975).

1.4.2.1 NADP-dependent GHB dehydrogenase

A cytosolic enzyme of 31-38 KDa was isolated from hamster liver and brain by (Kaufman *et al.*, 1979). The enzyme catalyzes the oxidation of GHB to SSA using $NADP^+$ as a cofactor. Favourite substrates are GHB, SSA, D-glucuronate, and L-gulonate. The K_m for GHB was determined to be 2.2 mM and 2.5 mM for liver and brain enzyme respectively. When coupling the reaction to the reduction of D-glucuronate, the K_m was five-fold lower (Kaufman and Nelson, 1981) which may indicate a favoured route *in vivo.* Given that GHB dehydrogenase is inhibited by anticonvulsant drugs, the similarity between GHB dehydrogenase and AKR1A1 in molecular weight, preferred substrates, cofactors and inhibitors suggests that they are identical.

1.4.2.2 HOT

Following the characterization of the NADP-dependent GHB-dehydrogenase, an antibody to it was prepared to investigate the presence of other enzymes that catalyze the first step in GHB degradation. The antibody suppressed effectively 95% of the ability of rat kidney and brain cytosol to degrade GHB while it inhibited only 50% of the activity in total rat kidney homogenate, implying the presence of at least one non cytosolic enzyme that oxidizes GHB. The enzyme was then isolated from rat liver, kidney and brain mitochondria (Kaufman *et al.*,

1988b, Kaufman *et al.*, 1988a). Unlike the first GHB dehydrogenase, this enzyme does not use NAD or NADP as a cofactor, but α-ketoglutarate as an electron acceptor. It transfers the hydrogen connected to the hydroxyl-bearing carbon in GHB to the ketone-bearing carbon in α-ketoglutarate so it requires two substrates rather than a substrate and a cofactor (Figure 1.8). The presence of a hydroxyacid and an oxoacid is necessary in this reaction; therefore the enzyme was named hydroxyacid oxoacid transhydrogenase (HOT). Other substrates include D-α-hydroxyglutarate, L-β-hydroxybutyrate as hydroxyacids, and SSA, α-ketoadipate and oxalacetate (Kaufman *et al.*, 1988b).

Following rodent studies, human tissues were investigated for the presence of HOT and the data obtained provide a better understanding of its characteristics (Struys *et al.*, 2005b). Human liver and fibroblast cell lines were used as a model in the study and enzyme activity was monitored by GC/MS using a stable isotope of γ-hydroxybutyrate and α-ketoglutarate. HOT activity was present in both models and also in fibroblast homogenates from patients with D-2-hydroxyglutarate aciduria, showing that deficiency in HOT is not the cause of this inborn disease. However, the activity in these models was lower than in rat brain and kidney mitochondria.

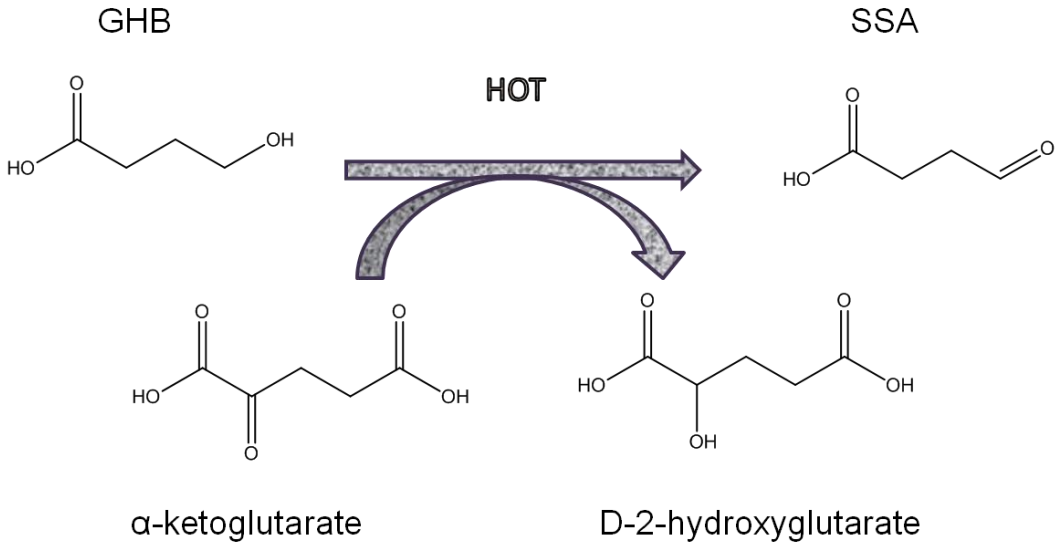

Figure 1.8: The transhydrogenase reaction of HOT. HOT transfers the hydrogen from the hydroxyl group in GHB to the ketone group in α-ketoglutarate. This reaction produces SSA and D-2-hydroxyglutarate.

More recently, a study identified the gene encoding HOT and revealed it is an iron containing alcohol dehydrogenase (Kardon *et al.*, 2006). In this study, HOT was purified partially from rat liver and its activity was measured by coupling it to SSADH and monitoring NADH formation by the later enzyme at 340 nm. HOT activity was not affected by EDTA but was inhibited by cyanide and phenanthroline which suggested that it used a divalent or trivalent cation for its activity. Metals did not stimulate the activity when were used in the range of 10-50 μM. Analyzing the two bands obtained for HOT at SDS-PAGE at 45 and 50 KDa, revealed that it is an iron-containing alcohol dehydrogenase encoded by the ADHFe1 gene.

ADHFe1 gene was first isolated from a human fetal brain cDNA library in 2002 (Deng *et al.*, 2002) and was identified as the first iron-containing alcohol dehydrogenase in human. Iron-containing alcohol dehydrogenases are a subfamily of the NAD dependent alcohol dehydrogenase family which contains as well medium chain zinc-dependent dehydrogenases (MDR) and short chain zinc-independent dehydrogenases (SDR)(Reid and Fewson, 1994).

ADHFe1 is located on chromosome 8q12.3-13.1 and comprises 14 exons. The ORF is different from the other human ADHs but shares a significant sequence identity with homologues in the bacterial ADHIII alcohol dehydrogenase as well as mouse, Drosophila and *Caenorhabditis elegans*. ADHFe1 has only two of the three histidine residues that were proposed to be engaged in metal binding (Bairoch, 1991). The expression of this gene was confirmed in adult liver, kidney

(Deng *et al.*, 2002), adipogenesis (Kim *et al.*, 2007) and the neuroblastoma cell line (Lyon *et al.*, 2009)

As in rat liver where two bands on SDS-PAGE corresponded to HOT (Kardon *et al.*, 2006), two protein species were detected for tagged murine ADHFe1 by Western blot (Kim *et al.*, 2007). It was proposed that translation of the ADHFe1 gene was launched at two different ATG and thus it had two splice variants.

1.4.2.3 SSADH

Succinic semialdehyde dehydrogenase (SSADH) is the enzyme responsible for the oxidation of SSA to succinate and the latter enters the TCA cycle. Therefore SSADH is involved in GHB degradation.

It has been shown that SSADH favours NAD as cofactor (Embree and Albers, 1964), and is localized in the mitochondrion of the cell (Salganicoff and Derobertis, 1965). Lipid peroxidation products such as acrolein and HNE inhibited irreversibly the activity of SSADH in rat brain mitochondria when added prior to SSA which imply an effect of oxidative stress on the metabolism of SSA and GHB *in vivo* (Nguyen and Picklo, 2003).

The significant role of SSADH in GHB turnover came to light after the discovery of an inborn disorder named GHB aciduria or SSADH deficiency (Jakobs *et al.*, 1981). High concentrations of GHB were detected in a patient's urine by GC/MS screening system. As SSA was also increased by 5-15 fold comparing with the

normal levels (0.2-0.6 μmol/mmol creatinine) (Struys *et al.*, 2005a), this indicated a problem in the degradation of SSA.

In normal individuals, a large amount of SSA, the product of the transaminase of GABA, is oxidized by SSADH to succinate and the later goes through the TCA cycle, the last general step in aerobic oxidation. A small portion of SSA is reduced by succinic semialdehyde reductase to form GHB. When SSADH is deficient, the oxidation route for SSA is blocked leading to diversion to the alternative reduction pathway to remove excess SSA by reducing it to GHB. The accumulation of GHB in the central nervous system and in body fluids is manifested by developmental delay, mental retardation, hypotonia, ataxia and seizures.

SSADH deficiency is an "autosomal recessive inherited disorder" recognized in approximately 400 cases worldwide (Pearl *et al.*, 2009).There is no therapy for this disease and drugs are only prescribed to relieve the symptoms. Anticonvulsant drugs are often used to manage epilepsy and seizures. However, valproate is not included as it is an inhibitor of SSADH so it may hinder any residual SSADH activity (Pearl *et al.*, 2003).

1.5 GHB concentrations

1.5.1 Endogenous GHB concentrations

GHB is present in neuronal and peripheral tissues. In rats, concentrations were reported to be 1.85 μM in brain, 10.8 μM in heart, 21.6 μM in kidney,1.59 μM in liver, 1.12 μM in lung, 11.3 μM in muscle, 0.55 μM in blood and 0.42 μM in white fat (Nelson *et al.*, 1981).

In rats killed by microwave irradiation, GHB levels in brain regions were 1.86 μM in stratum, 2.04 μM in cerebellum, 1.87 μM in cerebral cortex, 1.41 μM in hippocampus, 2.42 μM in hypothalamus, and 1.73 μM in white matter (Eli and Cattabeni, 1983). However, an increase in GHB levels especially in the hypothalamus was observed when the animals were decapitated, which indicates a postmortem GHB formation in brain (Eli and Cattabeni, 1983, Fung *et al.*, 2004).

In humans, a cut-off concentration of 4-5 mg/L and 10 mg/L for blood and urine respectively was recommended to discriminate endogenous GHB levels from those resulting from exogenous exposure (Elian, 2002, Elliott, 2003). In Elian study, endogenous concentrations of GHB ranged between 1.17-1.51 mg/L in 240 blood samples, and between 0.34-5.75 mg/L in 670 urine samples. A recent study proposed to reduce the urinary cut-off to 6 mg/L (Andresen *et al.*, 2010), however, caution should be taken to avoid false positive results as endogenous urinary GHB levels above 6 mg/L have been reported (LeBeau et al., 2002), and *in vitro* production of GHB in refrigerated unpreserved urine samples has been

documented (LeBeau et al., 2007). Pregnant women have higher levels of GHB and its precursor GBL (Raknes *et al.*, 2010).

In saliva, endogenous GHB ranged from 0.15 to 3.33 mg/L in 120 samples (De Paoli *et al.*, 2011), while in hair, endogenous levels varied from 0.3-12 ng/mg (Kintz *et al.*, 2003, Goulle *et al.*, 2003).

1.5.2 Postmortem endogenous GHB concentrations

Contrary to low and often undetectable endogenous GHB levels in living subjects, studies have shown that endogenous GHB concentrations are relatively high in body fluids after death. GHB has been reported in the whole blood of cases where death was unrelated to GHB. The concentrations ranged between 3.2 to 168 mg/L (Fieler *et al.*, 1998). This finding was confirmed by other researchers (Sakurada *et al.*, 2002, Kintz *et al.*, 2004, Moriya and Hashimoto, 2005)

These results had prospective consequence on the elucidation of GHB levels after death and led for screening of GHB in other organs and body fluids. In mouse liver, the amount detected increased overtime (Sakurada *et al.*, 2002) referring that GHB might be a product of post mortem breakdown. Urine was also a sample of interest as it was not expected to contain a high amount of endogenous GHB in deceased subjects. In many studies, GHB was detected at low concentrations (Sakurada *et al.*, 2002, Moriya and Hashimoto, 2005, Berankova *et al.*, 2006). In contrast, one study reported considerably higher

endogenous GHB levels in urine from 13 hanging and drowning cases (Elliott, 2001).

To explain this contradiction, it was proposed that storage condition and sample preservation affect the formation of GHB in post mortem blood and urine. To investigate this hypothesis, tests were carried out on blood and urine samples stored over a period of 8 months at different temperatures and the presence and absence of sodium fluoride (Berankova *et al.*, 2006). Sodium fluoride impedes the synthesis of polysaccharides by the microorganism and therefore stops microbial growth (Lough and Fehn, 1993). Low temperature (-20 C°) inhibited GHB production in blood, while increased levels of GHB were detected in unpreserved refrigerated blood. GHB values did not surpass 10 mg/L in post mortem urine with lower levels in preserved or refrigerated samples.

As it was proven that certain species of bacteria have the ability to convert GABA to GHB (Hardman and Stadtman, 1960, Nirenberg and Jakoby, 1960), it was also suggested that microorganisms play a part in elevated GHB post-mortem concentrations. Unpreserved blood and urine incubated with *Pseudomonas aeruginosa* for 1 month yielded 2.3 and 1.7 mg/L of GHB respectively (Elliott *et al.*, 2004). The study examined six other microorganisms but did not find a relationship between their growth and levels of endogenous GHB. Yet, this doesn't exclude the effects of microbes on GHB formation because other species may be involved.

In general, post-mortem blood concentrations for most analytes are dependent on the site of the sample. Blood from central sites usually gives high values, therefore, pathologists and forensic toxicologists prefer to collect blood from the

femoral vein because it gives constant quantitative results. For endogenous GHB, a study screened 71 autopsy cases less than 3 days after death and reported an elevated levels of GHB in cardiac blood rather than femoral blood (Kintz *et al.*, 2004). Another study found that femoral blood had amounts of GHB higher than cardiac left chamber blood and aortic blood in 25 cases less than 2 days after death (Moriya and Hashimoto, 2005) and the amounts of GHB in all samples were significantly less than the first study. Sample preparation can be an explanation for this difference as the first study applied a protein precipitation protocol followed by derivatization of GHB, while the second study converted GHB to GBL without derivatization.

Blood and urine are not the only samples where post mortem GHB was detected. Vitreous humour and bile had also considerable concentrations of GHB (Kintz *et al.*, 2004). It was obvious from the autopsy cases mentioned above that there are no correlation between the cause of death and endogenous GHB concentrations.

1.6 GHB detection techniques

1.6.1 Samples

The narrow window of detection of GHB raises difficulties in drug facilitated sexual assault cases. GHB is only detectable in blood and saliva for 5 hours (Kintz *et al.*, 2001) and in urine for 12 hours (Brenneisen *et al.*, 2004). It is therefore of great importance that the samples are taken quickly after the incident and either stored at low temperatures or analyzed directly to prevent *in vitro* formation of GHB. In cases where the samples can not be obtained in the time specified, a hair sample is analyzed a few weeks later. Hair provides a longer window of detection that is extended to several months and has been very useful in documenting cases of sexual assault (Kintz *et al.*, 2003, Rossi *et al.*, 2009)

1.6.2 Gas chromatography/Mass spectrometry (GC/MS)

Gas chromatography has been considered the favoured method for the quantitative and qualitative analysis of GHB (Elliott, 2003, Meyers and Almirall, 2005, Lyon *et al.*, 2007, Andresen *et al.*, 2010, De Paoli *et al.*, 2011). In this technique the sample is dissolved in an organic solvent and is injected into a high temperature injection port to be volatilised. The volatilised sample is carried by an inert gas (mobile phase) such as helium or hydrogen over a long

column (meters) coated with a liquid layer (stationary phase). Based on their chemical and physical characters, the components of the sample separate between the two phases. The greater the affinity of the component for the stationary phase, the longer it is hold on the column. The retention time of each component on the column is static under the experiment's conditions so it is an important factor for identification.

As soon as the sample passes through the column it reaches a detector. There are several detectors for GHB but the most currently used one is mass spectrometry (MS).

The first part of the mass spectrometry is the MS source where the separated components are ionised either by Electron Impact (EI) or by Chemical Ionisation (CI). The produced ions are separated in the mass analyzer (quadruples or ion traps) by their mass/charge ratio. The mass detector creates a mass spectrum where the ion abundance is plotted against the m/z ratio. Figure 1.9 shows a diagram of GC/MS.

Since GHB is a small polar compound and thermally unstable, derivatization of GHB prior to GC/MS analysis is necessary. The best method is silylation where a trimethylsilyl (TMS) group substitutes the hydrogen in the functional groups of GHB.

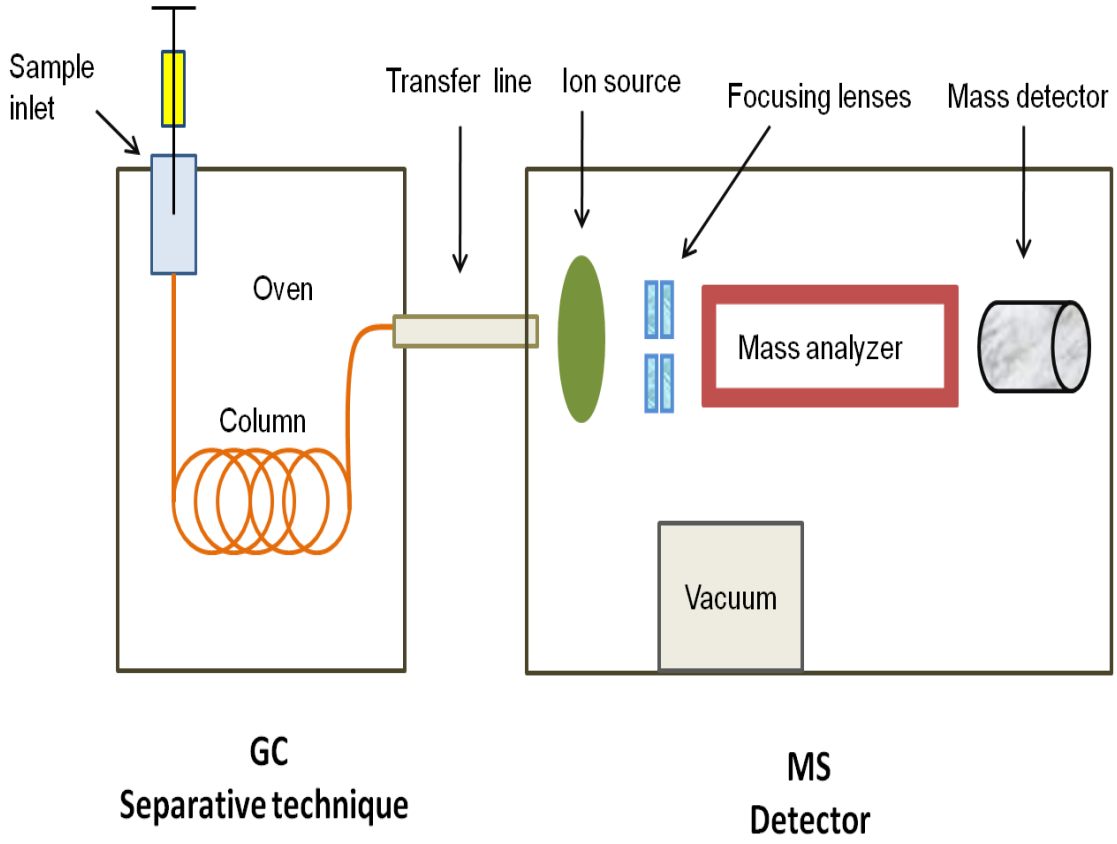

Figure 1.9: Gas Chromatography/Mass Spectrometry diagram. The injected sample is volatilised in the sample inlet and is carried by the mobile phase (inert gas) to the column where the components are separated. The retention time for each component on the column is important for identification. The separated elements are transferred to the MS detector where they are ionised. The ions are passed through the mass analyzer to the mass detector and a mass spectrum is generated.

1.6.3 Liquid chromatography/Mass spectrometry (LC/MS) and tandem mass spectrometry (LC/MS/MS)

In liquid chromatography, the mobile phase is liquid and the stationary phase is solid. The components in a sample are separated by their interaction with the stationary and the mobile phase and not only with the stationary phase as in GC.

The dissolved sample is injected into the mobile phase which is either a single solvent or a mixture of solvents constantly pumped through the system. The sample travels through the column where the components separate on the basis of their partition coefficient for the stationary and mobile phases (Figure 1.10). The separated components enter the MS where they are ionised by various methods such as Atmospheric Pressure Chemical Ionisation (APCI) or Electrospray Ionization (ESI). The two ionization methods are considered soft ionization techniques that do not fragment the ions into daughter ions. Therefore, the mass spectrum consists only of pseudomolecular ions either $[M+H]^+$ or $[M+H]^-$ or adducted ions such as $[M+Na]^+$.

Tandem mass spectrometry performs a fragmentation on a selected ion which allows the detection of very low levels of compounds.

There were some reports on the LC/MS(MS) analysis of GHB (Borgen *et al.*, 2004, Stout *et al.*, 2010), and some of them requires derivatization of the drug (Kaufmann and Alt, 2007). By far, GC/MS is the most commonly used chromatographic method for GHB analysis.

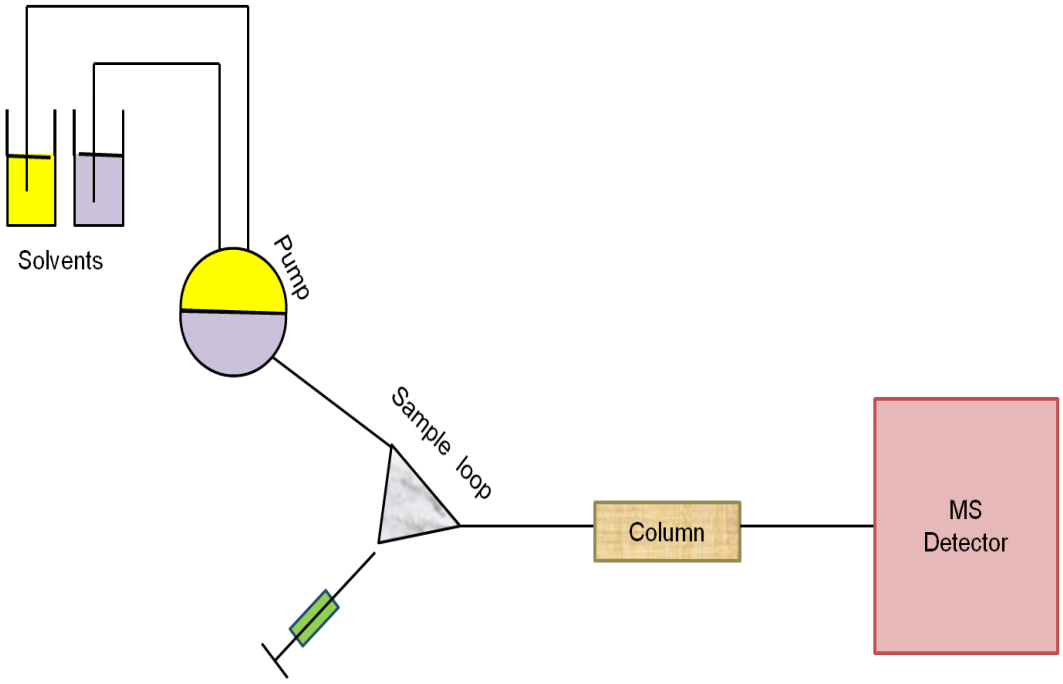

Figure 1.10: Liquid Chromatography/Mass Spectrometry diagram. The mobile phase is either a single or a mixture of solvents. Solvents are mixed in the pump and continuously flowed through the system. The sample is injected in the sample loop to the column where its components are separated by their partition coefficient between the mobile and the stationary phase. The separated elements are transferred to the MS detector to produce a mass spectrum for each element.

1.6.4 Enzymatic detection of GHB

Enzymatic techniques are considered a rapid screening method for the drug in a sample. It is a cost- and time-effective way to determine whether the drug of interest is present or not in the sample.

One way of detecting GHB is based on the conversion of GHB to SSA using GHB-dehydrogenase which uses NAD as a cofactor. GHB dehydrogenase reduces NAD to NADH and this reduction is correlated with an increase of absorbance at 340 nm (Sciotti *et al.*, 2010) (Figure 1.11 A). A commercially available kit employing this principle is developed by Buhlmann Laboratories, Schonenbuch, CH.

An alternative method is to couple the degradation of GHB to another reaction that produces a coloured compound. In one study GHB dehydrogenase from *Ralstonia eutropha* was used to oxidize GHB to SSA, and the reaction was coupled to diaphorase-mediated reduction of XTT (Bravo *et al.*, 2004) (Figure 1.11 B).

In another study GHB was oxidised by human AKR7A2 and the resultant NADPH reduce phenazine methosulfate (PMS). The reduced PMS reduces the blue dye 2,6 dichlorophenolindophenol (DCIP) to uncoloured product. The disappearance in colour is measured at 600 nm (Bendinskas *et al.*, 2011) (Figure 1.11 C). It should be noted, however, that AKR7A2 is a dominant SSA reductase and silencing the enzyme did not affect GHB dehydrogenase activity *in vitro* (Lyon *et al.*, 2007).

A

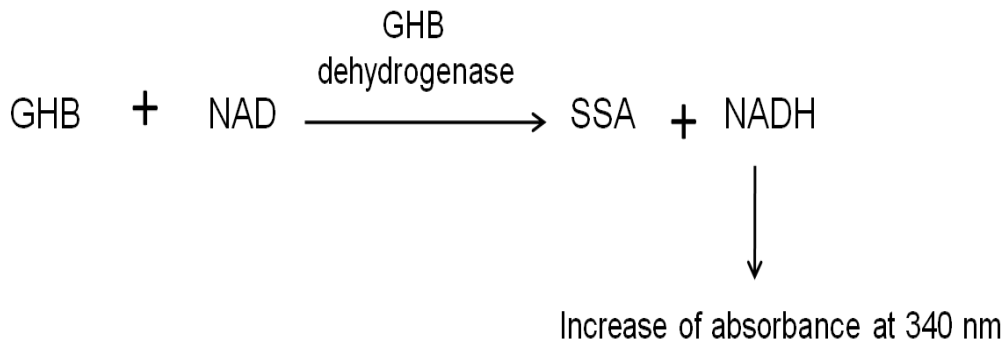
GHB
dehydrogenase
GHB + NAD
SSA + NADH
Increase of absorbance at 340 nm

B

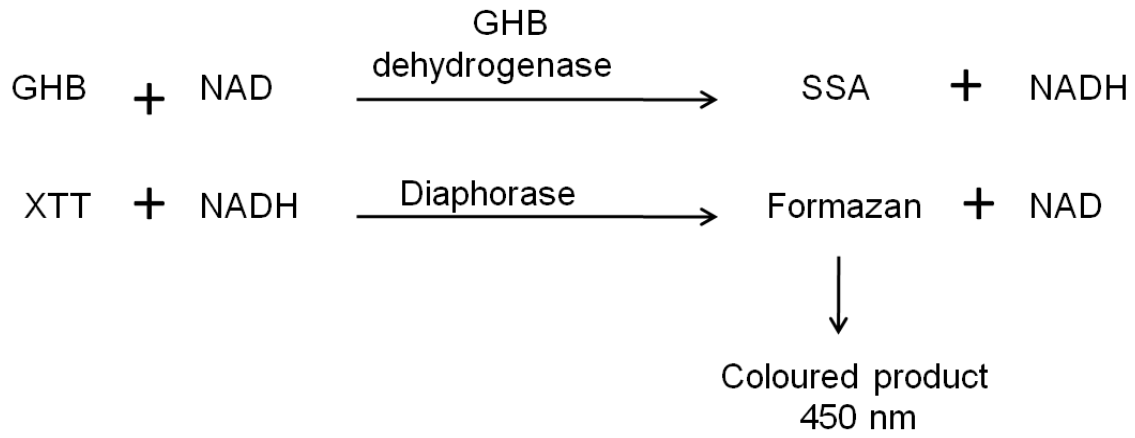
GHB
dehydrogenase
GHB + NAD
SSA + NADH
XTT + NADH
Diaphorase
Formazan + NAD
Coloured product
450 nm

C

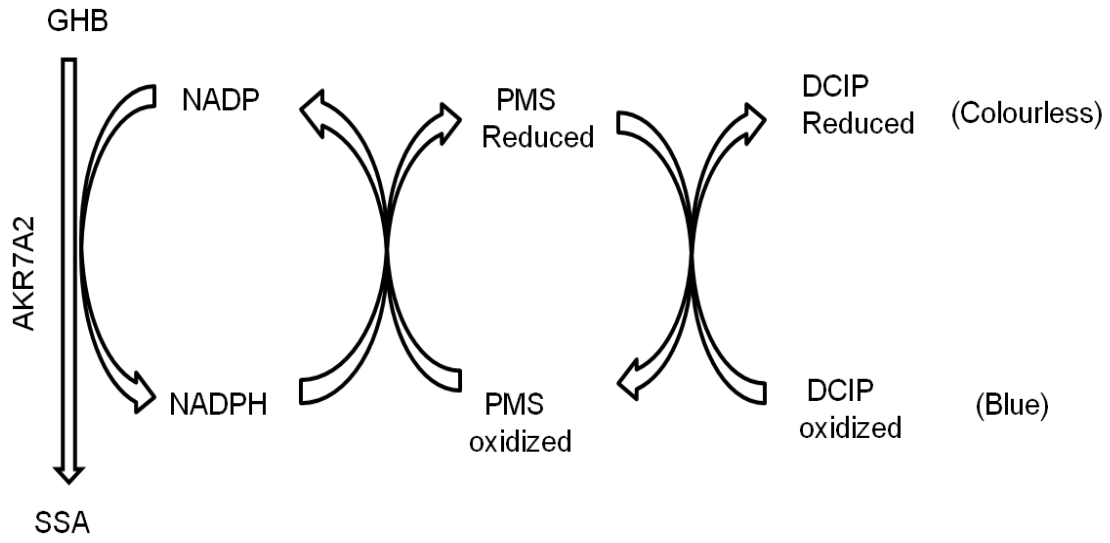

Figure 1.11: Principle of published enzymatic assays for GHB detection in beverages. A) Oxidation of GHB to SSA by GHB-dehydrogenase produces NADH and this formation is correlated with an increase of absorbance at 340 nm. **B)** The resultant NADH is used as a cofactor of diaphorase to reduce pro-dye XTT and thus producing a coloured product that can be measured at 450 nm. **C)** GHB is oxidised by AKR7A2 and produces NADPH. NADPH reduces PMS which in turn reduces the blue DCIP to a colourless product

1.7 Aim of this study

Understanding the GHB metabolic pathway is vital to interpret toxicological reports and to manage GHB overdose cases.

The first aim of this study is to characterize the role of the HOT enzyme in GHB metabolism and whether it works as a dehydrogenase or as a transhydrogenase enzyme, and explore the possibility of applying it in an enzymatic assay to detect GHB.

The second aim is to determine to what extent AKR1A1 is involved in endogenous and exogenous GHB metabolism in cell lines

The third aim is to investigate the effect of epidemiological factors on endogenous GHB levels in hair. This is to explore the metabolic pathway of GHB on the parent compound. The hair was chosen as a model because GHB is disposed in hair which enables monitoring these factors because of the long window of detection.

The objectives of this study are:

1- To express and purify the HOT enzyme as a recombinant protein, and to develop an enzymatic assay to measure its activity.

2- To knock down the expression of the gene encoding AKR1A1 in the human astrocytoma cell line 1321N1, and the human hepatoma cell line HepG2, and to measure the consequence of AKR1A1 silencing on endogenous GHB synthesis and catabolism, and on exogenous GHB metabolism.

3- To determine endogenous GHB concentrations in hair from GHB-free donors, and to examine the influence of some epidemiological factors on GHB levels between individuals.

CHAPTER TWO:

EXPRESSION, PURIFICATION AND REFOLDING OF A HYDROXYACID OXOACID TRANSHYDROGENASE ENZYME, AND ITS ROLE IN GHB METABOLISM

2 Expression, purification and refolding of a hydroxyacid oxoacid transhydrogenase and its role in GHB metabolism

2.1 Introduction

Although the presence and the activity of the hydroxyacid oxoacid transhydrogenase (HOT) was described more than 20 years ago (Kaufman *et al.*, 1988a, Kaufman *et al.*, 1988b), little progress has been made to understand this enzyme. This may be due to the fact that the gene encoding its protein was only identified recently (Kardon *et al.*, 2006), raising questions about its identity.

The HOT enzyme was first reported to be a transhydrogenase enzyme working on two substrates where one is a hydroxyacid and the other is an oxoacid. In this reaction, no cofactor is needed. The enzyme transfers the hydrogen attached to the hydroxyl group in GHB to the ketone group in α-ketoglutarate producing SSA and d-α-hydroxyglutarate.

However, the gene encoding HOT was identified as being identical to ADHFe1: a member of the NAD-dependent alcohol dehydrogenase group, indicating that the cofactor NAD is required in order for this enzyme to work. In these studies, the enzyme was isolated either from rat kidney (Kaufman *et al.*, 1988a), or from rat liver (Kardon *et al.*, 2006) but was not pure enough and was not in sufficient quantities to permit extreme investigations. The cloning of the gene encoding HOT enabled the use of recombinant DNA technology to produce the protein in large quantities and

to purify it in order to resolve the cofactor question and to characterize the enzyme.

Recombinant DNA technology is one of the most efficient ways of producing sufficient protein to studying *in vitro*, as it provides a high and pure amount of the protein that is not available naturally. The starting point is isolating the gene of interest and cloning it into an expression vector. The vector is inserted in to a host cell which allows controlled transcription and translation of the gene. Once the host cells are grown, the expressed protein can be isolated and purified.

Escherichia coli bacterium is a favourable host for expression studies as it grows rapidly on cheap media and expression plasmids are readily available (Baneyx, 1999).

The pET expression system (Novagen, 2002-2003) is a very powerful expression system that yields a high quantity of protein. It uses the T7 late promoter which is not recognized by *E. coli* RNA polymerase and permits the expression of the gene only when the T7 RNA polymerase is present. The vector is transformed into an *E. coli* strain that has the gene encoding T7 RNA polymerase under the control of the *Lac* promotor. This can be easily activated by the addition of IPTG, (isopropyl β-D-1-thiogalactopyranoside) a synthetic analogue of allolactose. This initiates transcription of the T7 RNA polymerase which subsequently leads to the transcription of the target gene (Figure 2.1).

The pET15b expression plasmid also contains a fusion poly histidine tag sequence in order to facilitate the purification of the recombinant protein by

immobilized metal affinity chromatography. The principal of this method lies in the ability of histidine to bind to nickel. Attaching an external sequence of this amino acid to a protein increases the binding power dramatically compared to other proteins. The His tag consists of six histidine residues, and given that histidine is not present in many proteins, a sequence of six histidine is extremely rare. The nickel is immobilized on the column through forming a chelating complex with an agent placed on an agarose resin. When a mixture of protein containing a His–tagged recombinant protein passes through the column, the recombinant protein is retained on the column while other proteins pass through, thus separating the target protein from its mixture. To elute the protein from the column, imidazole, which has a stronger affinity to nickel than histidine, is applied to the column to replace histidine from its binding sites.

In this chapter, the expression, purification and refolding of the recombinant enzyme from *E coli* are described, and two different enzyme activities are tested on the refolded enzyme; the transhydrogenase activity and the dehydrogenase activity in order to comprehend the manner of this unusual enzyme.

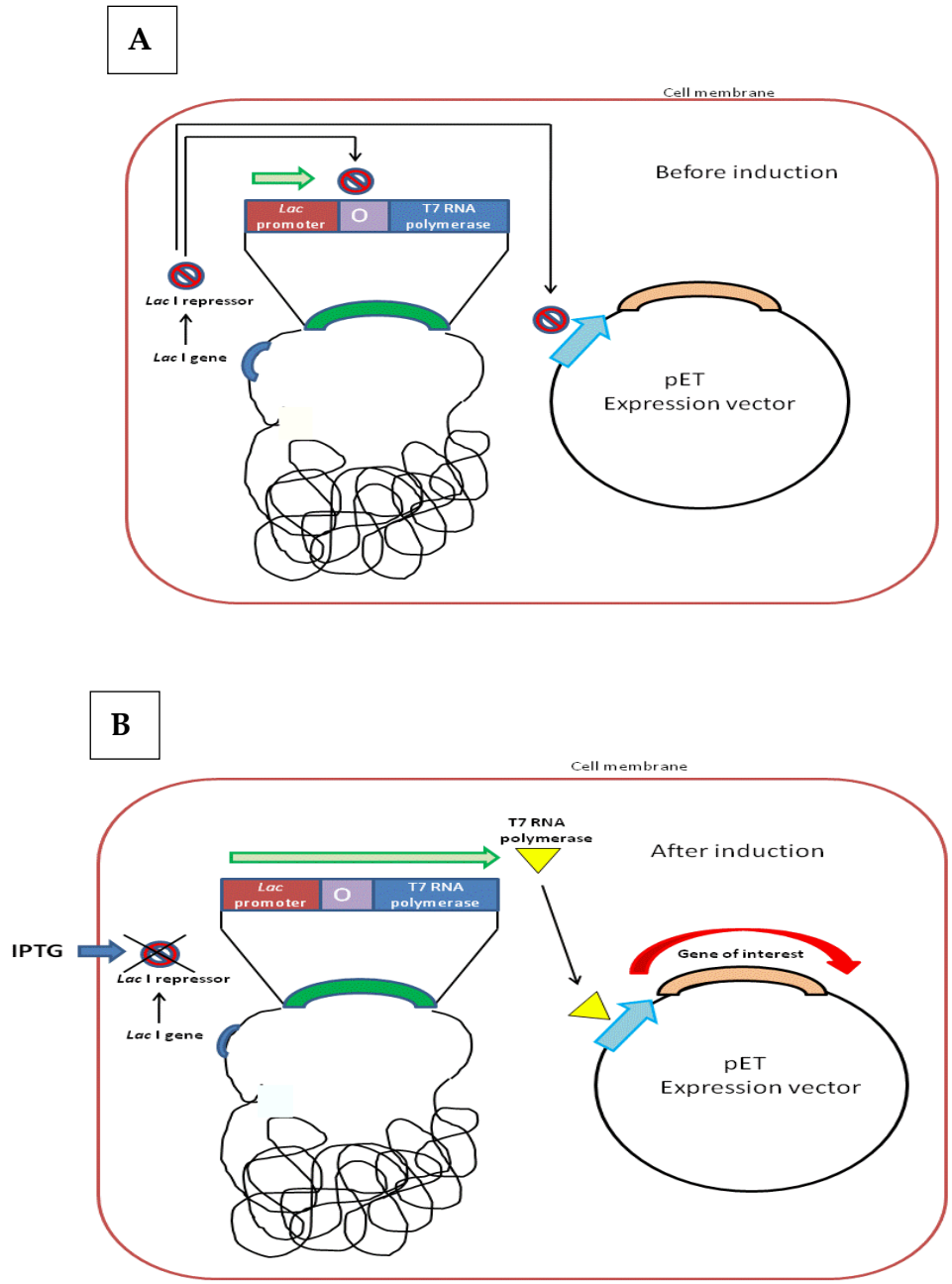

Figure 2.1: **Mechanism of Protein Expression in *E. coli*. A)** Before induction, the *Lac*I repressor binds to the *Lac* operator and inhibits expression of the T7 RNA polymerase. **B)** After induction, IPTG binds to the *Lac*I repressor and allows the transcription of the T7 RNA polymerase. The T7 RNA polymerase activates the T7 late promoter in the pET expression vector and thus the protein of interest is expressed.

2.2 Materials and methods

2.2.1 Materials

2.2.1.1 Plasmids

The plasmids used in this study are listed in table (2.1).

2.2.1.2 Bacterial strains:

2.2.1.2.1 Host strains

BL21(DE3) pLysS : genotype *E. coli* B F^- *dcm ompT hsdS*(r_B^- m_B^-) *gal* λ(DE3)[pLysS Cam^r] (Novagen, UK)

The BL21 DE3 pLYsS strain allows over expression of recombinant proteins without killing the host cell (Miroux and Walker, 1996), and does not contain an outer membrane protease to facilitate the recovery of the intact recombinant protein. DE3 lysogen produces T7 RNA polymerase upon IPTG induction while pLysS carries the T7 lysozyme encoding which suppresses basal level expression of the gene of interest.

2.2.1.2.2 Bacterial strains containing recombinant ADHFe1 and ALDH5A1 genes

BL21-HOT: The bacterial strain containing the expression plasmid with the ADHFe1 gene encoding recombinant HOT was prepared in our lab previously (Panopoulos, 2007)

The cleavage site of the mitochondrial targeting sequence (MTS) of the ADHFe1 gene was determined using TargetP 1.1 server to be at the 57th amino acid with a score of 0.952. The genetic sequence encoding the first 49 amino acids in the MTS sequence was excluded from the cloning, and only the sequence corresponding to the last 8 amino acids were included in order to start the protein sequence with a methionine, and to get the full length of the coding sequence of the protein.

The ADHFe1 gene was amplified from human liver cDNA as template. Figure (2.2) shows the nucleotide and aminoacid sequence of the HOT gene with the start and end of the genetic coding sequence (CDS). The position of the forward and reverse primers on the gene sequence, and the position of MTS on the protein sequence are highlighted. Restriction enzymes sites and two triple GC that were inserted for cloning purposes are illustrated on the genetic sequence.

The amplified gene was cloned into a Topo vector (Invitrogen ,UK) with a size of 3957bp. Sequencing the plasmid confirmed successful cloning and transformation of the ADHFe1 gene (Panopoulos, 2007). It was sub-cloned into a pET15b plasmid and named pAP2-HOT (Figure 2.3).

The plasmid was transformed into *E. coli* strain BL21pLysS (Novagen, UK) and the bacterial strain was named BL21-HOT.

BL21-SSADH: The preparation of bacterial strain containing the ALDH5A1 full length gene was described previously (Murphy *et al.*, 2003). Briefly, the full length ALDH5A1 gene was amplified from rat brain and was cloned on UA cloning vector (Qiagen). It was subcloned into pET15b plasmid and in this study the plasmid was named pALDH5 (Figure 2.4).

The plasmid was transformed into *E. coli* strain BL21pLysS (Novagen, UK) and the bacterial strain was named BL21-SSADH.

Plasmid	Description	Source
pAP2-HOT	pET15b expression vector containing the ADHFe1 coding sequence	Constructed in the laboratory by Andreas Panopoulos, MPhil (Panopoulos, 2007)
pALDH5	pET15b expression vector containing the ALDH5A1 coding sequence	Gift from Dr Matthew Picklo (Murphy *et al.*,2003). Originally cloned by Dr Michael Gibson

Table 2.1: Plasmids and their sources

CDS

AGCGACCCGAGGAGGGAAGAGGACTCCAAGCGCCATGGCCGCTGCCGCCCGAGCCCGGGTCGCGTACTTG

M A A A A R A R V A Y L

CTGAGGCAACTGCAACGCGCAGCGTGCCAGTGCCCAACTCATTCTCATACTTACTCCCAAGCCCCTGGA

L R Q L Q R A A C Q C P T H S H T Y S Q A P G

EcoRI NdeI

Forward Primer GGGGAATTCATATGGCTGTTTCAAATATTAGATATG

CTTTCACCTTCTGGGAAAACAACAGATTATGCCTTTGAGATGGCTGTTTCAAATATTAGATATGGAGCAG

L S P S G K T T D Y A F E M A V S N I R Y G A A

CAGTTACAAAGGAAGTAGGAATGGACCTAAAAAACATGGGTGCTAAAAATGTGTGCTTGATGACAGACAA

V T K E V G M D L K N M G A K N V C L M T D K

GAACCTCTCCAAGCTCCCTCCTGTGCAAGTAGCTATGGATTCCCTAGTGAAGAATGGCATCCCCTTTACGG

N L S K L P P V Q V A M D S L V K N G I P F T

TTTATGATAATGTGAGAGTGGAACCAACGGATTCAAGCTTCATGGAAGCTATTGAGTTTGCCCAAAAGGGA

V Y D N V R V E P T D S S F M E A I E F A Q K G

GCTTTTGATGCCTATGTTGCTGTCGGTGGTGGCTCTACCATGGACACCTGTAAGGCTGCTAATCTGTATGC

A F D A Y V A V G G G S T M D T C K A A N L Y A

ATCCAGCCCTCATTCTGATTTCCTAGATTATGTCAGTGCCCCCATTGGCAAGGGAAAGCCTGTGTCTGTGC

S S P H S D F L D Y V S A P I G K G K P V S V

CTCTTAAGCCTCTGATTGCAGTGCCAACTACCTCAGGAACCGGGAGTGAAACTACTGGGGTTGCCATTTTT

P L K P L I A V P T T S G T G S E T T G V A I F

GACTATGAACACTTGAAAGTAAAAATTGGCATCACTTCGAGAGCCATCAAACCCACACTGGGACTGATTGA

D Y E H L K V K I G I T S R A I K P T L G L I D

TCCTCTGCACACCCTCCACATGCCTGCCCGAGTGGTCGCCAACAGTGGCTTTGATGTGCTTTGCCATGCCC

P L H T L H M P A R V V A N S G F D V L C H A

TGGAGTCATACACCACCCTGCCCTACCACCTGCGGAGCCCCTGCCCTTCAAATCCCATCACACGGCCTGCG

L E S Y T T L P Y H L R S P C P S N P I T R P A

TACCAGGGCAGCAACCCAATCAGTGACATTTGGGCTATCCACGCGCTGCGGATCGTGGCTAAGTATCTGAA

Y Q G S N P I S D I W A I H A L R I V A K Y L K

GAGGGCTGTCAGAAATCCCGATGATCTTGAAGCAAGGTCTCATATGCACTTGGCAAGTGCTTTTGCTGGCA

R A V R N P D D L E A R S H M H L A S A F A G

TCGGCTTTGGAAATGCTGGTGTTCATCTGTGCCATGGAATGTCTTACCCAATTTCAGGTTTAGTGAAGATG

I G F G N A G V H L C H G M S Y P I S G L V K M

TATAAAGCAAAGGATTACAATGTGGATCACCCACTGGTGCCCCATGGCCTTTCTGTGGTGCTCACGTCCCC

Y K A K D Y N V D H P L V P H G L S V V L T S P

AGCGGTGTTCACTTTCACGGCCCAGATGTTTCCAGAGCGACACCTGGAGATGGCAGAAATACTGGGAGCCG

A V F T F T A Q M F P E R H L E M A E I L G A

ACACCCGCACTGCCAGGATCCAAGATGCAGGGCTGGTGTTGGCAGACACGCTCCGGAAATTCTTATTCGAT

D T R T A R I Q D A G L V L A D T L R K F L F D

CTGGATGTTGATGATGGCCTAGCAGCTGTTGGTTACTCCAAAGCTGATATCCCCGCACTAGTGAAAGGAAC

L D V D D G L A A V G Y S K A D I P A L V K G T

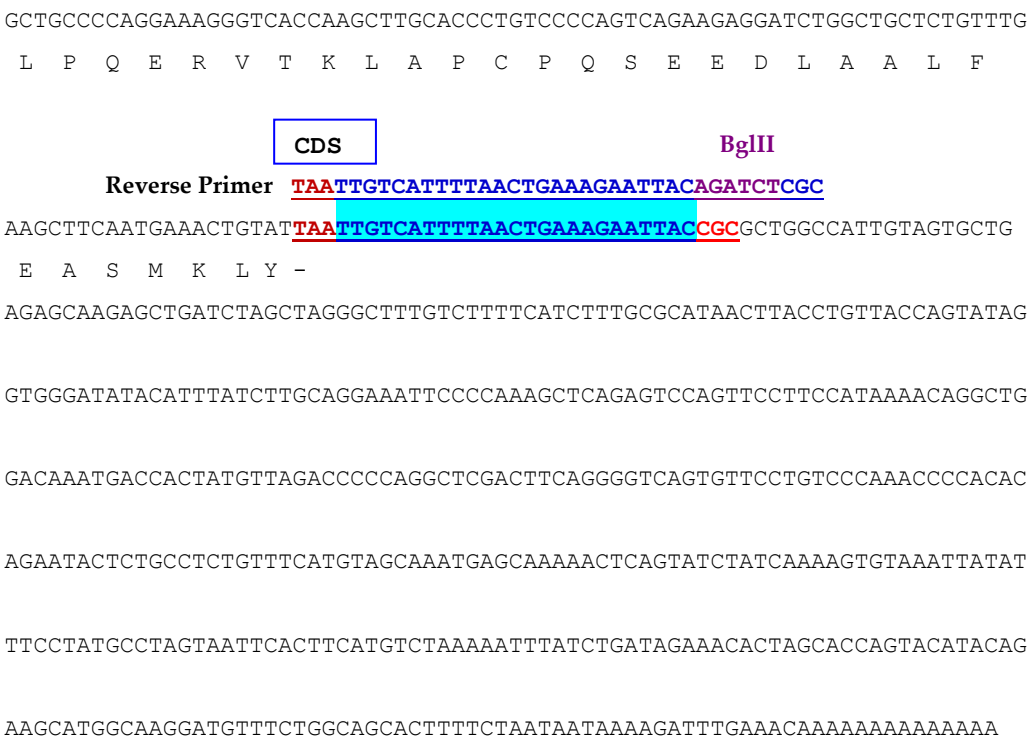

Figure 2.2: The ADHFe1 gene sequence. The ADHFe1 gene (NM_144650) and protein (NP_653251.2) sequences. The starting and the end of the genetic coding sequence CDS (35...1438) are shown in boxes on the gene sequence. The mitochondrial targeting sequence (MTS) is highlighted in yellow on the protein sequence. The genetic sequences of the primers are highlighted in blue. **EcoRI, NdeI** and **BglII** restriction enzymes sites which were included for cloning purposes are underlined. Two GC triplets were inserted at the beginning and at the end of the primer sequence, and they are shown in red.

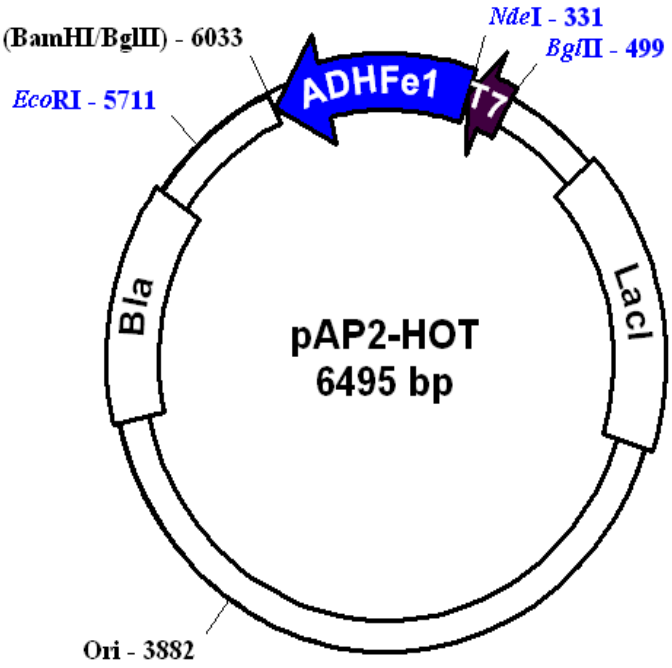

Figure 2.3: Map of pAP2-HOT. ADHFe1 gene that encodes the HOT enzyme was cloned into a pET15b vector. LacI coding sequence: bases: 866-1945. Bla coding sequence: Bases: 4643-5500

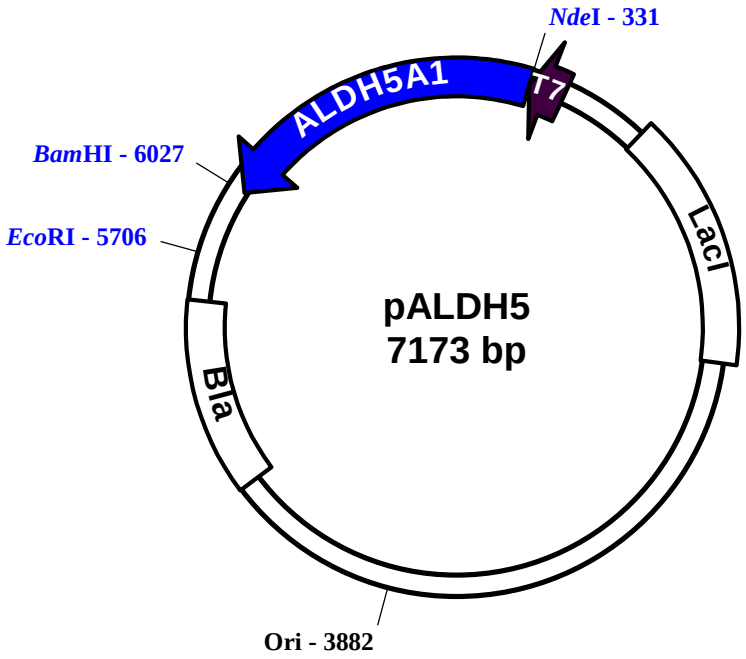

Figure 2.4: Map of pALDH5. SSADH gene (ALDH5A1) was cloned into a pET15b vector behind the T7 promotor. LacI coding sequence: bases 866-1945. Bla coding sequence: Bases 4643-5500.

2.2.1.3 Antibodies,

Primary antibody: Anti His antibody (Mouse IgG1) was obtained from Qiagen Ltd (Crawley,UK)

Secondary antibody: Goat anti-mouse IgG Biotin secondary antibody was a gift from Abcam.

2.2.1.4 Chemicals, Reagents and Biochemicals

Succinic semialdehyde, gamma hydroxybutyrate, cofactors (NAD, NADP, NADPH), N,N,N',N'-tetramethylethylenediame (TEMED), antibiotics (ampicillin and chloramphenicol), ferric chloride, 3-methyl-2-benzothiazolinone hydrazone hydrochloride hydrate (MBTH), tricholoroacetic acid, alcohols (octanol, butanol, methyl butanol, propanol and ethanol), dimethyl sulfoxide (DMSO), coumaric acid and luminol were supplied by Sigma-Aldrich (Poole, UK).

Yeast extract was purchased from Oxoid (Basingstoke, UK). Agar was obtained from Formedium LTD (Norwich,UK). Isopropyl-β-D-thiogalactoside (IPTG) was supplied from Melford Laboratories. Bio-Rad Protein Assay Reagents and prestained sodium dodecylsulphate (SDS) standards were supplied by Bio-Rad Laboratories (Hertfordshire, UK).

30% acrylamide/bisacrylamide solution was obtained from Severn Biotect Ldt, UK. Tris base, tryptone, sodium chloride and ammonium persulfate were from Fisher Scientific (UK). Phosphate monobasic and phosphate dibasic which used to prepare phosphate buffer were obtained from Reidel-Dettaen (Germany).

2.2.1.5 Columns

Affinity chromatography columns HisTrap 1 ml (17-5247-01) and 5 ml (17-5248-02), as well as desalting columns HiTrap desalting 5 ml (17-1408-01) were purchased from GE health care (Amersham, UK).

2.2.1.6 Instruments

GE Pharmacia FPLC (Fast Protein Liquid Chromatography) system was used for protein purification. This system was generally used for purification of large quantities of proteins. It includes two pumps capable of continuous flow to the purification columns, a peristaltic pump for column equilibration, a UV monitor to detect proteins on the column, a mixer to produce elution gradients, motor valves to assist with sample injection, column selection or flow reversal, and a controller with an integration function for computerized operation of various programs directing flow to the pumps and controlling the motor valves. The FPLC was placed at a cold room to perform purification at 4 °C.

Lambda 12 UV-Vis spectrophotometer from Perkin Elmer (USA) was used for enzyme kinetics. Absorbance at 340 nm and 280 nm was measured in a Quartz cuvette from VWR International (UK) with a 1 cm light path.

2.2.2 Methods

2.2.2.1 *E.coli* Growth Media

Luria-Bertani Broth (LB): 0.5% (w/v) Yeast Extract, 0.5% (w/v) NaCl and 1% (w/v) tryptone, made up to 1 ml in distilled water.

LB Agar (LB agar): 0.5% (w/v) yeast extract, 0.5% (w/v) NaCl, 1% (w/v) tryptone and 2% (w/v) agar, made up to 400 ml in distilled water.

Growth media were sterilized by heating at 121˚C for 15 minutes in an autoclave.

2.2.2.2 Antibiotics

Ampicillin was utilized at final concentration of 50 μg/ml. The stock solution was made at concentration of 50 mg/ml and sterilized by filtration through 0.22μm pore membranes.

Chloramphenicol was used at a final concentration of 30 μg/ml, with the stock solution (30 mg/ml) made up in ethanol.

Antibiotics were added to the LA agar and LB growth media after autoclaving.

2.2.2.3 Protein induction and cell lysis

BL21pLysS strains transformed with plasmids were grown from -80 °C glycerol stocks on LB agar plates supplied by ampicillin (50 μg/ml) and chloramphenicol (30 μg/ml). An isolated colony was picked carefully to grow in 4 ml LB starter culture with 50 μg /ml of ampicillin and 30 μg /ml of chloramphenicol in a 37 °C shaker overnight. The culture was transferred to a large flask containing 400 ml LB broth containing 0.1% of 50 mg/ml ampicillin and 30 mg/ml chloramphenicol at 37 ◦C shaking incubator and samples were taken every hour to check the growth by OD_{600} against LB media broth. When the optical density of the culture was between 0.4 and 0.5, expression was induced by adding IPTG (isopropyl β-D-1-thiogalactopyranoside) to the culture at a final concentration of 0.1 mM and 0.5 mM for HOT and SSADH proteins respectively. The culture was left for a further 3 hours in the shaking incubator at 30 ◦C. Cells were harvested by centrifugation and the pellet was retained and kept at -80 ◦C.

Cells were lysed in 20 ml start buffer (20 mM sodium phosphate, 0.5 M sodium chloride (NaCl), 1 mM imidazole, pH 7.4) and disrupted by a French Press with 40K cell. Lysate from the French press was centrifuged at 12,000 x g for 20 minutes. The supernatant was retained for SSADH purification while the pellet was retained for HOT purification under denaturing conditions.

2.2.2.4 His tag protein purification

2.2.2.4.1 SSADH purification under native conditions

The following buffers were prepared in distilled water, sterilized by filtration and the pH was adjusted to 7.4.

Start buffer: 20mM sodium phosphate, 0.5 M NaCl, 1mM imidazole.

Elution buffer: 20mM sodium phosphate, 0.5 M NaCl, 0.5 M imidazole.

The supernatant was retained and purification was carried out using FPLC. The protein was loaded to a 1 ml HisTrap nickel column (GE healthcare). Flow rate was 0.33 ml/min. The column was washed extensively (20 X column volume) with 96% start buffer and 4% elution buffer. The recombinant His-Tag protein was eluted in a step gradient starting from 4% elution buffer and 96% start buffer to 100% elution buffer. The collected fractions were assayed at 280 nm to detect the protein-containing fractions. The purity of the eluted protein was checked by SDS polyacrylamide gel electrophoresis and the protein amount was calculated via Bradford method (Bradford, 1976) against Bovine serum albumin.

2.2.2.4.2 HOT purification under denatured conditions

The method was modified from (Saurabh, 2007). The pellet was resuspended in 20 ml of start buffer (50 mM Na_2HPO_4 buffer + 0.3 M NaCl + 6 M urea, pH 7.5) and incubated at 30 °C for 1 hour. It was then centrifuged at 12000 rpm for 20 minutes. The supernatant was transferred to FPLC super loop and was injected into a 5 ml HisTrap nickel column (GE healthcare) at a flow rate of 1ml/min. The column was extensively washed (12X column volume) by 96 %

of start buffer and 4% of elution buffer (20 mM Tris base +100 mM NaCl + 6M Urea + 250 mM imidazole, pH 7.5).The recombinant His-tag protein was eluted in the denatured form by applying a step gradient from 96% start buffer and 4% elution buffer to 100% elution buffer. The collected fractions were assayed at 280 nm to detect the protein-containing fractions. The purity of the eluted protein was checked by SDS poly acrylamide gel electrophoresis and the protein amount was calculated via Bradford method against Bovine serum albumin.

2.2.2.5 Refolding Strategies

2.2.2.5.1 Refolding of the HOT protein by dialysis

Principle

Dialysis allows the movement of molecules from the high concentration to the low concentration by diffusion through a porous membrane. Proteins are bigger molecules which cannot diffuse through the pores while urea, salt and imidazole can easily cross the membrane to the low concentration.

Protocol

The pure protein was placed in dialysis tubing closed from both sides. The tubing was placed in a 500 ml shaking beaker containing 20 mM tris-Cl buffer, pH 8, 1 mM DTT and 5 M urea. The dialysis was performed at 4 °C and left on a shaker for 3 hours. Concentration of urea was dropped gradually from 5 M to 0.5 M every 2-3 hours.

2.2.2.5.2 Refolding of the HOT protein by dilution

The pure protein was diluted gradually to reduce the concentration of urea. Refolding buffer contained 20 mM tris buffer, pH8 and 1 mM DTT It was performed at 4 °C and a fresh buffer was added every few hours until the urea concentration reached 0.5 M. The diluted protein was concentrated using Amicon Ultra concentration tubes (Millipore, USA).

2.2.2.5.3 On-column refolding of the HOT protein

Principle:

On-column refolding allows the denatured protein to refold while loaded on nickel affinity chromatography column. This is achieved by performing a urea gradient to drop urea concentration to zero. The refolded protein is then eluted by a gradient of imidazole.

Protocol

The following four buffers were prepared according to (GE Lifesciences, 1999):

Start buffer: 50 mM Na_2HPO_4 buffer + 300 mM NaCl + 1 mM β–mercaptoethanol + 6M urea, pH 7.5

Second buffer: 20 mM Tris base + 100 mM NaCl + 6 M Urea + 1 mM β–mercaptoethanol + 250 mM imidazole, pH 7.5

Refolding buffer: 20 mM Tris buffer pH 8, 100 mM NaCl, and 1 mM β–mercaptoethanol .

Elution buffer: 20 mM Tris buffer pH 8, 100 mM NaCl, 1 mM β–mercaptoethanol , 250 mM imidazole.

The protein was loaded on the column and was washed at 10 mM imidazole (6 x column volume) by mixing 96% of start buffer with 4% of second buffer. A gradient of urea was performed on the column (10 x column volume) using start buffer and refolding buffer by moving from 100% start buffer containing 6M urea) to 100% refolding buffer (no urea). The protein was eluted using a gradient of imidazole by moving from 100% refolding buffer (no imidazole) to 100% elution buffer (250 mM imidazole).

2.2.2.5.4 Refolding of the HOT protein by size exclusion chromatography

Principle:

Size exclusion chromatography (SEC) separates molecules in a mixture according to their size, not to their molecular weight. The stationary phase is a crossed linked polymer such as agarose or dextran that contains pores able to accommodate small molecules (urea, imidazole, etc). Proteins are large molecules so they cannot infiltrate the pores, thus they elute with the mobile phase earlier than small molecules which are retained in the pores. When the mobile phase is an aqueous solution, the method called gel filtration.

Protocol

The denatured pure HOT protein was refolded by gel filtration (size exclusion chromatography) using Hitrap desalting column Sephadex™ G-25 Superfine (GE healthcare). The stationary phase is consisted of cross-linked dextran beads. The column was equilibrated by 25 ml of refolding buffer (20 mM Tris base, 1 mM DTT, pH 9) at a flow rate of 0.5 ml/min, and protein was refolded according to manufacturer's instructions. The elution was analyzed using gel electrophoresis to confirm the presence of the pure protein.

2.2.2.6 Gel electrophoresis

One dimensional electrophoresis on SDS - acrylamide gels separates proteins based on their molecular weight as described (Laemmli, 1970). The basis of this method is to produce a linear polpeptide chain by denaturing proteins. Denaturation is occurred by SDS; a strong detergent binds 1 g of protein per 1.4 g of SDS, and by boiling proteins in mercaptoethanol containing buffer which further denatures proteins by reducing the disulfide linkages. SDS-protein complexes are negatively charged due to the sulphate group of the SDS. Thus, the movement of the proteins is only dependent on their molecular weight: the smaller the protein, the faster it moves through the gel.

Solutions

4x Resolving buffer

90.8 g of Tris base; 2 g of SDS; made up to 450 ml with distilled water and the pH was adjusted to 8.8 with concentrated HCl. The solution was then made

up to 500 ml with distilled water and filtered through the Whatman # 1 filter paper.

4x Stacking buffer

15.14 g Tris base; 1 g SDS; made up to 200 ml with distilled water and the pH was adjusted to 6.8 with concentrated HCl. The solution was made up to 250 ml with distilled water and filtered through the Whatman # 1 filter paper.

10x Running buffer

30.28 g Tris base; 144 g glycine; 10 g SDS; made up to 1litre with distilled water.

10 x Running buffer was diluted (1:10) by distilled water to make 1 x Running buffer which was used to run the gel.

2 x LSB (Laemmli's Sample Buffer)

3.13 ml of 1 M Tris-Cl (pH 6.8); 2 g SDS; 9ml glycerol; 5 ml mercaptoethanol, 1 ml bromophenol blue (0.1%,v/v); made up to 50ml with distilled water.

Protocol

An Atto vertical gel apparatus (model-AE6450) from ATTO Corporation, Japan was used to run the gel. Two glass plated were wiped with ethanol and assembled.

Resolving gel (bottom gel) 10%

30% Acrylamide/bisacrylamide solution, 6.6 ml; 4 x Resolving Buffer, 5.0 ml; Ammonium persulphate (100 mg/ml fresh prepared), 100 µl; TEMED, 10 µl; distilled water 8.2 ml.

The resolving gel was poured between the two gel plates and overlayed by water-saturated isobutanol. It was left for 30 minutes to polymerize. The isobutanol layer was poured out, washed with distilled water and dried well.

Stacking gel (5%)

30% Acrylamide/bisacrylamide solution, 1.64 ml; 4 x Stacking Buffer, 2.5 ml; dH2O, 5.86 ml; Ammonium persulphate (100 mg/ml), 60 µl; TEMED, 10 µl.

The stacking gel was decanted on the top of the bottom gel and combs were inserted in the stacking gel. After complete polymerization, the combs were removed and the plates were transferred to the gel apparatus. The gel tank was filled with 1 x running buffer.

Sample preparation and loading

Loading Samples were prepared by mixing equal amounts of sample and 2 x LSB buffer and boiling them for 5 minutes. The samples were briefly centrifuged and then loaded on the gel. The gel was run at 125 V and 200 mA.

Gel staining

Staining solution 0.1% Coomassie stain blue R250 (w/v) in 20% methanol (v/v) and 7.5 % glacial acetic acid (v/v).

Destaining solution 20% methanol (v/v) and 7.5 % glacial acetic acid (v/v)

The gel was shaking in staining solution for 2 hours and then was destained by destaining solution until the bands were clearly visualized.

2.2.2.7 Western blotting

Western blotting is a powerful technique to detect a single protein in a mixture by using a specific antibody developed for this protein. The proteins are first separated by SDS-PAGE and then transferred to a membrane (nitrocellulose membranes are often used). The membrane has the capacity to bind both proteins and antibodies, thus, blocking non specific binding with the antibody is essential. Diluted protein solution of milk, BSA or Casein that contains a small percentage of detergent such as tween 20 is often used for this purpose. The protein binds to the specific antibody which is then binds to a secondary antibody. The secondary antibody is usually tied with an enzyme capable of cleaving a chemiluminescent agent to generate luminescence.

Solutions

1x Transfer buffer 14.4 g glycine; 3.0 g Tris base; 200 ml Methanol; made up to 1 litre with distilled Water.

10x TBS 100 ml of 1M Tris.Cl (pH 7.5); 375 ml of 4 M NaCl; made up to 1 litre with distilled water.

1x TBSTween 100 ml of 10 x TBS; 2 ml of Tween 20 (0.2% v/v); made up to 1 litre with distilled water.

Blocking solution 5% Alkali-soluble Casein was purchased from Merck and used according to the manufacturer's instructions

Procedure

The proteins were separated by SDS-PAGE as described in section (2.2.2.6). Four pieces of Whatman 3MM paper and 1 piece of nitrocellulose membrane were cut to the size of the gel and together with 2 sponges were all soaked in 1 x transfer buffer and were assembled in a (sandwich) form starting from the cathode (black) side of the plastic holder . The gel was put adjacent to the membrane between 2 Whatman papers and one sponge on each side, allowing the transfer from gel to membrane from cathode to anode. The transfer was carried out in a transfer tank (Bio-Rad gel apparatus) filled with 1x transfer buffer for 90 minutes at 300 mA. After the transfer, the membrane incubated with blocking solution for 1 hour, followed by incubation with the primary antibody diluted in a fresh blocking solution at 1:1000. The membrane was left in the primary antibody (Anti His antibody) on a shaker overnight. The membrane was washed in 1 x TBSTween 3 times (15 minutes each) and next incubated with the secondary antibody (goat anti mouse) for 2

hours. After that, the membrane was washed 3 times in 1X TBSTween (15 minutes each) and one time in TBS. The blots were ready to develop using ECL.

Antibody Detection using Enhanced Chemiluminescence (ECL)

250mM Luminol : 0.22 g of Luminol (Fluka) was dissolved in 5 ml DMSO. The solution was kept in the dark at -20°C in aliquots before use.

90mM Coumaric acid : 0.07 g Coumaric acid (Sigma) was dissolved in 5 ml DMSO and the solution was kept in the dark at -20°C in aliquots before use.

ECL 1 Solution 400 µl of 250 mM Luminol solution; 110 µl of 90 mM Coumaric acid solution; 4 ml of 1M Tris-Cl (pH 8.5); was made up to 40 ml with distilled water. It was kept at 4 °C in the dark before use.

ECL 2 Solution 256 µl of H_2O_2 30%; 4 ml of 1M Tris-Cl (pH 8.5); was made up to 40 ml with distilled water. It was kept at 4 °C in the dark.

Equal amount of ECL 1 and ECL 2 were mixed directly prior to use and poured over the membrane that had been probed into peroxidase conjugated secondary antibody. Bands were detected by measuring chemiluminescence using an intelligent dark box image reader (LAS3000) from Fujifilm.

2.2.2.8 Protein determination by Bio-Rad assay

The Bio-Rad protein assay employs the method described by Bradford (Bradford, 1976) to determine an unknown protein concentration by forming a complex between Bradford reagent (containing methanol and phosphoric

acid) and proteins with a characteristic absorbance at 595 nm. The amount of unknown protein is determined against a standard curve of a pure standard protein, commonly bovine serum albumin (BSA).

A stock of BSA is made in distilled water at 1 mg/ml. The stock was used to prepare several dilutions between 0 and 20 μg/ml in eppendorf tubes. 200 μl of Bio-Rad reagent was added to 800 μl of each dilution, raising the total volume to 1 ml. The tubes were mixed well and absorbance was measured at 595 nm. A standard curve for BSA was generated by plotting the absorbance at 595 nm against the amount of protein. Samples were prepared by diluting 10 μl of sample to 800 μl of distilled water, and 200 μl of Bio-Rad reagent was added. The amount of unknown protein was calculated from the standard curve.

2.2.2.9 Enzyme assays

2.2.2.9.1 Succinic semialdehyde dehydrogenase activity

Succinic semialdehyde dehydrogenase (SSADH) catalyzes the oxidation of SSA to succinate using NAD as a cofactor. To measure the activity of SSADH, the reduction of NAD to NADH was monitored at 340 nm.

The assay was carried out in a reaction volume of 1 ml at 25 ◦C in quartz glass cuvettes obtained from Hellma. Reaction mixture consisted of 20 mM HEPES buffer, pH7.1, 1 mM DTT, 50 μM SSA, 0.5 mM NAD and the purified enzyme to be tested. Results were expressed as nmol/min/mg of protein.

2.2.2.9.2 Transhydrogenase assay

Principle

A colorimetric assay to measure transhydrogenase activity of HOT was developed**.** The assay was used previously to determine GABA-transaminase activity by measuring the amount of SSA produced from the reaction. (Vasil'ev and Eremin, 1968, Taberner *et al.*, 1972). The method is based on measuring SSA, one of the products of the reaction between GHB and α-ketoglutarate. SSA is an aliphatic aldehyde and can react with 3-methyl-2-benzothiazolinone-2-hydrazone (MBTH) to form an azine. Another MBTH molecule is oxidized by ferric ions in acidic environment. The azine reacts with the oxidized MBTH to produce a coloured product that can be read at 660 nm. (Figure 2.5)

The method was modified to measure HOT activity by amending the initial reaction. However, the colorimetric reaction for SSA measurement was carried out as published previously.

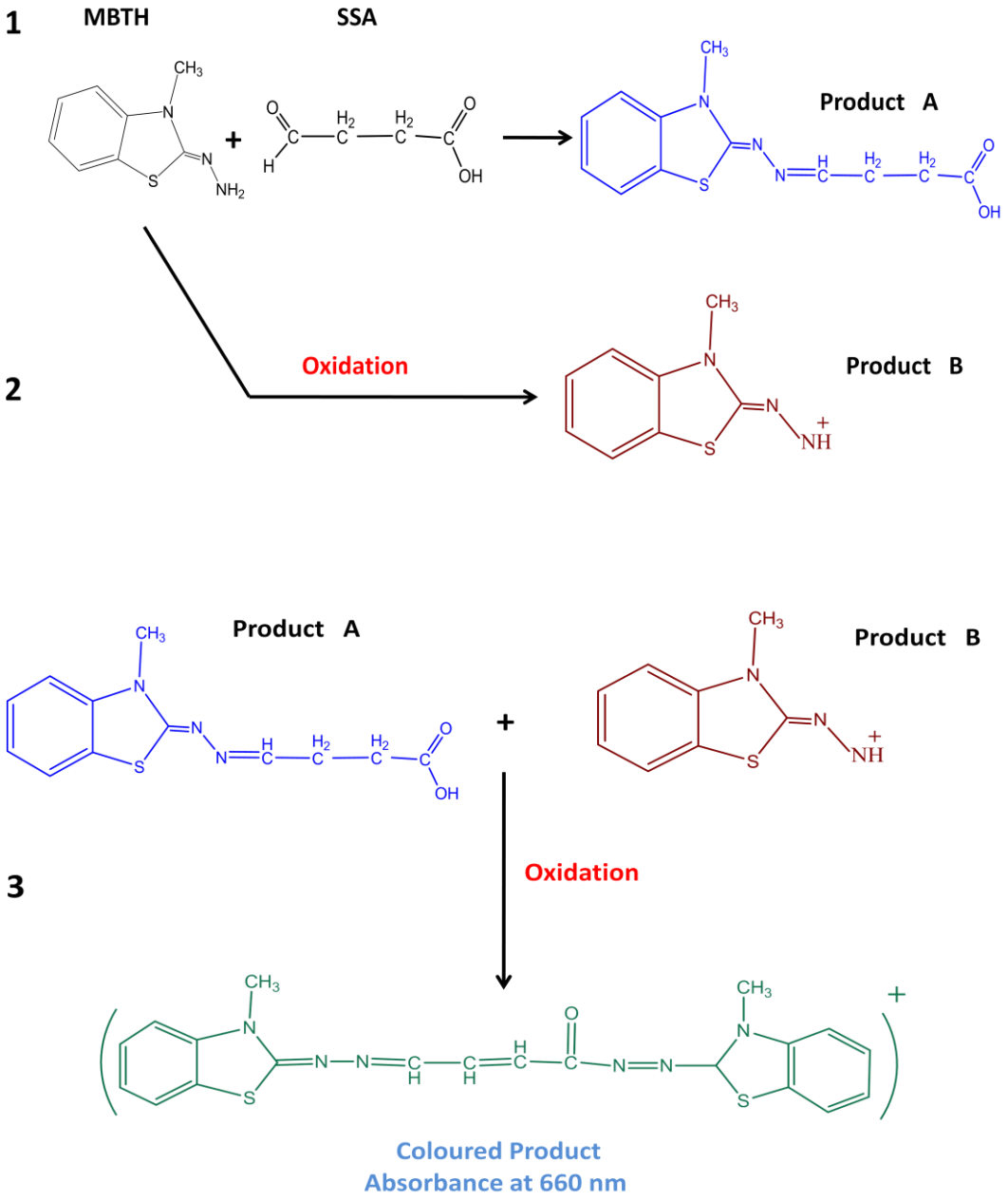

Figure 2.5: Principle of SSA determination by reaction with MBTH. 1) SSA reacts with MBTH to produce product A. **2)** Another MBTH molecule is oxidized by ferric ions to a reactive cation (product B). **3)** The reaction of product A and B produces a coloured product that has absorbance at 660 nm.

Procedure

The transhydrogenase reaction was carried out in a volume of 1 ml at 37 °C. The reaction mixture contained 80 mM HEPES buffer pH 7.5, 50 μM GHB, 50 μM α-ketoglutarate and 10 μg of the enzyme. The reaction was stopped after 30 minutes by the addition of 0.33 ml of 20% trichloroacetic acid. It was centrifuged at 5000 rpm for 5 minutes to precipitate the proteins. For each sample, a blank was prepared in the same way using refolding buffer instead of the enzyme.

100 μl of the supernatant was transferred to a fresh tube and mixed with 500 μl of 1% MBTH. After standing for 5 minutes, the mixture was boiled for 3 minutes then cooled in water for 8 minutes. 1 ml of 0.25 % ferric chloride prepared in 0.01 M hydrochloride acid (HCL) was added to each tube. After 5 minutes, 4 ml of acetone was added and the mixture shaken. The colour was left to completely develop for 40 minutes and then was read at 660 nm. A blank (reagent-only) reading was subtracted from the sample reading.

A standard curve was prepared using 25, 50,100, 200 and 400 μM of SSA. 100μl of each solution was moved to a fresh tube, mixed with 1% MBTH and the procedure carried out as above.

2.2.2.9.3 Alcohol dehydrogenase assay

GHB dehydrogenase reaction was performed either in 100 mM sodium phosphate pH 8 or 100 mM glycine pH 9, whether 50 μM or 1 mM GHB, 50 μM of NAD and 10 μg of enzyme. The increase in absorbance due to NADH production was monitored for 3 minutes at 30 sec interval at 340 nm. Results were expressed as nmol/min/mg of protein.

Other alcohols were also tested: Stocks of ethanol and propanol were made up in water while stocks of isobutanol, methyl butanol, benzylaclohol and octanol were made up in DMSO. Substrates were used at 1 mM and NAD was used at 50 and 200 μM in 0.1 M sodium phosphate buffer pH 8.

2.3 Results

2.3.1 Expression of recombinant HOT and SSADH

The HOT enzyme is proposed to participate in GHB catabolism by using α-ketoglutarate as a co- substrate and in a NAD(P) independent manner. With the purpose of characterizing the enzyme, a plasmid (pAP2-HOT) containing the cloned ADHFe1 gene encoding HOT was introduced into *E. coli* strain BL21pLysS (Panopoulos, 2007). In this plasmid, the full length of the ADHFe1 gene has been cloned under the control of the IPTG inducible promoter. Expression of the ADHFe1 gene was carried out described in materials and methods. The induction was initiated when the optical density of the bacterial cells reached between 0.4-0.5. At this optical density, the growth of the bacteria is at the log phase and induction was carried out for three hours using 0.1 mM of IPTG.

SSADH was also purified as a positive control for expression and purification of His-tagged protein. In addition, purified SSADH was needed for subsequent enzyme assays. The plasmid (pALDH5) was introduced in to the host and expressed in a similar manner using higher concentration of IPTG.

Protein extracts were prepared from samples before and after induction and analyzed by SDS-PAGE electrophoresis. An induced band of ~ 45 KDa was observed after induction of the ADHFe1 gene. An induced band of ~ 54 KDa was viewed for bacteria containing the pALDH5 which carries the ALDH5A1 gene (Figure 2.3A). These concur with the known molecular weights of HOT (45 KDa) and SSADH (54 KDa), indicating the production of both proteins has been successful (Figure 2.6).

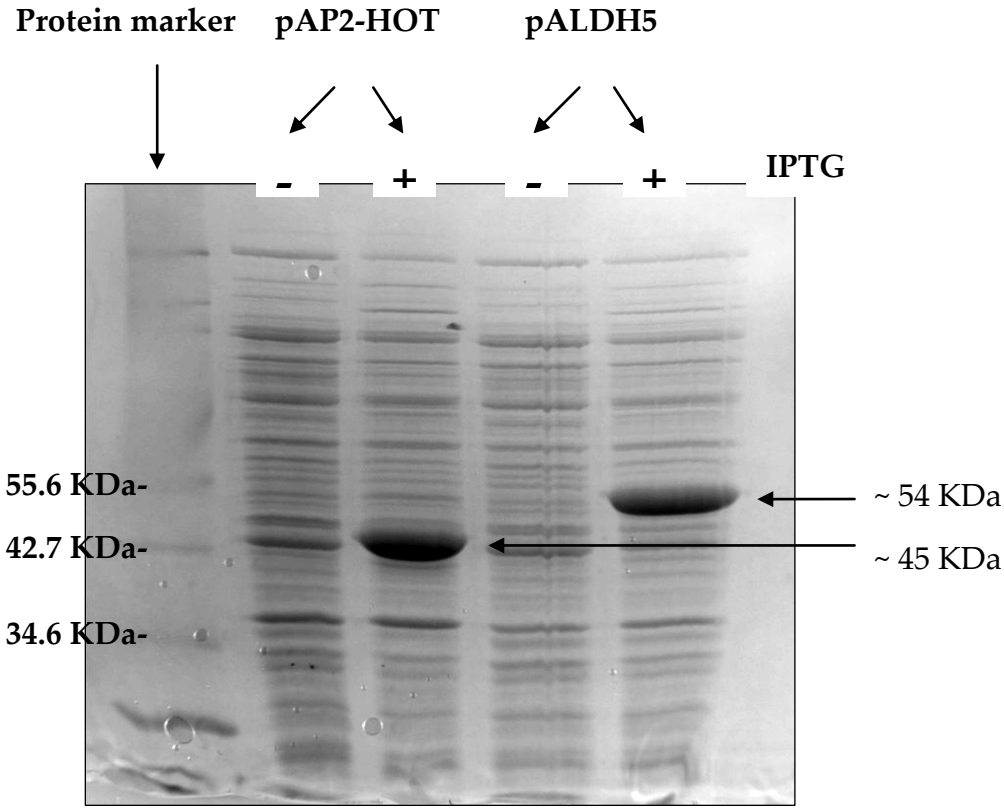

Figure 2.6: Expression of HOT and SSADH in *E coli* BL21PlysS. Bacterial cultures containing expressing plasmids pAP2 and pALDH5 were grown until OD 0.4-0.5 then 0.5 mM of IPTG was added to SSADH culture and 0.1 mM of IPTG was added to HOT culture and both were left for 3 hours at 30 °C. Protein samples were prepared from the cultures and 10 μg of samples along with 10 μl of protein marker were separated by SDS-PAGE.

To further verify that the observed bands corresponded to the two recombinant genes and to ensure that the His-tag is still intact and was not cleaved during the induction process, proteins were transferred to a nitrocellulose membrane and the His-tag was detected using anti-His antibodies as described in material and methods. Two strong bands appeared in the samples after induction, and were absent from the samples taken before induction. The position of these two bands was in accordance with their position on the SDS gel where the SSADH band has a higher molecular weight than the HOT band (Figure 2.7). As the presence of the intact His-tag is essential for protein purification by affinity chromatography, the Western results permitted progressing to the purification of the expressed proteins.

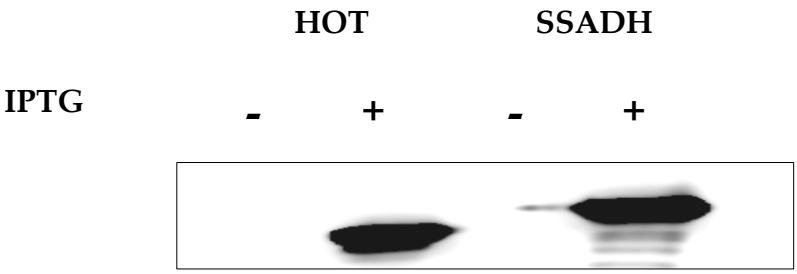

Figure 2.7: Western blot of induced HOT and SSADH. Western blot analysis of expressed HOT and SSADH; The two cultures were grown until OD 0.4-0.5 then 0.5 mM of IPTG was added to SSADH culture and 0.1 mM of IPTG was added to HOT culture and both were left for 3 hours at 30 °C . 10 µg of samples before and after induction were separated by SDS-PAGE and transferred to a nitrocellulose membrane. The His-tagged protein was detected using anti-His antibody by chemiluminescence.

2.3.2 Purification of recombinant SSADH:

After induction of expression, 400 ml of bacterial cells were lysed using the French press as described in materials and methods and centrifuged to remove cell debris and unbroken cells. Purification of SSADH was carried out on the supernatant using nickel affinity column automated by FPLC at 4 ˚C as described in material and methods. Crude extract containing SSADH was loaded onto a 1 ml nickel agarose column to which the His-tagged protein was attached while other bacteria proteins passed through the column (Flow-through). A gradient of imidazole (0 to 0.5 M) was used to elute the SSADH protein and fractions were collected with a flow rate of 0.3 ml/min.

The results (Figure 2.8) show protein fractions 26-29 which contain a strong band at 54 KDa. There are some contaminating bands but the protein appears to be 98% pure. Protein concentrations were determined by Bio-Rad Bradford method and the enzyme was kept at 4 °C for up to two weeks.

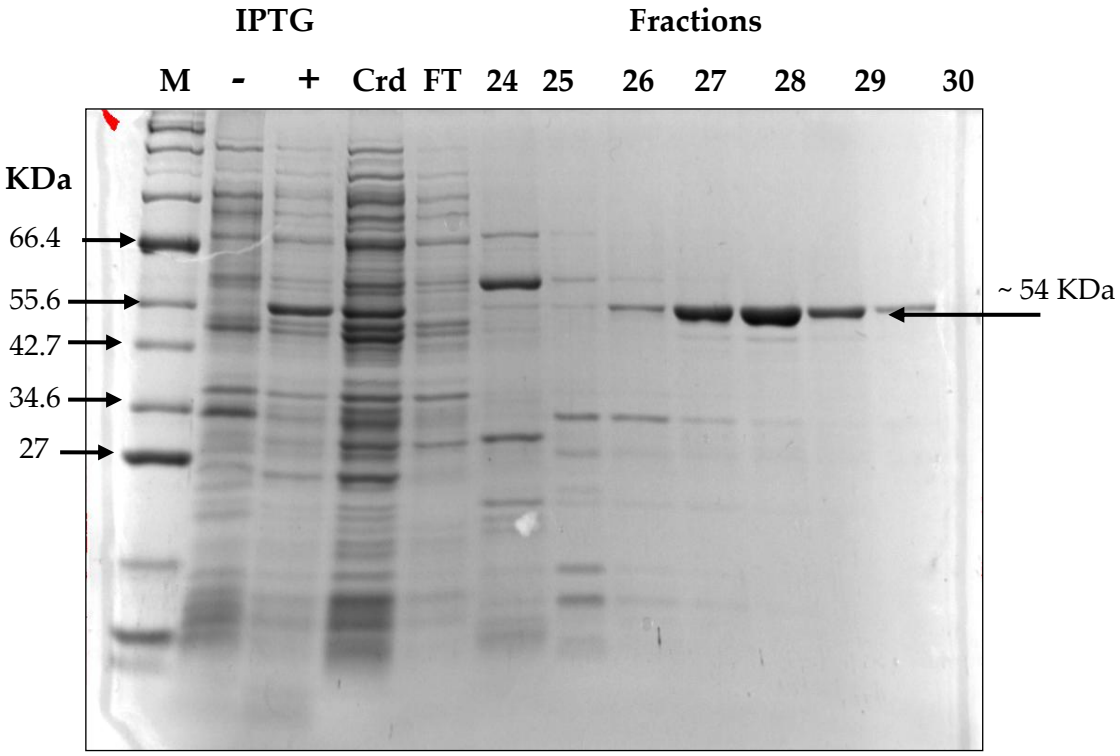

Figure 2.8: Purification of SSADH by affinity chromatography. Bacterial cells (BL21pLysS containing plasmid pALDH5 were grown to OD600 of 0.4 and the expression of SSADH was induced by adding 0.5 mM of IPTG for 3 hours at 30 °C. The cells were lysed by French press and centrifuged .The supernatant was loaded onto a nickel column, washed and purified by a gradient of imidazole. Samples before (-) and after (+) induction, crude (Crd), Flow through (FT) and eluted fractions (24-30) were separated on SDS-PAGE along with wide range protein marker (M)

2.3.3 Purification of recombinant HOT

Localization of the HOT protein in the bacterial cell

After induction with IPTG, the cells expressing HOT were lysed using French press. Samples from both the supernatant and the pellet were run on SDS-PAGE and transferred to a nitrocellulose membrane. The anti-His antibody showed the presence of the His tag recombinant HOT protein in the pellet in a vast amount, but not in the soluble fraction. Purified SSADH was used as a positive control (Figure 2.9 A).

To investigate possible reasons for not detecting HOT in the supernatant, the sensitivity of the His-tag antibody was tested by serial dilution of the pellet. The protein can be detected at 1/10 and 1/100 dilution (Figure 2.9 B). This was to exclude the possibility that the HOT protein may be expressed in the supernatant at minor levels that may not be detectable by the antibody. Levels lower than 100 times dilution are insufficient for enzyme assays.

Being present in the pellet indicates that the protein is expressed at high levels and is forming insoluble inclusion bodies. It is a phenomenon often noticed when inducing eukaryotic proteins in *E. coli* where the protein is misfolded, misdirected and/or aggregated.

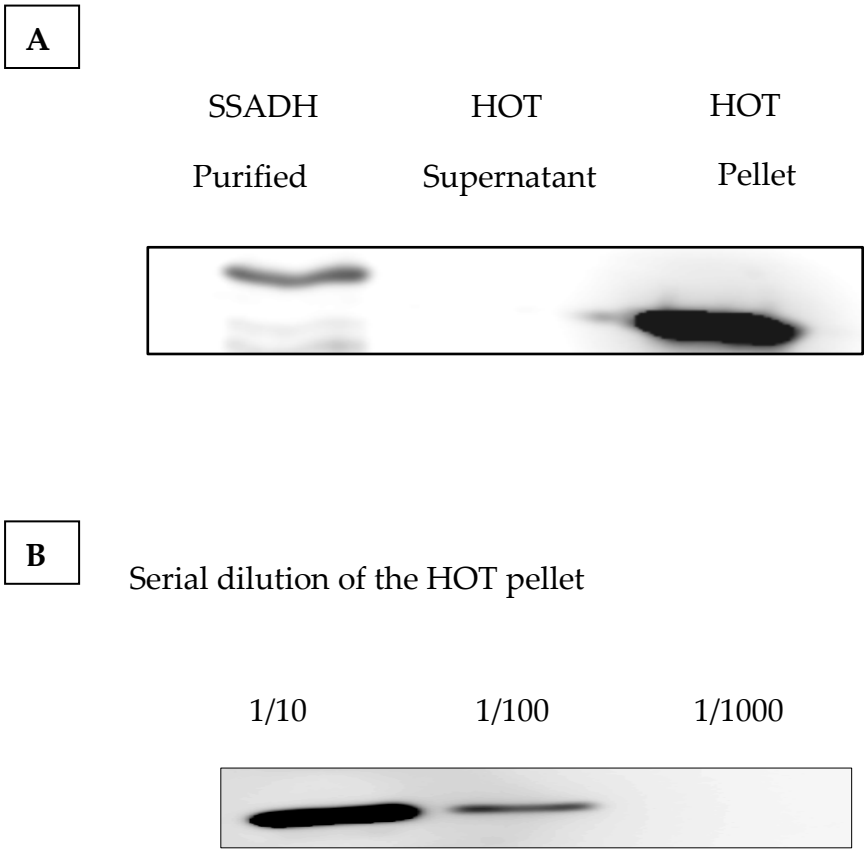

Figure 2.9: Expression and localization of the HOT protein by Western blot. Expression of the HOT protein was induced by 0.1 mM of IPTG for 3 hours at 30 °C, and the bacterial cells were lysed using French press and centrifuged. **A)** Samples from the supernatant and the pellet were separated by SDS-PAGE and transferred to a nitrocellulose membrane. The His-tagged recombinant HOT protein was detected using anti-His antibody and purified SSADH was used as a positive control. **B)** The HOT pellet was diluted 10, 100 and 1000 times and analyzed by Western blot to investigate the sensitivity of the anti-His antibody

Optimization of HOT expression

In an attempt to prevent insolubility of the protein, the expression conditions were changed to slow the growth of the bacteria, but this did not result in any solubilisation of the protein. Attempts were made to express the protein at lower temperatures and different IPTG amounts. The culture was induced at 16 and 20 °C overnight, or at 25 °C for 3 hours at 0.5, 0.2, 0.1 or 0.05 mM IPTG and although a band appeared in the same position as the HOT protein when induced by 0.1 mM of IPTG for 3 hours at 25 °C (Figure 2.10), the western blot analysis using anti-His-antibody provided negative results. Adding 1 mM of ATP and/or ferrous ions to the culture media did not produce any effect on the protein solubility. Therefore, it was necessary to attempt to purify the protein from the pellet, but in order to do that; the protein needed to be denatured by a strong detergent to solubilise the inclusion bodies.

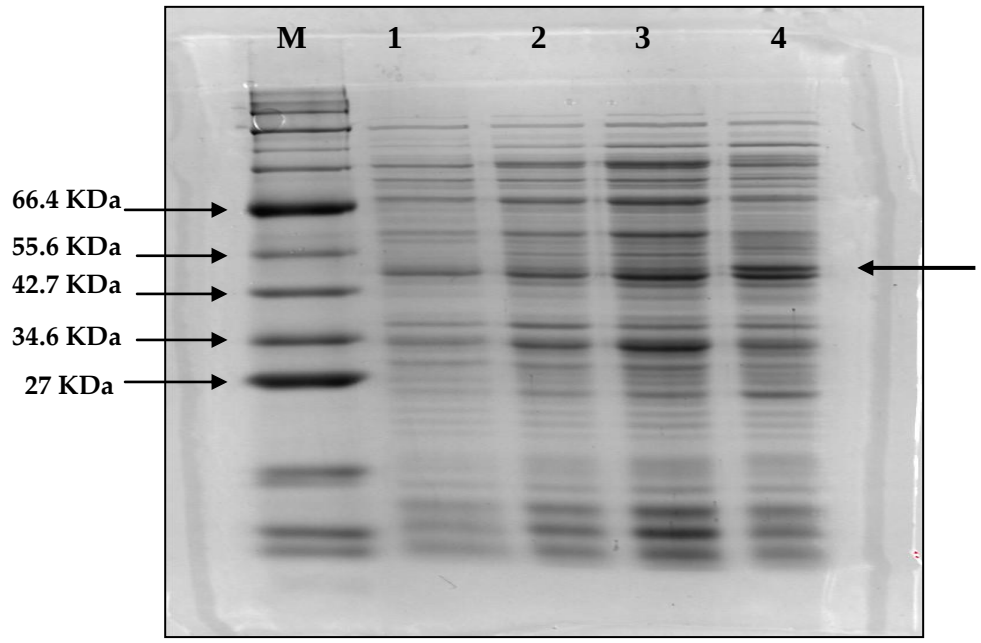

Figure 2.10: Optimization of HOT expression. Three bacterial cell cultures were grown until OD600 is between 0.4 and 0.6 and expression of HOT protein was attempted under various conditions. Lane 1 is pre-induced culture, lane 2 is induced culture at 20 °C by 0.2 mM IPTG, lane 3 is induced culture at 20 °C by 0.5 mM IPTG and lane 4 is induced culture at 25 °C by 0.1 mM IPTG. A band appeared in lane 4 but Western blot analysis using anti-His antibody was negative.

Purification of the HOT protein from the bacterial cell pellet

Dissolving the insoluble inclusion bodies requires the use of a high concentration of a denaturant such as urea to disturb the three dimensional structure of proteins. Urea was included in the start and elution buffer at a high level (6 M). The inclusion bodies were lysed in the start buffer by incubation for 1 hour at 30 °C. The lysate was centrifuged and the clear supernatant was passed through a 5 ml HisTrap nickel column. The column was washed extensively 10 times column volume at 20 mM imidazole and eluted with a gradient of imidazole from 20 to 250 mM at 1 ml/min flow rate (Figure 2.11). Analysis of the samples by SDS-PAGE electrophoresis showed a single band present in the eluted fractions. The purity of this band was around 95%. The yield of purified protein was calculated to be 1 mg for each 1 L of bacterial culture. Protein amount in inclusion bodies was 22 mg/L of culture.

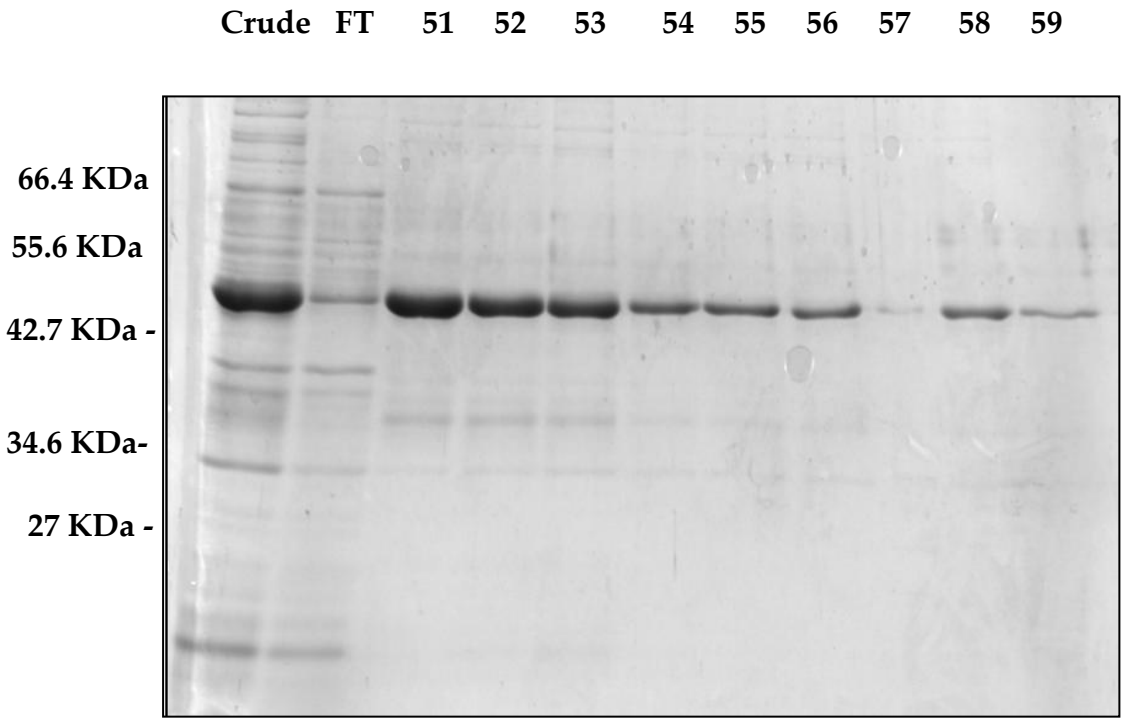

Figure 2.11: Purification of HOT enzyme under denatured conditions. HOT was expressed in *E. coli* BL21plysS from plasmid pAP2 by 0.1 mM of IPTG for 3 hours and the bacterial cells were lysed and centrifuged. The pellet was dissolved in urea and then was loaded onto a 5 ml HisTrap nickel column. Crude, flow through and HOT fractions (55-59) were separated on 10% SDS-PAGE gel.

2.3.4 Identification of purified protein

To verify that the purified protein corresponds to the HOT protein, the band was sequenced by the Proteomics centre in the University of Glasgow by MS/MS after trypsin digestion, and the data were analyzed by Mascot software (Matrix Science). The threshold ion score was calculated to be above 42 for 5% confidence. Results of analysis are listed in table 2.2 and table 2.3.

Table 2.2 showed five peptides entries that matched the database with their observed and expected masses. Three of the entries correspond to the same peptide, so the queries match number is three. According to the software instruction, two peptides or more are enough for confidant identification. Trypsin digestion was complete as the miss score was zero in all peptides. One of the ion score was statistically different with an ion score above 42 and expect value less than 0.1 (Expect shows the probability that the match happened by chance).

Table 2.3 showed proteins that match the same set of peptides. With a score of 54, the five queries showed a match with the HOT protein sequence. There are many entries for the HOT protein in the database resulting from different isoforms. The molecular weight for these proteins ranged between 45 and 50 KDa. Figure 2.12 highlights the matched peptides on the HOT protein sequence, and Figure 2.13 shows multiple sequence alignment of identified proteins.

Query	Observed	Mr(expt)	Mr(calc)	Delta	Miss	Score	Expect	Rank	Peptide
88	400.6849	799.3553	799.4188	-0.0635	0	19	17	1	K.GTLPQER.V
171	465.1842	928.3538	928.4250	-0.0712	0	54	0.0053	1	R.NPDDLEAR.S
172	465.2024	928.3903	928.4250	-0.0347	0	(15)	43	1	R.NPDDLEAR.S
173	465.2074	928.4003	928.4250	-0.0247	0	(25)	3.8	1	R.NPDDLEAR.S
274	466.2288	1395.6645	1395.7796	-0.1151	0	9	1.1e+02	7	K.LPPVQVAMDSLVK.N

Table 2.2: **Analysis of HOT band.** Analysis of purified HOT band was carried out by MS/MS after trypsin digestion. First column shows matched query number. Second, third and forth columns show observed, expected and calculated mass respectively. The miss column shows number of missed trypsin cleavage sites. Score shows ion score. Expect shows the frequency of the match occurrence by chance. Last column shows the matched peptides

Protein	Mass	Score	**Queries matched**	Identity
gi|119607307	45985	54	5	alcohol dehydrogenase, iron containing,1,isoform CRA_a [Homo sapiens]
gi|119607310	45442	54	5	alcohol dehydrogenase, iron containing,1,isoform CRA_d [Homo sapiens]
gi|133922590	50732	54	5	hydroxyacid-oxoacid transhydrogenase,mitochondrial precursor [Homo sapiens]
gi|194374233	43116	54	5	unnamed protein product [Homo sapiens]

Table 2.3: Proteins matching the same sets of peptides. NCBInr database search results of proteins that match the same set of peptides

MAVSNIRYGAAVTKEVGMASIRDDLKNMGAKNVCLMTDKNLSKLPPVQVAMDSLVKNGIPFTVYD
NVRVEPTDSSFMEAIEFAQKGAFDAYVAVGGGSTMDTCKAANLYASSPHSDFLDYVSAPIGKGKP
VSVPLKPLIAVPTTSGTGSETTGVAIFDYEHLKVKIGITSRAIKPTLGLIDPLHTLHMPARVVAN
SGFDVLCHALESYTTLPYHLRSPCPSNPITRPAYQGSNPISDIWAIHALRIVAKYLKRAVRNPDD
LEARSHMHLASAFAGIGFGNAGVHLCHGMSYPISGLVKMYKAKDYNVDHPLVPHGLSVVLTSPAV
FTFTAQMFPERHLEMAEILGADTRTARIQDAGLVLADTLRKFLFDLDVDDGLAAVGYSKADIPAL
VKGTLPQERVTKLAPCPQSEEDLAALFEASMKLY

Figure 2.12: Hydroxyacid oxoacid transhydrogenase sequence. NCBI protein sequence accession Q8IWW8

http://www.ncbi.nlm.nih.gov/protein/74714449

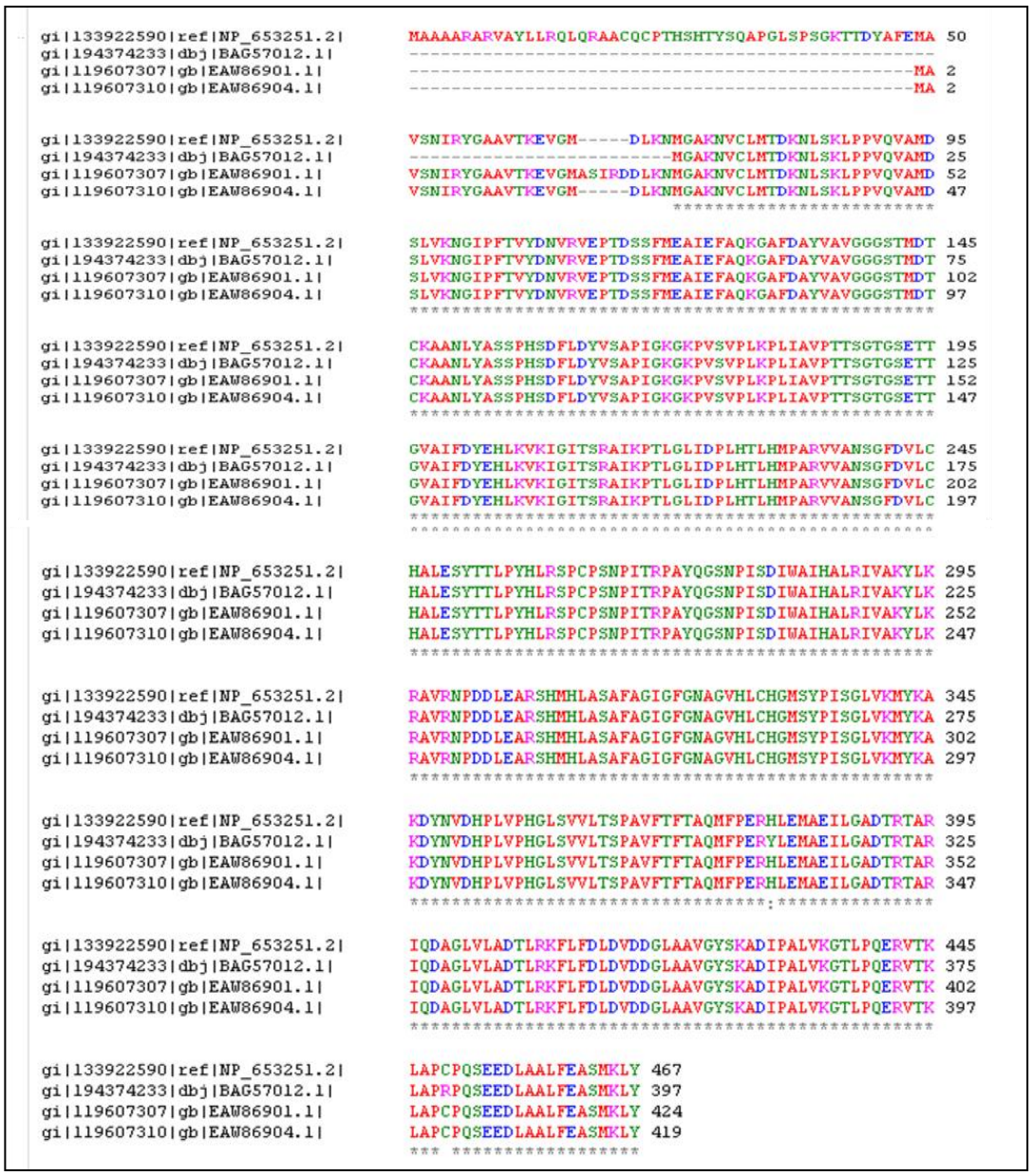

Figure 2.13: Sequence alignments of identified proteins. ClustalW2 multiple sequence alignments of match proteins stated in table 2.3

2.3.5 Refolding of the denatured HOT protein

As the HOT protein was denatured in order to be purified, the enzyme was not active and the protein needed to be refolded to regain activity. Four different methods were carried out in order to refold the denatured recombinant HOT protein. Three of these methods (dialysis, dilution and size exclusion chromatography) were performed after collecting the pure HOT fractions. The fourth method (on-column refolding) was carried out before HOT elution from the column.

2.3.5.1 Refolding by dialysis

When using dialysis, the purified fractions were dialyzed against a large volume of buffer containing 1 mM of DTT and 5M urea. DTT is a powerful reducing agent that prevents the formation of unnatural disulfide bonds between cysteine residues presented in the denatured protein, thus assists in protein refolding (Braakman *et al.*, 1992). Urea concentration in the buffer (5 M) was less than urea concentration in the sample (6 M) and was dropped gradually over a period of time to permit the movement of urea molecules from the high concentration to the low concentration through the dialysis tubing. However protein precipitation occurred once the urea concentration dropped below 1.5 M. As ADHFe1 is a NAD dependent and iron containing gene, 1 mM of NAD and/or ferrous ions were added to the refolding buffer in the assumption that they may play a role in protein refolding but did not prevent protein aggregation.

2.3.5.2 Refolding by dilution

Dilution was applied in order to prevent the aggregation of the recombinant protein observed when dialyzed; protein was diluted gradually at 4 °C in 20 mM Tris-Cl buffer pH 8 in the presence of 1 mM DTT and/or 1 mM of NAD and ferrous ions to diminish urea concentrations from 6 M to 0.5 M. Few hours were left for each step to allow proper refolding of the protein .The diluted protein was concentrated using Amicon Ultra concentration tubes (Millipore, USA).

2.3.5.3 On-column refolding

Another established refolding technique is on column protein refolding where the protein is refolded before eluting from the column. The method involves two subsequent gradients, a gradient of urea followed by a gradient of imidazole. The method was adapted from the manufacturer's application notes (GE Lifesciences, 1999)

β–Mercaptoethanol (another powerful reducing agent) was included in all buffers. The solubilised inclusion bodies were loaded on the column and washed at a low concentration (10 mM) of imidazole at pH of 7.5. Urea concentration was dropped gradually at pH 8 from 6 M to zero molar while maintaining imidazole concentrations at 10 mM. The HOT protein was washed with a urea-free buffer before performing an imidazole gradient from 10 mM to

250 mM at pH 8. The eluted fractions were analyzed by SDS-PAGE and protein concentrations were determined by Bio-Rad assay.

2.3.5.4 Refolding by size exclusion chromatography

Refolding by size exclusion chromatography was performed after obtaining the pure HOT protein fractions. The fractions were combined and 1.5 ml was passed through a Sephadex ™ G-25 column equilibrated with 20 mM Tris-Cl pH 9 and 1 mM DTT. The HOT protein was detected in the second collected elution.

2.3.6 Enzyme assays

To test whether the renatured HOT enzyme is active, enzyme assays were carried out on the refolded enzyme.

2.3.6.1 Coupled assay: SSADH

Testing the activity of HOT by coupling the enzyme to SSADH was reported previously (Kardon *et al.*, 2006), so in addition to the use of purified SSADH as a positive control for HOT purification, the enzyme was also used in the coupled assay. Figure 2.14 explains the principle of the coupled assay using SSADH. In the first reaction GHB is oxidized to SSA by HOT with the participation of α-ketoglutarate. In the second reaction SSADH oxidize SSA to succinate, and reduce NAD to NADH. The increase of absorbance at 340 nm due to NADH

formation is directly proportional to the amount of SSA in the reaction, and therefore to the activity of HOT in the first reaction.

For this purpose the activity of SSADH itself was tested using SSA as a substrate and NAD as a cofactor in 20 mM HEPES buffer pH 7.1 as described in material and methods. Assaying the activity of this enzyme required the addition of DTT to the reaction mixture to reduce disulfide bridges. The activity of the enzyme was directly proportional to the amount of NADH formed in the mixture which was monitored at 340 nm in a quartz cuvette.

Specific activities of purified fractions of SSADH were summarized in table 2.4. Fraction 28 was chosen for the subsequent measurement of HOT activity. It retained activity for approximately two weeks when stored at 4 °C.

The coupled assay was performed as described by (Kardon *et al.*, 2006) with the addition of DTT to restore SSADH activity. However, the assay gave a high background reading which was due to the presence of α-ketoglutarate. Elimination of DTT or reducing its concentration to 50 μM abolished SSADH activity. Therefore, determination of HOT activity by the coupled assay was unfeasible

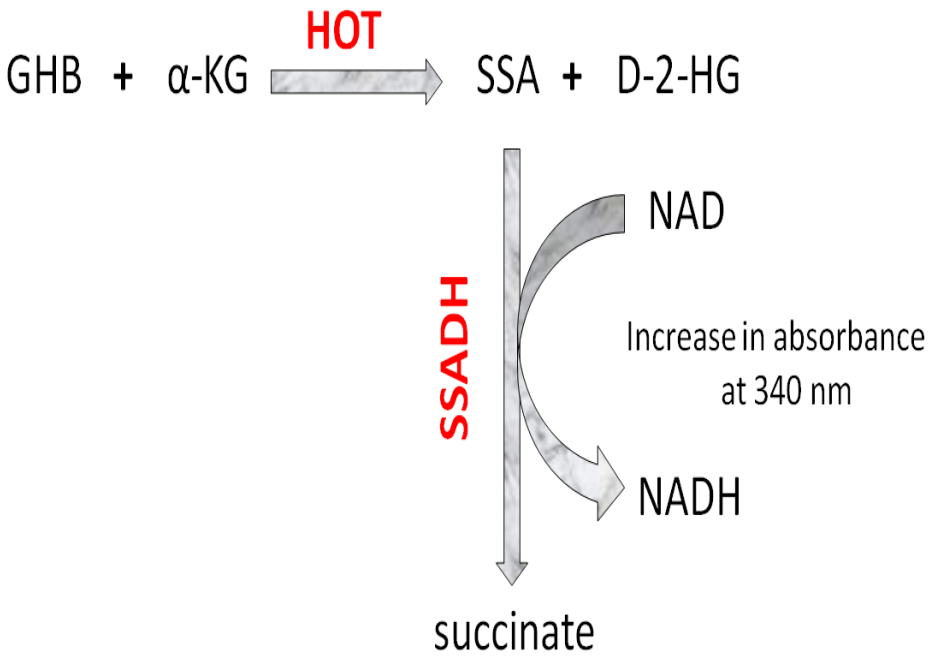

Figure 2.14 Principle of coupled assay using SSADH. GHB is oxidized to SSA by HOT and SSA is further oxidized to succinate by SSADH. SSADH uses NAD as a cofactor and the oxidation of SSA to succinate is parallel with the reduction of NAD to NADH. The formation of NADH is monitored at 340 nm.

Fraction	Specific activity (nmol/min/mg of protein)
27	440 ± 19
28	1553± 152
29	1237± 6
30	536. ± 22

Table 2.4: Specific activity of purified SSADH fractions. Activities of purified SSADH fractions (27-30) were assayed in 20 mM HEPES buffer pH7.1, 1 mM DTT, 50 μM SSA, 0.5 mM NAD, and 7 μg of SSADH. Protein amount was determined by Bio-Rad assay. Specific activities are expressed in nmol/min/mg of protein. Results are expressed as mean ± SEM of assays performed in triplicate.

2.3.6.2 Transhydrogenase activity

This is a discontinuous assay based on the measurement of SSA produced from the reaction between GHB and α-ketoglutarate. SSA is detected by forming an azine with 3-methyl-2-benzothiazolinone-2-hydrazone (MBTH), and then oxidizing the azine by ferric ions to form a coloured product that has absorbance at 660 nm.

In order to test the linearity and the sensitivity of SSA measurement, stock SSA standards were prepared in distilled water at 25, 50, 100, 200 and 400 nmoles/ml. 100 µl of 0.1 M HEPES buffer pH7.5 was used as blank . The assay was carried out on 100 µl of each solution and the results were expressed in amount (nmoles) after being corrected for 100 µl. The assay demonstrated sensitivity as the limit of detection (LOD) was 2.5 nmoles. The assay was linear over the range of the measured concentrations and the correlation of coefficient (R2) was greater than 0.99 (0.9996) (Figure 2.15).

The reaction mixture to determine transhydrogenase activity contained equal concentrations (50 µM) of GHB and α-ketoglutarate, and 10 µg of the refolded HOT enzyme in 80 mM HEPES buffer pH 7.5. The reaction was performed at 37 °C for 30 minutes and was stopped by adding 0.33 ml of TCA 20%. After removing proteins by centrifuging, the amount of SSA in 100 µl of the supernatant was analyzed using the colorimetric assay above. For each analyzed sample, a blank was prepared in the same way with the addition of refolding buffer instead of the enzyme. The reading was subtracted from the background reading and the amount of SSA produced in 30 minutes by the transhydrogenase assay was calculated from the standard curve.

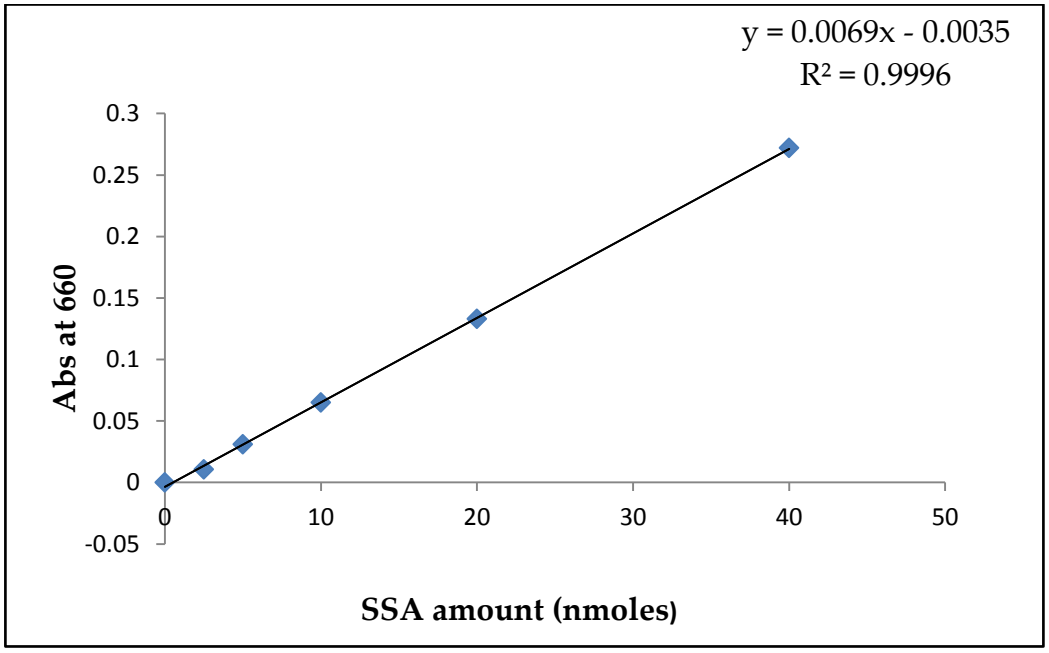

Figure 2.15: Standard curve of succinic semialdehyde amount measured using MBTH. Standard solutions of 25, 50, 100, 200 and 400 µM of SSA were prepared in distilled water, and the amount of SSA in 100 µl was assayed by the MBTH test as described in material and methods. Absorbance at 660 nm was plotted against amount of SSA in nmoles

The highest activity observed (439 nmol/min/mg) was for the protein refolded by gel filtration chromatography (Table 2.5). This indicates that the protein has refolded correctly and that active enzyme has successfully been assayed. No measurable activity was observed for the refolded protein by dialysis or by dilution.

Refolding method	Specific activity (nmol/min/mg)
Gel filtration	439.81 ± 19.64
On column refolding	103.83
Dialysis	n/ma
Dilution	n/ma

Table 2.5: Specific activity of HOT after refolding. Recombinant HOT protein was purified by nickel affinity chromatography under denatured conditions, and was refolded by four different methods. Transhydrogenase activity for the refolded protein was assayed by the MBTH test. Results were expressed as nmol/min/mg of protein, n/ma: no measurable activity.

2.3.6.3 GHB dehydrogenase activity

NAD-dependent dehydrogenase activity for the HOT enzyme refolded by gel filtration was measured using 0.2 mM of NAD as a cofactor and 10 μM, 50 μM or 1 mM of GHB as substrate in 100 mM phosphate buffer pH 8 or in glycine-NaOH pH 9 by following the increase of absorbance at 340 nm. The reaction was performed at 37 °C for 5 minutes in the presence and absence of ferrous ions in order to determine their role. No measurable activity was observed for all the examined reactions. It was clear that HOT does not use NAD directly to oxidize GHB to SSA. Also ferrous ions are not involved in GHB oxidation.

2.3.6.4 Alcohol dehydrogenase

Other alcohols were tested at 1 mM final concentration for general alcohol dehydrogenase activity; ethanol and propanol were prepared in distilled water and butanol, octanol, benzyl alcohol and methylbutanol were prepared in DMSO. Only the reaction using 1 mM octanol produced measurable activity (407± 32 nmoles/min/mg). The K_m for octanol was 22 mM.

2.4 Discussion

2.4.1 Summary

The work in this chapter describes the expression, purification and refolding of hydroxyacid oxoacid transhydrogenase (HOT) as a recombinant protein. HOT was expressed and purified under denatured conditions and different refolding methods were applied. Size exclusion chromatography and on column refolding gave the best activity. HOT works as a transhydrogenase enzyme using equal amounts of GHB and α-ketoglutarate, and works as alcohol dehydrogenase with octanol. It does not appear to possess NAD(P)-dependent GHB dehydrogenase activity.

2.4.2 Protein expression and purification

In this chapter, recombinant HOT protein was expressed under the control of the T7 promoter and purified in *E. coli* to provide sufficient amounts to measure its activity as a transhydrogenase enzyme, and to determine whether it works as a typical alcohol dehydrogenase, given that the gene belongs to NAD-dependent alcohol dehydrogenase superfamily. Other questions regarding the role of iron in its function, and if other cofactors are involved can now be investigated.

The HOT gene was successfully expressed in large quantities. However, purifying the enzyme in the native state was not possible since the expressed HOT was located in the insoluble portion of the cell, meaning that it cannot be

purified directly, and has no biological activity. It is a general problem observed when expressing eukaryotic proteins in *E. coli*, where the bacterial cell accumulates a highly expressed heterogeneous protein in insoluble particles called inclusion bodies (Wang, 2009). The formation of inclusion bodies in *E. coli* is not only dependent on the level of expression (which can be reduced by controlling the expressing temperature, length of induction and inducer levels) (Wang and Morris, 2007) but also as a way of protecting the bacterial cell from the heterogeneous protein. Inclusion bodies consist mainly of the recombinant protein so they are advantageous in terms of obtaining a vast amount of pure protein in a relatively easy isolation procedure (Park *et al.*, 2009). However, due to protein misfolding and aggregating, and the need to subsequently utilize a strong detergent such as urea in order to dissolve and isolate them, they are not suitable for kinetics studies. The tertiary structure of the protein may be achieved by refolding to obtain a native protein with an active site.

2.4.3 Reasons for insolubility

As the HOT protein contains six cysteine residues, formation of unnatural disulfide bonds between them might be the reason for protein misfolding. Reducing agents such as DTT and β–mercaptoethanol need to be included in the refolding buffer to break such formation. The importance of reducing state is exemplified when purifying another enzyme SSADH. Under native conditions, the enzyme displayed no activity in the absence of DTT. SSADH contains 15 cysteines residues in its protein sequence (NP_001071).

Mitochondrial proteins such as HOT have additional sequence on the N terminus of the protein called mitochondrial targeting sequence (MTS) that direct newly synthesized proteins to the mitochondria. The MTS is cleaved afterwards and has no role in enzyme activity. When cloning an eukaryote protein in *E. coli*, it is advisable to exclude the MTS, because it has been demonstrated that MTS in eukaryote proteins bear some similarity with integral membrane bacterial proteins (Saier *et al.*, 1988) so it may trigger the expressed protein to be membrane–bound in *E. coli*, and therefore insoluble. The SSADH clone used in this study lacks the MTS completely, while the HOT clone contains 8 amino acids from the MTS. Although this short sequence cannot work as a guiding signal, it is possible that it may influence the solubility of the protein.

2.4.4 Protein refolding

Different strategies have been reported in the literature towards protein refolding including the most traditionally used techniques dialysis (Katoh *et al.*, 2005, Kohyama *et al.*) and dilution (Remmert *et al.*, 2000) or a combination of both (McConnell and Pachon, Zhuo et al., 2005) to eliminate the detergent and permit the formation of the native protein. Although they are relatively simple to apply, they are time-consuming and require a large volume of buffers to reach the folding point. Alternative methods include size exclusion chromatography and on-column refolding (Batas and Chaudhuri, 1996, Werner *et al.*, 1994, Fursova *et al.*, 2009, Sun *et al.*, Wang *et al.*, 2008a) . Both are time-saving and more effective comparing to dilution and dialysis. In this study,

dialysis and dilution were not effective in restoring enzyme activity while size exclusion chromatography produced the highest activity. On column refolding was the quickest method to perform and to obtain urea-free enzyme.

2.4.5 Enzyme activity

Different methods were reported for assaying HOT transhydrogenase activity either in a continuous way by coupling the transhydrogenase reaction to another enzymatic reaction that uses SSA as substrate and can be monitored spectrophotometrically; or by discontinuous assays where the reaction is allowed to run for a certain period of time, then the reaction is stopped and the amount of the product (SSA) during this time is measured.

The continuous assay was described by (Kardon *et al.*, 2006) where HOT was coupled to NAD-dependent SSADH and the formation of NADH from the coupled reaction was recorded at 340 nm. As highly active SSADH was purified as a recombinant protein, attempts were made to couple HOT to SSADH following the published method. The only addition to the assay was DTT as it was necessary to restore recombinant SSADH activity (Murphy *et al.*, 2003). However, the assay gave a high background absorbance which was due to the presence of ketoglutarate. Eliminating DTT from the assay or reducing its concentration to 50 μM abolished SSADH activity which compromised the coupled assay. In coupled reactions, the second enzyme should have a high activity to turn over the entire formed product from the first reaction. The high

background reading and the limited time for initial rate activity complicated the measuring of HOT activity.

Discontinuous assays were reported by (Kaufman *et al.*, 1988a, Struys *et al.*, 2005b) where the reaction was incubated at 37 °C for a period of time then the reaction was stopped and either the formation of SSA or the consumption of GHB was measured. Kaufman uses GABAse enzyme (contain GABA transaminase and crude SSADH) to measure SSA, while Struys measured GHB and 2 hydroxyglutarate by GC/MS. However, chromatographic methods require longer preparation time and a level of experience, compared to colorimetric assays. In this study a colorimetric method was adapted and developed to measure SSA. The linearity and the sensitivity of the assay were demonstrated using a standard SSA solution.

In this study, the measured specific activity for purified recombinant HOT was 440 nmol/min/mg. Previously, the activity was measured for partially purified enzyme from rat mitochondria to be 38 nmol/min/g of tissue in kidney and 46 nmol/min/g of tissue in liver (Kaufman *et al.*, 1988a). In (Struys *et al.*, 2005b), the specific activity in homogenates from cultured fibroblast was 18 pmol/hour/mg, and in (Kardon *et al.*, 2006) specific activity was 120 and 90 nmol/min/g of tissue in liver and kidney respectively. From the above indications the specific activity for recombinant HOT was expected to be higher. If the purification had not been performed under denaturing conditions, perhaps higher activity would have been observed as some activity may have lost by the denaturing and refolding

process. HOT specific activities that were measured in different study are compared in table 2.6.

Dehydrogenase activity for HOT was measured to determine whether HOT is indeed an alcohol dehydrogenase enzyme as revealed by its gene classification. Surprisingly, only octanol was a substrate for HOT. Octanol is primarily a substrate for octanol dehydrogenase (EC 1.1.1.73), a NAD-dependent enzyme from the long chain alcohol dehydrogenase family which was mainly found in *Drosophila* (Danielsson *et al.*, 1994).

Sample	Specific activity	unit	Reference
Recombinant HOT	440	nmol/min/mg of protein	This study
Rat kidney mitochondria	38	nmol/min/g of tissue	(Kaufman *et al.*, 1988a)
Rat liver mitochondria	46	nmol/min/g of tissue	(Kaufman *et al.*, 1988a)
cultured fibroblast	0.0003	nmol/min/mg of protein	(Struys *et al.*, 2005b)
Rat liver	120	nmol/min/g of tissue	(Kardon *et al.*, 2006)
Rat kidney	90	nmol/min/g of tissue	(Kardon *et al.*, 2006)

Table 2.6: Comparison between specific activity of HOT measured in this study and reported specific activities reported previously. Specific activities for HOT enzyme from different tissues and locations are summarized. Activities are expressed in different units, and their references are included in the last column.

2.5 Conclusions

In conclusion, this study presents the first report on producing and purifying HOT as a recombinant protein in *E. coli*. The ability to produce purified HOT in large quantities is necessary to study the enzyme function and structure, and to synthesize a specific antibody for this enzyme.

A time-saving refolding method has been developed in order to test enzyme activity. A colorimetric assay to measure SSA has been applied to determine HOT transhydrogenase activity.

To date, this is the first attempt to link the classification of the ADHFe1 gene with enzyme activity by testing different alcohols as substrates for this enzyme. For the first time, octanol was demonstrated to be a substrate for this enzyme

2.6 Future work:

The purification of HOT in a large amount will allow the development of a specific antibody for this enzyme, and this in turn will help to understand the role of this enzyme *in vitro* and *in vivo* by using different approaches such as gene silencing to determine the degree of HOT involvement in GHB metabolism. During the course of this work, Attempts were made to silence HOT in cell lines but the measurement of protein levels after knocking down the gene was not possible due to the absence of a specific antibody for HOT.

Characterization of HOT and determining its structure is also possible after producing milligrams amount of the protein and eliminating the urea by the refolded methods described in this work. Concerning the insolubility of recombinant HOT, another expression vector could be prepared by removing totally the mitochondrial targeting sequence of the gene, or by switching to an eukaryotic expression vectors, where this sequence will lead to the expressed protein accumulating in the mitochondria of the cells and the mitochondria could be isolated by subcellular fractionation.

To date, this is the first attempt to link the classification of the ADHFe1 gene with enzyme activity by testing different alcohols as a substrate for this enzyme. As octanol is a substrate for HOT, it is of interest to test whether octanol affect GHB metabolism by competing with GHB. The possible interaction of octanol with GABAergic pathway is important as well, as a study demonstrated that octanol was a weak agonist of $GABA_A$ receptor. Octanol displayed concentration-dependent dual actions on GABA induced current in the presence of different concentrations of GABA in HEK293 cells (Kurata *et al.*, 1999) . Octanol also interacts with neurotransmitter pathways (Zuo *et al.*, 2004) by inhibiting neuronal nicotinic acetylcholine receptors (AChRs). Testing whether the HOT enzyme has a role in these pathways in the presence of octanol may highlight a new role for this enzyme.

CHAPTER THREE:

THE ROLE OF AKR1A1 IN THE METABOLISM OF GHB IN 1321N1 AND HEPG2 CELLS

3 The Role of AKR1A1 in the metabolism of GHB in 1321N1 and HepG2 cells

3.1 Introduction

Aldehyde reductase (AKR1A1), one of the founder members of the aldo-keto reductase superfamily, has been the focus of many studies and reviews, given its wide distribution in all tissues and organs, and the broad range of substrate activity (Barski *et al.*, 2008). This has included its proposed contribution to GABA metabolism via SSA reduction and GHB oxidation. It had been assumed that AKR1A1 is identical to an enzyme named the high K_m aldehyde reductase which was purified and characterized before adapting the new nomenclature for the aldo-keto reductases super family in the 1990s (Cromlish and Flynn, 1985, Kaufman *et al.*, 1979, Cromlish *et al.*, 1985). SSA was shown to be a substrate for this enzyme which indicated that it may be involved in GHB synthesis. However, another *in vitro* study provided evidence that the enzyme acts as GHB dehydrogenase, converting GHB to GABA in rat brain under certain circumstances (Vayer *et al.*, 1985b, Vayer *et al.*, 1985a). To investigate the actual role of AKR1A1 in GHB metabolism and whether it works as a dehydrogenase or as a reductase, RNAi technology has been employed in this chapter.

The discovery of RNA interference (Elbashir *et al.*, 2001, Caplen *et al.*, 2001) was a breakthrough in biological research and gene function studies. It is a powerful tool that suppresses the mRNA levels of a specific gene and therefore its translation to protein. The effects resulting from stopping protein synthesis are observed to determine its function.

To silence a gene, a specific double stranded RNA molecule is designed. Upon entering the cells, this is cut by an enzyme named Dicer to short sequences named small interfering RNA (siRNA) in the cytosol of the cell. The two strands disassociate and the antisense strand incorporates with a ribonucleoprotein complex named RNA-Induced Silencing Complex (RISC) and directs the cleavage of a complementary sequence of mRNA (Figure 3.1).

Introducing a synthesized siRNA into the cells requires the usage of a transfection reagent (vehicle). However, this process can be detrimental to some cell types as the reagent weakens the cells during the process of the transfection. Other methods include the use of plasmid vectors to introduce DNA encoding siRNA into the cells.

In this *in vitro* functional study, two models representing the liver and the central nervous system were chosen. AKR1A1 is highly expressed in liver (Barski *et al.*, 1999) , a tissue that also has high endogenous GHB (Nelson *et al.*, 1981), and which is the main organ in the body responsible for drug metabolism. HepG2 cells were chosen to represent this organ. To investigate the CNS, astrocytes were chosen as they are the most widespread type of glial cells

in the brain and spinal cord. They are star-shaped cells that are involved in synaptic functions by evoking Ca^{2+} in response to neurotransmitters and by producing gliotransmitters and neuroactive substances such as ATP and glutamate (Newman, 2003). There is evidence that astrocytes are able to synthesize GABA, either from glutamate by GAD67, or from putrescine (Angulo *et al.*, 2008), and have been shown to possess both GABAergic and GABAceptive properties (Lee *et al.*, 2011) as they have GABA receptors and they are able to uptake GABA (Tardy *et al.*, 1979). The captured GABA is metabolized in the astrocytes to SSA and then to GHB. Therefore, astrocytes play important role in endogenous GHB metabolism. The astrocytoma cell line 1321N1 has therefore chosen to represent this cell type.

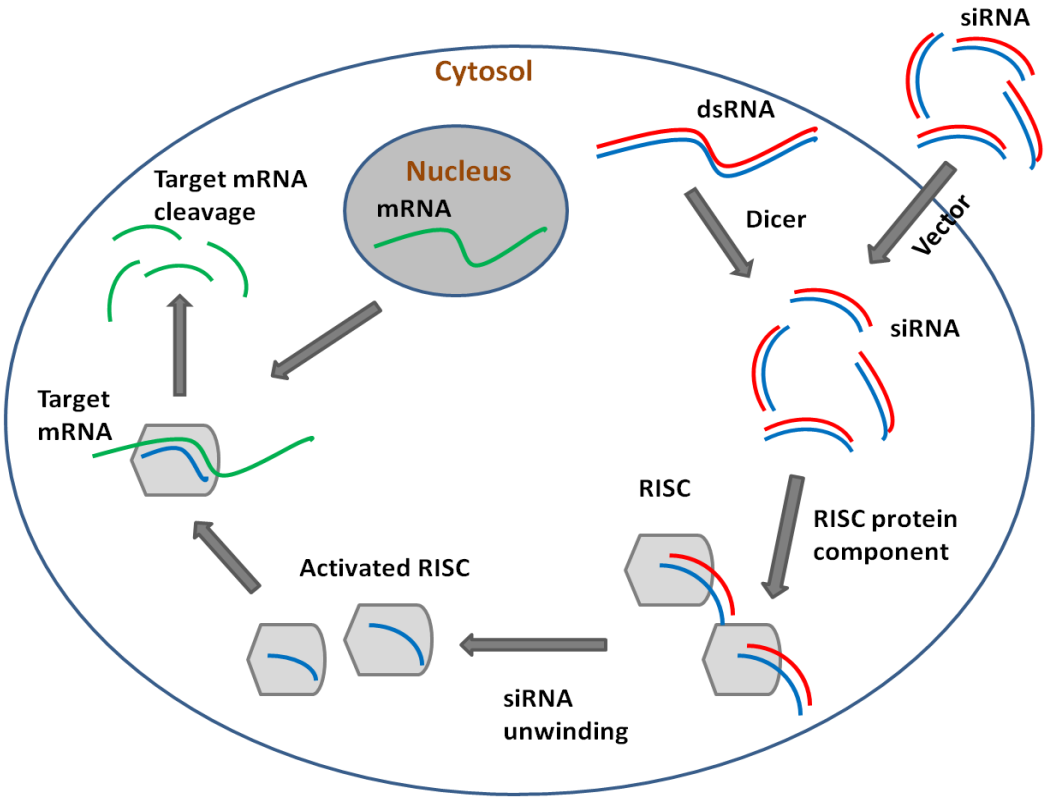

Figure 3.1:RNA interference pathway inside in the cell. Small interfering RNA (siRNA) is produced from double strand RNA (dsRNA) by dicer enzyme, or synthesized and introduced into the cell using a vector. It goes through many steps leading to the degradation of the target gene's mRNA.

3.2 Aim of the chapter

The aim of this chapter is to determine the role of AKR1A1 in the metabolism of GHB in two models representing the central nervous system and liver by:

- Knocking down the expression of AKR1A1 in 1321N1 and HepG2 cells.
- Examining the effect of silencing AKR1A1 on reductase and dehydrogenase activities in these cells.
- Investigating the effect of silencing AKR1A1 on intracellular and extracellular endogenous GHB levels.
- Determining whether AKR1A1 is involved in exogenous GHB metabolism as a reductase or a dehydrogenase enzyme.

3.3 Materials and methods

3.3.1 Materials

3.3.1.1 Human cell lines

Human 1321N1 astrocytoma cells were a gift from Dr Eve Lutz. They were obtained from human astrocytes in the brain (Ponten and Macintyre, 1968, Macintyre *et al.*, 1972).

Human hepatoma HepG2 cells (Knowles *et al.*, 1980) were obtained from America Type Culture Collection (ATCC) .

3.3.1.2 Cell culture media and reagents

The following cell culture media and reagents were obtained from Sigma Aldrich, UK:

- Dulbecco's modified Eagle's medium (DMEM)
- Phosphate buffer saline (PBS)
- Trypsin-EDTA Solution (1x)
- Penicillin-Streptomycin (10,000 units penicillin; 10 mg streptomycin/ml 0.9% NaCl) Solution
- Sodium Pyruvate (11.0 mg/ml sodium pyruvate in tissue culture water)
- Non-Essential Amino Acid (100x) Solution

Fetal bovine serum (FBS) was purchased from Sigma Aldrich, Germany.

3.3.1.3 Cell culture apparatus

- The tissue culture hood was supplied by ICN Gelaire (England).
- The incubator was manufactured by Heraeus (Germany).
- Carbon dioxide (CO2) cylinder was supplied by BOC.
- Bright-line haemocytometer was obtained from Sigma-Aldrich (Germany).
- Olympus CK40 inverted Microscope was from Olympus (Japan).

3.3.1.4 Cell culture plastic wares

All plastic were supplied by Fisher Scientific (UK): Easy Flask 75 cm^2 Vent/Close tissue culture flasks, 100 mm dishes and 6well plates wares used in this experiment.

Cell scrapers were obtained from BD bioscience (UK).

All plastic wares were free from DNAse and RNAse activity.

3.3.1.5 Chemicals

All chemicals were obtained from Fisher Scientific, UK except for:

Deuterated GHB was purchased from LGC standards, Teddington, UK.

GHB, SSA, cofactors (NADPH, NADP, and NAD), D-glucuronate, p-nitrobenzaldehyde and Diethylpyrocarbonate (DEPC) were purchased from Sigma Aldrich, UK.

Bio-Rad Protein Assay Reagents was supplied by Bio-Rad Laboratories (Hertfordshire, UK).

3.3.1.6 Oligonucleotide primers

The oligonucleotides were synthesized by Eurofins MWG operon (UK) and are listed in table 3.1

3.3.1.7 Antibodies

The antibodies use in this study are listed in table 3.2

3.3.1.8 RNAi

The following materials were obtained from Invitrogen, Paisley, UK

- The siRNA sequence for AKR1A1 (s20198) were obtained from the silencer select library.

  Sense (5′ > 3′) GCUGUUAAGUAUGCCCUUATT

  Antisense (5′ > 3′) UAAGGGCAUACUUAACAGCTG
- Opti-MEM reduced serum transfection media
- Lipofectamine RNAiMAX transfection reagent.

Scrambled oligonucleotide sequence was provided by Santa Cruz Biotechnology Inc., Santa Cruz, California.

Oligonucleotide	Sequence	Annealing Temperature
AKR1A1-forward AKR1A1-reverse	5′-TGC TGC TAT CTA CGG CAA TG-3′ 5′-TGC ATC AGG TAC AGG TCC AG-3′	56 °C
AKR7A2- forward AKR7A2- reverse	5′-AAC TGG ACA CGG CCT TCA TG-3′ 5′-CAG GAT CCA GCC ATT GCT CT-3′	50 °C
GAPDH –forward GAPDH –reverse	5′-GGA GTC AAC GGA TTT GGT-3′ 5′-GTG ATG GGA TTT CCA TTG-3′	46 °C

Table 3.1: Oligonucleotide Primers

Antibody	Source	Dilution
AKR1A1	A gift from John Hayes, University of Dundee.	1:3000
AKR7A2	Developed in the laboratory (Li *et al*., 2006)	1:3000
GAPDH	Santa Cruz Biotechnology Inc., Santa Cruz, California	1:3000
Goat anti-rabbit IgG-HRP secondary Ab	bio-rad, UK	1:3000

Table 3.2: Antibodies for western blot

3.3.2 Methods

3.3.2.1 Cell culture

1321N1 cells were grown in Dulbecco's Modified Eagle Medium supplemented with 10% FBS and 1 % penicillin/ streptomycin (10,000 units penicillin; 10 mg streptomycin/ml 0.9% NaCl) solution. The cells were maintained at 37 °C incubator with 5% CO2. The media was changed every three days and the cells were passaged every 5-6 days.

HepG2 cells (HB-8065) were cultured in Dulbecco's Modified Eagle Medium enhanced with 10% FBS , 1% MEM nonessential amino acid solution (100x), 1% sodium pyruvate (11.0mg/ml sodium pyruvate in tissue culture sterile water) solution and 1% penicillin-streptomycin solution (10,000 units penicillin; 10 mg streptomycin/ml 0.9% NaCl). The cells were maintained at 37 °C in a humidified atmosphere of 5% CO2. The media were changed every three days and the cells were passaged every 5-6 days.

3.3.2.2 Cell counting

The media were aspirated and the cells were washed with 1X PBS. To detach the adherent cells, 2 ml of 1 x trypsin-EDTA were added to the flask and incubated for 2-3 minutes at 37 °C. The flask was gently tapped to lift the cells and fresh media were added to the flask to dilute the trypsin. The cells were removed to a sterile 15 ml tube and centrifuged for 5 minutes at 1000 rpm. The supernatant

was discarded and the pellet was resuspended thoroughly in 1 ml of fresh media. The cells were diluted 10 times by adding 900 µl of fresh media to a 100 µl of the resuspended cells. The number of cells was determined using a haemocytometer (sigma) by counting the four corner squares and calculating the average. The area of each square is $1mm^2$ and the depth is 0.1 mm so the number counted is the number of cells × 10^4 per ml. The final number of the cells was determined using the following equation

$$\text{Number of cells} = \text{Average of cells count} \times 10^4 \times \text{dilution factor}$$

3.3.2.3 Knocking down the expression of AKR1A1 by siRNA

1321N1 cells

1321N1 cells were cultured in 6 well plates (2.5×10^5/well) in 2.5 ml of antibiotic -free media, and left for 24 hours to reach a confluency of 30-50%.

Transfection was performed in RNAse–free environment.

6 µl of 10 µM siRNA (s20198) (final concentration 20 nM) was diluted in 250 µl of Opti-MEM media, while 4 µl of Lipofectamine RNAiMAX was diluted separately in 250 µl of Opti-MEM media. The two dilutions were combined, mixed gently and left at room temperature for 20 minutes. The transfection mixture was added drop-wise to the cells raising the total volume in the well to 3 ml.

500 µl of Opti-MEM media was added to the control wells and 500 µl of scrambled siRNA-Lipofectamine complex prepared in the same way as the silencing complex was added to the scrambled wells. The plate were rocked back and forth and returned to the 37 °C incubator/ 5% CO2. The media was changed after 24 hours by whole growth media and the cells were further left for 48 hours before accessing the knocking down efficiency at 72 hours.

For enzyme assay and determination of GHB endogenous levels, cells were seeded in 100 mm dishes (10^6) in 7.5 ml antibiotic free media and the total volume in the dish was 9 ml. siRNA and Lipofectamine were used at the same final concentration after adjusting the final volume to 9 ml.

HepG2 cells

As HepG2 cells are known to be a (difficult to transfect) cell line, a reverse protocol was applied where the seeding and transfection were carried in the same day. Transfection mixture was prepared as mentioned in 1321N1 cells (also final concentration 20 nM) and placed in the wells. The cells were diluted in anti biotic–free media and added to the well (5×10^5/well) to a total volume of 3 ml or in the dish to a total volume of 9 ml. The procedure was followed as mentioned above

3.3.2.4 RNA isolation

Total RNA was isolated from the cells using SV total RNA isolation system From Promega, USA (Cat.No: Z3100) according to the manufacturer's instructions. The protocol used spin chromatography and ethanol precipitation and it also includes DNAse treatment to reduce genomic DNA contamination (Chirgwin *et al.*, 1979, Otto, 1998). Samples were stored at -80 °C.

3.3.2.5 Determination of RNA yield and integrity

The yield of RNA was determined spectrophotometrically at 260nm after diluting RNA sample 1:100 by RNAse-free water. OD260 is 1 for 40μg/ml of RNA. The ratio of 260/280 nm was used as an indicator for RNA purity.

The integrity of RNA was determined by agarose gel electrophoresis as described below.

3.3.2.6 Agarose gel electrophoresis

The following buffers were prepared

50 x TAE buffer: 242 g Tris base; 57.1 ml glacial acetic acid, 100 ml of 0.5 M EDTA pH 8.0, made up to 1 litre by H_2O

1 x TAE buffer was made by diluting 20 ml of 50 x TAE buffer to 1 L by distilled water.

1% Agarose gel was prepared by melting 0.5 g of agarose (Flowgen, UK) in 50 ml of 1x TAE buffer in microwave and left to cool to 50 °C before adding 3 µl of 10 mg/ml ethidium bromide. The agarose was poured into a gel caster with combs inserted and left for 20 minutes for complete settlement of the gel. 6 µl of RNA or DNA samples was mixed with 1 µl of 6 x DNA loading dye (Promega) and loaded into the gel. 1kb DNA ladder (Promega) was utilised to determine the size of the band and 5. The gel was run in 1x TAE buffer at 100 mA for 30 minutes and the bands were viewed under ultraviolet light.

3.3.2.7 First-strand cDNA Synthesis

The following materials were purchased from Promega, USA:

- M-MLV Reverse Transcriptase (200 µg/µl)
- M-MLV Reverse Transcriptase Buffer (5x)
- PCR Nucleotide Mix (dNTP mix) (10 mM)
- Random Primers (500 µg/ml)

10 µl of RNA (around 0.5 µg) was mixed with 1 µl of random primers. The mixture was heated for 5 minutes in 70 °C water bath then cooled directly on ice for 5 minutes and the following components were added respectively;

5 µl of 5 x first strand buffer, 1.25 µl of 10 mM dNTP, 1 µl of reverse transcriptase and RNAse –free water to 25 µl. Synthesis of first strand cDNA was carried out in a PCR machine where the mixture was incubated at 42 °C for

50 minutes then it was further incubated at 70 °C for 15 minutes. Samples were diluted to 100 µl by RNAse -free water and stored at -20 °C.

3.3.2.8 Polymerase chain reaction (PCR)

Standard PCR reaction was carried out using a Thermo Hybaid PCR Express Thermal Cycler. The gene was amplified using AKR1A1 specific primers listed in table 3.1 and the cDNA prepared from 1321N1 and HepG2 cells as template. Reagents were purchased from Promega.

PCR reaction was set up in a total volume of 50 µl per sample with 10 µl of 5× Go *taq* reaction buffer, 1 µl of 10 mM PCR nucleotide mix (dNTPs), 1 µl of forward primer (10 µM), 1 µl of reverse primer (10 µM) , 0.5 µl of Go *taq* DNA polymerase (5U/µl) , 2 µl of cDNA and 34.5 µl of PCR grade water . Go *taq* reaction buffer contains 7.5 mM $MgCl_2$ so the final concentration of $MgCl_2$ in the reaction was 1.5 mM. Final concentration of primers was 0.2 µM.

PCR conditions were as follow:

Initial denaturation at 94 °C for 2 minutes	
30 cycles of	Denaturation at 94 °C for 30 seconds Annealing at 56 °C for 30 seconds Extension at 72 °C for 60 seconds
Final extension at 72 °C for 10 minutes	

PCR product was analyzed by agarose gel electrophoresis and the expected product size was 201 base pairs (bp).

3.3.2.9 Quantitative real time polymerase chain reaction (RT-PCR)

The levels of RNA expression were determined using LightCycler FastStart DNA Master SYBR Green I (Roche Applied Science, Germany). The PCR master mix contained per sample:

Perfecta SYBR green fastmix (Quanta)	10 μl
Forward primer 10 μM	1 μl
Reverse primer 10 μM	1 μl
PCR grade water	3 μl

The master mix volume was scaled up to the number of samples and gently mixed by pipetting. 15 μl was pipetted into a LightCycler ®Capillary and 5 μl of cDNA was added to make the total reaction volume 20 μl. The capillaries were sealed, spun down in LC Carousel Centrifuge and placed in the LightCycler®Sample Carousel.

1- The first stage was denaturing the samples at 95 °C for 30 seconds.

2- The second stage was amplifying the gene of interest for 45 cycles by

- Denaturation at 95 °C,

- Annealing for 5 seconds at the annealing temperature mentioned in table (3.1)
- Extension at 72 °C. Extension time was calculated by dividing the amplicon size by 25.

Acquisition was performed at the end of each cycle in the single mode.

3- The third stage was the melting curve where samples were heated at 95°C, cooled at 65°C for 15 seconds and melted at 95 °C with continuous acquisition for 1 cycle.

4- The last stage was cooling the samples at 40 °C for 30 seconds.

3.3.2.10 Relative quantification of mRNA levels

The comparative C_T method ($\Delta\Delta C_T$) (Winer *et al.*, 1999, Livak and Schmittgen, 2001) was used to quantify the level of target gene (AKR1A1) by normalizing to the levels of a house –keeping gene (GAPDH) and then measuring the fold change in gene expression in controls and knocking down samples. C_T is the cycle threshold and it is defined as the number of cycles required for a constant level of fluorescence to go beyond the threshold. The level of fluorescence was 1 in all measurements. The method was described by Applied Biosystems (UK),2003 and it applies the following equations:

The target gene was normalized against the house keeping gene

$\Delta C_T = C_{T\ target} - C_{T\ reference}$

The knock down sample was compared with calibrator sample

$\Delta\Delta C_T = \Delta C_{T\ test\ sample} - \Delta C_{T\ calibrator\ sample}$

The fold change in gene expression was determined by

$2^{-\Delta\Delta CT}$

3.3.2.11 Western blot

Cells from 6 well plates were washed with PBS and scraped in 100 µl of 2 X lysis buffer (3.13 ml of 1 M Tris-Cl (pH 6.8); 2 g SDS; 9 ml glycerol; 5 ml mercaptoethanol). The samples were boiled at 100 °C for 5 minutes then centrifuged at 13000 for 1 minute. Protein levels were determined by Bio-Rad assay (section 2.2.2.9).

2 µl of 0.1% of bromophenol blue was added to each sample before running the samples on SDS-PAGE and transferring the proteins to a nitrocellulose membrane. Detailed protocol and buffers' compositions were mentioned in chapter 2 (refer to sections 2.2.2.8)

Image J software (www.imagejdev.org)was used to quantify the intensities of the bands.

3.3.2.12 Preparation of cell extract for enzyme assay

A freeze-thaw protocol was used to prepare cell extract in order to keep enzyme activity. The cells in 100 mm dishes were washed with PBS and harvested by centrifuging .The cell pellet was resuspended in 150 µl of 250 mM tris buffer, pH 7.5. The resuspended cells were frozen at - 80 °C for 5 minutes and then directly transferred to 37 °C for 5 minutes. The process was repeated 3 times. After that, the cells were centrifuged at 10000 rpm for 5 minutes and the supernatant retained and store at – 80 °C until use.

3.3.2.13 Enzyme assays

All enzyme assays were carried out using Nanodrop 2000 UV-Vis Spectrophotometer from Thermo scientific (Leicestershire, UK). The change of absorbance at 340 nm was measured at 37 °C in a Quartz cuvette from VWR International (UK) in a 1 cm light path. Extinction coefficient for NADPH is 6.22 mM^{-1} cm^{-1} at 340 nm. Amount of protein was calculated as described in chapter 2 (section 2.2.2.8). Results were expressed as nmoles per minute per mg of protein.

3.3.2.13.1 Aldehyde reductase activity

Aldehyde reductase activity was determined by monitoring the decrease of absorbance of NADPH at 340 nm. Assays were performed in a reaction volume of 1 ml at 37 °C and mixture contained 100 mM phosphate buffer pH 6.6 and 50 μM of NADPH. Substrates used were 1 mM of p-nitrobenzaldehyde, 10 μM or 1 mM of SSA, and 1mM or 10 mM of D-glucuronate. The reaction was started by the addition of cell extract and monitored for 5 minutes at 20 seconds interval.

3.3.2.13.2 GHB dehydrogenase assay

GHB dehydrogenase activity was measured at 37 °C by monitoring the increase of absorbance at 340 nm, resulting from the conversion of NADP to NADPH. Assay mixture contained 100 mM glycine buffer pH 9, 200 μM of NADPH and 10 μM or 10 mM of GHB. Assay was started by the addition of cell extract and results were expressed as nmol/min/mg of protein.

3.3.2.14 MTT assay

Cell viability was determined by following the ability of cells to reduce a tetrazolium dye MTT (3-(4,5-dimethylthiazol-2-yl)-2,5-diphenyltetrazolium bromide) to insoluble purple formazan (Mosmann, 1983). The concentration of formazan is determined spectrophotometrically, and used as indicator of cell growth.

Cytotoxicity assay of GHB was performed in a 96-well plate bought from Fisher Scientific. The cells were counted using a haemocytometer. Cells were seeded in triplicate (1×10^4 per well), and grown until reaching 70-80% confluent. Different concentration of the drug was added and left for an incubation period of 24 hours. 20 µl of MTT (1.2 mg/ml) was added to the cells and further incubated for 2 hours. The media containing MTT was removed and the cells were lysed using 100 µl of DMSO to dissolve the purple formazan. Absorbance at 540 nm was measured using a 96-well Labsystems iEMS plate-reader (Labsystems and Life Sciences International Limited, UK). Cell viability was calculated using the following formula:

% of cell viability = (OD_{540} of the treated samples/OD_{540} of the control) x 100.

3.3.2.15 GHB determination by gas chromatography-mass spectrometry

3.3.2.15.1 Preparation of samples

Extracellular endogenous GHB

The media of the cells was retained for extracellular GHB measurement, centrifuged briefly and 200 µl was transferred to a 1.5 ml Eppendorf tube. 500 µl of acetonitrile was added and the sample was centrifuged for 5 minutes at 13000 rpm to precipitate the proteins. The supernatant was removed to a 4 ml glass vial along with 50 µl of GHB-d6 which was served as internal standard, and the samples were frozen at -80 °C until analysis. When ready, the samples were blown to complete dryness under a moderate flow of nitrogen at room temperature, and derivatized using 75 µl of BSTFA at 70 °C for 30 minutes. The

samples were allowed to cool to room temperature, transferred to a small GC/MS vial and 75 µl of ethyl acetate was added to each sample.

Intracellular endogenous GHB

The method was adapted from (Villain *et al.*, 2003), and described in (Lyon *et al.*, 2007). The cells were washed by PBS, harvested by centrifuging and counted to normalize the results. Cell extract was prepared as mentioned in section (3.2.2.12) and transferred to a 1.5 ml Eppendorf tube along with 500 µl of acetonitrile. The samples were centrifuged at 13000 rpm for 5 minutes and the supernatant was placed in a 4 ml glass vial and kept at -80 °C. Before analysis, samples were blown to complete dryness under a moderate flow of nitrogen at room temperature and heated and derivatized by 75 µl of BSTFA at 70 °C for 30 minutes. The samples were allowed to cool to room temperature before shifting to a small GC/MS vial and adding 75 µl of ethyl acetate.

Exogenous GHB

The cells were cultured and transfected as stated in section (3.2.2.3). After 72 hours of transfection, cells were treated with 1 and 50 µM of GHB and left for 24 hours. Intracellular and extracellular samples for GC/MS analysis were prepared as mentioned above.

3.3.2.15.2 GC/MS conditions

Analysis was carried out using a Trace GC Thermoquest functioned in the splitless mode combined with Finnigan Polaris Q detector with AS2000 autosample, all from Thermo Finnigan. GC column DB-5ms Ultra Inert (30 mt , 0.25 mm ID internal diameter and 0.25 μmdf thickness of film) was purchased from Agilent.

2 μl was injected in the splitless mode at 250 °C. The oven was programmed to start at 60 °C, held for 1 minute, and then ramped to 250 °C at 10 °C/min. The total analysis time was 20 minutes. Helium flow rate was 1 ml/min. The two ions monitored for quantificational purposes were 233 for GHB and 239 for GHB-d6. Data were analyzed using Xcalibur TM version 1.2 software.

3.3.2.16 Statistical analysis

Graph pad Prism software version 4.00 for Windows, GraphPad Software, San Diego California USA was used to analyze the results. Student t-test and one way ANOVA with Dunnett's post test were used to compare two groups and more than two groups respectively.

3.4 Results

3.4.1 Verifying the presence of AKR1A1 in 1321N1 and HepG2 cells

Before, functional analysis could be carried out, the presence of the AKR1A1 gene in 1321N1 and HepG2 cells was confirmed by amplifying the AKR1A1 gene using the specific primers listed in table (3.1) at a final concentration of 0.2 μM. Total mRNA was isolated from 1321N1 and HepG2 cells by the SV total RNA isolation system from Promega, and cDNA was prepared as detailed in materials and methods. The PCR reaction was run for 30 cycles and PCR products were analyzed by agarose gel electrophoresis.

Figure 3.2 shows the presence of a single clear band in each sample at the expected amplicon size of 201 bp as determined by comparing with 100 bp DNA ladder. The result demonstrated that the AKR1A1 gene was successfully amplified and its existence in these cell lines was confirmed. The band was stronger in HepG2 cells than 1321N1 cells.

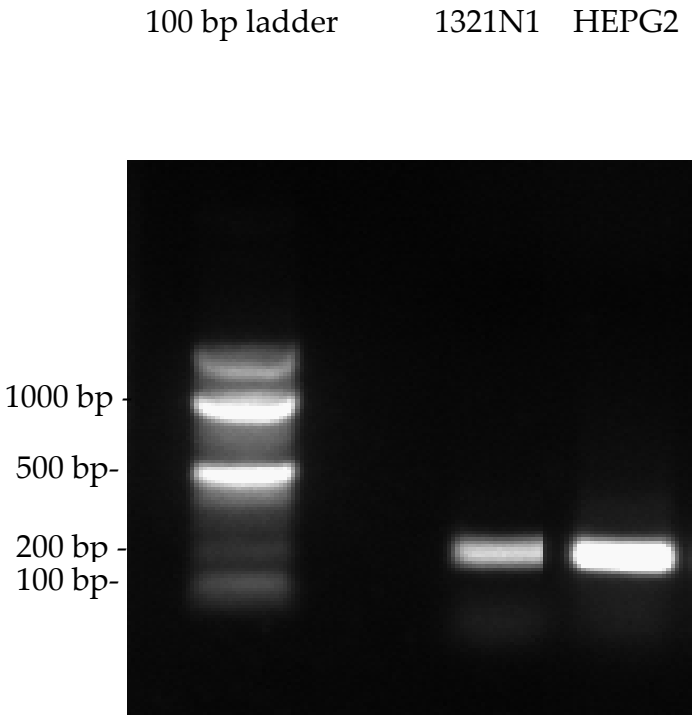

Figure 3.2: PCR product of AKR1A1 gene transcription in 1321N1 and HepG2 cells. Total RNA was isolated from 1321N1 and HepG2 cells and the AKR1A1 gene was amplified by RT-PCR using AKR1A1 specific primers. 1321N1 and HepG2 PCR products were run on 1% agarose gel electrophoresis along with 100 bp (base pairs) ladder. Product size is ~ 200 bp.

3.4.2 Knocking down the expression of AKR1A1 in 1321N1 and HepG2 cells

In order to investigate the effect of AKR1A1 in GHB metabolism, human 1321N1 and HepG2 cells were used as *in vitro* models for the central nervous system and the liver respectively. Cells were transfected with double-stranded siRNA designed to target the mRNA of the AKR1A1 gene. Cells transfected with scrambled non-specific siRNA in the same way served as a negative control for the transfection process in order to exclude effects due to the transfection reagent. Delivering targeted or scrambled siRNA into the cells did not affect cell growth and did not provoke cell death. The efficiency of knocking down the gene was assayed 72 hours post transfection on mRNA and protein levels.

To determine the silencing effectiveness on AKR1A1 mRNA levels in 1321N1 cells, total RNA was isolated from the cells and cDNA was synthesized using random primers as described in materials and methods. Isolation of RNA and synthesis of cDNA were carried out on the same day when possible to avoid any degradation of RNA. Otherwise, RNA samples were preserved at – 80 °C. mRNA levels of AKR1A1 were quantified relative to GAPDH (a house keeping gene) in triplicate using the ($\Delta\Delta C_T$) method to calculate fold difference in expression between control and silenced cells. The results in Figure (3.3) shows an 88 % reduction in AKR1A1 mRNA levels in knocking down cells comparing to control cells, indicating that silencing the gene was effective.

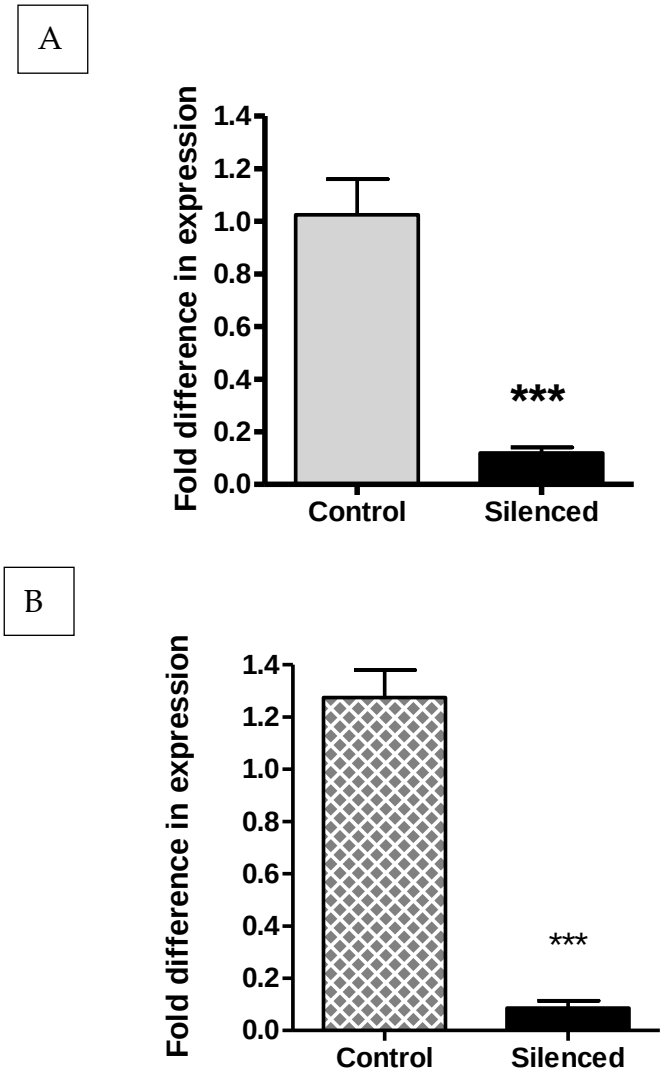

Figure 3.3: mRNA levels in control and silenced 1321N1 cells. Total RNA was isolated from **A)** 1321N1 cells and **B)** HepG2 cells. Relative quantification of mRNA levels of AKR1A1 to GAPDH was carried out by RT-PCR following the ($\Delta\Delta C_T$) method as detailed in the method section. Values represent the mean ± SEM of experiments performed in triplicate. Column bars show the fold difference between control and silenced cells. Statistical analysis was performed using student t-test. Asterisks indicate significant difference (***$p < 0.001$) compared to control.

To evaluate the effect of silencing AKR1A1 on protein levels in 1321N1 and HepG2 cells, extracts were prepared from control, silenced and scrambled cells and samples were analyzed by Western blot 72 hours after transfection using AKR1A1 specific antibody. Levels of GAPDH expression were used as a loading control. Results revealed a 92 % reduction in AKR1A1 expression in HepG2 cells (Figure 3.4) and 94 % reduction in expression in 1321N1 cells (Figure 3.5), indicating a successful knocking down of translation to protein.

AKR1A1 protein levels in scrambled cells were the same as control cells, signifying that the observed decrease of AKR1A1 protein levels in the silenced cells was solely due to the specific designed siRNA, excluding off-target effects.

To verify that the designed siRNA targeted only AKR1A1, protein levels of AKR7A2, another human gene from the AKR superfamily that is also involved in GHB metabolism, were measured in HepG2 and 1321N1 cells by western blotting. Results showed equal level of expression between control, silenced and scrambled cells.

The significant reduction in mRNA and protein levels of AKR1A1 does not appear to affect cell growth or viability.

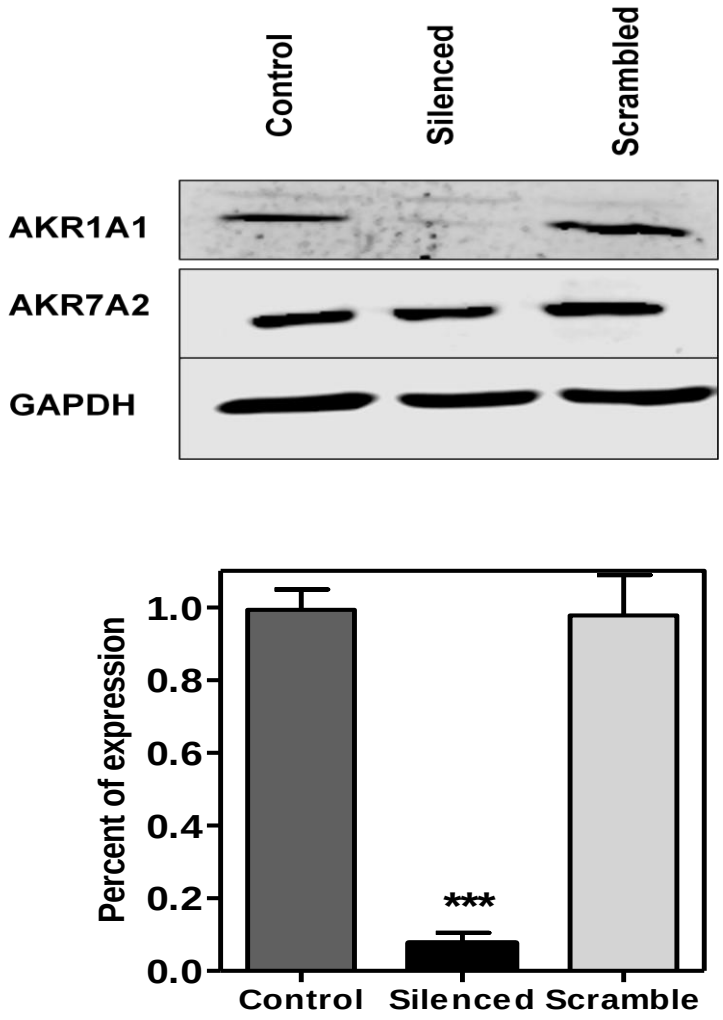

Figure 3.4: Silencing AKR1A1 in HepG2 cells. HepG2 cells were transfected with AKR1A1-targeted siRNA, and AKR1A1, AKR7A2 (positive control) and GAPDH (loading control) protein levels were assayed 72 hours after transfection by western blotting. Scrambled cells were used as a negative control for the transfection. Protein bands were quantified by ImageJ and data represents the mean of three different experiments ± SEM. One –way ANOVA with Dunnett's post test indicated a significant difference between silenced and control AKR1A1 levels (***$p<0.005$)

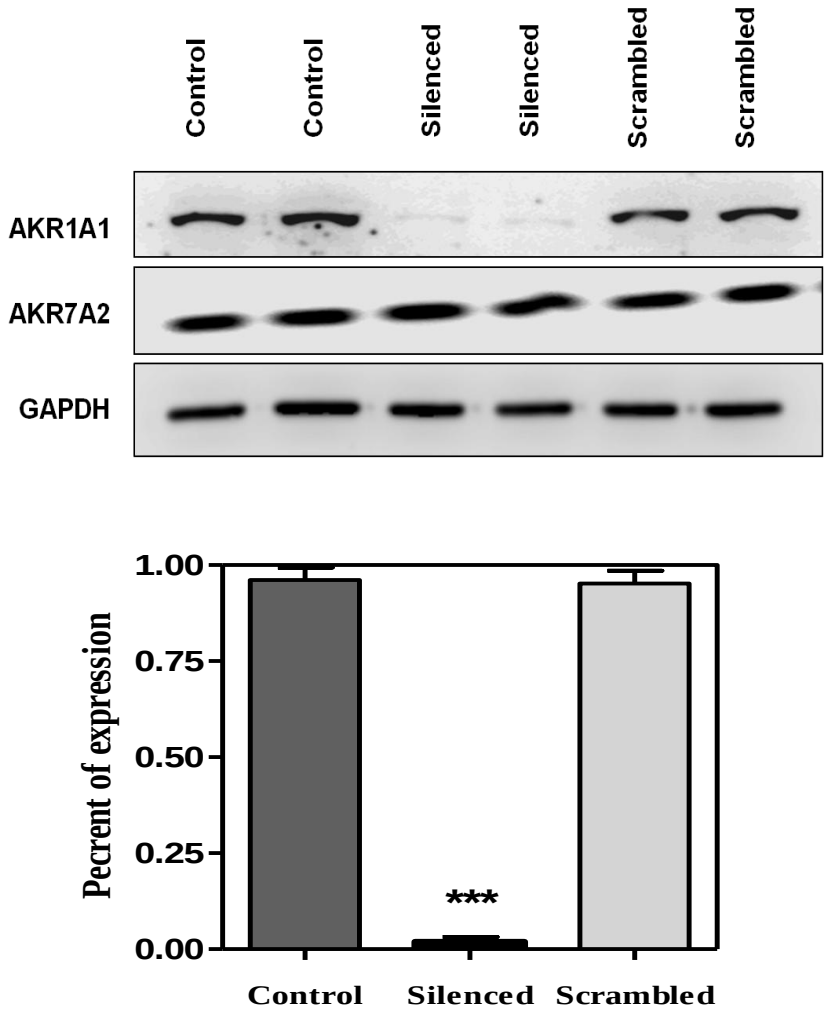

Figure 3.5: Silencing AKR1A1 in 1321N1 cells. 1321N1 cells were transfected with AKR1A1-targeted siRNA, and AKR1A1, AKR7A2 (positive control) and GAPDH (loading control) protein levels were assayed 72 hours after transfection by western blot. Samples were run in duplicate. Scrambled cells were used as a negative control for the transfection. Protein bands were quantified by ImageJ and data represent the mean of three different experiments ± SEM. One way ANOVA with Dunnett's post test indicated a significant difference between silenced and control AKR1A1 levels (***$p<0.001$)

3.4.3 Effect of silencing AKR1A1 on the ability of 1321N1 and HepG2 cells to reduce aldehydes

The contribution of AKR1A1 to the ability of 1321N1 and HepG2 cells to reduce aldehydes was investigated using p-nitrobenzaldehyde (p-NBA) as substrate. pNBA is a model substrate for most AKRs including AKR1A1 (Wermuth *et al.*, 1977, Iwata *et al.*, 1990). The assay monitored the change in absorbance at 340 nm using 1mM of substrate and 50 μM of NADPH in 100mM phosphate buffer. Figure 3.6 showed that 72 hours post transfection; pNBA specific activity was reduced by 30% in 1321N1 silenced cells and by 42% in HepG2 silenced cells. The K_m for p-NBA determined previously for the high K_m aldehyde reductase was 450 μM in pig brain (Cromlish and Flynn, 1985), and 150 μM in human liver (Wermuth *et al.*, 1977) which agrees with the concentration used in this study. The relative contribution of AKR1A1 to aldehyde reductase activity was greater in HepG2 cells, although total aldehyde reductase activity was higher in 1321N1 cells. Differences in the expression of the enzyme between the cell lines might be an explanation for that.

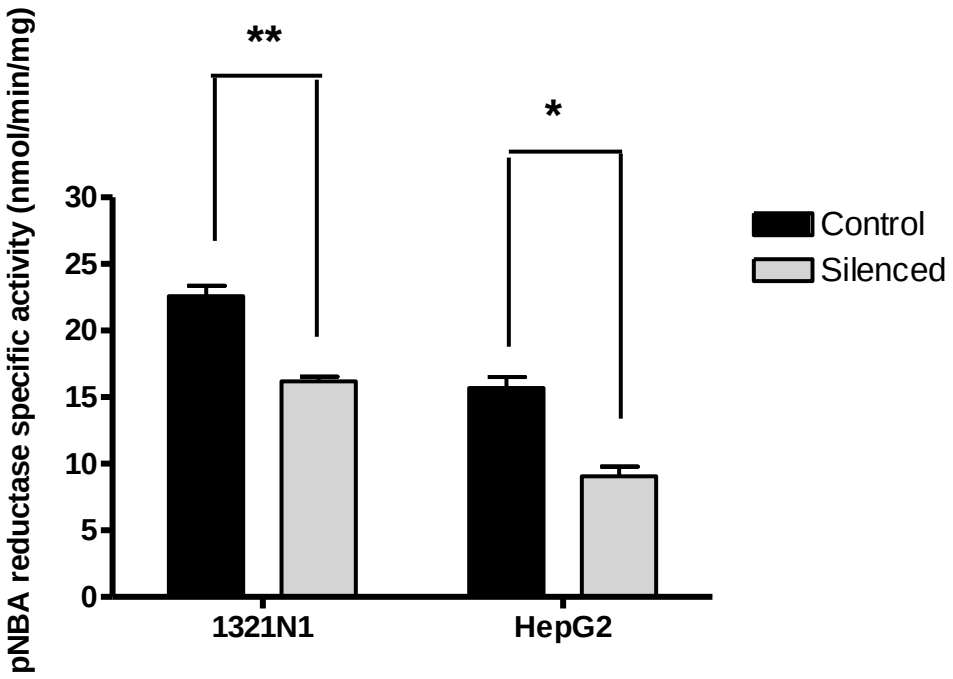

Figure 3.6: Effect of silencing AKR1A1 on pNBA specific activity in 1321N1 and HepG2 cells. p-nitrobenzaldehyde (pNBA) reductase activity was carried out on 1321N1 and HepG2 cell extracts from normal and AKR1A1-targeted siRNA transfected cells. Assay mixture contained 100 mM sodium phosphate buffer pH 6.6, 1 mM pNBA, 50 μM NADPH and 10 μl of cell extract and the reduction of absorbance at 340 nm was monitored at 25 °C. Protein concentrations were measured by Bradford assay. Data represent the mean + SEM of three different experiments. Asterisks indicate significant reduction in pNBA specific activity between control and silenced cells using student t-test (**$p<0.01$ *$p<0.05$)

3.4.4 Effect of silencing AKR1A1 on the reduction of D-glucuronate to L-gulonate

The ability of the 1321N1 and HepG2 cells to reduce D-glucuronate in the absence of AKR1A1 was investigated. D-glucuronate is a known substrate for AKR1A1 and the reduction of D-glucuronate to L-gulonate is the only reported biological activity for AKR1A1 in rodents.

The K_m for D-glucuronate determined previously for the high K_m aldehyde reductase was 4.5 mM in brain (Rivett *et al.*, 1981) and 3.2 mM in human liver (Wermuth and von Wartburg, 1980), therefore, two concentrations above and below the K_m were chosen. The assay was carried out 72 hours post transfection by monitoring the change in absorbance at 340 nm. Assay mixture contained 100 mM phosphate buffer pH 6.6, 1 mM or 10 mM of D-glucuronate, 50 μM of NADPH and 10 μl of cell extract.

Figure 3.7 shows that at 1 mM concentration of substrate, D-glucuronate reductase activity in 1321N1 cells was not affected by AKR1A1 knocking down , while it was significantly decreased by 67.5% in HepG2 silenced cells comparing to control. At 10 mM concentration of substrate, D-glucuronate reductase activity was reduced significantly by 74% in HepG2 cells and by 52% in 1321N1 cells. The relative contribution of AKR1A1 to D-glucuronate activity as well as total D-glucuronate reductase was greater in HepG2 cells.

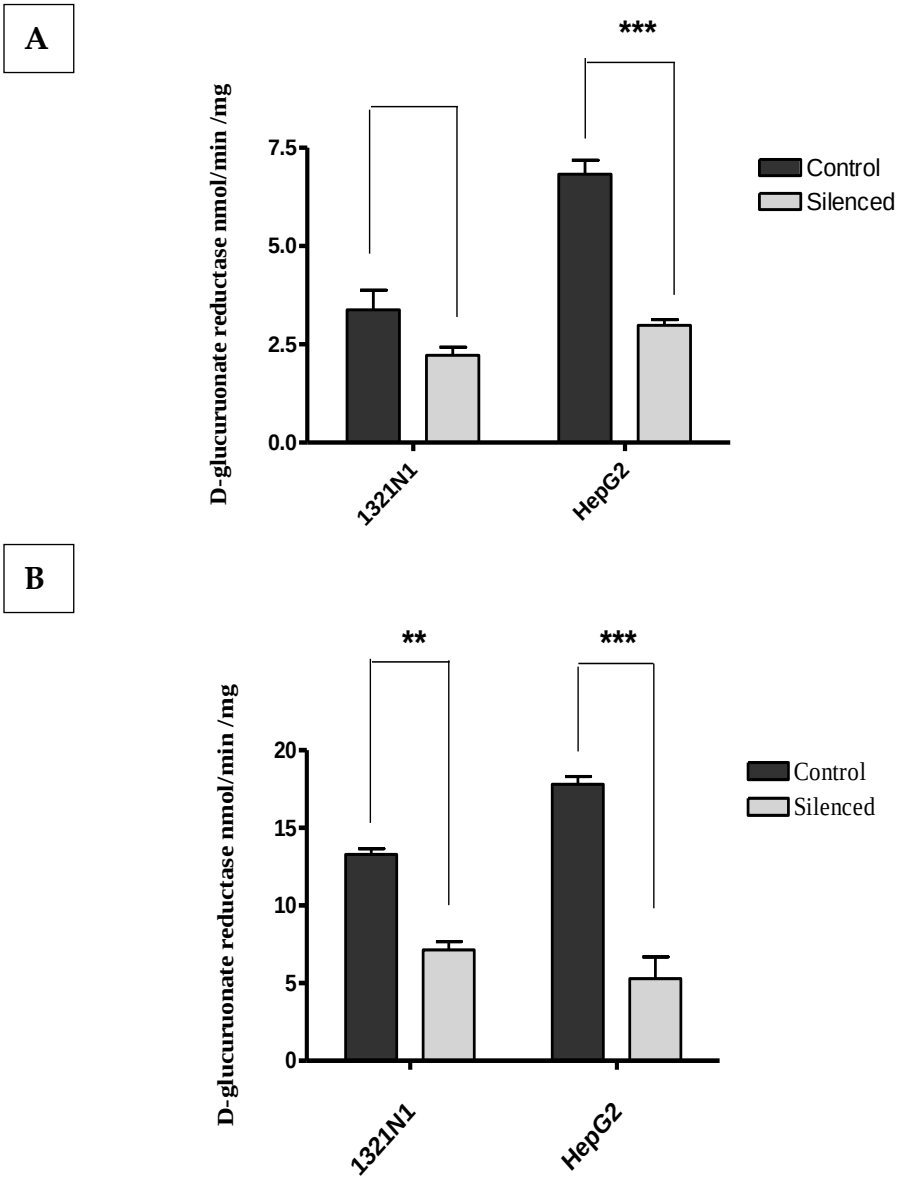

Figure 3.7: Effect of D-glucuronate reductase activity in 1321N1 and HepG2 cells. D-glucuronate reductase activity in cell lines at **A)** 1 mM and **B)** 10 mM of D-glucuronate. Assays were carried out on 1321N1 and HepG2 cell extracts from normal and silenced cells 72 hours post transfection in 100 mM sodium phosphate buffer pH 6.6, 50 µM NADPH and 10 µl of cell extract .The reduction of absorbance at 340 nm was monitored at 25 °C. Data represent the mean + SEM of three different experiments. Asterisks indicate significant reduction in D-glucuronate specific activity between control and silenced cells using student t-test (***$p<0.001$**$p<0.01$ *$p<0.05$)

3.4.5 Effect of silencing AKR1A1 on SSA reductase activity in 1321N1 and HepG2 cells

To investigate the role of AKR1A1 on the synthesis of GHB in 1321N1 and HepG2 cells, the ability of the cells to reduce SSA at high and low concentrations were tested. The reaction was performed at 37 °C in sodium phosphate buffer pH 6.6 by measuring the conversion of NADPH to NADP at 340 nm. At 1 mM of SSA, silencing of AKR1A1 lowered SSA reductase activity by 36% and 31% in 1321N1 cells and HepG2 cell respectively (Figure 3.8). This was significantly different with a p value of less than 0.01. This shows that AKR1A1 is important for the reduction of SSA, when SSA levels are high. However, at 10 μM of SSA, no difference in activity was observed between control and silenced cells (Figure 3.9), indicating that AKR1A1 is unlikely to play a major role in the reduction of SSA to GHB when concentrations of SSA are low. The effect is not cell specific as it was observed in both 1321N1 and HepG2 cells, demonstrating that AKR1A1 plays a similar role in GHB synthesis inside and outside of the central nervous system.

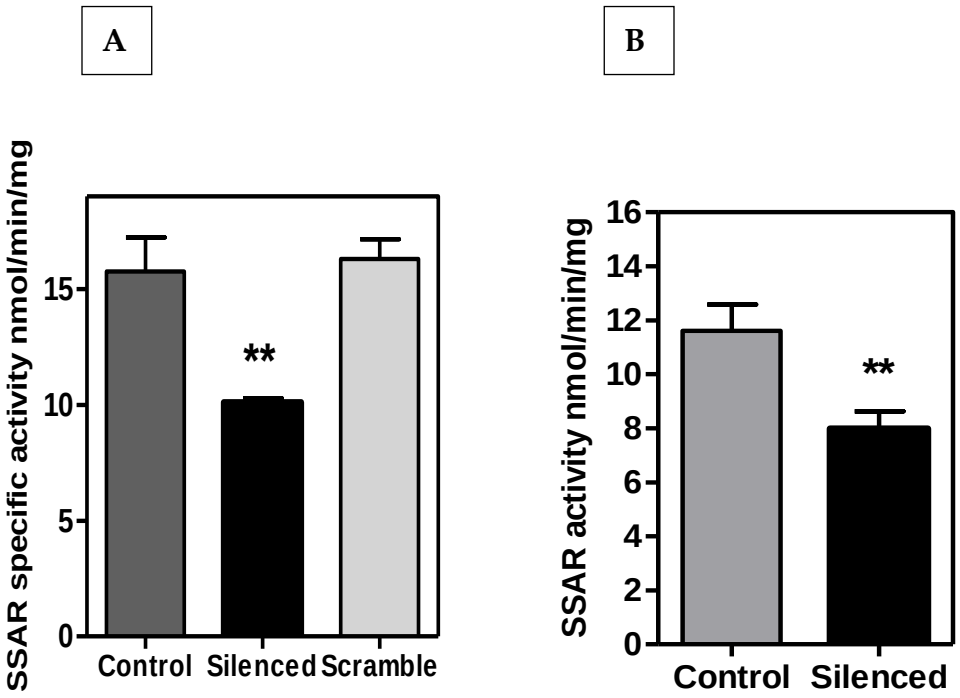

Figure 3.8: Effect of silencing AKR1A1 on SSAR specific activity in 1321N1 and HepG2 cells using high concentration of SSA. SSAR activity was measured in cell extracts prepared from **A**) 1321N1 and **B**) HepG2 cells using 1 mM of SSA. The consumption of NADPH was monitored at 340 nm for 5 minutes and specific activity of the enzyme was expressed as nmol/min/mg of protein. Data represent the mean of three experiments + SEM. Asterisks indicate significant reduction in SSAR activity compared to control and scrambled cells using one-way ANOVA followed by Dunnett's post test in **A**, and student t-test in **B** (**$p<0.01$)

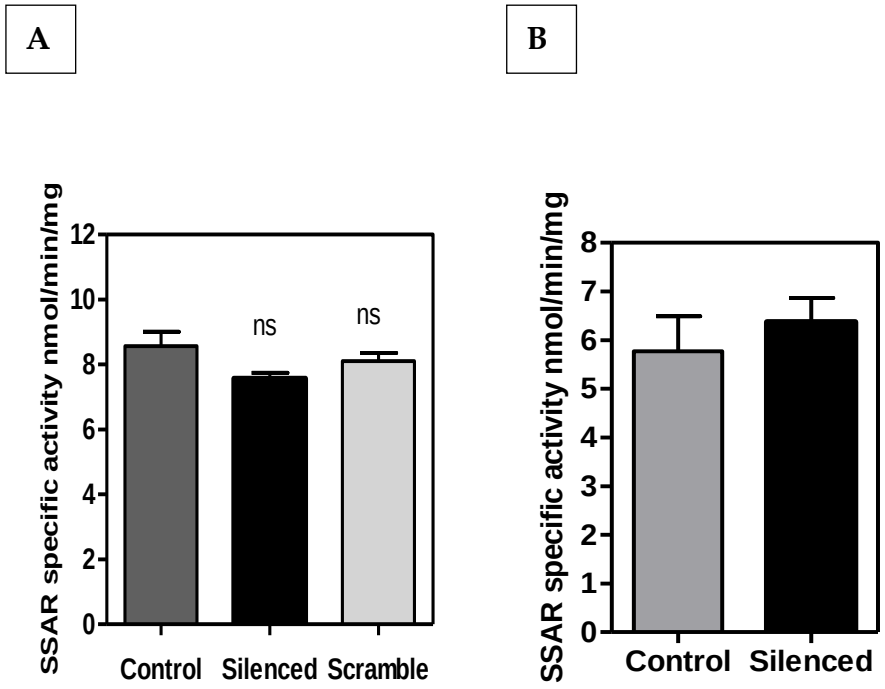

Figure 3.9: Effect of silencing AKR1A1 on SSAR specific activity in 1321N1 and HepG2 cells using low concentration of SSA. SSAR activity was measured in cell extract prepared from **A)** 1321N1 and **B)** HepG2 cells using 10 μM of SSA. Specific activity of the enzyme was expressed as nmol/min/mg of protein. Data represent the mean of three experiments + SEM. ns not significant.

3.4.6 Effect of silencing AKR1A1 on endogenous GHB levels in 1321N1 and HepG2 cells

In order to verify the involvement of AKR1A1 in GHB biosynthesis in 1321N1 and HepG2 cells, levels of extracellular and intracellular GHB 72 hours post transcription were assayed by GC/MS and cell number (counted by haemocytometer) was used for normalization. The results in Figure 3.10 and Figure 3.11 showed that GHB levels in both cell types were not affected by the knocking down of AKR1A1, illustrating that AKR1A1 does not participate significantly in endogenous GHB metabolism. This is reasonable taking into consideration the earlier findings which suggests that AKR1A1 is responsible for 30% of SSA reductase activity at high levels but not at endogenous levels. The data also exemplify that extracellular levels of GHB are significantly higher than intracellular levels in both 1321n1 and HepG2 cells. It is clear that much of endogenous GHB produced by the cells is exported to the surrounding media after synthesis.

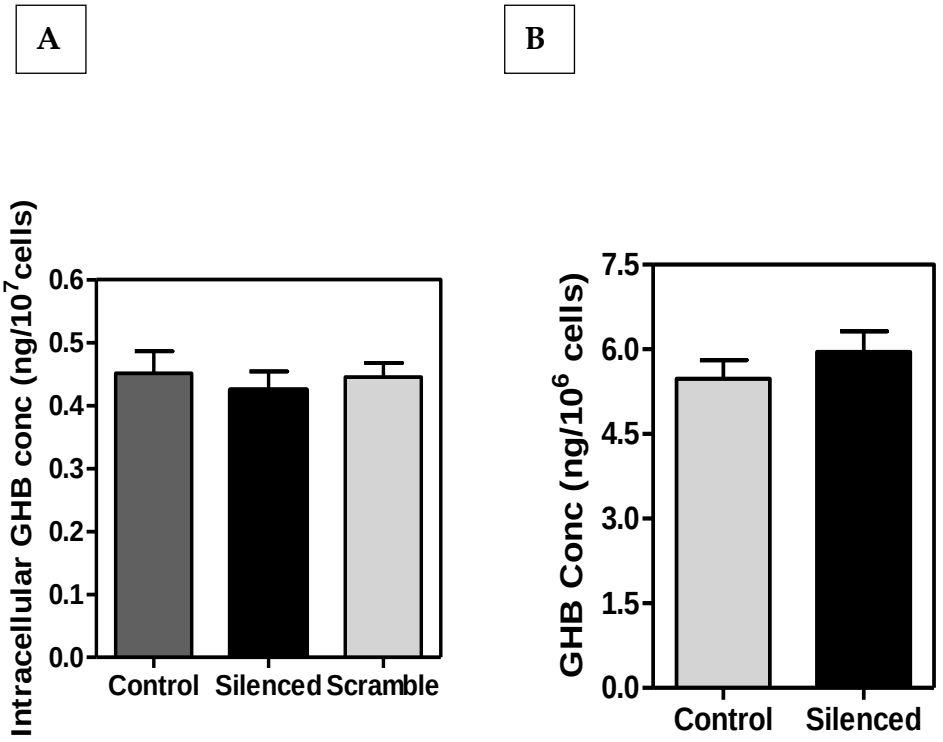

Figure 3.10: Effect of silencing AKR1A1 on intracellular endogenous GHB level in 1321N1 and HepG2 cells. A) 1321N1 cells, **B)** HepG2 cells; 72 hours after transfection, intracellular GHB was extracted from control, silenced and scrambled cells by protein precipitation using acetonitrile, derivatized by BSTFA, and measured by GC/MS. Concentration was expressed as ng per number of cells. Data represent the mean +SEM of three experiments.

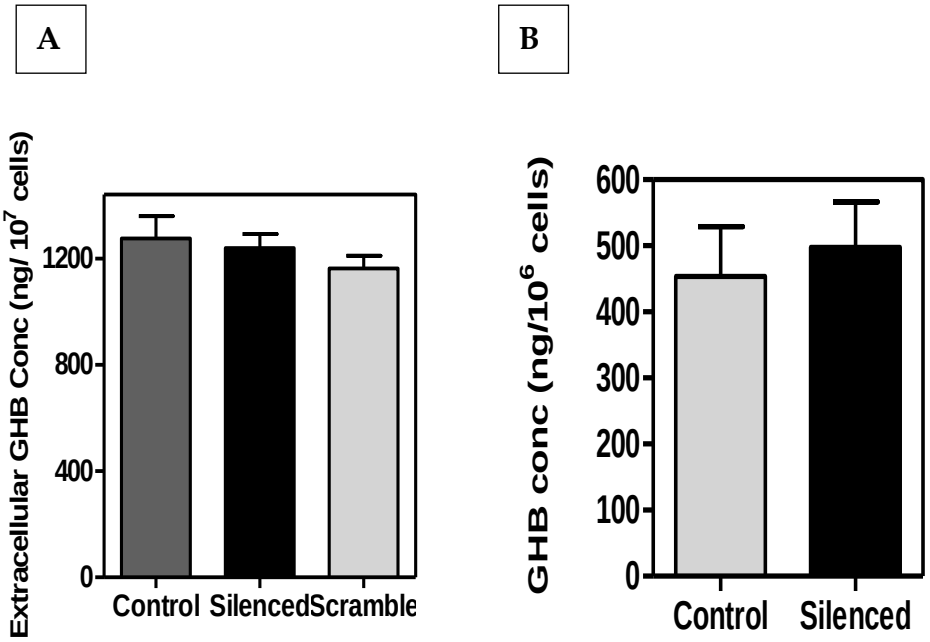

Figure 3.11: Effect of silencing AKR1A1 on extracellular endogenous GHB level in 1321N1 and HepG2 cells. A) 1321N1 cells, **B)** HepG2 cells ; 72 hours after transfection, GHB was extracted from 200 ul of media from control, silenced and scrambled cells by protein precipitation using acetonitrile, derivatized by BSTFA, and analyzed by GC/MS. Concentration was expressed as ng per number of cells. Data represent the mean +SEM of three experiments.

3.4.7 Effect of silencing AKR1A1 on GHB dehydrogenase activity in 1321N1 and HepG2 cells

To investigate the involvement of AKR1A1 in GHB catabolism, the ability of the cells to oxidize GHB at high and low levels was tested. The NADP dependent oxidation of GHB to SSA was carried out in 100 mM glycine buffer pH 9 using 10 mM or 10 μM of GHB. The higher concentration (10 mM) was chosen based on a previous study (Vayer *et al.*, 1985b) where the high K_m aldehyde reductase was able to convert GHB to GABA.

Figure (3.12) showed that silencing AKR1A1 significantly affected NADP dependent GHB dehydrogenase activity which dropped by 50 % in 1321N1 cells and by 82% in HepG2 cells when using a high concentration (10 mM) of GHB. This is a significant difference when applying statistical analysis with a p value <0.01 and < 0.001 for 1321N1 and HepG2 cells respectively.

In contrast, Figure (3.13) showed that at low levels of GHB (10 μM), GHB dehydrogenase activity was not affected by AKR1A1 silencing. This indicated that AKR1A1 is the predominant GHB dehydrogenase in HepG2 cells when high levels of GHB are present, while it plays no role at endogenous GHB levels. In 1321N1 cells AKR1A1 represents a large part of GHB dehydrogenase activity but this is smaller than the effect observed in HepG2 cells.

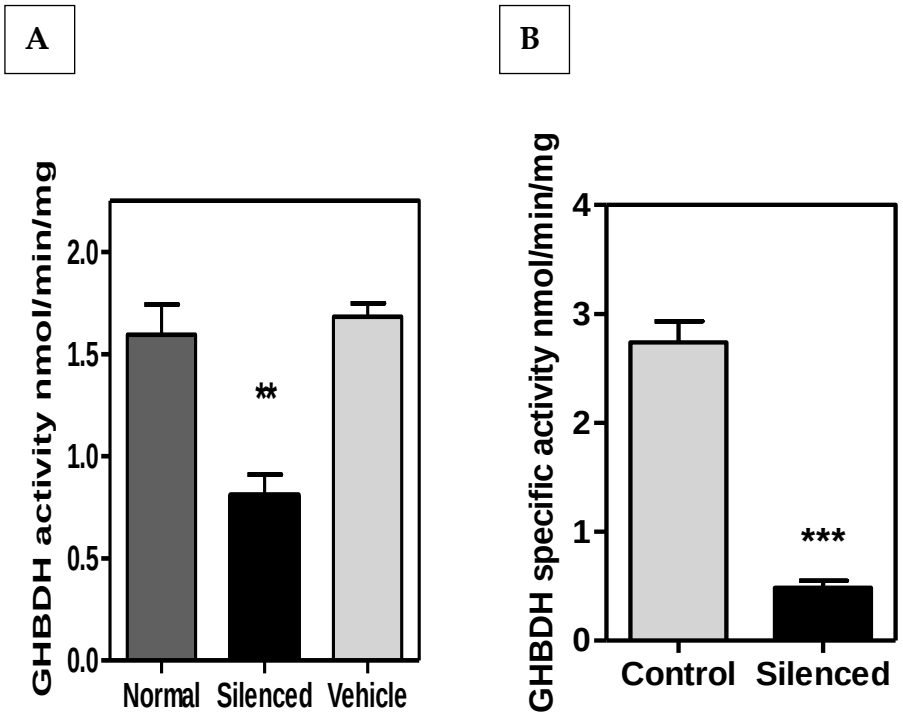

Figure 3.12: Effect of silencing AKR1A1 on GHB dehydrogenase specific activity in 1321N1 and HepG2 cells using high concentration of GHB. A) 1321N1 cells and **B)** HepG2 cells. Extracts were prepared from control, silenced and scrambled cells, and NADP-dependent GHB dehydrogenase activity was measured at 37 °C using 10 mM of GHB. The increase in absorbance was monitored at 340 nm. Results were expressed as nmol/min/mg of protein. Data represent the mean of three experiments +SEM. Asterisks indicate significant difference in silenced sample vs control using one way ANOVA followed by Dunnett's post test in **A**, and student t-test in **B** (**p<0.01,***p<0.001)

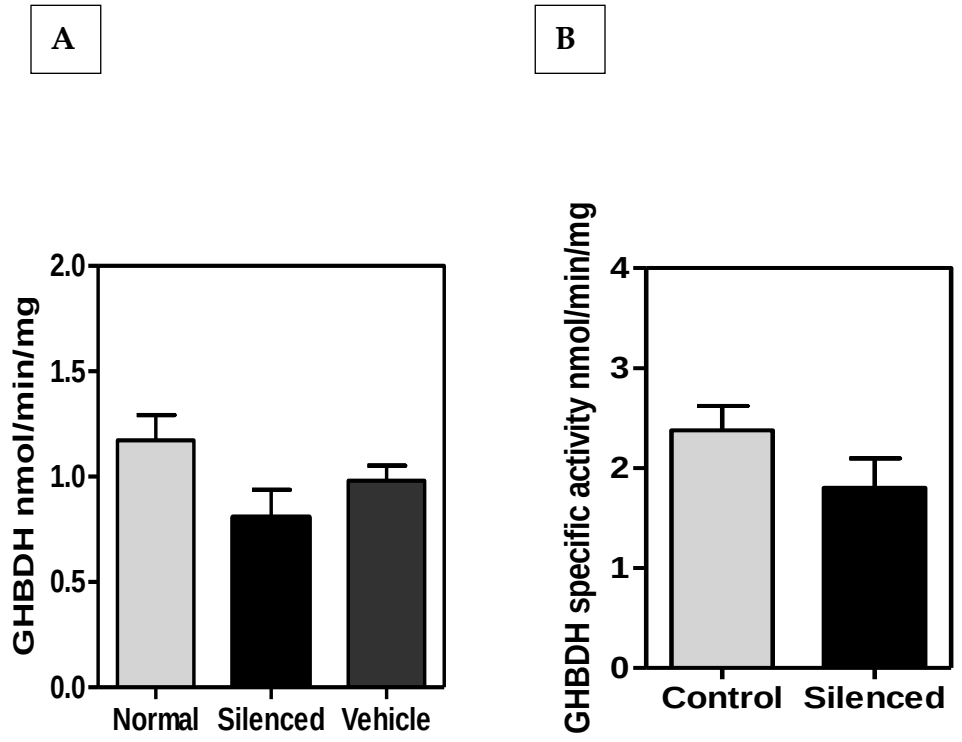

Figure 3.13: Effect of silencing AKR1A1 on GHB dehydrogenase specific activity in 1321N1 and HepG2 cells using low concentration of GHB. A) 1321N1 cells and **B)** HepG2 cells. Extracts were prepared from control, silenced and scrambled cells, and NADP-dependent GHB dehydrogenase activity was measured at 37 °C using 10 μM of GHB. The increase in absorbance was monitored at 340 nm. Results were expressed as nmol/min/mg of protein. Data represent the mean of three experiments +SEM.

3.4.8 Effect of GHB on 1321N1 and HepG2 cells

To investigate the effect of silencing AKR1A1 when cells are exposed to exogenous GHB, the cytotoxic effect of GHB on 1321N1 and HepG2 cells was first determined using the MTT assay as described in material and methods. Cells were seeded in a 96 well-plate and treated with 1, 10, 25, 50, 100 and 500 μM of GHB for 24 hours. Figure (3.14) shows that GHB produced a proliferative effect on both 1321N1 and HepG2 cells. The maximum effect was observed at 1 μM treatment. The impact on 1321N1 was much stronger than HepG2 cells where treatment with 1 μM of GHB was statistically different from untreated control (p value < 0.05). No toxicity was observed at higher concentrations in 1321N1 cells while in HepG2 cells, 90% of the cells were still viable at 500 μM of GHB

Based on this observation, a concentration of 50 μM was chosen to treat the cells in order to investigate the role of AKR1A1 in exogenous GHB metabolism.

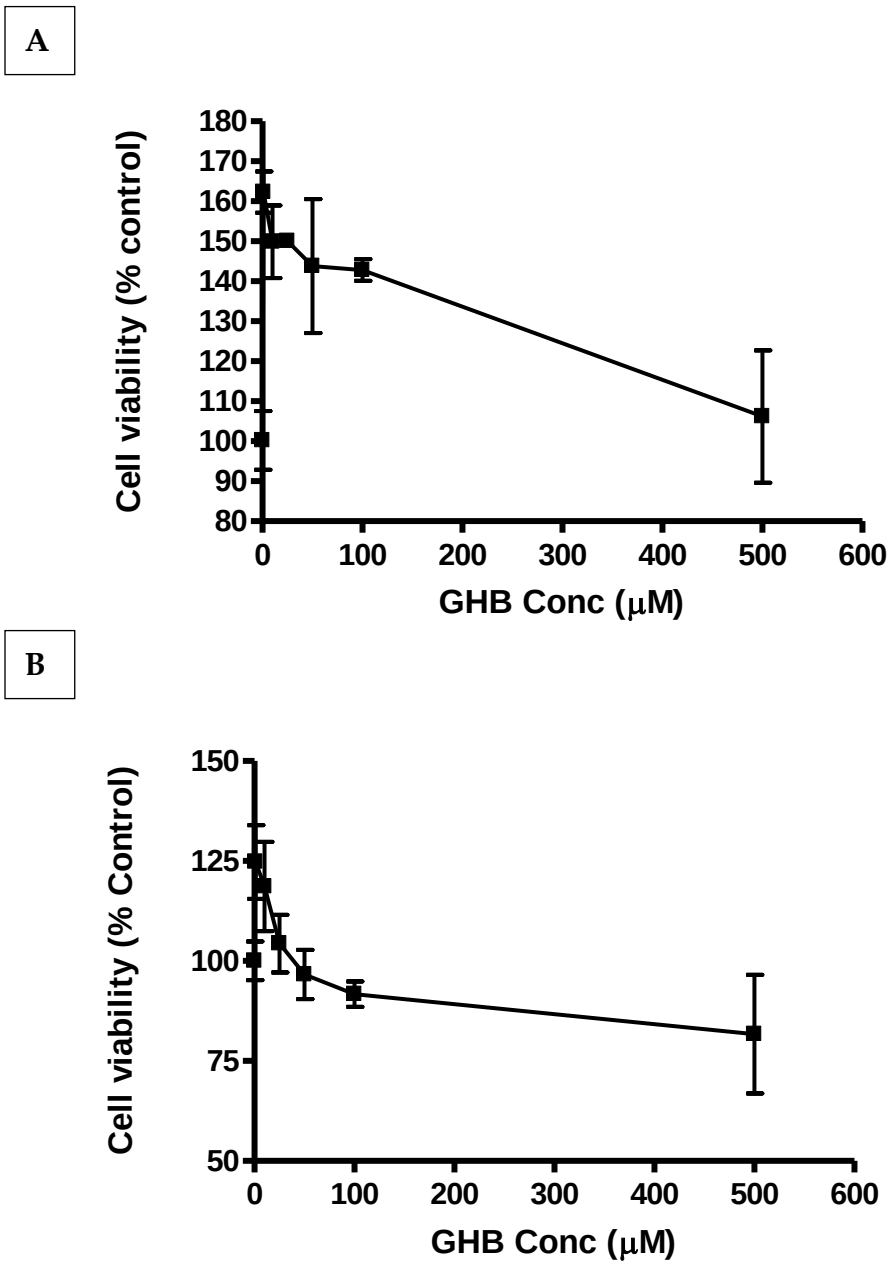

Figure 3.14: Effect of GHB on 1321N1 and HepG2 cells. Effect of GHB on **A)** 1321N1 and **B)** HepG2 cells. Cells were treated for 24 hours with 1-10-25-50-100 and 500 μM of GHB and cytotoxicity was determined by MTT assay. Cell viability was expressed as % of control cells and plotted against the concentration of the drug.

3.4.9 Effect of silencing AKR1A1 on exogenous GHB levels in 1321N1 and HepG2 cells

Following the observation from SSA reductase and GHB dehydrogenase assays and the significant involvement of AKR1A1 at high concentration of GHB, control, silenced and scrambled 1321N1 and HepG2 cells were treated with 50 μM of GHB for 24 hours, and levels of intracellular and extracellular GHB were measured using GC/MS and expressed by ng per number of cells. Figure (3.15) demonstrates a significant increase in intracellular GHB levels in silenced HepG2 cells compared to control and scrambled cells, while extracellular GHB levels remained constant. Taken together with the reduction in GHB-dehydrogenase activity in HepG2 cells, the results suggest that AKR1A1 is involved in GHB catabolism in these cells.

In 1321N1 cells the effect on extracellular GHB levels was statistically significant as shown in Figure (3.16), while having no significant effect on intracellular GHB levels, despite the reduction in GHB dehydrogenase activity by 50% in these cells.

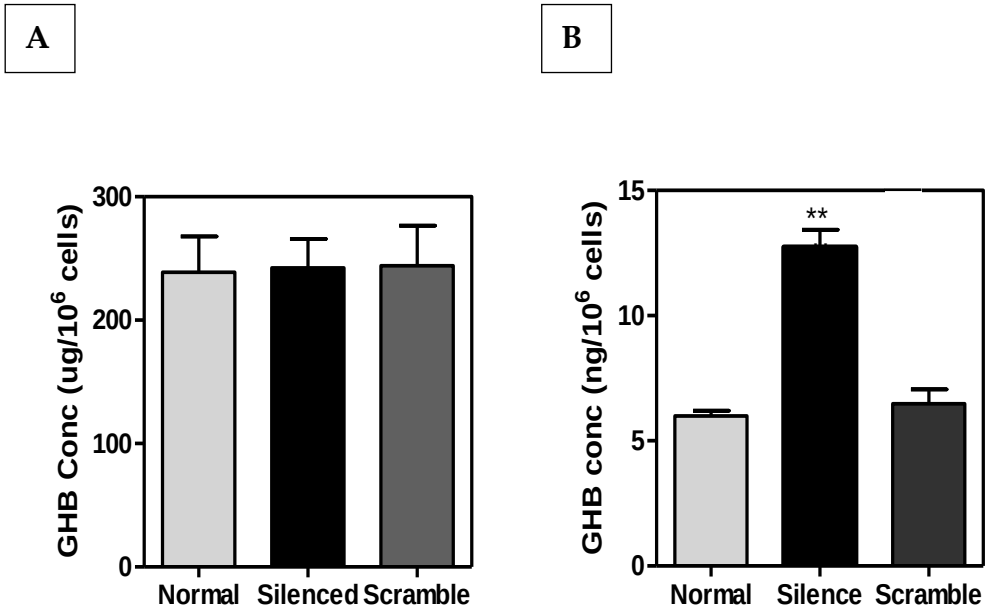

Figure 3.15: Effect of silencing AKR1A1 on extracellular and intracellular GHB level in HepG2 cells after 24 h treatment with 50 μM of GHB. A) Extracellular GHB levels **B)** Intracellular GHB levels. Control silenced and scrambled HepG2 cells were treated with 50 μM of GHB for 24 hours and GHB levels were measured by GC/MS. Data represent the mean of three experiment +SEM. Asterisks indicate significant difference (**$p < 0.01$) when results were analyzed statistically by one-way ANOVA followed by Dunnett's post test.

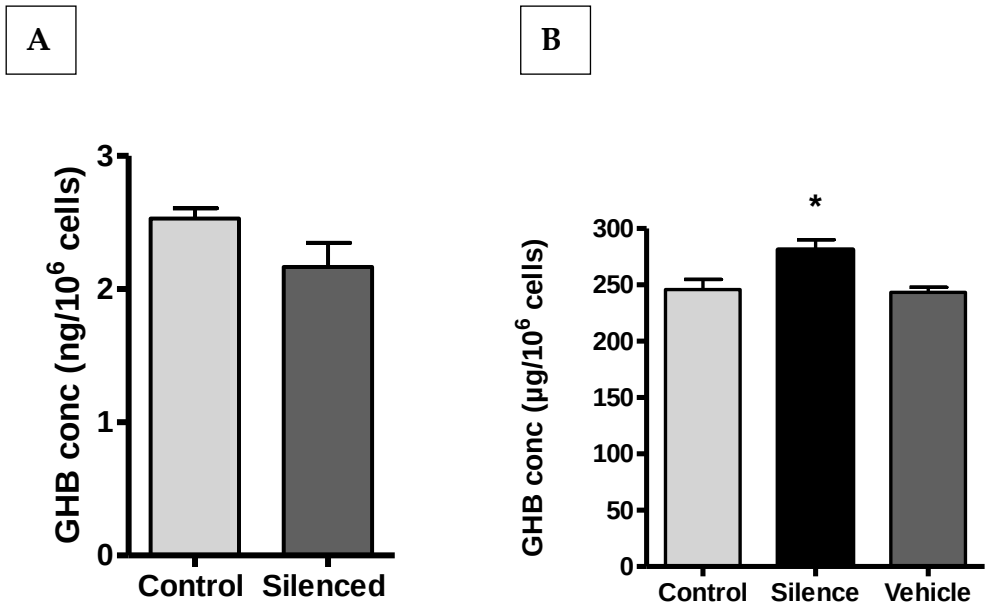

Figure 3.16: Effect of silencing AKR1A1 on extracellular and intracellular endogenous GHB level in 1321N1 cells after 24 h treatment with 50 µM of GHB. Control and silenced 1321N1 cells were treated with 50 µM of GHB for 24 hours. **A)** Intracellular GHB levels and **B)** Extracellular GHB levels were determined by GC/MS and expressed by µg /number of cells. Asterisks indicate significant difference (*$p < 0.05$) in extracellular GHB levels when analyzed statistically by one-way ANOVA followed by Dunnett's post test.

3.5 Discussion

The work carried out in this chapter was aimed at understanding the role of aldehyde reductase AKR1A1 in GHB metabolism by silencing its encoding gene in 1321N1 and HepG2 cell lines and observing the impact on GHB synthesis and breakdown. The results provide evidence that AKR1A1 is identical to the high K_m aldehyde reductase, previously shown to be involved in GHB metabolism, and that AKR1A1 participates in exogenous, but not endogenous GHB catabolism.

p-NBA reductase and D-glucuronate reductase activities of AKR1A1

p-NBA and D-glucuronate are model substrates for AKR1A1 and were employed in different studies to determine AKR1A1 properties. In particular, the reduction of D-glucuronate by AKR1A1 plays an important biological role in rodents (Gabbay *et al.*, 2010). In this study, AKR1A1 contributed significantly to p-NBA and D-glucuronate reductase activities in HepG2 cells, and to a less extent in 1321N1 cells, indicating that AKR1A1 is more functional in liver. Although the K_m for D- glucuronate was reported to be 3.2 mM in human liver (Wermuth and von Wartburg, 1980), a significant reduction in D-glucuronate reductase activity was observed when using 1 mM of substrate. The difference in pH assay conditions might explain this question as the K_m was determined in the cited paper at pH 7.4 , while in this study reductase assays were carried out at pH 6.6. Furthermore, AKR1A1 reductase activity was shown to be reduced when pH is increased (Rivett *et al.*, 1981)

SSA reductase activity of AKR1A1

It has been speculated that AKR1A1 is identical to the high K_m aldehyde reductase purified from different sites (Rivett *et al.*, 1981, Cromlish and Flynn, 1985, Kaufman *et al.*, 1979, Cash *et al.*, 1979). The high K_m aldehyde reductase was shown to work as an SSA reductase with a K_m of 130 μM in rat brain (Rivett and Tipton, 1981), and 49 μM and 37 μM in hamster liver and brain respectively (Kaufman *et al.*, 1979). The data in this study support this observation, as SSA reductase activity at 10 μM was not affected by AKR1A1 silencing in both cells. In contrast, at 1 mM SSA concentration, 30-36 % of SSA reductase activity was attributed to AKR1A1.

Previously, AKR7A2 (aflatoxin aldehyde reductase), which has a lower K_m for SSA than AKR1A1 (O'Connor et al., 1999), was shown to be the dominant SSA reductase in human neuroblastoma cell line SHSY5Y at the two concentrations tested (Lyon *et al.*, 2007). Given that AKR7A2 is localized mainly in glial cells throughout the central nervous system (Picklo *et al.*, 2001), and expressed in human hepatocytes (Ireland *et al.*, 1998) , AKR7A2 might act similarly in 1321N1 and HepG2 cells as well. This remains to be investigated.

As AKR1A1 does not effectively reduce SSA at low concentrations, it is logical that it does not have an impact on endogenous GHB concentration. Both extracellular and intracellular levels of GHB were unaffected by AKR1A1 knocking down. Interestingly, extracellular levels of GHB were much higher

than intracellular levels in both cells, indicating that both 1321N1 and HepG2 cells secrete GHB to the medium after synthesis.

GHB dehydrogenase activity of AKR1A1

In this study, GHB dehydrogenase activity was significantly affected by AKR1A1 silencing when assayed using 10 mM of GHB. However, at 10 μM of GHB, dehydrogenase activity was not altered in silenced cells. This coincides with the K_m for GHB calculated previously for the high K_m aldehyde reductase in hamster liver and brain to be 2.2 mM and 2.5 mM respectively (Kaufman *et al.*, 1979) and 10 mM in rat brain (Vayer *et al.*, 1985b). It further emphasizes that AKR1A1 on its own does not participate in endogenous GHB metabolism. However, when coupling AKR1A1 to GABA-T enzyme, the K_m value for GHB was reduced to 175 μM (Vayer *et al.*, 1985b). Altogether, this suggests that at micromolar GHB concentrations, AKR1A1 oxidizes GHB to produce GABA as a final product, and the reaction does not proceed to enter the Krebs cycle via succinate. By this way, the coupled reaction via AKR1A1 serves as a compensatory route to synthesize new GHB from GABA and this can feed into metabolism.

In terms of GHB catabolism, proof is provided here that AKR1A1 is a major GHB-dehydrogenase in HepG2 cells, contributing to 82% of GHB dehydrogenase activity. In 1321N1 cells, half of GHB dehydrogenase activity was attributed to AKR1A1. This indicates that at cases where high levels of GHB

are present such as in overdose cases or in SSADH deficiency patients, AKR1A1 eliminates excess GHB by reducing it to SSA. Given that the K_m values for GABA-transaminase were 0.31 mM , 0.32 mM and 0.76 mM in human brain, human liver and cultured astrocytes respectively(White and Sato, 1978, Larsson and Schousboe, 1990), while the K_m values for SSADH were 1 μM in human brain and less than 1 μM in human liver (Ryzlak and Pietruszko, 1988, Dockham *et al.*, 1992), the favourable route for SSA is to be oxidized to succinate rather than to be converted to GABA. In this case, AKR1A1 assists in removing GHB via SSA and succinate and the TCA cycle.

Cell proliferation effect of GHB on 1321N1 and HepG2 cells

To examine whether the reduction in GHB-dehydrogenase activity associates with alteration in exogenous GHB levels, cells need to be exposed to GHB. For this purpose, the cytotoxic effect of GHB on 1321N1 and HepG2 cells was determined using the MTT assay after treating the cells with various concentrations of GHB. Interestingly, at micromolar concentrations, GHB promotes cell proliferation of these cells. In 1321N1 cells, the effect was statistically significant at 1 μM of GHB.

A possible explanation is the stimulation in growth hormone release following GHB administration (Volpi *et al.*, 2000). In addition, GABA, the main precursor of GHB, manifests a similar effect on HepG2 cells where concentrations between 1μM and 40 μM induced cell proliferation, while concentrations between 100

μM to 400 μM had no effect on cell growth (Liu *et al.*, 2008). The proliferation effect of GABA seems to be mediated by $GABA_A$ receptor α3 subunit (Liu *et al.*, 2008, Takehara *et al.*, 2007). Consequently, the impact of GHB in HepG2 cells is not likely to be a direct activation of GABA receptor, as GHB only binds to $GABA_B$ receptor not to alpha receptors, and baclofen, a $GABA_B$ receptor agonist, inhibits HepG2 cell proliferation (Wang *et al.*, 2008b).

In the central nervous system, the proliferative effect of GABA was observed in immature cerebellar granule cells when using GABA between 0.1 and 100 μM (Fiszman *et al.*, 1999). In contrast, this was not observed in chronically treated rats with gamma butyrolactone GBL, a pro-drug for GHB. The rats were injected with GBL 8 times at 100 mg/kg for two weeks. The number of cells was determined by measuring bromodeoxyuridine which labels dividing cells. In this case, the chronic administration of GBL did not affect cell numbers in the dentate gyrus in the hippocampus, confirming that the GHB proliferative effect is dose and time-dependent (Scott *et al.*, 2010).

AKR1A1 in exogenous GHB metabolism

In HepG2 cells, treating the cells with 50 μM of GHB after silencing AKR1A1 confirmed the significant role for this enzyme in exogenous GHB metabolism as a two-fold increase in intracellular GHB levels was observed in silenced cells. However, in 1321N1 cells, the significant difference was on the extracellular level, not the intracellular level. The ability of cells to catabolise GHB seemed to be affected, leading to higher concentrations in the media. It appeared that 1321N1 cells did not store GHB inside the cells, as intracellular levels were similar to endogenous levels.

The concentration tested on cells in this study 50 μM is equivalent to 6.3 mg/L of sodium GHB. Attempts to correlate between brain or liver and plasma GHB concentrations have been reported previously. In one experiment, the relationship between GHB concentrations in plasma and whole brain were studied in rat following two different doses of GHB (Lettieri and Fung, 1979). GHB was administered either intracardially (400 mg/kg) or intravenously (800 mg/kg), and levels in plasma and brain were determined following animal awaking. At the lower dose, the sleeping time was 58 minutes, plasma concentration was 474 μg/ml, and whole brain concentration was 100 μg/ml. At the higher dose, sleeping time was 138 minutes, plasma level was 566 μg/ml, and brain level was 135 μg/ml. Although GHB brain levels seem to be independent from dose (which coincides with non linear pharmacokinetics), the ratio between brain and plasma levels is rather consistent; 0.21 and 0.24 at lower dose and higher dose respectively. Similar results were obtained in a recent

study after a single dose of GHB (Raybon and Boje, 2007). Rodents were injected with 548 mg/kg of GHB, and concentrations after 20 minutes were 307 μg/ml and 32.8 μg/ml in plasma and extracellular brain respectively, while after 199 minutes, plasma levels were 214 μg/ml and extracellular brain levels were 36 μg/ml. Both studies showed that a small percent of the dose is able to penetrate the blood brain barrier.

In humans, a case study of GHB-related death showed that post-mortem GHB levels in brain and liver were 102 mg/kg and 52 mg/kg, while in urine, femoral and heart blood levels were 1665 μg/ml , 461 μg/ml and 276 μg/ml respectively (Mazarr-Proo and Kerrigan, 2005). However, the actual lethal dose taken was not known but estimated to be between 2 and 4 g.

3.6 Conclusions

In conclusion, this is the first report of knocking down the gene encoding AKR1A1 in cell lines. This achievement opens the door to investigate the role of AKR1A1 in several biological activities and pathways.

In this study, proof was provided that AKR1A1 is identical to the high K_m aldehyde reductase and to the NADP-dependent GHB dehydrogenase purified by Kaufman (Kaufman *et al.*,1979) . This was proposed previously but without evidence.

This work throws additional light on GHB metabolism and in particular, on the role of AKR1A1 in this pathway. The involvement of AKR1A1 in the metabolism of GHB at high concentrations is useful to differentiate between participating enzymes in endogenous and exogenous levels, which may help when studying overdoses of GHB. Factors that affect the level of this enzyme such as genetic polymorphisms may influence the metabolism of overdoses of GHB among humans.

3.7 Future work

The *in vitro* data presented in this study encourage the progressing for *in vivo* experiments in knockout mice. A model for the murine enzyme (AKR1A4) had already been established to investigate its role in ascorbic acid biosynthesis (conversion of D-glucuronate to L-glulonate) (Gabbay *et al.*, 2010). The pharmacokinetics and toxicity of GHB can be assessed in these mice and compared to the pharmacokinetics and toxicity of GHB in control mice.

Alternatively, overexpression of AKR1A1 in transgenic mice prior to GHB treatment, and studying the impact on GHB elimination, is a way to establish the exact role of this enzyme in GHB overdoses.

CHAPTER FOUR:

INVESTIGATION OF FACTORS AFFECTING ENDOGENOUS GHB CONCENTRATIONS IN HAIR

4 Investigation of factors affecting endogenous GHB concentrations in hair

4.1 Introduction

4.1.1 Preface to hair testing

Since the detection of opiate metabolites in human hair in 1979 (Baumgartner *et al.*, 1979), hair has been considered as an alternative biological matrix for investigation of drug abuse history. When compared with other traditional toxicological matrices such as blood and urine, hair posses several advantages that encourage its use in forensic analysis.

First, sample collection is easy, and does not require specialist skills. Second, samples can be stored indefinitely at room temperature without the need to use preservatives, which eliminates the risk of sample degradation observed with other types of samples. Finally, the detection window is extended to several weeks and sometimes up to several months (depending on the hair length), so it is very useful to document chronic use and drug abuse history while this is not possible with blood or urine samples (Pragst and Balikova, 2006).

On the other hand, the necessity to use a large ball of hair is a drawback to the analysis. Another restriction is exogenous contamination from the environment which may lead to false positive results in certain drug examinations.

The most important use of hair in toxicological analysis is the determination of drug abuse history or the ingestion of a drug in a specific time and this is

determined via hair segmentation. Hair is divided into short lengths where each segment represents a specific time period starting from the proximal segment. By analyzing all the segments, a time course of drug exposure can be determined taking individual hair growth rate into account (Gallardo and Queiroz, 2008). Individual growth rate is determined by obtaining a second sample after a month and comparing its length with the first sample.

Although the exact mechanism for drug incorporation in hair is still unclear, there is evidence that drugs can enter hair by several routes: from the blood stream (Borges *et al.*, 2002); sweat (Raul *et al.*, 2004); or from the environment (Potsch and Moeller, 1996). Incorporation of a certain drug in hair from the blood stream depends on the melanin content of the hair, and the lipophilicity and basicity of the compound itself which control its passage through the cell membrane (Joseph *et al.*, 1996).

The Society Of Hair Testing (SOHT) recommends the collection of hair samples from the posterior vertex area of the head as close as possible to the scalp (Society of Hair Testing, 2004). This is because of the uniformity in growth rate in this site and the lack of age-related and gender-related influences, as most hair is in the anagen stage (growth phase). Collection is performed about 4 weeks after an incident in order to allow the hair to grow off the scalp. In order to exclude the possibility of external contamination, hair undergoes a decontamination procedure to remove impurities from hair care products and any adherent compounds from the environment. An organic solvent must be included in hair washing to eradicate oils. The use of dichloromethane for this purpose has been reported (Kintz *et al.*, 2009, Villain *et al.*, 2006); because it is a non protic solvent which does not swell the hair so

does not extract materials from it. In routine laboratory analysis, the washing is retained and analyzed to eliminate contamination. However, it has been shown that different washing procedures produce different analytical concentrations (Paulsen *et al.*, 2001)

The next step is separating drugs from the hair matrix. In order to effectively extract drugs from hair, many factors need to be considered including the chemical structure of the drug, its binding to proteins, its polarity, pH and its sensitivity to the substances employed during sample preparation (Pragst and Balikova, 2006). It is advisable to develop one extraction procedure that allows the detection and quantification of many drugs simultaneously. Sonication with methanol is the most commonly used extraction method because it is compatible with most drug groups. Nevertheless, high impurities are presented in the extract and the recovery is deficient (Pragst and Balikova, 2006). Digestion of the hair with sodium hydroxide is preferable to extract alkaline-resistant drugs (Klein *et al.*, 2004, Couper *et al.*, 1995). Samples are then cleaned-up by either solid-phase extraction (SPE), or by liquid-liquid extraction, before applying chromatographic techniques to determine drug concentrations (Figure 4.1)

Interpretation of hair results requires a complete understanding of the compound properties, the circumstances of sample collection, and the surrounding environment such as the detection of nicotine in the hair of a person living in a smoking environment. A further complication is when a compound is excreted endogenously to the hair where it is preferable to use each subject as his own control.

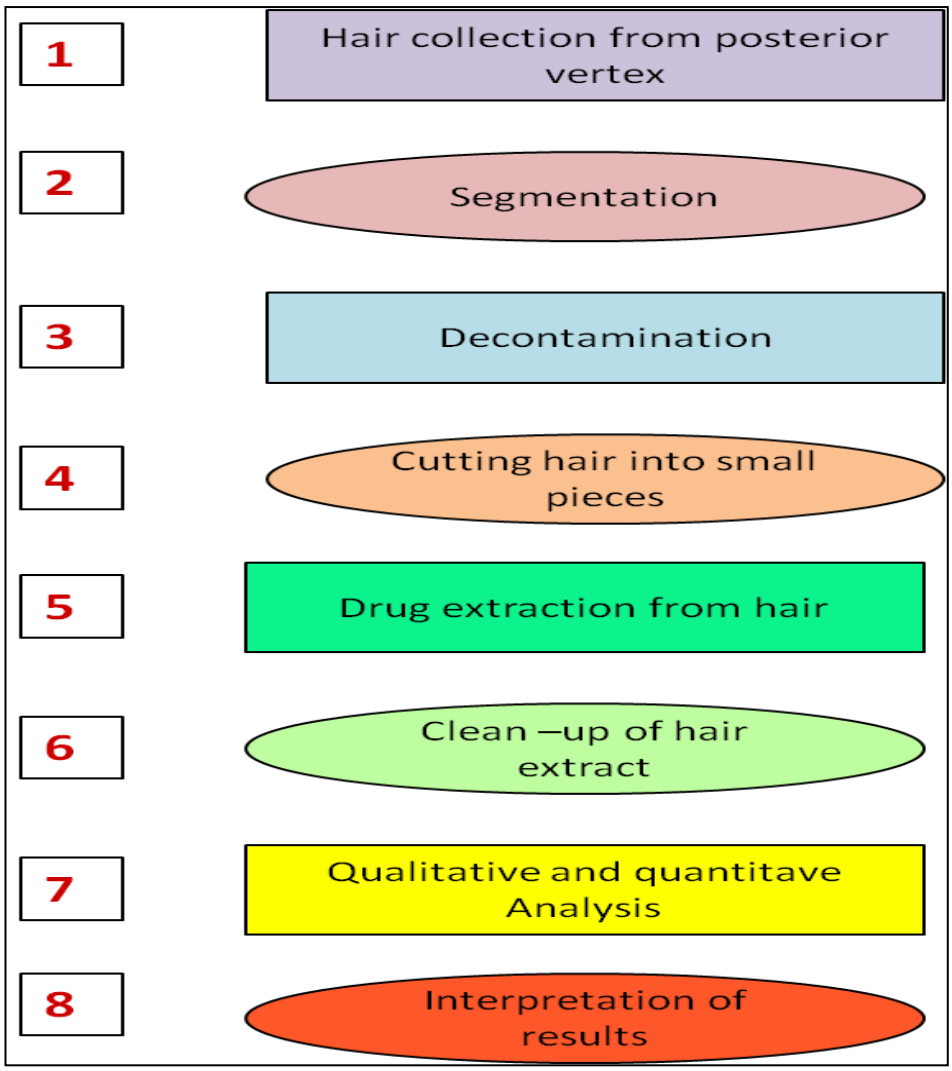

Figure 4.1: Steps of hair analysis. Steps of hair analysis adapted from (Pragst and Balikova, 2006). Other recommendations put decontamination prior to segmentation.

4.1.2 GHB in hair

The use of hair to detect GHB intake in forensic cases has gained significant interest due to the narrow window of detection in blood and oral fluid (5 hours) (Kintz *et al.*, 2001), and in urine (up to 12 hours) (Brenneisen *et al.*, 2004). In GHB–related sexual assault cases, amnesia is a common symptom (Nicholson and Balster, 2001), so the time between the incident and sample collection is generally extended to 1-2 days, which limits the opportunity to detect GHB in body fluids.

Using hair, GHB ingestion has been confirmed one month after the incident in a rape case by analyzing the victim's hair via segmental analysis (Kintz *et al.*, 2003). In another case, the repeated co-ingestion of GHB and morphine over a period of 7 months was verified by hair analysis (Rossi *et al.*, 2009).

Given that GHB is an endogenous product, it is expected to be present in the hair at low levels even if ingestion has not taken place. However, variation in the normal levels among people has been reported (Kintz *et al.*, 2003) ranging from 0.5 to 12 ng/mg of hair. Therefore, determining whether the detected GHB is endogenous or as a result of drug exposure, may be problematic in some cases. In a recent study, endogenous GHB interfered with the results of the analysis of a sample eleven months after an assault (Scott, 2009). Although GHB was elevated in a hair segment corresponding to the time period of the alleged ingestion, it could not be concluded that it was from exposure because of the variation in the results. Therefore, studying

endogenous GHB in hair and identifying the factors affecting its variation is necessary for successful interpretation of toxicological results.

One of the factors proposed to influence natural GHB levels is melanin content. Two studies examined this hypothesis by grouping hair samples into three categories: black, brown, and blond. The number of samples were 24 (Kintz *et al.*, 2003) , and 61 samples (Goulle *et al.*, 2003) . No significant difference was observed in either study, so it was concluded that hair colour does not affect endogenous GHB levels in hair which is perhaps not surprising since melanin binds mostly basic and hydrophobic drugs (Howells *et al.*, 1994).

The first study examined also the gender factor by grouping the 24 samples into male and female sets, and the difference was not significant as well.

To date, hair colour and gender are the only factors that have been studied in hair. Other factors may influence GHB endogenous levels in hair. Age for example affects hair growth rate and anagen ratio (Tajima *et al.*, 2007), and race affect drug incorporation in hair. In an *in vitro* study, hair samples from different ethnic groups were exposed to cocaine and morphine and when analyzed, the two drugs in African American hair samples were 31 fold higher than Caucasian or Asian samples although all samples were black in colour (Kidwell *et al.*, 2000). This may be due for genetic or cultural reasons. Race may also influence GHB levels by the different in expression levels of alcohol dehydrogenase (ADH) and aldehyde dehydrogenase (ALDH)

presented in hair cells (Potsch *et al.*, 1997, Goedde *et al.*, 1980) and their genetic polymorphism.

Besides, daily habit factors such as smoking or drinking may influence endogenous GHB levels in hair. Administration of alcohol increased endogenous GHB levels in rat liver and brain (Roth, 1970) which may be a result of ethanol and GHB competition for NAD^+ dependent degradation. In addition, smoking is considered a factor because of the interaction of nicotine and GHB on $GABA_B$ receptors. Baclofen, a well known agonist for $GABA_B$ receptor, antagonised GHB and nicotine self-administration in mice (Fattore *et al.*, 2001, Fattore *et al.*, 2002).

To determine the influence of these factors on endogenous GHB levels in hair, hair samples from subjects varying in ages, races and dietary preference were obtained and analyzed.

4.2 Aim of this chapter

The aim of this chapter is to investigate the effect of some epidemiological factors on the endogenous levels of GHB in hair.

The objectives in this research are:

- To obtain hair samples from individuals differing in their background and lifestyle, and who have had no contact with GHB.

- To determine endogenous GHB levels in hair by GC/MS

- Interpretation of the results by considering one epidemiological factor at a time, and applying an appropriate statistical analysis to observe any significant difference

4.3 Materials and methods:

4.3.1 Chemicals:

Deuterated GHB (GHB-d6) was obtained from Cerilliant at a concentration of 1 mg/ml in methanol. GHB sodium salt and N,O-Bis(trimethylsilyl)trifluoroacetamide (BSTFA) were purchased from Sigma Aldrich. Ethyl acetate, dichloromethane, all HPLC grade, 98% sulphuric acid and hydrochloride acid AR grade were also from Sigma Aldrich (UK) and sodium hydroxide was bought from Fisher Scientific (UK).

4.3.2 Sample collection:

As hair is considered a biological sample in Scotland, ethical approval from the University of Strathclyde was obtained before starting the experiment. 28 subjects volunteered to participate in this experiment and all of them completed an epidemiological survey where they provided information about their age, ethnic background, smoking and drinking habits. The subjects also stated clearly that they had not taken any exogenous GHB. Each survey was anonymously given a reference number which was also recorded on the collected hair sample. Hair samples were collected according to the recommendation of the Society of Hair Testing (Society of Hair Testing, 2004). Briefly, hair was collected from the posterior vertex by cutting the hair as near as possible from the scalp. Each sample was kept aligned and wrapped in aluminium foil then was saved in a paper envelope away from light at room temperature.

The first proximal cm of every hair sample was chosen to compare endogenous GHB between individuals for two main reasons;

First: The first proximal cm was obtainable in male and female hair, regardless of hair length, so this allows an accurate judgment on the levels of endogenous GHB in the same segment of the hair between people.

Second: In real GHB cases hair is recommended to cut into 3 mm long segments. However, it was shown that the first 3 mm proximal segment of the hair can be contaminated by sweat which has high levels of endogenous GHB (Goulle *et al.*, 2003, Kintz *et al.*, 2003), and the authors recommended waiting 4-5 weeks before hair collection. Therefore, analyzing the whole 1 cm will minimize the possibility of contamination by sweat to one third.

4.3.3 Washing procedure:

Hair samples were cut and washed following the recommendation of the Forensic science department in Glasgow University (Scott, 2009). In brief, the first cm of each hair sample was cut and placed carefully in a capped glass beaker. Each hair segment was sonicated for 3 minutes in distilled water then the water was poured out. This procedure was repeated once with distilled water and twice with dichloromethane. After drying completely, each segment was cut finally into very short pieces.

4.3.4 Measuring endogenous GHB concentration using the standard addition method:

A standard addition method was previously used by (Elliott, 2003) in order to determine endogenous GHB concentrations in urine by GC/MS. Applying a standard addition method in this experiment was necessary in order to obtain accurate measurements of the very low levels of GHB with the GC/MS technique. 10 µl of GHB (1 µg/ml) was added to the hair samples, producing GHB levels above the limit of detection of the assay. To further control the addition and to determine the exact concentration of supplemented GHB, standard samples of 10 µl of GHB (1 µg/ml) were treated, extracted and analyzed exactly in the same way and at the same time as hair samples. This permitted accurate measurement of the GHB concentration added to the hair samples. Consequently, GHB levels in hair were determined by subtracting the mean concentration of GHB in standard samples from the hair GHB concentration measured. One hair sample was spiked with 0.5, 1, 2, 5 and 10 µl of GHB (1 µg/ml) and 50 µl of GHB-d6 (1 µg/ml) as internal standard in order to evaluate the method precision and linearity.

4.3.5 Extraction of GHB from hair:

GHB is an acidic compound and therefore it is stable in alkaline environment. An extraction method for GHB has been validated previously and was the method of choice for endogenous GHB in hair in the literature (Kintz *et al.*, 2003, Goulle *et al.*, 2003, Stout *et al.*, 2010). The method was used

in this study with minor modifications. Briefly, 10 mg of each hair sample was weighed and placed into 4 ml glass tube. 50 µl of GHB-d6 (1 µg/ml), and 1 ml of sodium hydroxide (0.01 M) were added to the tube. 10 µl of GHB (1 µg/ml) was also added for the standard addition method. The mixture was incubated for 16 hours at 56 °C with agitation at 80 rpm. After incubation, samples were allowed to cool at room temperature then 100 µl of HCL (0.1 M) was used to neutralize the solution. GHB then was extracted by the addition of 100 µl of sulphuric acid (0.05 M) and 3 ml of ethyl acetate (HPLC grade), followed by mixing by inversion for 5 minutes, and the sample was then centrifuged at 2500 rpm/5 minutes. The organic layer was transferred into fresh 4 ml glass tube, dried under moderate flow of nitrogen and derivatized with 75 µl of BSTFA for 30 minutes at 70 °C.

4.3.6 Gas chromatography–mass spectrometry conditions:

The samples were analyzed by GC/MS .Gas chromatography (Focus GC), mass spectrometry (DS QII) and autosampler (AS 3000) were all from Thermo Scientific (UK). The column used was from Varian LTD (UK) (Factor four capillary column, VF-1ms 30m x 0.25mm x 0.25 µm, 100% dimethylpolysiloxane). 2 µl was injected in the splitless mode at 250 °C. The oven was programmed to start at 60 °C, held for 2 minutes, then ramped to 180 °C at 15 °C/min, held for 1 minutes, then ramped again to 300 °C at 50°C/min and held for 8 minutes. The total analysis time was 26 minutes. Scanning was performed in the selected ion monitoring (SIM) mode. Helium flow rate was 1 ml/min. The two ions monitored for quantification purposes were 233 for GHB and 239 for GHBD6. 204 and 117 were chosen for identification purposes. Data were analyzed using Xcalibur software.

4.3.7 Calculation of the LOD and the LOQ

The limit of detection (LOD) and the limit of quantification (LOQ) were calculated as described by (Daneshvar *et al.*, 2003).

LOD = 3.3 (SD/S)

LOQ= 10 (SD/S)

Where S is the slope of the calibration curve, and SD is the standard deviation of the Y intercept.

4.3.8 Statistical analysis:

Graph Pad Prism software version 4.00 for Windows, GraphPad Software, (San Diego California, USA) was used for statistical analysis and non-parametric tests were applied. The Mann–Whitney test was used to compare between two independent groups. The Kruskal-Wallis test was used to compare between more than two independent groups

4.4 Results

4.4.1 Extraction and detection of GHB in hair

In order to determine GHB concentration in hair samples, GHB was extracted from hair using alkaline hydrolysis which was performed in mild conditions using 0.01 M of NaOH at 56 °C for 16 hours. This method was shown to successfully extract GHB from hair, and produce a relatively clean chromatogram (Goulle *et al.*, 2003). After cooling to room temperature, the mixture was neutralized using HCl, and then was acidified with 0.05 M of sulphuric acid. GHB is an acidic compound and has a pKa of 4.72 (Nord *et al.*, 1983), so in a pH less than 4, GHB is present mainly in the uncharged form. Therefore, it can move from the aqueous phase to the organic phase, allowing liquid–liquid extraction of the compound. At a pH between 3 and 4, GHB is stable and is not converted to GBL, as the lactone conversion of GHB requires a pH lower than 2, and a long incubation time (Chappell et al., 2004, LeBeau et al., 2000)

GHB was derivatized using BSTFA, and was injected into the GC/MS in the selected ion monitoring (SIM) mode. Deuterated GHB served as internal standard. Ion 233 was quantified for GHB (Figure 4.2) and 239 for GHB-d6, and the peak area ratio of 233 to 239 was calculated to determine GHB concentrations. Based on the mass spectrum of derivatized GHB in the full scan mode in Figure (4.3), ions 204 and 117 were chosen for identification purposes. Retention time was 7.02 minutes for GHB and 6.95 minutes for GHB-d6 (Figure 4.4)

A

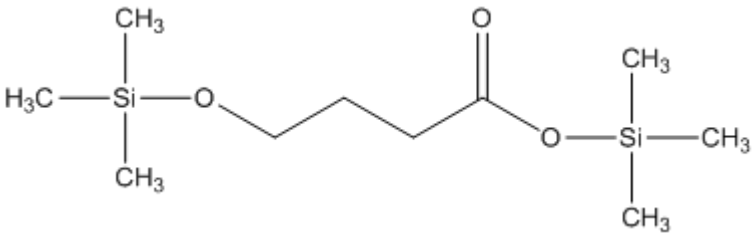

B

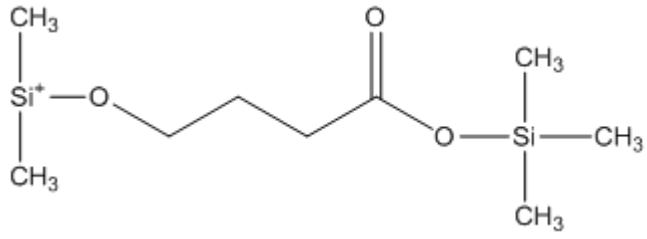

Figure 4.2: Derivatized GHB and origin of *m/z* 233. A) Derivatized GHB: The molecular weight (m) is 248 **. B)** Precursor ion 233**:** Positive ion 233 is generated by the loss of a methyl group (m-15).

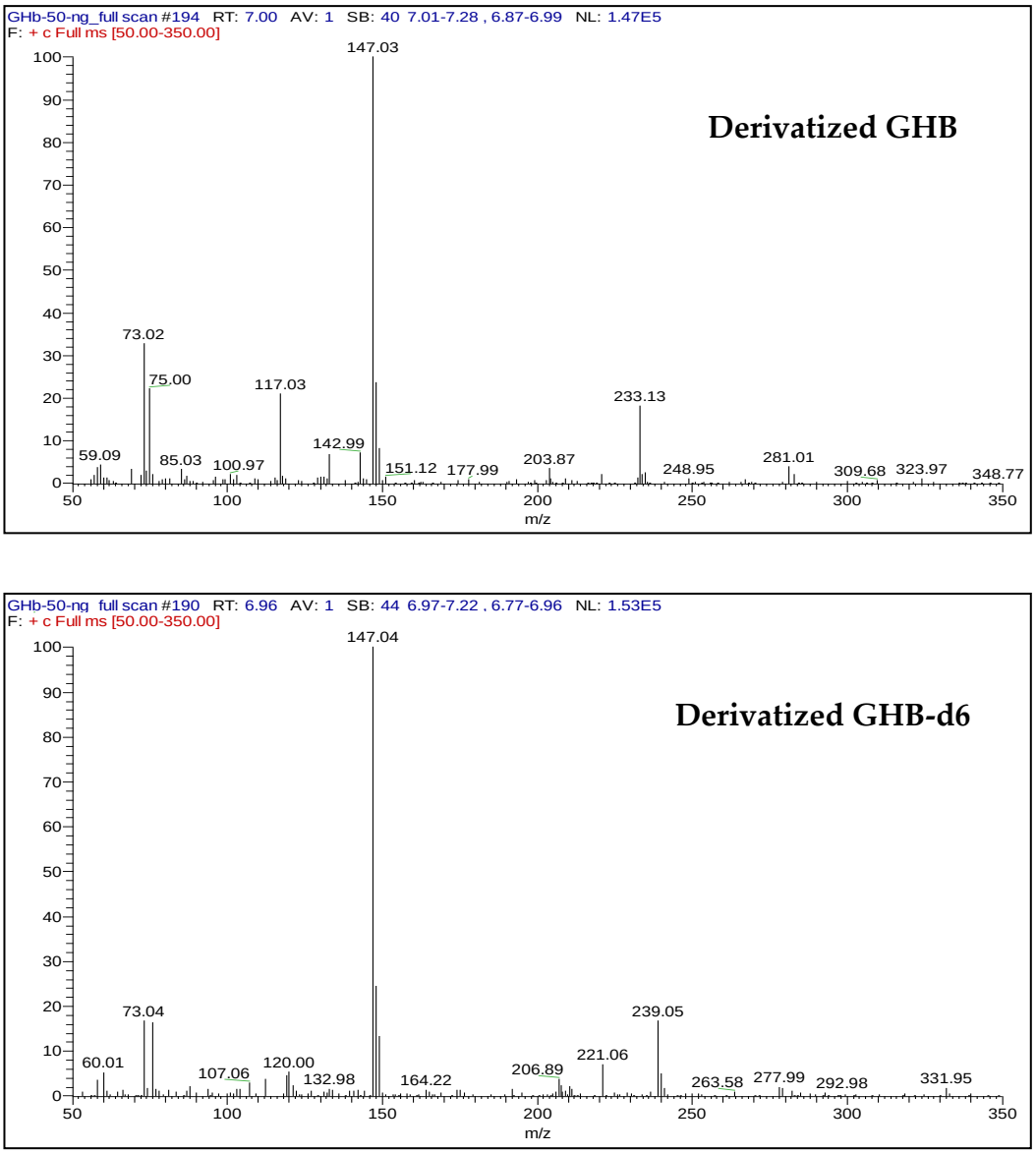

Figure 4.3: Mass spectrum of derivatized GHB by GC/MS. Mass spectrum of a derivatized GHB (50 µl of 1 µg/ml) and derivatized GHB-d6 (50 µl of 1 µg/ml) obtained using the electron impact (EI) ionization in the positive mode

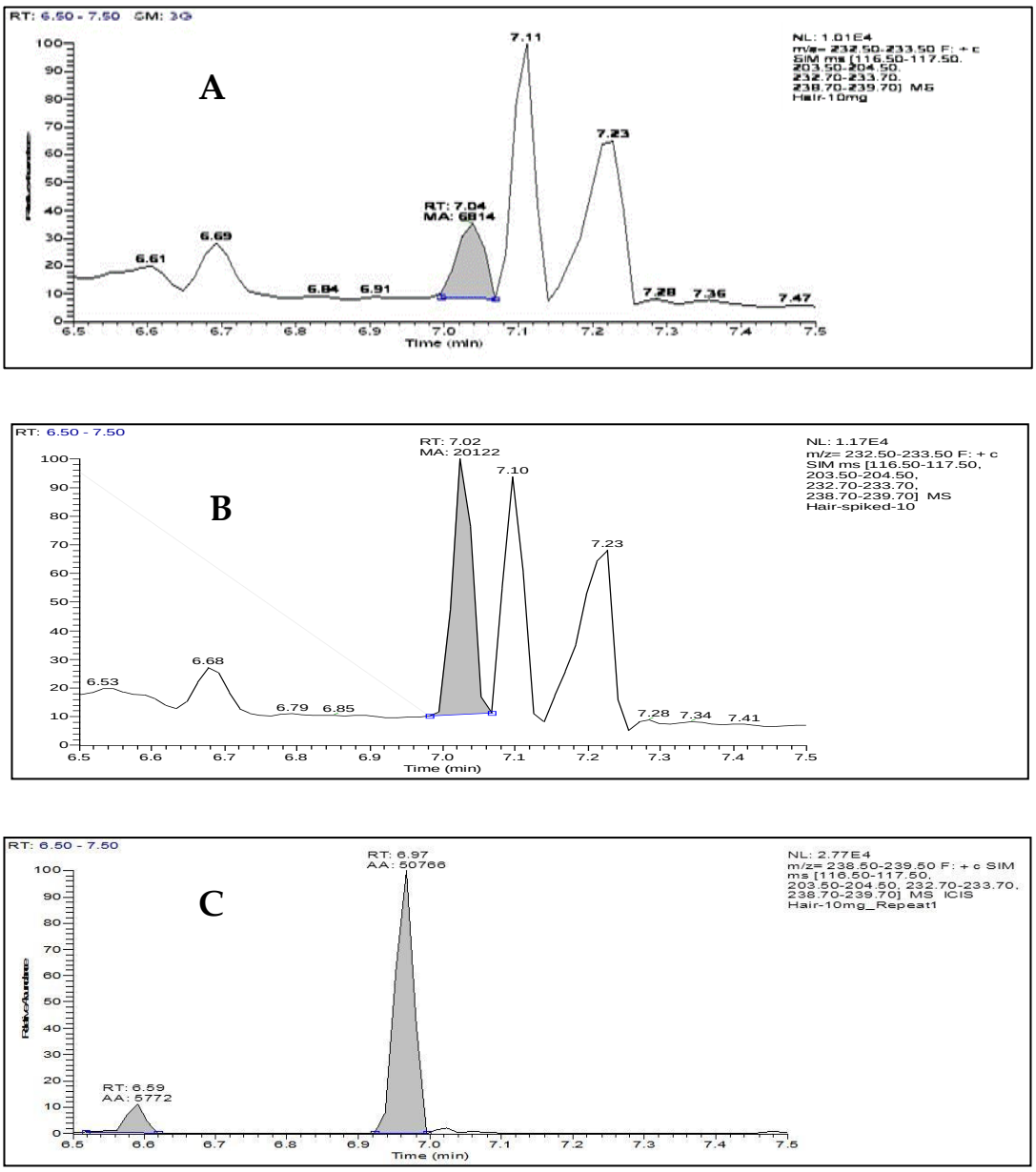

Figure 4.4: GC/MS chromatogram of hair samples spiked with GHB and GHB-d6. 10 mg of hair sample was extracted and analyzed in the SIM mode and two ions (233 and 239) were monitored for GHB and GHB-d6 respectively.**A)** Endogenous GHB in hair sample **B)** Hair sample spiked with 10 µl of GHB (1µg/ml) and, **C)** Hair sample spiked with 50 µl of GHB-d6 (1µg/ml) and. RT is 7.02 minutes for GHB and 6.98 minutes for GHB-d6

4.4.2 Validation of GC/MS method

The same hair sample was used in the creation of a calibration curve. 10 mg of hair was spiked with 0.5, 1, 2, 5, 10 ng/ml of GHB. Samples were extracted and analyzed as mentioned in materials and methods. The peak area ratio of GHB to GHB-d6 was calculated and a calibration curve was created by plotting the area ratio against the amount of GHB. The correlation of coefficient (R2) in this range was determined by linear regression analysis to be 0.994 (Figure 4.5). The LOD and LOQ for the assay were 1.13 ng and 3.49 ng respectively. Therefore, spiking all hair samples with a standard addition of 10 μl of GHB (1 μg/ml) produced concentrations the above the LOD and the LOQ of the assay, allowing accurate measurement of GHB.

The relative standard deviation (RSD) was determined for each sample (n = 3), and the mean minus the RSD was greater than zero. Absolute recovery was assayed by spiking hair samples (n = 3) with 10 ng/ ml of GHB. The samples were extracted as described, but the internal standard GHB-d6 (50 ng/ml) was added prior to evaporation. The absolute recovery was determined to be 98.9 % by comparing the extracted GHB/GHB-d6 ratio to that of the unextracted samples at the same concentrations.

Intraday precision: hair samples (n = 3) and water samples were spiked at 3 concentrations of GHB (10, 20 and 50 ng/ml), and were extracted and injected 3 times at the same day. The RSD for each concentration are listed in table 4.1. Intraday precision was determined for control samples of GHB prepared in distilled water (n = 10) and injected on different days. The RSD was 7.8 %

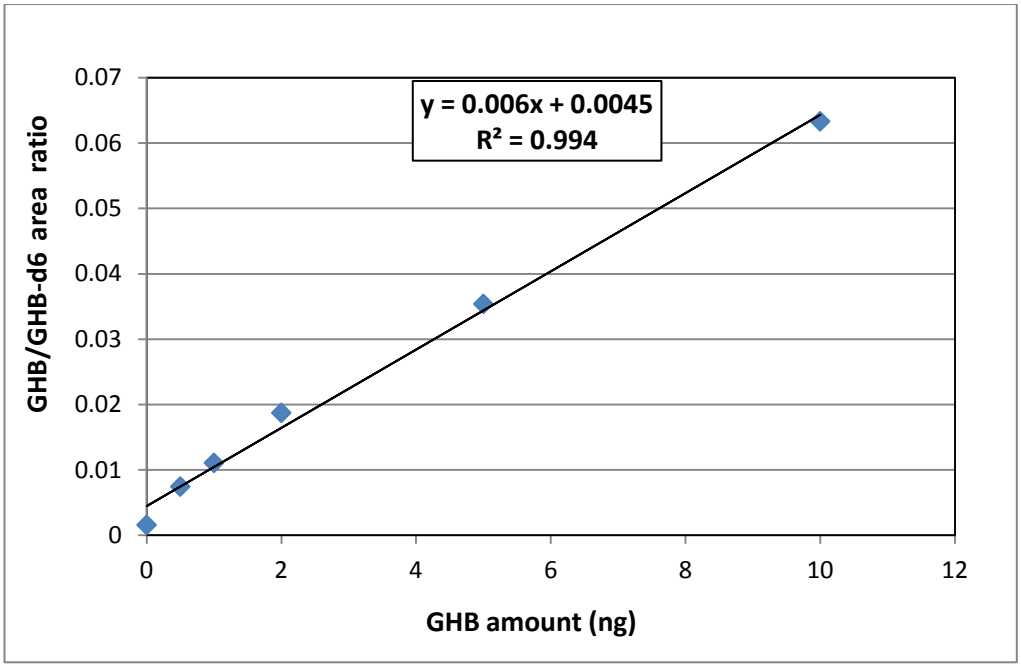

Figure 4.5: Calibration curve of GHB in hair. One hair sample was spiked with 0.5 ,1, 2, 5, 10 µl of GHB (µg/ml), before it was extracted and analyzed as described in materials and methods. The peak area ratio of GHB /GHB-d6 was plotted against the amount of spiked GHB in hair. The method was linear between 1 and 10 ng of GHB

GHB concentration	Intraday precision (%RSD) Hair	Intraday precision (%RSD) water
10	5.1	8.3
20	7.6	10
50	2.6	4.4

Table 4.1: Intraday precision results for GHB

4.4.3 Influence of gender on GHB endogenous concentration in hair:

In order to evaluate the effect of gender on endogenous GHB concentration in hair, samples from 20 males and 8 females were collected and analyzed by GC/MS. Endogenous concentrations were determined as described in the methods and materials section .The results are shown in Figure (4.6).

Table 4.2 showed the comparison between the two groups. GHB in male samples (n = 20) ranged from 0.02 to 0.65 ng/mg with an average of 0.24 ng/mg and a median of 0.2 ng/mg. In female samples (n = 8) GHB ranged from 0.04 to 0.35 ng/mg with an average of 0.19 ng/mg and a median of 0.18 ng/mg. The medians of the two groups were compared using the Mann Whitney test. Two tailed p value was more than 0.05 and Mann Whitney U statistic was 73.

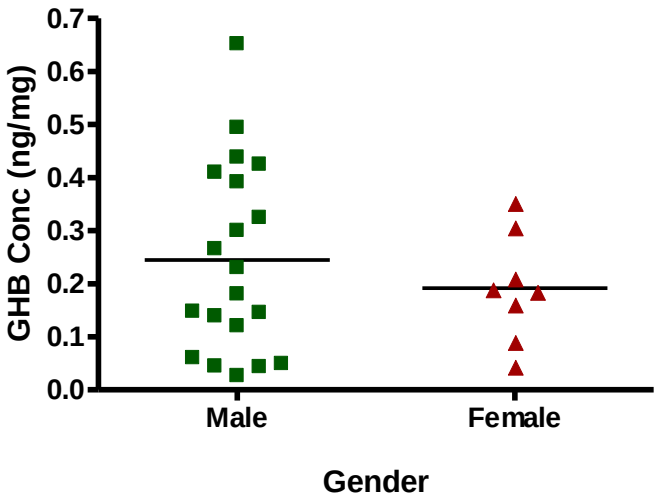

Figure 4.6: Endogenous GHB levels in males and females. A scatter plot of GC/MS analysis of GHB in male and females hair samples

Table 4.2: Comparison of endogenous concentrations of GHB (ng/mg) in hair samples based on gender

	Male	Female
n	20	8
%	71.4%	28.5 %
Range	0.02-0.65	0.04-0.35
Mean	0.24	0.19
Median	0.2	0.18

4.4.4 Influence of ethnicity and age on GHB endogenous concentration in hair:

The effect of ethnicity was assessed by grouping the samples into six ethnic groups; Middle-Eastern, Caucasians, Asians, Africans, Indians, and individuals who come from two or more ethnic groups. Kruskal –Wallis test was used to compare the groups. The results are plotted in Figure (4.7). Table 4.3 summarises the comparison between the ethnic groups. Middle Eastern group had a median of 0.11 ng/mg (n=12) while the Caucasian group had a median of 0.23 ng/mg (n=11). One Asian participant has a concentration of 0.35 ng/mg, and one participant from Indian/Pakistani origin had a concentration of 0.41 ng/mg. One participant from African origin had a concentration of 0.04 ng/mg. Two subjects who were of mixed ethnicities had a median of 0.41 ng/mg. The medians of the Middle Eastern and Caucasian groups were significantly different when compared by the Mann-Whitney test.

The influence of age on GHB metabolism was also evaluated. The participants were divided into three groups; Less than 30 years, 30-50 years, more than 50 years (Figure 4.8). Half of the samples were in the 30-50 years group. A smaller increase was observed in GHB levels as age increased but was not significant (Table 4.4).

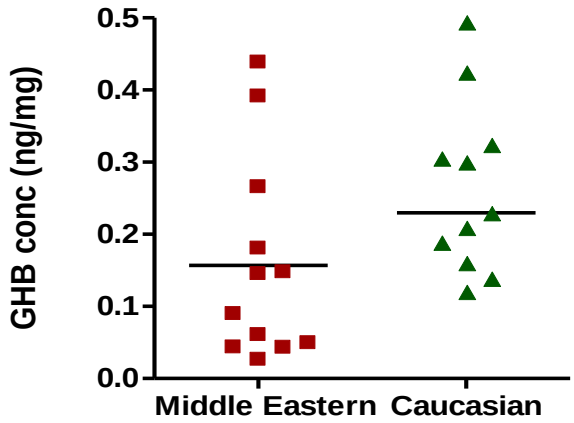

Figure 4.7: Endogenous GHB levels in ethnic groups. A scatter plot of GHB determined by GC/MS in Middle Eastern and Caucasian hair samples.

Table 4.3: Comparison of endogenous concentrations of GHB (ng/mg) in hair samples based on Ethnicity		
	Middle eastern	**Caucasian**
n	12	11
%	42.8 %	39.2 %
Range	0.02-0.43	0.12-0.49
Mean	0.15	0.26
Median	0.11	0.23

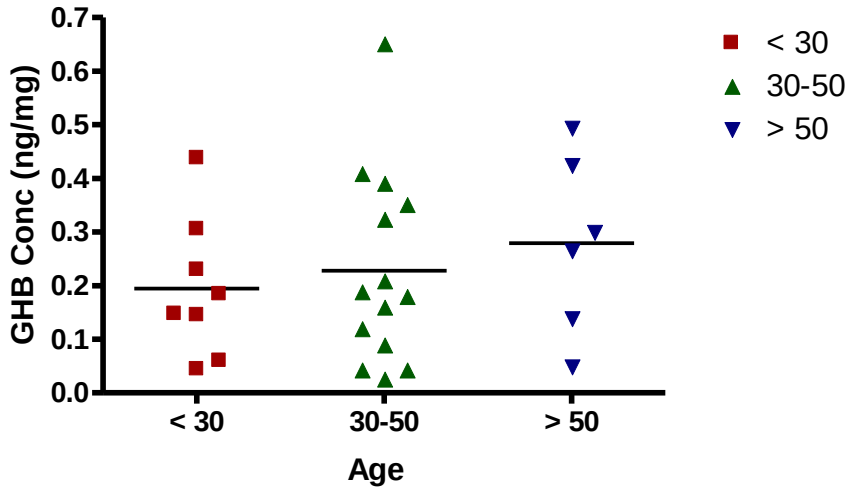

Figure 4.8: Endogenous GHB levels in different age groups. A scatter plot of GC/MS analysis of GHB in hair samples from subjects less than 30 years, 30-50 years, and more than 50 years

Table 4.4: Comparison of endogenous concentrations of GHB (ng/mg) in hair samples based on age

	< 30	**30-50**	**> 50**
n	8	14	6
%	28.5 %	50 %	21.4%
Range	0.04-0.43	0.02-0.65	0.05-0.49
Mean	0.19	0.22	0.27
Median	0.16	0.18	0.28

4.4.5 Effect of smoking and drinking on endogenous GHB level in hair:

Smoking and drinking are popular habits in some parts of the world. To investigate whether smoking influences GHB levels, hair samples were assembled into smokers and non-smokers groups (Figure 4.9). Of the total number of 28 samples, 12 were from individuals who declared that they smoked regularly and the remaining 16 were from individuals who did not smoke at all. The results in Table 4.5 show that smokers had a mean and median of 0.20 and 0.16 ng/mg GHB respectively. The mean for non-smokers was 0.24 ng/mg and the median was 0.19 ng/mg. The 12 smoker subjects were 11 males and one female. The 16 non-smoking subjects were 9 males and 7 females. The medians were not statistically different using the Mann Whitney test (Table 4.5).

To examine the effect of drinking, hair samples were divided in to two categories according to alcohol consumption: 14 samples from individuals who declared they consume alcohol regularly, and 14 samples from donors who did not consume alcohol at all (Figure 4.10). The Mann Whitney test was used for statistical analysis and results are summarized in Table 4.6

Although drinkers had higher values of GHB when compared to abstainers, this was not statistically different using the non parametric Mann-Whitney test.

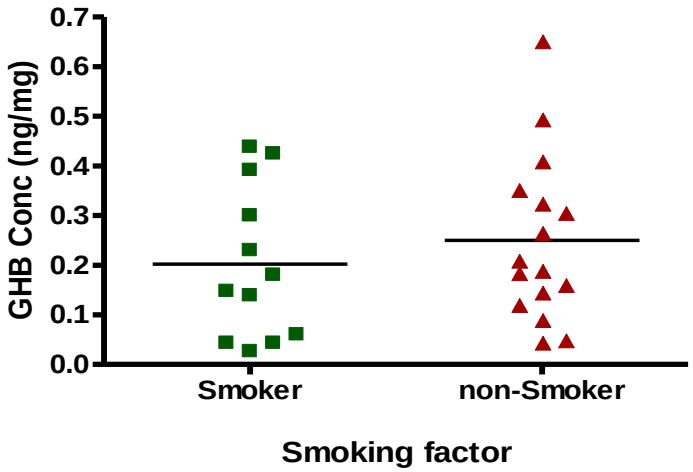

Figure 4.9: Endogenous GHB levels in smokers and non-smokers groups. A scatter plot of GC/MS analysis of GHB in hair samples from smokers and non-smokers individuals

Table 4.5: Comparison of endogenous concentrations of GHB (ng/mg) in hair samples based on smoking habit

	smoker	non smoker
n	12	16
%	42.8 %	57.1 %
Range	0.02-0.43	0.04-0.65
Mean	0.20	0.24
Median	0.16	0.19

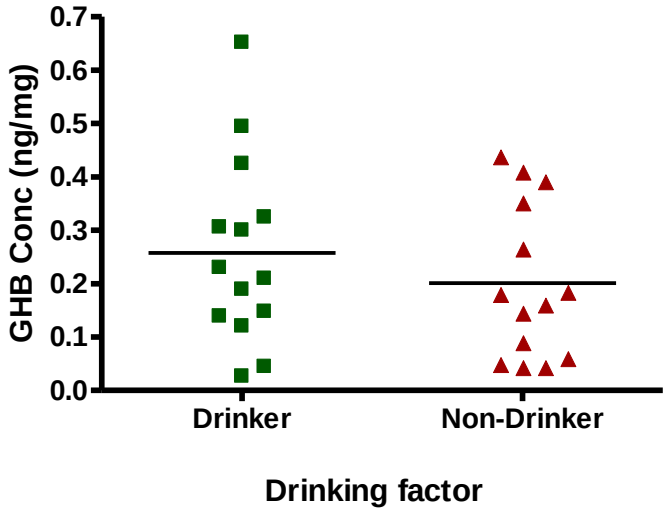

Figure 4.10: Endogenous GHB levels in drinkers and abstainers groups. A scatter plot of GC/MS analysis of GHB in smokers and non-drinkers hair samples

Table 4.6: Comparison of endogenous concentrations of GHB (ng/mg) in hair samples based on drinking habit

	Drinker	non drinker
n	14	14
%	50 %	50 %
Range	0.02-0.65	0.04-0.43
Mean	0.25	0.2
Median	0.21	0.17

4.5 Discussion

The work described in this chapter aimed to examine the effect of some epidemiological factors on the endogenous levels of GHB in hair. The factors examined in this study were gender, ethnicity, age, smoking, and drinking.

Hair is a useful matrix to study GHB metabolism, as it contains endogenous GHB, and it offers the opportunity to observe the endogenous levels of GHB over a period of several months. By using different hair samples, GHB metabolism between individuals can be compared, by evaluating the parent compound that is excreted into hair cells.

It has already been demonstrated that endogenous GHB levels in hair is widely distributed between individuals. This indicates a difference in GHB metabolism in the population, leading to the variation in the amount of GHB excreted into hair. However, it was not clear whether this variation is solely due to the amount of GHB in circulation, or to the factors influencing drug transportation and incorporation in hair. To verify this point, several epidemiological factors were examined.

In this study, hair samples from 28 volunteers were analyzed and assembled in to groups based on one factor at a time. Non parametric tests were applied because GHB endogenous levels are not normally distributed in humans. A

great variability in GHB endogenous levels was observed among the 28 samples tested.

The gender factor was examined and found to not influence GHB levels in hair. This agrees with a previous study which reported that there is no difference in the endogenous level of GHB in hair between males and females (Kintz *et al.*, 2003). That study compared only 8 male and 16 female samples, and the type of statistical test used was not mentioned. Nevertheless, in urine, a study reported that GHB concentration is significantly higher in males. However, the study compared only 5 males to 3 females and 7 of the subjects were African Americans (LeBeau et al., 2002)

In addition, ethnicity did not significantly alter endogenous GHB levels. Yet, the number of samples in three groups (Asian, Indian, and African) was not sufficient to draw a conclusion. A large-scale study including participants from mixed ethnicities is necessary in order to evaluate the influence of ethnicity of the endogenous levels in hair. This is particularly important as variation in the single nucleotide polymorphism (SNP) in GHB metabolizing enzymes may be influenced by ethnic –related factors.

A small increase of GHB was observed with age, agreeing with an earlier study that measured endogenous GHB in urine in large populations (n = 207) where a small increase of GHB was noted with age (Moriya *et al.*, 2006)

No significant difference was observed between smoking and non smoking groups. These results are in agreement with a preliminary study that measured endogenous GHB in urine samples (Moriya *et al.*, 2006). This previous study had been carried out on a population of 20 subjects including 4 drinkers and 4 smokers and samples were collected 3 times a day from each subject for 5 days. Endogenous GHB was higher in smokers than non-smokers although it was not statistically different and inter-day variation was recorded.

Nicotine has a known pharmacological effect on $GABA_B$ receptors to which GHB binds at higher concentrations (Lingenhoehl *et al.*, 1999). The interaction between GHB and nicotine has been observed previously in a systematic study in 125 subjects during acute administration of GHB. Current smokers developed greater acute intoxication symptoms from administered GHB than former or never smokers (Kim *et al.*, 2008). However at endogenous levels, GHB binds to a specific receptor distinct from $GABA_B$ receptor which may explain the lack of nicotine effect at endogenous levels (Moriya *et al.*, 2006).

Although drinkers had higher values of GHB when compared to abstainers, this was not statistically different using the non parametric Mann-Whitney test. Previously, the presence of GHB and its prodrug GBL were reported in alcoholic beverages (Elliott and Burgess, 2005) such as red wine and white wine. In red wine, GHB concentrations ranged from 4.1 to 21.4 mg/L (mean = 12.6 mg/L) in different types of red wine and GBL concentrations were more than 5 mg/L while in white wine GHB levels were lower (range 3-9.6 mg/L, mean = 5.7 mg/L) and GBL was also detected above 5 mg/L . GHB and GBL were not detected in beer, rum, vodka or whisky. It is therefore possible the higher GHB concentrations in alcohol consumers were due to its presence in some alcoholic drinks. However, participants in the current study did not identify the type of alcoholic drink consumed

4.6 Conclusions:

The endogenous GHB concentrations quantified in our study fit within the range reported by other investigators. In addition, our results have shown that GHB endogenous levels are not altered by the epidemiological factors investigated.

To our knowledge, this is the first report that has looked into the possible effect of drinking and smoking on GHB endogenous concentrations in hair. Given that hair can be used to document drug history and lifestyle, we investigated the hypothesis that smoking or drinking had an effect on endogenous GHB levels in

hair. If there is an effect, it will be more observable in hair rather other type of samples because of the long-term window that can be used.

Although no significant difference in GHB levels between drinkers and abstainers was found, it would be valuable to include the type of alcoholic drink in the toxicological report when investigating a GHB-related case as this may influence detectable GHB levels.

4.7 Future work

The ethnicity factor needs further investigation with a large number of samples for each ethnic group.

An alternative approach to determine the reasons beyond GHB variation is to study this variation on the genetic level. Identifying single nucleotide polymorphism (SNPs) in the genes corresponding to GHB-metabolizing enzymes may provide valuable information that help to understand the difference of GHB levels in hair.

CHAPTER FIVE:

SUMMARY AND GENERAL DISCUSSION

5 Summary and general discussion

Gamma hydroxybutyrate (GHB) has gained importance given the multiple facets of the compound. GHB has been prescribed for therapeutic purposes (Fuller and Hornfeldt, 2003, Addolorato *et al.*, 1999), has been sold over the counter as an anabolic supplement (Van Cauter *et al.*, 1997) and has been abused as a recreational drug and as a date-rape drug (Rodgers *et al.*, 2004, Stillwell, 2002). Furthermore, GHB was discovered to be of endogenous origin (Bessman and Fishbein, 1963), and was assigned the role of a neurotransmitter and neuromodulator (Vayer *et al.*, 1987).

GHB metabolism has been a key issue for all these roles. Understanding the pathway and the fate of the drug are essential for medical and forensic applications as well as for neurological studies. A range of experiments have been carried out to determine the steps of the pathway, and have identified SSA, succinate, and GABA as metabolites of GHB. Additional experiments have been performed to reveal the enzymes responsible for these reactions and have isolated specific enzymes from different organs and species. Despite this progress, little was known about the degree of their involvements and the required conditions for their work.

The HOT enzyme was originally recognized as a hydroxyacid oxoacid transhydrogenase (Kaufman *et al.*, 1988a), but its encoding gene was only recently identified as an iron containing alcohol dehydrogenase (Kardon *et al.*, 2006). AKR1A1 was proposed to be identical to the high K_m aldehyde reductase

(Vayer *et al.*, 1985b), but it was uncertain whether it works mainly as a SSA reductase or as a GHB dehydrogenase (Cash *et al.*, 1979, Kaufman *et al.*, 1979).

The work in this thesis investigated several different aspects of GHB metabolism. The HOT enzyme has been produced in *E. coli* as a recombinant protein in order to characterize the enzyme and to explore its use in GHB detection. The gene encoding AKR1A1 was knocked down in 1321N1 and HepG2 cell lines to determine the participation of this enzyme in GHB synthesis and breakdown. Finally, the correlation between endogenous GHB levels in hair and some epidemiological factors have been examined in an attempt to bridge the molecular analysis gap in hair testing.

5.1 Summary and Discussion

The major findings of this thesis are summarized below.

5.1.1 Recombinant HOT can be expressed and purified from *E. coli*

The work described in **Chapter 2** aimed to produce human HOT enzyme in large quantities using recombinant DNA technology, in order to enable the characterization of the enzyme *in vitro*. The HOT protein was expressed artificially in *E. coli* and purified using immobilized metal affinity chromatography. Induction was optimised to give the best expression in a

limited time using low IPTG concentrations. Purification of recombinant HOT protein was performed under denaturing conditions since the protein was located in the insoluble fraction of *E. coli* cells. This method was time and cost – saving and can be applied for large –scale purification. The HOT protein was successfully recovered from inclusion bodies in high purity for subsequent investigations.

Since the HOT protein was denatured during purification, a refolding step needed to be carried out before assaying the activity of the enzyme. In the literature, variable refolding methodologies were reported as the refolding step is highly protein-specific. In this work, four established refolding techniques were compared over the activity of HOT. Refolding by size exclusion chromatography was the method of choice for this enzyme.

5.1.2 HOT can be used to assay GHB

A new enzymatic assay was developed to assay the transhydrogenase activity of HOT by measuring the resultant SSA in a simple colorimetric assay. The methods described previously for HOT transhydrogenase activity were performed by coupling the reaction to NAD-dependent SSADH either in a continuous reaction using recombinant SSADH (Kardon *et al.*, 2006) or in a discontinuous assay using GABAse (Kaufman *et al.*, 1988a). However, when applying the continuous assay to measure HOT activity, the purified

recombinant SSADH had a high background activity with α-ketoglutarate which obstructed the accurate measurement of initial rate. Chromatographic assays have been reported elsewhere (Struys *et al.*, 2005b), but it is time-consuming and costly for enzymatic studies.

In **Chapter 2**, the transhydrogenase activity of HOT was assayed in a discontinuous assay using equal amounts GHB and α-ketoglutarate. The reaction was stopped and SSA was measured (Vasil'ev and Eremin, 1968, Taberner *et al.*, 1972). The assay showed linearity in the range of concentrations measured and was sensitive to nanomolar amount of SSA. Therefore, the HOT enzyme can be used to monitor GHB. This assay is better than previously published enzymatic assays because of the ability of HOT to metabolize low levels of GHB, and the lack of interaction with alcohols as HOT does not use ethanol as a substrate. The development of the HOT assay in order to apply it forensically to detect GHB in alcoholic beverages and body fluids are considered in future studies.

5.1.3 HOT does not require NAD for GHB-dehydrogenase activity

HOT only catalyzes GHB oxidation to SSA if α-ketoglutarate is present to work as hydrogen acceptor. In reactions lacking α-ketoglutarate, no activity was recorded. Therefore, in the context of GHB metabolism, HOT manifests transhydrogenase activity between GHB and α-ketoglutarate, and this reaction does not need any supplemented elements such as iron or NAD^+.

The results are intriguing given that HOT is an ADHFe1, generally considered to be NAD-dependent. It was previously postulated that HOT is similar to lactate-malate transhydrogenase (EC 1.1.99.7) from *Micrococcus lactilyticus* which contains a tightly bound NAD^+/NADH prosthetic group (Allen and Patil, 1972). Further support to this assumption was provided by the identification of the gene encoding HOT to be from the NAD dependent iron containing alcohol dehydrogenase subfamily (Kardon *et al.*, 2006). In this study, HOT was denatured during the purification process, so if a NAD^+ prosthetic group was present in the enzyme structure, it would have been released following denaturation of the protein. Consequently, addition of NAD^+ would have been essential for enzyme activity. Nevertheless, this was not the case as HOT maintained transhydrogenase activity in the absence of NAD^+, and the addition of 1 mM of NAD^+ to the reaction did not improve the activity. However, elucidating the structure of HOT can only confirm or refute the presence of a NAD prosthetic group.

5.1.4 HOT can oxidize octanol using NAD as a cofactor

The dehydrogenase activity of HOT in relation to GHB metabolism was assayed (**Chapter 2**). Although the ADHFe1 gene encoding HOT belongs to the NAD dependent iron-containing alcohol dehydrogenase group, HOT does not have a $NAD(P)^+$- dependent GHB dehydrogenase activity even when including ferric or ferrous ions in the reaction. However, when other alcohols were tested, HOT was shown to possess NAD-dependent octanol dehydrogenase activity. It seems

that when HOT uses $NAD(P)^+$ as hydrogen acceptor, it prefers a long aliphatic alcohol as a substrate. Given that the ADHFe1 gene encoding HOT is the only human member in the iron-dependent group which consists mainly of bacterial proteins (Deng *et al.*, 2002), it may refer to a diversity in the catalyzing activity between the members, despite the similarity in their gene sequences.

Since the structure of HOT has not been resolved yet, the NAD binding site is still a question. Figure 5.1 shows multiple sequence alignment of several members of the iron-containing ADH group including HOT and 1,2-propanediol oxidoreductase from *E. coli* (FucO) . The structure of FucO which shares a 45% similarity in protein sequence to HOT (Blast analysis) is shown in Figure 5.2. The active site is located in the cleft between the two domains of the enzyme, one domain is consisted of α helics and β sheets, while the other includes only α helices (Figure 5.2A). Four amino acids (Asp196, His200, His263, and His277) are involved in metal binding where the iron ion is coordinated tetrahedrally (Figure 5.2B). NAD binds in the cleft and interrelates with the residues in the N-terminal domain.

As the HOT protein was successfully purified and refolded, structure studies which require large quantities of purified protein free of urea and imidazole can also be performed in future.

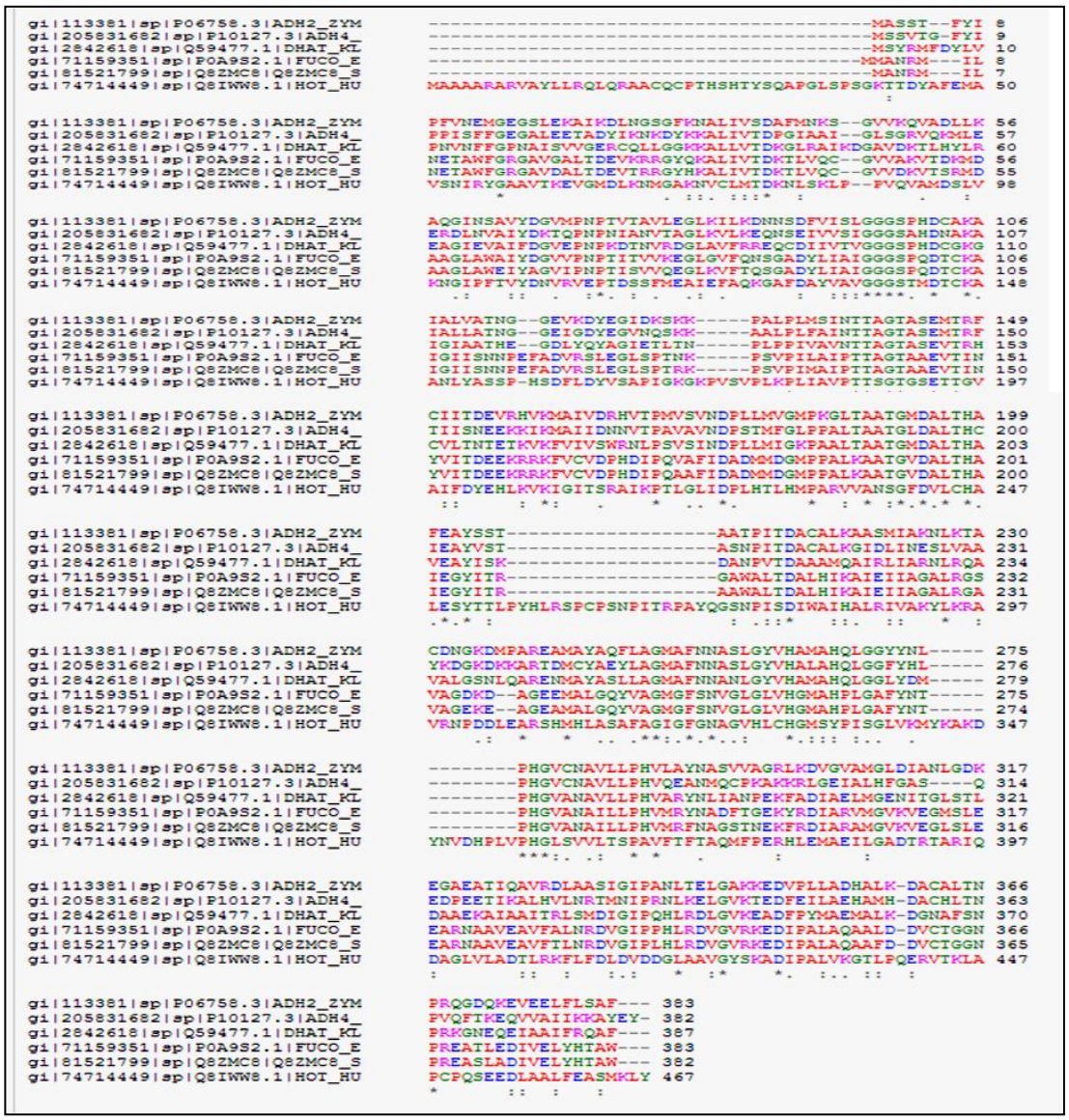

Figure 5.1: Sequence alignments of iron-containing alcohol dehydrogenases. ClustalW2 multiple sequence alignments of alcohol dehydrogenase II from *Z. mobilis* (ADH2) (accession no.P06758), alcohol dehydrogenase IV from *S. cerevisiae* (ADH4) (accession no P10127), 1,3-propanediol oxidoreductase from *K. pneumonia* (accession no Q59477), 1,2-propanediol oxidoreductase from *E. coli* (FucO) (accession no P11549), 1,2-propanediol dehydrogenase from S. enteric (1,2-Prd) (accession no Q8ZMC8), and the HOT protein (accession no Q8IWW8)

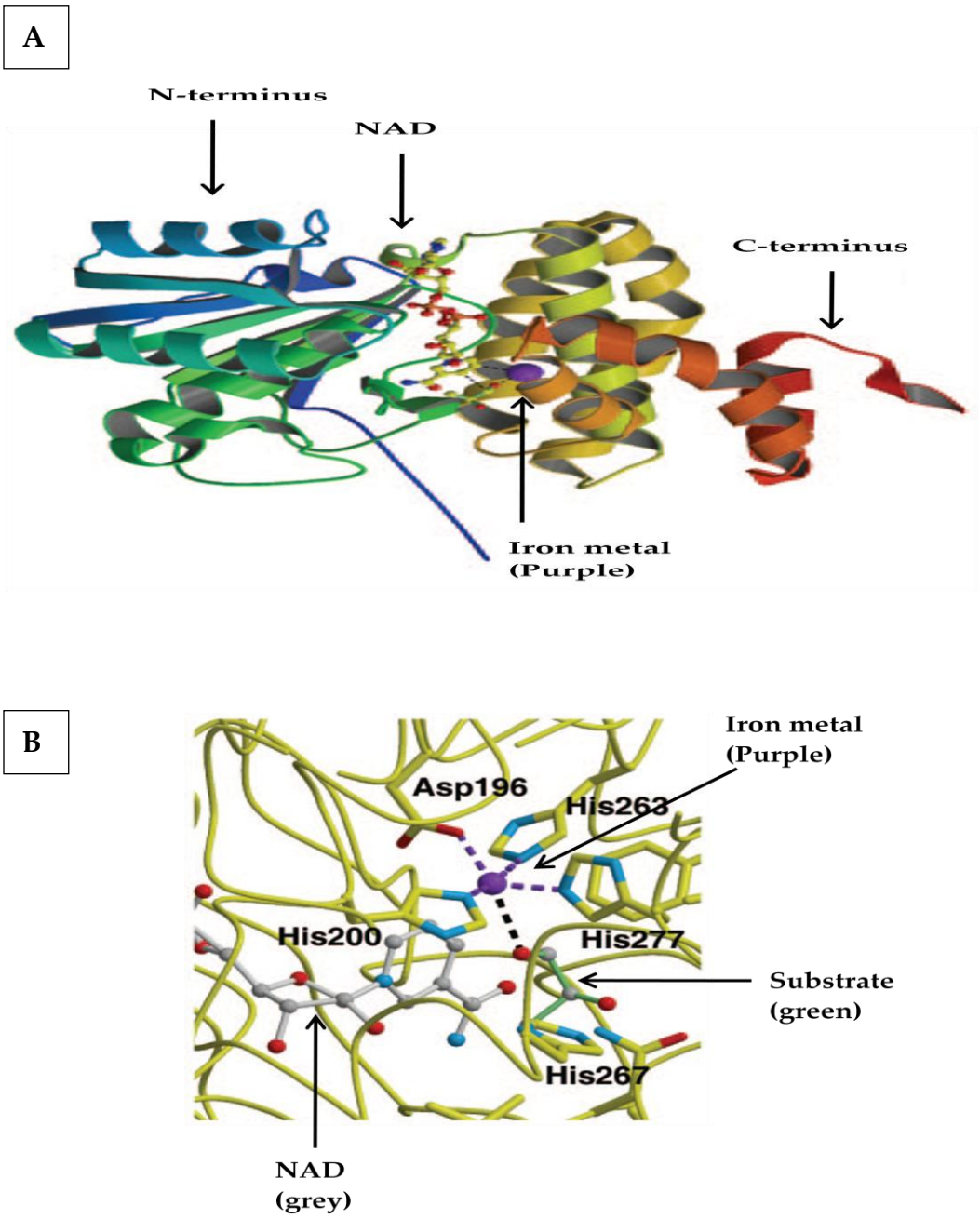

Figure 5.2: A ribbon diagram of the 1,2-propanediol oxidoreductase (FucO). A) The N-terminus starts from residue 1 and the S-terminus starts at residue 183. The active site is located between the two subunits and the binding sites of iron and NAD are displayed. **B)** Stereo representation of the active site of FucO. The substrate, NAD and iron binding sites are displayed and the important residues are labelled. Adopted from (Montella *et al.*, 2005)

5.1.5 Aldehyde reductase (AKR1A1) does not play a role in endogenous GHB metabolism

Aldehyde reductase has been proposed to be involved in GHB metabolism for some years. In order to determine the extent of AKR1A1 participation in GHB metabolic pathway, RNA interference technology was utilised in **Chapter 3**. The gene encoding AKR1A1 was silenced in 1321N1 and HepG2 cell lines using double-stranded specific siRNA, and measurement of RNA and protein levels demonstrated a successful knocking down of the AKR1A1 gene.

In GHB synthesis, the ability of 1321N1 and HepG2 cells to reduce SSA to GHB was considerably decreased by AKR1A1 silencing. However, this reduction was only observed at millimolar concentration of SSA, and not at micromolar concentration which is in agreement with the postulation that AKR1A1 is the high K_m aldehyde reductase (Vayer *et al.*, 1985b). Thus, it is compatible with GHB endogenous levels in 1321N1 and HepG2 cells being insensitive to AKR1A1 silencing, and consequently, this excludes AKR1A1 from the endogenous GHB biosynthesis pathway. Other enzymes such as AKR7A2 may take a part (Lyon *et al.*,2007)

In GHB catabolism, AKR1A1 also appear to have no impact on endogenous GHB degradation since GHB dehydrogenase activity was not affected by knocking down AKR1A1.

5.1.6 Aldehyde reductase (AKR1A1) may play a role in the catabolism of exogenous GHB

Silencing of AKR1A1 leads to a significant decrease in the ability of cells to degrade millimolar concentrations of GHB, and this effect was mostly noticeable in HepG2 cells. This indicated a role of AKR1A1 in exogenous GHB catabolism. To clarify this point, the cells were treated with 50 μM of GHB and extracellular and intracellular GHB levels were measured by GC/MS. The results revealed a significant increase in extracellular GHB levels in 1321N1 cells and intracellular GHB levels in HepG2 cells. Taken together, these results show that AKR1A1 is actively involved in the catabolism of exogenous GHB catabolism in 1321N1 and HepG2 cells. It also shows different behaviours of 1321N1 and HepG2 cells in response to GHB administration, revealing that HepG2 cells store GHB inside the cells while 1321N1 cells secrete it into the media. This indicates that HepG2 cells may use excessive GHB for cellular processes, possibly for energy production through the TCA cycle, while 1321N1 cells use GHB as a neurotransmitter regardless of its origin. However, it also shows that high doses of GHB may damage liver cells prior to CNS cells, but neurological symptoms which are resulted from GHB secretion and binding to receptors are initially apparent.

The role of AKR1A1 in GHB catabolism *in vivo* will be the focus of future studies to determine the extent of AKR1A1 participation in knock-out models following a dose of GHB.

5.1.7 Mechanism of endogenous and exogenous GHB catabolism by AKR1A1 and HOT

The HOT enzyme was sensitive to 50 μM of GHB (**Chapter 2)**, unlike AKR1A1 which has a high K_m for GHB (10 mM)(Vayer *et al.*, 1985b). Therefore, it is likely that HOT is involved in endogenous GHB catabolism, while AKR1A1 is responsible for exogenous GHB degradation (**Chapter 3).** The subcellular localization of the two enzymes offers further evidence to this hypothesis. Endogenous GHB is synthesized from GABA by mitochondrial GABA-T (Reijnierse *et al.*, 1975), and AKR7A2 which is believed to be mitochondrial in some cell types such as SHSY5Y (Keenan *et al.*, 2006). GHB is then oxidized to SSA which is further oxidized to succinate by the mitochondrial enzyme SSADH in order to enter the TCA cycle in the mitochondria. It is therefore appropriate for the enzyme oxidizing endogenous GHB to SSA to be mitochondrial which raises preference for HOT. In this approach the entire endogenous GHB metabolic pathway occurs in the mitochondria without the interference of cytosolic AKR1A1. However, it is yet to be determined whether AKR7A2 is mitochondrial in 1321N1 and HepG2 cells. When GHB is administrated exogenously, it is transported into the cells. As a result, high levels of GHB are present in the cytosol where AKR1A1 is localized. Therefore, AKR1A1 is likely to be the major enzyme responsible for degrading excessive GHB to SSA which is transported to the mitochondria so as to be converted to succinate or to GABA (Figure 5.3).

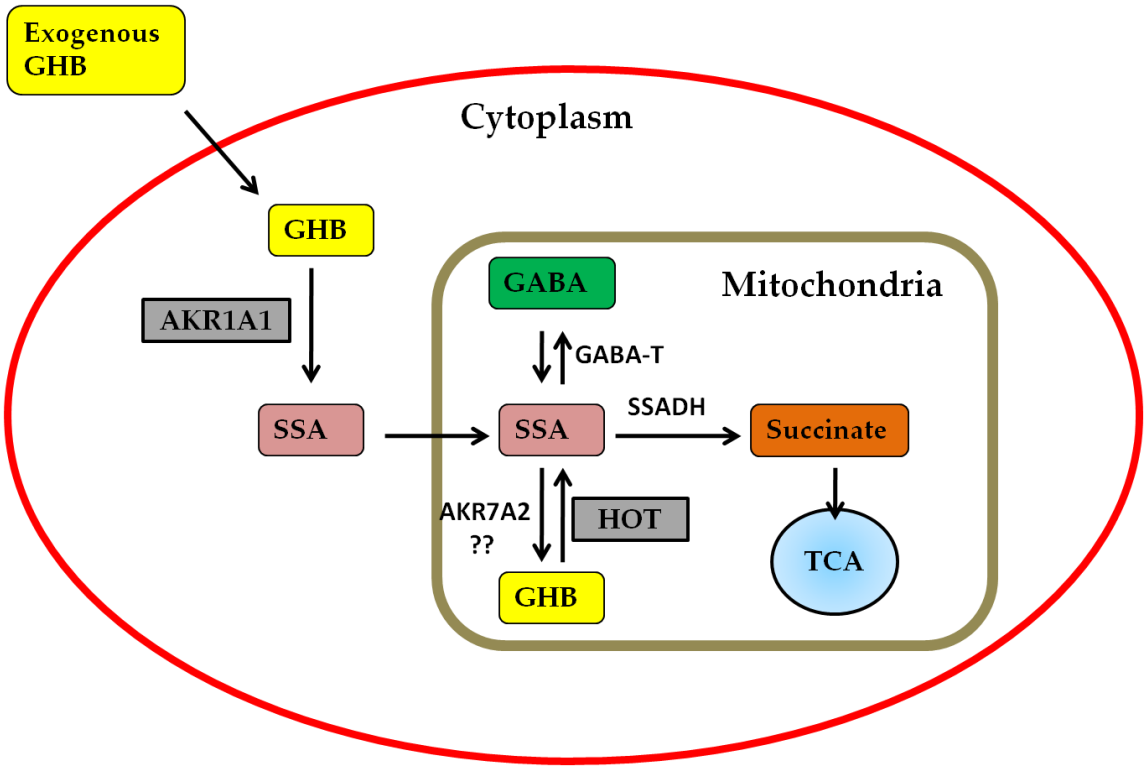

Figure 5.3: Proposed mechanism of endogenous and exogenous GHB metabolic pathway. The proposed enzymes are drawn in grey boxes.

5.1.8 GHB causes proliferation in 1321N1 and HepG2 cells

The cell viability assay (MTT assay) revealed a proliferative effect of low concentrations of GHB on 1321N1 and HepG2 cells (**Chapter 3**). Cell proliferation was mostly observed at the lowest concentration of GHB used in this study (1 μM), and was inversely proportional to GHB concentrations. 1321N1 cells were more responsive to proliferation than HepG2 cells, where even the highest tested concentration (500 μM) caused cell proliferation. GHB also causes proliferation in the neuroblastoma cell line SH-SY5Y cells (data not shown). GHB display no toxicity on 1321N1 and HepG2 cells in the range of concentrations tested. More than 80% of HepG2 cells were still viable after 24 hours treatment with 500 μM of GHB.

Cell proliferation is a cellular response for abnormal conditions such as oxidative stress when low amount of reactive oxygen species (ROS) is produced (Martindale and Holbrook, 2002). Since it was previously shown that GHB induced oxidative stress in rat cerebral cortex when it was administered at 10 mg/kg for 1 hour (Sgaravatti *et al.*, 2007), it is possible that the proliferative effect is another reaction to oxidative stress provoked by GHB. However, the link between GHB and oxidative stress was only studied *in vivo (Sgaravatti et al., 2007, Sgaravatti et al., 2009)*, so cell proliferation was not included as a marker for oxidative stress in these studies. Nevertheless, it is worth noting that higher doses of GHB (more than 100 mg/kg) had a protective effect against oxidative stress (Mamelak, 2007).

5.1.9 Endogenous GHB levels in hair are not dependent on gender, age, ethnicity, smoking or drinking

Endogenous GHB is not restricted to the central nervous system or to the liver. It is disposed into body fluids such as urine (LeBeau et al., 2002), sweat (Abanades *et al.*, 2007), saliva (De Paoli *et al.*, 2011) as well as in hair (Goulle *et al.*, 2003). In forensic cases, these samples are usually collected to determine exposure, but in GHB case, the endogenous origin may interfere with the results. This is particularly observed in hair and sweat where a great variability was reported between individuals (Kintz *et al.*, 2003, Abanades *et al.*, 2007). Therefore, the work in **Chapter 4** aimed to explain the reasons behind this variation in hair. Several epidemiological factors such as gender, ethnicity, age, smoking and drinking were examined in relation to endogenous GHB levels in 28 hair samples from GHB-free donors. It was hypothesised that these factors may interfere with GHB synthesis or transportation to the hair cells, or with hair cell growth cycle. The results in hair confirmed the variation in GHB endogenous levels, but non parametric statistical tests did not illustrate any correlation between GHB natural levels and any of the factors. It seems that GHB disposition in hair is far complex than to be correlated with one factor. However, the study here has some limitations in the number of samples and in the use of standard addition method. Hence, a large-scale study is required to release the causes behind GHB variation in hair.

The lack of correlation between endogenous GHB in hair and the factors studied accentuates the importance of using the subject own hair as control in forensic cases. It also suggests the examination of GHB disposition in hair on a

molecular level to determine whether this variation is resulted from different levels in the blood stream or from a various rate in GHB transportation to the hair cells.

5.2 Conclusions

In conclusions, the present work contributes to the comprehension of GHB catabolism by determining the level of AKR1A1 and HOT contribution to GHB metabolic pathway. The study provides a mechanistic insight into endogenous and exogenous GHB degradation by AKR1A1 and HOT. The research was novel in terms of silencing AKR1A1 in cell lines, and of producing HOT as a recombinant protein for use in GHB assays. In addition, the study describes the first attempt to link endogenous GHB concentrations in hair to factors such as ethnicity, smoking and drinking.

BIBLIOGRAPHY

Abanades, S., Farre, M., Segura, M., Pichini, S., Pastor, A., Pacifici, R., Pellegrini, M. & de la Torre, R. 2007. Disposition of gamma-hydroxybutyric acid in conventional and nonconventional biologic fluids after single drug administration: issues in methodology and drug monitoring. *Ther Drug Monit,* **29,** 64-70.

Addolorato, G., Balducci, G., Capristo, E., Attilia, M. L., Taggi, G., Gasbarrini, G. & Ceccanti, M. 1999. Gamma-hydroxybutyric acid (GHB) in the treatment of alcohol withdrawal syndrome: a randomized comparative study versus benzodiazepine. *Alcohol Clin. Exp. Res.,* **23,** 1596–1604.

Addolorato, G., Castelli, E., Stefanini, G. F., Casella, G., Caputo, F., Marsigli, L., Bernardi, M. & Gasbarrini, G. 1996. An open multicentric study evaluating 4-hydroxybutyric acid sodium salt in the medium-term treatment of 179 alcohol dependent subjects. *Alcohol,* **31,** 341-345.

Albers, R. W. & Salvador, R. A. 1958. Succinic semialdehyde oxidation by a soluble dehydrogenase from brain. *Science,* **128,** 359-60.

Allen, S. H. & Patil, J. R. 1972. Studies on the structure and mechanism of action of the malate-lactate transhydrogenase. *J Biol Chem,* **247,** 909-16.

Anderson, I. B., Kim, S. Y., Dyer, J. E., Burkhardt, C. B., Iknoian, J. C., Walsh, M. J. & Blanc, P. D. 2006. Trends in gamma-hydroxybutyrate (GHB) and related drug intoxication: 1999 to 2003. *Ann Emerg Med,* **47,** 177-83.

Anderson, R. A., Ritzmann, R. F. & Tabakoff, B. 1977. Formation of gamma-hydroxybutyrate in brain. *J Neurochem,* **28,** 633-9.

Andrade, R., Malenka, R. C. & Nicoll, R. A. 1986. A G protein couples serotonin and GABAB receptors to the same channels in hippocampus. *Science,* **234,** 1261-5.

Andresen, H., Sprys, N., Schmoldt, A., Mueller, A. & Iwersen-Bergmann, S. 2010. Gamma-hydroxybutyrate in urine and serum: additional data supporting current cut-off recommendations. *Forensic Sci Int,* **200,** 93-9.

Andresen, H., Stimpfl, T., Sprys, N., Schnitgerhans, T. & Muller, A. 2008. Liquid ecstasy - a significant drug problem. *Dtsch Arztebl Int,* **105,** 599-603.

Andriamampandry, C., Taleb, O., Kemmel, V., Humbert, J. P., Aunis, D. & Maitre, M. 2007. Cloning and functional characterization of a gamma-hydroxybutyrate receptor identified in the human brain. *Faseb J,* **21,** 885-95.

Andriamampandry, C., Taleb, O., Viry, S., Muller, C., Humbert, J. P., Gobaille, S., Aunis, D. & Maitre, M. 2003. Cloning and characterization of a rat brain receptor that binds the endogenous neuromodulator gamma-hydroxybutyrate (GHB). *FASEB J. ,* **17,** 1691-1693.

Angulo, M. C., Le Meur, K., Kozlov, A. S., Charpak, S. & Audinat, E. 2008. GABA, a forgotten gliotransmitter. *Prog Neurobiol,* **86,** 297-303.

Bairoch, A. 1991. PROSITE: a dictionary of sites and patterns in proteins. *Nucleic Acids Res,* **19 Suppl,** 2241-5.

Banerjee, P. K. & Snead, O. C., 3rd 1995. Presynaptic gamma-hydroxybutyric acid (GHB) and gamma-aminobutyric acidB (GABAB) receptor-mediated release of GABA and glutamate (GLU) in rat thalamic ventrobasal nucleus (VB): a possible mechanism for the generation of absence-like seizures induced by GHB. *J Pharmacol Exp Ther,* **273,** 1534-43.

Baneyx, F. 1999. Recombinant protein expression in Escherichia coli. *Curr Opin Biotechnol,* **10,** 411-21.

Bania, T. C. & Chu, J. 2005. Physostigmine does not effect arousal but produces toxicity in an animal model of severe gamma-hydroxybutyrate intoxication. *Acad Emerg Med,* **12,** 185-9.

Barker, S. A., Snead, O. C., Poldrugo, F., Liu, C. C., Fish, F. P. & Settine, R. L. 1985. Identification and quantitation of 1,4-butanediol in mammalian tissues: an alternative biosynthetic pathway for gamma-hydroxybutyric acid. *Biochem Pharmacol,* **34,** 1849-52.

Barski, O. A., Gabbay, K. H. & Bohren, K. M. 1999. Characterization of the human aldehyde reductase gene and promoter. *Genomics,* **60,** 188-98.

Barski, O. A., Tipparaju, S. M. & Bhatnagar, A. 2008. The aldo-keto reductase superfamily and its role in drug metabolism and detoxification. *Drug Metab Rev,* **40,** 553-624.

Batas, B. & Chaudhuri, J. B. 1996. Protein refolding at high concentration using size-exclusion chromatography. *Biotechnol Bioeng,* **50,** 16-23.

Baumgartner, A. M., Jones, P. F., Baumgartner, W. A. & Black, C. T. 1979. Radioimmunoassay of hair for determining opiate-abuse histories. *J Nucl Med,* **20,** 748-52.

Becher, A., White, J. H. & McIlhinney, R. A. 2001. The gamma-aminobutyric acid receptor B, but not the metabotropic glutamate receptor type-1, associates with lipid rafts in the rat cerebellum. *J Neurochem,* **79,** 787-95.

Beghè, F. & Campanini, M. T. 2000. Safety and tolerability of gamma-hydroxybutyric acid in the treatment of alcohol-dependents patients. *Alcohol* **20,** 223-225.

Benavides, J., Rumigny, J. F., Bourguignon, J. J., Cash, C., Wermuth, C. G., Mandel, P., Vincendon, G. & Maitre, M. 1982a. High affinity binding sites for gamma-hydroxybutyric acid in rat brain. *Life Sci,* **30,** 953-961.

Benavides, J., Rumigny, J. F., Bourguignon, J. J., Wermuth, C. G., Mandel, P. & Maitre, M. 1982b. A high-affinity, Na+-dependent uptake system for gamma-hydroxybutyrate in membrane vesicles prepared from rat brain. *J Neurochem,* **38,** 1570-5.

Bendinskas, K., Sattelberg, P., Crossett, D., Banyikwa, A., Dempsey, D. & MacKenzie, J. A. 2011. Enzymatic detection of gamma-hydroxybutyrate using aldo-keto reductase 7A2. *J Forensic Sci,* **56,** 783-7.

Berankova, K., Mutnanska, K. & Balikova, M. 2006. Gamma-hydroxybutyric acid stability and formation in blood and urine. *Forensic Sci Int,* **161,** 158-62.

Bernasconi, R., Mathivet, P., Bischoff, S. & Marescaux, C. 1999. Gamma-hydroxybutyric acid: an endogenous neuromodulator with abuse potential? *Trends Pharmacol Sci,* **20,** 135-41.

Bessman, S. P. & Fishbein, W. N. 1963. Gamma-Hydroxybutyrate, a Normal Brain Metabolite. *Nature,* **200,** 1207-1208

Bessman, S. P. & McCabe, E. R., 3rd 1972. 1,4-Butanediol--a substrate for rat liver and horse liver alcohol dehydrogenases. *Biochem Pharmacol,* **21,** 1135-42.

Bessman, S. P., Rossen, J. & Layne, E. C. 1953. Gamma-Aminobutyric acid-glutamic acid transamination in brain. *J Biol Chem,* **201,** 385-91.

Bhattacharya, I. & Boje, K. M. 2004. GHB (gamma-hydroxybutyrate) carrier-mediated transport across the blood-brain barrier. *J Pharmacol Exp Ther,* **311,** 92-98.

Bohren, K. M., Bullock, B., Wermuth, B. & Gabbay, K. H. 1989. The aldo-keto reductase superfamily. cDNAs and deduced amino acid sequences of human aldehyde and aldose reductases. *J Biol Chem,* **264,** 9547-51.

Borgen, L. A., Okerholm, R., Morrison, D. & Lai, A. 2003. The influence of gender and food on the pharmacokinetics of sodium oxybate oral solution in healthy subjects. *J Clin Pharmacol,* **43,** 59-65.

Borgen, L. A., Okerholm, R. A., Lai, A. & Scharf, M. B. 2004. The pharmacokinetics of sodium oxybate oral solution following acute and chronic administration to narcoleptic patients. *J Clin Pharmacol,* **44,** 253-7.

Borges, C. R., Martin, S. D., Meyer, L. J., Wilkins, D. G. & Rollins, D. E. 2002. Influx and efflux of amphetamine and N-acetylamphetamine in keratinocytes, pigmented melanocytes, and nonpigmented melanocytes. *J Pharm Sci,* **91,** 1523-35.

Bowery, N. G. & Hudson, A. L. 1979. gamma-Aminobutyric acid reduces the evoked release of [3H]-noradrenaline from sympathetic nerve terminals [proceedings]. *Br J Pharmacol,* **66,** 108P.

Braakman, I., Helenius, J. & Helenius, A. 1992. Manipulating disulfide bond formation and protein folding in the endoplasmic reticulum. *Embo J,* **11,** 1717-22.

Bradford, M. M. 1976. A rapid and sensitive method for the quantitation of microgram quantities of protein utilizing the principle of protein-dye binding. *Anal Biochem,* **72,** 248-54.

Brancucci, A., Berretta, N., Mercuri, N. B. & Francesconi, W. 2004a. Gamma-hydroxybutyrate and ethanol depress spontaneous excitatory postsynaptic currents in dopaminergic neurons of the substantia nigra. *Brain Res,* **997,** 62-6.

Brancucci, A., Berretta, N., Mercuri, N. B. & Francesconi, W. 2004b. Presynaptic modulation of spontaneous inhibitory postsynaptic currents by gamma-hydroxybutyrate in the substantia nigra pars compacta. *Neuropsychopharmacology,* **29,** 537-43.

Branlant, G. & Biellmann, J. F. 1980. Purification and some properties of aldehyde reductases from pig liver. *Eur J Biochem,* **105,** 611-21.

Bravo, D. T., Harris, D. O. & Parsons, S. M. 2004. Reliable, sensitive, rapid and quantitative enzyme-based assay for gamma-hydroxybutyric acid (GHB). *J Forensic Sci,* **49,** 379-87.

Brenneisen, R., Elsohly, M. A., Murphy, T. P., Passarelli, J., Russmann, S., Salamone, S. J. & Watson, D. E. 2004. Pharmacokinetics and excretion of gamma-hydroxybutyrate (GHB) in healthy subjects. *J Anal Toxicol,* **28,** 625-30.

Broughton, R. & Mamelak, M. 1979. The treatment of narcolepsy-cataplexy with nocturnal gamma-hydroxybutyrate. *Can J Neurol Sci,* **6,** 1-6.

Brown, G. K., Cromby, C. H., Manning, N. J. & Pollitt, R. J. 1987. Urinary organic acids in succinic semialdehyde dehydrogenase deficiency: evidence of alpha-oxidation of 4-hydroxybutyric acid, interaction of succinic semialdehyde with pyruvate dehydrogenase and possible secondary inhibition of mitochondrial beta-oxidation. *J Inherit Metab Dis,* **10,** 367-75.

Cammalleri, M., Brancucci, A., Berton, F., Loche, A., Gessa, G. L. & Francesconi, W. 2002. Gamma-hydroxybutyrate reduces GABA(A)-mediated inhibitory postsynaptic potentials in the CA1 region of hippocampus. *Neuropsychopharmacology,* **27,** 960-9.

Caplen, N. J., Parrish, S., Imani, F., Fire, A. & Morgan, R. A. 2001. Specific inhibition of gene expression by small double-stranded RNAs in invertebrate and vertebrate systems. *Proc Natl Acad Sci U S A,* **98,** 9742-7.

Carai, M. A., Colombo, G., Brunetti, G., Melis, S., Serra, S., Vacca, G., Mastinu, S., Pistuddi, A. M., Solinas, C., Cignarella, G., Minardi, G. & Gessa, G. L. 2001. Role of GABA(B) receptors in the sedative/hypnotic effect of gamma-hydroxybutyric acid. *Eur J Pharmacol,* **428,** 315-21.

Cash, C. D., Maitre, M. & Mandel, P. 1979. Purification from human brain and some properties of two NADPH-linked aldehyde reductases which reduce succinic semialdehyde to 4-hydroxybutyrate. *J Neurochem,* **33,** 1169-75.

Castelli, M. P., Ferraro, L., Mocci, I., Carta, F., Carai, M. A., Antonelli, T., Tanganelli, S., Cignarella, G. & Gessa , G. L. 2003. Selective gamma-hydroxybutyric acid receptor ligands increase extracellular glutamate in the hippocampus, but fail to activate G protein and to produce the sedative/hypnotic effect of gamma-hydroxybutyric acid.. *J Neurochem.* , **87,** 722-732.

Center for Disease Control 1990. Multistate outbreak of poisonings associated with illicit use of gamma hydroxy butyrate. *MMWR Morb Mortal Wkly Rep,* **39,** 861-3.

Chappell, J. S., Meyn, A. W. & Ngim, K. K. 2004. The Extraction and Infrared Identification of Gamma-Hydroxybutyric Acid (GHB) from Aqueous Solutions. *J Forensic Sci,* **49,** 52- 59.

Chin, M. Y., Kreutzer, R. A. & Dyer, J. E. 1992. Acute poisoning from gamma-hydroxybutyrate in California. *West J Med,* **156,** 380-4.

Chirgwin, J. M., Przybyla, A. E., MacDonald, R. J. & Rutter, W. J. 1979. Isolation of biologically active ribonucleic acid from sources enriched in ribonuclease. *Biochemistry,* **18,** 5294-9.

Choi, S. & Silverman, R. B. 2002. Inactivation and inhibition of gamma-aminobutyric acid aminotransferase by conformationally restricted vigabatrin analogues. *J Med Chem,* **45,** 4531-9.

Coune, P., Taleb, O., Mensah-Nyagan, A. G., Maitre, M. & Kemmel, V. 2010. Calcium and cAMP signaling induced by gamma-hydroxybutyrate receptor(s) stimulation in NCB-20 neurons. *Neuroscience,* **167,** 49-59.

Couper, F. J., McIntyre, I. M. & Drummer, O. H. 1995. Extraction of psychotropic drugs from human scalp hair. *J Forensic Sci,* **40,** 83-6.

Cromlish, J. A. & Flynn, T. G. 1985. Identification of pig brain aldehyde reductases with the high-Km aldehyde reductase, the low-Km aldehyde reductase and aldose reductase, carbonyl reductase, and succinic semialdehyde reductase. *J Neurochem,* **44,** 1485-93.

Cromlish, J. A., Yoshimoto, C. K. & Flynn, T. G. 1985. Purification and characterization of four NADPH-dependent aldehyde reductases from pig brain. *J Neurochem,* **44,** 1477-84.

Cruz, H. G., Ivanova, T., Lunn, M. L., Stoffel, M., Slesinger, P. A. & Luscher, C. 2004. Bi-directional effects of GABA(B) receptor agonists on the mesolimbic dopamine system. *Nat Neurosci,* **7,** 153-9.

Daneshvar, P., Yazdanpanah, M., Cuthbert, C. & Cole, D. E. 2003. Quantitative assay of plasma homocysteine thiolactone by gas chromatography/mass spectrometry. *Rapid Commun Mass Spectrom,* **17,** 358-62.

Danielsson, O., Atrian, S., Luque, T., Hjelmqvist, L., Gonzalez-Duarte, R. & Jornvall, H. 1994. Fundamental molecular differences between alcohol dehydrogenase classes. *Proc Natl Acad Sci U S A,* **91,** 4980-4.

De Biase, D., Barra, D., Simmaco, M., John, R. A. & Bossa, F. 1995. Primary structure and tissue distribution of human 4-aminobutyrate aminotransferase. *Eur J Biochem,* **227,** 476-80.

De Paoli, G., Walker, K. M. & Pounder, D. J. 2011. Endogenous gamma-hydroxybutyric acid concentrations in saliva determined by gas chromatography-mass spectrometry. *J Anal Toxicol,* **35,** 148-52.

Deng, Y., Wang, Z., Gu, S., Ji, C., Ying, K., Xie, Y. & Mao, Y. 2002. Cloning and characterization of a novel human alcohol dehydrogenase gene (ADHFe1). *DNA Seq,* **13,** 301-6.

Dockham, P. A., Lee, M. O. & Sladek, N. E. 1992. Identification of human liver aldehyde dehydrogenases that catalyze the oxidation of aldophosphamide and retinaldehyde. *Biochem Pharmacol,* **43,** 2453-69.

Doherty, J. D., Stout, R. W. & Roth, R. H. 1975. Metabolism of (1-14C)gamma-hydroxybutyric acid by rat brain after intraventricular injection. *Biochem Pharmacol,* **24,** 469-74.

Donjacour, C. E., Aziz, N. A., Roelfsema, F., Frölich, M., Overeem, S., Lammers, G. J. & Pijl, H. 2011. Effect of sodium oxybate on growth hormone secretion in narcolepsy patients and healthy controls. *Am J Physiol Endocrinol Metab.,* **300,** 1069-1075.

Drasbek, K. R., Christensen, J. & Jensen, K. 2006. Gamma-hydroxybutyrate--a drug of abuse. *Acta Neurol Scand,* **114,** 145-56.

Elbashir, S. M., Harborth, J., Lendeckel, W., Yalcin, A., Weber, K. & Tuschl, T. 2001. Duplexes of 21-nucleotide RNAs mediate RNA interference in cultured mammalian cells. *Nature,* **411,** 494-8.

Eli, M. & Cattabeni, F. 1983. Endogenous gamma-hydroxybutyrate in rat brain areas: postmortem changes and effects of drugs interfering with gamma-aminobutyric acid metabolism. *J Neurochem,* **41,** 524-30.

Elian, A. A. 2002. Determination of endogenous gamma-hydroxybutyric acid (GHB) levels in antemortem urine and blood. *Forensic Sci Int,* **128,** 120-2.

Elliott, S. 2001. The presence of gamma-hydroxybutyric acid (GHB) in postmortem biological fluids. *J Anal Toxicol,* **25,** 152.

Elliott, S. & Burgess, V. 2005. The presence of gamma-hydroxybutyric acid (GHB) and gamma-butyrolactone (GBL) in alcoholic and non-alcoholic beverages. *Forensic Sci Int,* **151,** 289-92.

Elliott, S., Lowe, P. & Symonds, A. 2004. The possible influence of micro-organisms and putrefaction in the production of GHB in post-mortem biological fluid. *Forensic Sci Int,* **139,** 183-90.

Elliott, S. P. 2003. Gamma hydroxybutyric acid (GHB) concentrations in humans and factors affecting endogenous production. *Forensic Sci Int,* **133,** 9-16.

Embree, L. J. & Albers, R. W. 1964. Succinic Semialdehyde Dehydrogenase from Human Brain. *Biochem Pharmacol,* **13,** 1209-17.

Fattore, L., Cossu, G., Martellotta, M. C., Deiana, S. & Fratta, W. 2001. Baclofen antagonises intravenous self-administration of gamma-hydroxybutyric acid in mice. *Neuroreport,* **12,** 2243-2246.

Fattore, L., Cossu, G., Martellotta, M. C. & Fratta, W. 2002. Baclofen antagonizes intravenous self-administration of nicotine in mice and rats. *Alcohol Alcohol.,* **37,** 495-498.

Felmlee, M. A., Roiko, S. A., Morse, B. L. & Morris, M. E. 2010. Concentration-effect relationships for the drug of abuse gamma-hydroxybutyric acid. *J Pharmacol Exp Ther,* **333,** 764-71.

Ferrara, S. D., Zotti, S., Tedeschi, L., Frison, G., Castagna, F., Gallimberti, L., Gessa, G. L. & Palatini, P. 1992. Pharmacokinetics of gamma-hydroxybutyric acid in alcohol dependent patients after single and repeated oral doses. *Br J Clin Pharmacol,* **34,** 231-5.

Fieler, E. L., Coleman, D. E. & Baselt, R. C. 1998. gamma-Hydroxybutyrate concentrations in pre- and postmortem blood and urine. *Clin Chem,* **44,** 692.

Fishbein, W. N. & Bessman, S. P. 1964. Gamma-Hydroxybutyrate in Mammalian Brain. Reversible Oxidation by Lactic Dehydrogenase. *J Biol Chem,* **239,** 357-61.

Fiszman, M. L., Borodinsky, L. N. & Neale, J. H. 1999. GABA induces proliferation of immature cerebellar granule cells grown in vitro. *Brain Res Dev Brain Res,* **115,** 1-8.

Fuller, D. E. & Hornfeldt, C. S. 2003. From club drug to orphan drug: sodium oxybate (Xyrem) for the treatment of cataplexy. *Pharmacotherapy,* **23,** 1205-9.

Fung, H. L., Haas, E., Raybon, J., Xu, J. & Fung, S. M. 2004. Liquid chromatographic-mass spectrometric determination of endogenous gamma-hydroxybutyrate concentrations in rat brain regions and plasma. *J Chromatogr B Analyt Technol Biomed Life Sci,* **807,** 287-91.

Fursova, K. K., Laman, A. G., Melnik, B. S., Semisotnov, G. V., Kopylov, P., Kiseleva, N. V., Nesmeyanov, V. A. & Brovko, F. A. 2009. Refolding of scFv mini-antibodies using size-exclusion chromatography via arginine solution layer. *J Chromatogr B Analyt Technol Biomed Life Sci,* **877,** 2045-51.

Gabbay, K. H., Bohren, K. M., Morello, R., Bertin, T., Liu, J. & Vogel, P. 2010. Ascorbate synthesis pathway: dual role of ascorbate in bone homeostasis. *J Biol Chem,* **285,** 19510-20.

Gallardo, E. & Queiroz, J. A. 2008. The role of alternative specimens in toxicological analysis. *Biomed Chromatogr,* **22,** 795-821.

Galloway, G. P., Frederick, S. L., Staggers, F. E., Jr., Gonzales, M., Stalcup, S. A. & Smith, D. E. 1997. Gamma-hydroxybutyrate: an emerging drug of abuse that causes physical dependence. *Addiction,* **92,** 89-96.

GE Lifesciences 1999. Rapid and efficient purification and refolding of a (His)6-tagged recombinant protein produced in E. coli as inclusion bodies. *Application note,* **18-1134-37 AB**.

Gervasi, N., Monnier, Z., Vincent, P., Paupardin-Tritsch, D., Hughes, S. W., Crunelli, V. & Leresche, N. 2003. Pathway-specific action of gamma-hydroxybutyric acid in sensory thalamus and its relevance to absence seizures. *J Neurosci,* **23,** 11469-78.

Gessa, G. L., Agabio, R., Carai, M. A., Lobina, C., Pani, M., Reali, R. & Colombo, G. 2000. Mechanism of the antialcohol effect of gamma-hydroxybutyric acid. *Alcohol,* **20,** 271-276.

Gibson, K. M., Gupta, M., Pearl, P. L., Tuchman, M., Vezina, L. G., Snead, O. C., 3rd, Smit, L. M. & Jakobs, C. 2003. Significant behavioral disturbances in succinic semialdehyde dehydrogenase (SSADH) deficiency (gamma-hydroxybutyric aciduria). *Biol Psychiatry,* **54,** 763-8.

Gobaille, S., Hechler, V., Andriamampandry, C., Kemmel, V. & Maitre, M. 1999. gamma-Hydroxybutyrate modulates synthesis and extracellular

concentration of gamma-aminobutyric acid in discrete rat brain regions in vivo. *J Pharmacol Exp Ther,* **290,** 303-9.

Gobaille, S., Schleef, C., Hechler, V., Viry, S., Aunis, D. & Maitre, M. 2002. Gamma-hydroxybutyrate increases tryptophan availability and potentiates serotonin turnover in rat brain. *Life Sci,* **70,** 2101-12.

Goedde, H. W., Agarwal, D. P. & Harada, S. 1980. Genetic studies on alcohol-metabolizing enzymes: detection of isozymes in human hair roots. *Enzyme,* **25,** 281-6.

Gold, B. I. & Roth, R. H. 1977. Kinetics of in vivo conversion of gamma-[3H]aminobutyric acid to gamma-[3H]hydroxybutyric acid by rat brain. *J Neurochem,* **28,** 1069-73.

Goulle, J. P., Cheze, M. & Pepin, G. 2003. Determination of endogenous levels of GHB in human hair. Are there possibilities for the identification of GHB administration through hair analysis in cases of drug-facilitated sexual assault? *J Anal Toxicol,* **27,** 574-80.

Hardman, J. K. & Stadtman, T. C. 1960. Metabolism of omega-amino acids. I. Fermentation of gamma-aminobutyric acid by Clostridium aminobutyricum n. sp. *J Bacteriol,* **79,** 544-8.

Howells, L., Godfrey, M. & Sauer, M. J. 1994. Melanin as an adsorbent for drug residues. *Analyst,* **119,** 2691-3.

Hu, R. Q., Banerjee, P. K. & Snead, O. C., 3rd 2000. Regulation of gamma-aminobutyric acid (GABA) release in cerebral cortex in the gamma-hydroxybutyric acid (GHB) model of absence seizures in rat. *Neuropharmacology,* **39,** 427-39.

Ingels, M., Rangan, C., Bellezzo, J. & Clark, R. F. 2000. Coma and respiratory depression following the ingestion of GHB and its precursors: three cases. *J Emerg Med,* **19,** 47-50.

Ireland, L. S., Harrison, D. J., Neal, G. E. & Hayes, J. D. 1998. Molecular cloning, expression and catalytic activity of a human AKR7 member of the aldo-keto reductase superfamily: evidence that the major 2-carboxybenzaldehyde reductase from human liver is a homologue of rat aflatoxin B1-aldehyde reductase. *Biochem J,* **332 (Pt 1),** 21-34.

Iwata, N., Inazu, N. & Satoh, T. 1990. The purification and properties of aldose reductase from rat ovary. *Arch Biochem Biophys,* **282,** 70-7.

Jakobs, C., Bojasch, M., Monch, E., Rating, D., Siemes, H. & Hanefeld, F. 1981. Urinary excretion of gamma-hydroxybutyric acid in a patient with neurological abnormalities. The probability of a new inborn error of metabolism. *Clin Chim Acta,* **111,** 169-78.

Jensen, K. & Mody, I. 2001. GHB depresses fast excitatory and inhibitory synaptic transmission via GABA(B) receptors in mouse neocortical neurons. *Cereb Cortex,* **11,** 424-9.

Jez, J. M., Bennett, M. J., Schlegel, B. P., Lewis, M. & Penning, T. M. 1997a. Comparative anatomy of the aldo-keto reductase superfamily. *Biochem J,* **326 (Pt 3),** 625-36.

Jez, J. M., Flynn, T. G. & Penning, T. M. 1997b. A new nomenclature for the aldo-keto reductase superfamily. *Biochem Pharmacol,* **54,** 639-47.

Jones, K. A., Borowsky, B., Tamm, J. A., Craig, D. A., Durkin, M. M., Dai, M., Yao, W. J., Johnson, M., Gunwaldsen, C., Huang, L. Y., Tang, C., Shen, Q., Salon, J. A., Morse, K., Laz, T., Smith, K. E., Nagarathnam, D., Noble, S. A., Branchek, T. A. & Gerald, C. 1998. GABA(B) receptors function as a heteromeric assembly of the subunits GABA(B)R1 and GABA(B)R2. *Nature,* **396,** 674-9.

Joseph, R. E., Jr., Su, T. P. & Cone, E. J. 1996. In vitro binding studies of drugs to hair: influence of melanin and lipids on cocaine binding to Caucasoid and Africoid hair. *J Anal Toxicol,* **20,** 338-44.

Kam, P. C. & Yoong, F. F. 1998. Gamma-hydroxybutyric acid: an emerging recreational drug. *Anaesthesia,* **53,** 1195-8.

Kardon, T., Noel, G., Vertommen, D. & Schaftingen, E. V. 2006. Identification of the gene encoding hydroxyacid-oxoacid transhydrogenase, an enzyme that metabolizes 4-hydroxybutyrate. *FEBS Lett,* **580,** 2347-50.

Katoh, S., Murata, K., Kubota, Y., Kumeta, H., Ogura, K., Inagaki, F., Asayama, M. & Katoh, E. 2005. Refolding and purification of recombinant OsNifU1A domain II that was expressed by Escherichia coli. *Protein Expr Purif,* **43,** 149-56.

Kaufman, E. E. & Nelson, T. 1981. Kinetics of coupled gamma-hydroxybutyrate oxidation and D-glucuronate reduction by an NADP+-dependent oxidoreductase. *J Biol Chem,* **256,** 6890-4.

Kaufman, E. E., Nelson, T., Fales, H. M. & Levin, D. M. 1988a. Isolation and characterization of a hydroxyacid-oxoacid transhydrogenase from rat kidney mitochondria. *J Biol Chem,* **263,** 16872-9.

Kaufman, E. E., Nelson, T., Goochee, C. & Sokoloff, L. 1979. Purification and characterization of an NADP+-linked alcohol oxido-reductase which catalyzes the interconversion of gamma-hydroxybutyrate and succinic semialdehyde. *J Neurochem,* **32,** 699-712.

Kaufman, E. E., Nelson, T., Miller, D. & Stadlan, N. 1988b. Oxidation of gamma-hydroxybutyrate to succinic semialdehyde by a mitochondrial pyridine nucleotide-independent enzyme. *J Neurochem,* **51,** 1079-84.

Kaufmann, E. & Alt, A. 2007. Determination of GHB in urine and serum by LC/MS using a simple one-step derivative. *Forensic Sci Int,* **168,** 133-7.

Kaupmann, K., Cryan, J. F., Wellendorph, P., Mombereau, C., Sansig, G., Klebs, K., Schmutz, M., Froestl, W., van der Putten, H., Mosbacher, J., Brauner-Osborne, H., Waldmeier, P. & Bettler, B. 2003. Specific gamma-hydroxybutyrate-binding sites but loss of pharmacological effects of gamma-hydroxybutyrate in GABA(B)(1)-deficient mice. *Eur J Neurosci,* **18,** 2722-30.

Kaupmann, K., Huggel, K., Heid, J., Flor, P. J., Bischoff, S., Mickel, S. J., McMaster, G., Angst, C., Bittiger, H., Froestl, W. & Bettler, B. 1997. Expression cloning of GABA(B) receptors uncovers similarity to metabotropic glutamate receptors. *Nature,* **386,** 239-46.

Kaupmann, K., Malitschek, B., Schuler, V., Heid, J., Froestl, W., Beck, P., Mosbacher, J., Bischoff, S., Kulik, A., Shigemoto, R., Karschin, A. & Bettler, B. 1998. GABA(B)-receptor subtypes assemble into functional heteromeric complexes. *Nature,* **396,** 683-7.

Keenan, C., Ghaffar, S., Grant, A. W., Hinshelwood, A., Li, D. & McGarvie, G. 2006. Succinic semialdehyde reductases: contribution to gamma-hydroxybutyrate catabolism and subcellular localization. *In:* WEINER, H. P., B.; LINDAHL, R.; MASER, E., EDITORS (ed.) *Enzymology and Molecular Biology of Carbonyl Metabolism.* West Lafayette, IN: Purdue University Press.

Kelly, V. P., Sherratt, P. J., Crouch, D. H. & Hayes, J. D. 2002. Novel homodimeric and heterodimeric rat gamma-hydroxybutyrate synthases that associate with the Golgi apparatus define a distinct subclass of aldo-keto reductase 7 family proteins. *Biochem J,* **366,** 847-61.

Kemmel, V., Miehe, M., Roussel, G., Taleb, O., Nail-Boucherie, K., Marchand, C., Stutz, C., Andriamampandry, C., Aunis, D. & Maitre, M. 2006. Immunohistochemical localization of a GHB receptor-like protein isolated from rat brain. *J Comp Neurol,* **498,** 508-524.

Kemmel, V., Taleb, O., Andriamampandry, C., Aunis, D. & Maitre, M. 2003. Gamma-hydroxybutyrate receptor function determined by stimulation of rubidium and calcium movements from NCB-20 neurons. *Neuroscience,* **116,** 1021-1031.

Kidwell, D. A., Lee, E. H. & DeLauder, S. F. 2000. Evidence for bias in hair testing and procedures to correct bias. *Forensic Sci Int,* **107,** 39-61.

Kim, J. Y., Tillison, K. S., Zhou, S., Lee, J. H. & Smas, C. M. 2007. Differentiation-dependent expression of Adhfe1 in adipogenesis. *Arch Biochem Biophys,* **464,** 100-11.

Kim, S. Y., Barker, J. C., Anderson, I. B., Dyer, J. E., Earnest, G. & Blanc, P. D. 2008. Systematic assessment of gamma hydroxybutyrate (GHB) effects during and after acute intoxication. *Am J Addict,* **17,** 312-8.

King, L. A., McDermott, S. D., Jickells, S. & Negrusz, A. 2008. Drugs of abuse. *in Clarke's analytical forensic toxicology.* Pharmaceutical press.

King, M. A., Thinschmidt, J. S. & Walker, D. W. 1997. Gammahydroxybutyrate (GHB) receptor ligand effects on evoked synaptic field potentials in CA1 of the rat hippocampal slice. *J Neural Transm,* **104,** 1177-93.

Kintz, P., Cirimele, V., Jamey, C. & Ludes, B. 2003. Testing for GHB in hair by GC/MS/MS after a single exposure. Application to document sexual assault. *J Forensic Sci,* **48,** 195-200.

Kintz, P., Evans, J., Villain, M., Chatterton, C. & Cirimele, V. 2009. Hair analysis to demonstrate administration of sildenafil to a woman in a case of drug-facilitated sexual assault. *J Anal Toxicol,* **33,** 553-6.

Kintz, P., Goulle, J. P., Cirimele, V. & Ludes, B. 2001. Window of detection of gamma-hydroxybutyrate in blood and saliva. *Clin Chem,* **47,** 2033-4.

Kintz, P., Villain, M., Cirimele, V. & Ludes, B. 2004. GHB in postmortem toxicology. Discrimination between endogenous production from exposure using multiple specimens. *Forensic Sci Int,* **143,** 177-81.

Klein, J., Blanchette, P. & Koren, G. 2004. Assessing nicotine metabolism in pregnancy--a novel approach using hair analysis. *Forensic Sci Int,* **145,** 191-4.

Knowles, B. B., Howe, C. C. & Aden, D. P. 1980. Human hepatocellular carcinoma cell lines secrete the major plasma proteins and hepatitis B surface antigen. *Science,* **209,** 497-9.

Knudsen, K., Jonsson, U. & Abrahamsson, J. 2010. Twenty-three deaths with gamma-hydroxybutyrate overdose in western Sweden between 2000 and 2007. *Acta Anaesthesiol Scand,* **54,** 987-92.

Kohyama, K., Matsumoto, T. & Imoto, T. Refolding of an unstable lysozyme by gradient removal of a solubilizer and gradient addition of a stabilizer. *J Biochem,* **147,** 427-31.

Kurata, Y., Marszalec, W., Yeh, J. Z. & Narahashi, T. 1999. Agonist and potentiation actions of n-octanol on gamma-aminobutyric acid type A receptors. *Mol Pharmacol,* **55,** 1011-9.

Laborit, H. 1964. Sodium 4-hydroxybutyrate *Int J Neuropharmacol,* **3,** 433-451.

Laemmli, U. K. 1970. Cleavage of structural proteins during the assembly of the head of bacteriophage T4. *Nature,* **227,** 680-5.

Larsson, O. M. & Schousboe, A. 1990. Kinetic characterization of GABA-transaminase from cultured neurons and astrocytes. *Neurochem Res,* **15,** 1073-7.

LeBeau, M. A., Christenson, R. H., Levine, B., Darwin, W. D. & Huestis, M. A. 2002. Intra- and interindividual variations in urinary concentrations of endogenous gamma-hydroxybutyrate. *J Anal Toxicol,* **26,** 340-6.

LeBeau, M. A., Montgomery, M. A., Miller, M. L. & Burmeister, S. G. 2000. Analysis of Biofluids for Gamma-Hydroxybutyrate (GHB) and Gamma-Butyrolactone (GBL) by Headspace GC-FID and GC-M. *J Anal Toxicol,* **24,** 421-428.

LeBeau, M. A., Montgomery, M. A., Morris-Kukoski, C., Schaff, J. E. & Deakin, A. 2007. Further evidence of in vitro production of gamma-hydroxybutyrate (GHB) in urine samples. *Forensic Sci Int,* **169,** 152-6.

Lee, M., Schwab, C. & McGeer, P. L. 2011. Astrocytes are GABAergic cells that modulate microglial activity. *Glia,* **59,** 152-65.

Lenz, D., Jubner, M., Bender, K., Wintermeyer, A., Beike, J., Rothschild, M. A. & Kaferstein, H. 2011. Inhibition of 1,4-butanediol metabolism in human liver in vitro. *Naunyn Schmiedebergs Arch Pharmacol,* **383,** 647-54.

Leone, M. A., Vigna-Taglianti, F., Avanzi, G., Brambilla, R. & Faggiano, F. 2010. Gamma-hydroxybutyrate (GHB) for treatment of alcohol withdrawal and prevention of relapses. *Cochrane Database Syst Rev***,** CD006266.

LeTourneau, J. L., Hagg, D. S. & Smith, S. M. 2008. Baclofen and gamma-hydroxybutyrate withdrawal. *Neurocrit Care,* **8,** 430-3.

Lettieri, J. T. & Fung, H. L. 1979. Dose-dependent pharmacokinetics and hypnotic effects of sodium gamma-hydroxybutyrate in the rat. *J Pharmacol Exp Ther,* **208,** 7-11.

Lingenhoehl, K., Brom, R., Heid, J., Beck, P., Froestl, W., Kaupmann, K., Bettler, B. & Mosbacher, J. 1999. Gamma-hydroxybutyrate is a weak agonist at recombinant GABA(B) receptors. *Neuropharmacology,* **38,** 1667-73.

Liu, Y., Li, Y. H., Guo, F. J., Wang, J. J., Sun, R. L., Hu, J. Y. & Li, G. C. 2008. Gamma-aminobutyric acid promotes human hepatocellular carcinoma

growth through overexpressed gamma-aminobutyric acid A receptor alpha 3 subunit. *World J Gastroenterol,* **14,** 7175-82.

Livak, K. J. & Schmittgen, T. D. 2001. Analysis of relative gene expression data using real-time quantitative PCR and the 2(-Delta Delta C(T)) Method. *Methods,* **25,** 402-8.

Lough, P. S. & Fehn, R. 1993. Efficacy of 1% sodium fluoride as a preservative in urine samples containing glucose and Candida albicans. *J Forensic Sci,* **38,** 266-71.

Lyon, R. C., Johnston, S. M., Panopoulos, A., Alzeer, S., McGarvie, G. & Ellis, E. M. 2009. Enzymes involved in the metabolism of gamma-hydroxybutyrate in SH-SY5Y cells: identification of an iron-dependent alcohol dehydrogenase ADHFe1. *Chem Biol Interact,* **178,** 283-7.

Lyon, R. C., Johnston, S. M., Watson, D. G., McGarvie, G. & Ellis, E. M. 2007. Synthesis and catabolism of gamma-hydroxybutyrate in SH-SY5Y human neuroblastoma cells: role of the aldo-keto reductase AKR7A2. *J Biol Chem,* **282,** 25986-92.

Macintyre, E. H., Ponten, J. & Vatter, A. E. 1972. The ultrastructure of human and murine astrocytes and of human fibroblasts in culture. *Acta Pathol Microbiol Scand A,* **80,** 267-83.

Madea, B. & Musshoff, F. 2009. Knock-out drugs: their prevalence, modes of action, and means of detection. *Dtsch Arztebl Int,* **106,** 341-7.

Mahr, G., Bishop, C. L. & Orringer, D. J. 2001. Prolonged withdrawal from extreme gamma-hydroxybutyrate (GHB) abuse. *Psychosomatics,* **42,** 439-40.

Maitre, M. 1997. The gamma-hydroxybutyrate signalling system in brain: organization and functional implications. *Prog Neurobiol,* **51,** 337-61.

Maitre, M., Cash, C., Weissmann-Nanopoulos, D. & Mandel, P. 1983. Depolarization-evoked release of gamma-hydroxybutyrate from rat brain slices. *J Neurochem,* **41,** 287-90.

Maitre, M., Ciesielski, L., Cash, C. & Mandel, P. 1975. Purification and studies on some properties of the 4-aminobutyrate : 2-oxoglutarate transaminase from rat brain. *Eur J Biochem,* **52,** 157-69.

Maitre, M., Hechler, V., Vayer, P., Gobaille, S., Cash, C. D., Schmitt, M. & Bourguignon, J. J. 1990. A specific gamma-hydroxybutyrate receptor ligand possesses both antagonistic and anticonvulsant properties. *J Pharmacol Exp Ther,* **255,** 657-63.

Mamelak, M. 2007. Alzheimer' s disease, oxidative stress and gammahydroxybutyrate. *Neurobiol Aging,* **28,** 1340-60.

Mamelak, M. 2009. Narcolepsy and depression and the neurobiology of gammahydroxybutyrate. *Prog Neurobiol,* **89,** 193-219.

Martindale, J. L. & Holbrook, N. J. 2002. Cellular response to oxidative stress: signaling for suicide and survival. *J Cell Physiol,* **192,** 1-15.

Maxwell, R. & Roth, R. H. 1972. Conversion of 1,4-butanediol to -hydroxybutyric acid in rat brain and in peripheral tissue. *Biochem Pharmacol,* **21,** 1521-33.

Mazarr-Proo, S. & Kerrigan, S. 2005. Distribution of GHB in tissues and fluids following a fatal overdose. *J Anal Toxicol,* **29,** 398-400.

McConnell, M. J. & Pachon, J. Expression, purification, and refolding of biologically active Acinetobacter baumannii OmpA from Escherichia coli inclusion bodies. *Protein Expr Purif,* **77,** 98-103.

Meyers, J. E. & Almirall, J. R. 2005. Analysis of gamma-hydroxybutyric acid (GHB) in spiked water and beverage samples using solid phase microextraction (SPME) on fiber derivatization/gas chromatography-mass spectrometry (GC/MS). *J Forensic Sci,* **50,** 31-6.

Miroux, B. & Walker, J. E. 1996. Over-production of proteins in Escherichia coli: mutant hosts that allow synthesis of some membrane proteins and globular proteins at high levels. *J Mol Biol,* **260,** 289-98.

Montella, C., Bellsolell, L., Perez-Luque, R., Badia, J., Baldoma, L., Coll, M. & Aguilar, J. 2005. Crystal structure of an iron-dependent group III dehydrogenase that interconverts L-lactaldehyde and L-1,2-propanediol in Escherichia coli. *J Bacteriol,* **187,** 4957-66.

Moriya, F. & Hashimoto, Y. 2005. Site-dependent production of gamma-hydroxybutyric acid in the early postmortem period. *Forensic Sci Int,* **148,** 139-42.

Moriya, F., Nishimura, H., Furumiya, J. & Hashimoto, Y. 2006. Effects of drinking and smoking on endogenous levels of urinary gamma-hydroxybutyric acid, a preliminary study. *Leg Med (Tokyo),* **8,** 231-4.

Morris, M. E., Hu, K. & Wang, Q. 2005. Renal clearance of gamma-hydroxybutyric acid in rats: increasing renal elimination as a detoxification strategy. *J Pharmacol Exp Ther,* **313,** 1194-202.

Mosmann, T. 1983. Rapid colorimetric assay for cellular growth and survival: application to proliferation and cytotoxicity assays. *J Immunol Methods,* **65,** 55-63.

Murphy, T. C., Amarnath, V., Gibson, K. M. & Picklo, M. J., Sr. 2003. Oxidation of 4-hydroxy-2-nonenal by succinic semialdehyde dehydrogenase (ALDH5A). *J Neurochem,* **86,** 298-305.

Nava, F., Carta, G., Bortolato, M. & Gessa, G. L. 2001. gamma-Hydroxybutyric acid and baclofen decrease extracellular acetylcholine levels in the hippocampus via GABA(B) receptors. *Eur J Pharmacol,* **430,** 261-3.

Nelson, T., Kaufman, E., Kline, J. & Sokoloff, L. 1981. The extraneural distribution of gamma-hydroxybutyrate. *J Neurochem,* **37,** 1345-8.

Newman, E. A. 2003. New roles for astrocytes: regulation of synaptic transmission. *Trends Neurosci,* **26,** 536-42.

Nguyen, E. & Picklo, M. J., Sr. 2003. Inhibition of succinic semialdehyde dehydrogenase activity by alkenal products of lipid peroxidation. *Biochim Biophys Acta,* **1637,** 107-12.

Nicholson, K. L. & Balster, R. L. 2001. GHB: a new and novel drug of abuse. *Drug Alcohol Depend,* **63,** 1-22.

Nimmerrichter, A. A., Walter, H., Gutierrez-Lobos, K. E. & Lesch, O. M. 2002. Double blind controlled trial of gamma-hydroxybutyrate and clomethiazole in the treatment of alcohol withdrawal. *Alcohol Alcohol* **37,** 67-73.

Nirenberg, M. W. & Jakoby, W. B. 1960. Enzymatic utilization of gamma-hydroxybutyric acid. *J Biol Chem,* **235,** 954-60.

Nord, E. P., Wright, S. H., Kippen, I. & Wright, E. M. 1983. Specificity of the Na+-dependent monocarboxylic acid transport pathway in rabbit renal brush border membranes. *J Membr Biol,* **72,** 213-221.

Novagen 2002-2003. *Protein Expression: Prokaryotic Expression: pETBlue and pET System Overview. Novagen 2002-2003 Catalog*.

O'Connor, T., Ireland, L. S., Harrison, D. J. & Hayes, J. D. 1999. Major differences exist in the function and tissue-specific expression of human aflatoxin B1 aldehyde reductase and the principal human aldo-keto reductase AKR1 family members. *Biochem J,* **343 Pt 2,** 487-504.

Odagaki, Y., Nishi, N. & Koyama, T. 2000. Functional coupling of GABA(B) receptors with G proteins that are sensitive to N-ethylmaleimide treatment, suramin, and benzalkonium chloride in rat cerebral cortical membranes. *J Neural Transm,* **107,** 1101-16.

Odagaki, Y. & Yamauchi, T. 2004. Gamma-hydroxybutyric acid, unlike gamma-aminobutyric acid, does not stimulate Gi/Go proteins in rat brain membranes. *Basic Clin Pharmacol Toxicol.,* **94,** 89-98.

Otto, P., Kephart, D., Bitner, R., Huber, S. & Volkerding, K. 1998. Separate isolation of genomic DNA and total RNA from single samples using the SV Total RNA Isolation System. *Promega Notes,* **69,** 19-23.

Palatini, P., Tedeschi, L., Frison, G., Padrini, R., Zordan, R., Orlando, R., Gallimberti, L., Gessa, G. L. & Ferrara, S. D. 1993. Dose-dependent absorption and elimination of gamma-hydroxybutyric acid in healthy volunteers. *Eur J Clin Pharmacol,* **45,** 353-6.

Panopoulos, A. 2007. *"The Role of a Hydroxyacid-Oxoacid Transhydrogenase in GHB Metabolism"*. MPhil thesis, University of Strathclyde.

Park, T. J., Kim, J. S., Choi, S. S. & Kim, Y. 2009. Cloning, expression, isotope labeling, purification, and characterization of bovine antimicrobial peptide, lactophoricin in Escherichia coli. *Protein Expr Purif,* **65,** 23-9.

Paulsen, R. B., Wilkins, D. G., Slawson, M. H., Shaw, K. & Rollins, D. E. 2001. Effect of four laboratory decontamination procedures on the quantitative determination of cocaine and metabolites in hair by HPLC-MS. *J Anal Toxicol,* **25,** 490-6.

Pearl, P. L., Gibson, K. M., Acosta, M. T., Vezina, L. G., Theodore, W. H., Rogawski, M. A., Novotny, E. J., Gropman, A., Conry, J. A., Berry, G. T. & Tuchman, M. 2003. Clinical spectrum of succinic semialdehyde dehydrogenase deficiency. *Neurology,* **60,** 1413-7.

Pearl, P. L., Gibson, K. M., Cortez, M. A., Wu, Y., Carter Snead, O., 3rd, Knerr, I., Forester, K., Pettiford, J. M., Jakobs, C. & Theodore, W. H. 2009. Succinic semialdehyde dehydrogenase deficiency: lessons from mice and men. *J Inherit Metab Dis,* **32,** 343-52.

Perez, E., Chu, J. & Bania, T. 2006. Seven days of gamma-hydroxybutyrate (GHB) use produces severe withdrawal. *Ann Emerg Med,* **48,** 219-20.

Picklo, M. J., Sr., Olson, S. J., Hayes, J. D., Markesbery, W. R. & Montine, T. J. 2001. Elevation of AKR7A2 (succinic semialdehyde reductase) in neurodegenerative disease. *Brain Res,* **916,** 229-38.

Pierce, R. C. & Kumaresan, V. 2006. The mesolimbic dopamine system: the final common pathway for the reinforcing effect of drugs of abuse? *Neurosci Biobehav Rev,* **30,** 215-38.

Ponten, J. & Macintyre, E. H. 1968. Long term culture of normal and neoplastic human glia. *Acta Pathol Microbiol Scand,* **74,** 465-86.

Potsch, L. & Moeller, M. R. 1996. On pathways for small molecules into and out of human hair fibers. *J Forensic Sci,* **41,** 121-5.

Potsch, L., Skopp, G. & Moeller, M. R. 1997. Biochemical approach on the conservation of drug molecules during hair fiber formation. *Forensic Sci Int,* **84,** 25-35.

Pragst, F. & Balikova, M. A. 2006. State of the art in hair analysis for detection of drug and alcohol abuse. *Clin Chim Acta,* **370,** 17-49.

Rainesalo, S., Saransaari, P., Peltola, J. & Keranen, T. 2003. Uptake of GABA and activity of GABA-transaminase in platelets from epileptic patients. *Epilepsy Res,* **53,** 233-9.

Raknes, G., Aronsen, L. & Fuskevag, O. M. 2010. Urinary concentrations of gamma-hydroxybutyric acid and related compounds in pregnancy. *J Anal Toxicol,* **34,** 394-9.

Raul, J. S., Cirimele, V., Ludes, B. & Kintz, P. 2004. Detection of physiological concentrations of cortisol and cortisone in human hair. *Clin Biochem,* **37,** 1105-11.

Raybon, J. J. & Boje, K. M. 2007. Pharmacokinetics and pharmacodynamics of gamma-hydroxybutyric acid during tolerance in rats: effects on extracellular dopamine. *J Pharmacol Exp Ther,* **320,** 1252-60.

Reid, M. F. & Fewson, C. A. 1994. Molecular characterization of microbial alcohol dehydrogenases. *Crit Rev Microbiol,* **20,** 13-56.

Reijnierse, G. L., Veldstra, H. & Van den Berg, C. J. 1975. Subcellular localization of gamma-aminobutyrate transaminase and glutamate dehydrogenase in adult rat brain. Evidence for at least two small glutamate compartments in brain. *Biochem J,* **152,** 469-75.

Remmert, K., Vullhorst, D. & Hinssen, H. 2000. In vitro refolding of heterodimeric CapZ expressed in E. coli as inclusion body protein. *Protein Expr Purif,* **18,** 11-9.

Rivett, A. J., Smith, I. L. & Tipton, K. F. 1981. Purification of the high-Km aldehyde reductase from rat brain and liver and from ox brain. *Biochem J,* **197,** 473-81.

Rivett, A. J. & Tipton, K. F. 1981. Kinetic studies of the reduction of succinic semialdehyde by rat-brain aldehyde reductase. *Eur J Biochem,* **118,** 635-9.

Rodgers, J., Ashton, C. H., Gilvarry, E. & Young, A. H. 2004. Liquid ecstasy: a new kid on the dance floor. *Br J Psychiatry,* **184,** 104-6.

Roland, J. J., Mark, K., Vetreno, R. P. & Savage, L. M. 2008. Increasing hippocampal acetylcholine levels enhance behavioral performance in an animal model of diencephalic amnesia. *Brain Res,* **1234,** 116-27.

Rossi, R., Lancia, M., Gambelunghe, C., Oliva, A. & Fucci, N. 2009. Identification of GHB and morphine in hair in a case of drug-facilitated sexual assault. *Forensic Sci Int,* **186,** e9-e11.

Roth, R. H. 1970. Formation and regional distribution of gamma-hydroxybutyric acid in mammalian brain. *Biochem Pharmacol,* **19,** 3013-3019.

Roth, R. H., Delgado, J. M. & Giarman, N. J. 1966. Gamma-butyrolactone and gamma-hydroxybutyric acid. II. The pharmacologically active form. *Int J Neuropharmacol,* **5,** 421-8.

Roth, R. H. & Giarman, N. J. 1965. Preliminary Report on the Metabolism of Gamma-Butyrolactone and Gamma-Hydroxybutyric Acid. *Biochem Pharmacol,* **14,** 177-8.

Roth, R. H. & Giarman, N. J. 1968. Evidence that central nervous system depression by 1,4-butanediol in mediated through a metabolite, gamma-hydroxybutyrate. *Biochem Pharmacol,* **17,** 735-9.

Roth, R. H. & Giarman, N. J. 1970. Natural occurrence of GHB in mammalian brain. *Biochem Pharmacol* **19,** 1087-1093.

Ryzlak, M. T. & Pietruszko, R. 1988. Human brain "high Km" aldehyde dehydrogenase: purification, characterization, and identification as NAD+ -dependent succinic semialdehyde dehydrogenase. *Arch Biochem Biophys,* **266,** 386-96.

Saier, M. H., Jr., Yamada, M., Suda, K., Erni, B., Rak, B., Lengeler, J., Stewart, G. C., Waygood, E. B. & Rapoport, G. 1988. Bacterial proteins with N-terminal leader sequences resembling mitochondrial targeting sequences of eukaryotes. *Biochimie,* **70,** 1743-8.

Sakaba, T. & Neher, E. 2003. Direct modulation of synaptic vesicle priming by GABA(B) receptor activation at a glutamatergic synapse. *Nature,* **424,** 775-8.

Sakurada, K., Kobayashi, M., Iwase, H., Yoshino, M., Mukoyama, H., Takatori, T. & Yoshida, K. 2002. Production of gamma-hydroxybutyric acid in postmortem liver increases with time after death. *Toxicol Lett,* **129,** 207-17.

Salganicoff, L. & Derobertis, E. 1965. Subcellular Distribution of the Enzymes of the Glutamic Acid, Glutamine and Gamma-Aminobutyric Acid Cycles in Rat Brain. *J Neurochem,* **12,** 287-309.

Saurabh, A. 2007. *Putative aldo-keto reductase from Streptomyces coelicolor.* M.Res Thesis., Unversity of Strathclyde.

Schaller, M., Schaffhauser, M., Sans, N. & Wermuth, B. 1999. Cloning and expression of succinic semialdehyde reductase from human brain. Identity with aflatoxin B1 aldehyde reductase. *Eur J Biochem,* **265,** 1056-60.

Schmidt, C., Gobaille, S., Hechler, V., Schmitt, M., Bourguignon, J. J. & Maitre, M. 1991. Anti-sedative and anti-cataleptic properties of NCS-382, a gamma-hydroxybutyrate receptor antagonist. *Eur J Pharmacol,* **203,** 393-7.

Schneir, A. B., Ly, B. T. & Clark, R. F. 2001. A case of withdrawal from the GHB precursors gamma-butyrolactone and 1,4-butanediol. *J Emerg Med,* **21,** 31-3.

Sciotti, M. A., Hasan, L., Scholer, A., Jermann, T. M., Weber, J. M. & Gygax, D. 2010. Development and characterization of an enzymatic method for the rapid determination of gamma hydroxybutyric acid. *Chimia (Aarau),* **64,** 793-8.

Scott, B. W., Chan, K. F., Wong, G., Ahmed, M., Chieverton, L., Liu, R. R., Wood, J. & Burnham, W. M. 2010. Cytogenesis in the adult rat dentate gyrus is increased following kindled seizures but is unaltered in pharmacological models of absence seizures. *Epilepsy Behav,* **18,** 179-85.

Scott, K. S. 2009. The use of hair as a toxicological tool in DFC casework. *Sci Justice,* **49,** 250-3.

Sgaravatti, A. M., Magnusson, A. S., Oliveira, A. S., Mescka, C. P., Zanin, F., Sgarbi, M. B., Pederzolli, C. D., Wyse, A. T., Wannmacher, C. M., Wajner, M. & Dutra-Filho, C. S. 2009. Effects of 1,4-butanediol administration on oxidative stress in rat brain: study of the neurotoxicity of gamma-hydroxybutyric acid in vivo. *Metab Brain Dis,* **24,** 271-82.

Sgaravatti, A. M., Sgarbi, M. B., Testa, C. G., Durigon, K., Pederzolli, C. D., Prestes, C. C., Wyse, A. T., Wannmacher, C. M., Wajner, M. & Dutra-Filho, C. S. 2007. Gamma-hydroxybutyric acid induces oxidative stress in cerebral cortex of young rats. *Neurochem Int,* **50,** 564-70.

Sivilotti, M. L., Burns, M. J., Aaron, C. K. & Greenberg, M. J. 2001. Pentobarbital for severe gamma-butyrolactone withdrawal. *Ann Emerg Med,* **38,** 660-5.

Snead, O. C. 2000. Evidence for a G protein-coupled gamma-hydroxybutyric acid receptor. *J Neurochem.,* **75,** 1986-1996.

Snead, O. C., 3rd 1991. The gamma-hydroxybutyrate model of absence seizures: correlation of regional brain levels of gamma-hydroxybutyric acid and gamma-butyrolactone with spike wave discharges. *Neuropharmacology,* **30,** 161-7.

Snead, O. C., 3rd, Bearden, L. J. & Pegram, V. 1980. Effect of acute and chronic anticonvulsant administration on endogenous gamma-hydroxybutyrate in rat brain. *Neuropharmacology,* **19,** 47-52.

Snead, O. C., 3rd, Furner, R. & Liu, C. C. 1989. In vivo conversion of gamma-aminobutyric acid and 1,4-butanediol to gamma-hydroxybutyric acid in rat brain. Studies using stable isotopes. *Biochem Pharmacol,* **38,** 4375-80.

Snead, O. C., 3rd & Gibson, K. M. 2005. Gamma-hydroxybutyric acid. *N Engl J Med,* **352,** 2721-32.

Snead, O. C. & Liu, C. C. 1984. Gamma-hydroxybutyric acid binding sites in rat and human brain synaptosomal membranes. *Biochem Pharmacol,* **33,** 2587-2590.

Society of Hair Testing 2004. Recommendations for hair testing in forensic cases. *Forensic Sci Int,* **145,** 83-4.

Stillwell, M. E. 2002. Drug-facilitated sexual assault involving gamma-hydroxybutyric acid. *J Forensic Sci,* **47,** 1133-4.

Stout, P. A., Simons, K. D. & Kerrigan, S. 2010. Quantitative analysis of gamma-hydroxybutyrate at endogenous concentrations in hair using liquid chromatography tandem mass spectrometry. *J Forensic Sci,* **55,** 531-7.

Struys, E. A., Jansen, E. E., Gibson, K. M. & Jakobs, C. 2005a. Determination of the GABA analogue succinic semialdehyde in urine and cerebrospinal fluid by dinitrophenylhydrazine derivatization and liquid chromatography-tandem mass spectrometry: application to SSADH deficiency. *J Inherit Metab Dis,* **28,** 913-20.

Struys, E. A., Verhoeven, N. M., Ten Brink, H. J., Wickenhagen, W. V., Gibson, K. M. & Jakobs, C. 2005b. Kinetic characterization of human hydroxyacid-oxoacid transhydrogenase: relevance to D-2-hydroxyglutaric and gamma-hydroxybutyric acidurias. *J Inherit Metab Dis,* **28,** 921-30.

Sun, W., Dai, X., Zheng, Y., Wang, J., Hou, L., Du, J. & Hu, H. G. On-column refolding purification of DT389-hIL13 recombinant protein expressed in Escherichia coli. *Protein Expr Purif,* **75,** 83-8.

Tabakoff, B. & von Wartburg, J. P. 1975. Separation of aldehyde reductases and alcohol dehydrogenase from brain by affinity chromatography: metabolism of succinic semialdehyde and ethanol. *Biochem Biophys Res Commun,* **63,** 957-66.

Taberner, P. V., Barnett, J. E. & Kerkut, G. A. 1972. Preparation of succinic semialdehyde: its colorimetric estimation as an assay for GABA aminotransferase. *J Neurochem,* **19,** 95-9.

Tajima, M., Hamada, C., Arai, T., Miyazawa, M., Shibata, R. & Ishino, A. 2007. Characteristic features of Japanese women's hair with aging and with progressing hair loss. *J Dermatol Sci,* **45,** 93-103.

Takehara, A., Hosokawa, M., Eguchi, H., Ohigashi, H., Ishikawa, O., Nakamura, Y. & Nakagawa, H. 2007. Gamma-aminobutyric acid (GABA) stimulates pancreatic cancer growth through overexpressing GABAA receptor pi subunit. *Cancer Res,* **67,** 9704-12.

Tardy, M., Bardakdjian, J. & Gonnard, P. 1979. GABA metabolism in cultured glial cells. *Adv Exp Med Biol,* **123,** 177-87.

Tedeschi, L., , , Carai, M. A., Frison, G., Favretto, D., Colombo, G., Ferrara, S. D. & Gessa, G. L. 2003. Endogenous gamma-hydroxybutyric acid is in the rat, mouse and human gastrointestinal tract. *Life Sci,* **72,** 2481-2488.

Van Cauter, E., Plat, L., Scharf, M. B., Leproult, R., Cespedes, S., L'Hermite-Balériaux, M. & Copinschi, G. 1997. Simultaneous stimulation of slow-wave sleep and growth hormone secretion by gamma-hydroxybutyrate in normal young Men. *J Clin Invest,* **100,** 745-753.

van Noorden, M. S., Kamal, R., de Jong, C. A., Vergouwen, A. C. & Zitman, F. G. 2009. [Gamma-hydroxybutyric acid (GHB) dependence and the GHB withdrawal syndrome: diagnosis and treatment]. *Ned Tijdschr Geneeskd,* **154,** A1286.

Van Sassenbroeck, D. K., De Paepe, P., Belpaire, F. M., Rosseel, M. T., Martens, P., Boon, P. A. & Buylaert, W. A. 2001. Relationship between gamma-hydroxybutyrate plasma concentrations and its electroencephalographic effects in the rat. *J Pharm Pharmacol,* **53,** 1687-96.

Varela, M., Nogue, S., Oros, M. & Miro, O. 2004. Gamma hydroxybutirate use for sexual assault. *Emerg Med J,* **21,** 255-6.

Vasil'ev, V. & Eremin, V. P. 1968. [A rapid method of determining gamma-aminobutyrate-alpha-ketoglutarate transaminase activity]. *Biull Eksp Biol Med,* **66,** 123-5.

Vayer, P., Mandel, P. & Maitre, M. 1985a. Conversion of gamma-hydroxybutyrate to gamma-aminobutyrate in vitro. *J Neurochem,* **45,** 810-4.

Vayer, P., Mandel, P. & Maitre, M. 1987. Gamma-hydroxybutyrate, a possible neurotransmitter. *Life Sci,* **41,** 1547-57.

Vayer, P., Schmitt, M., Bourguignon, J. J., Mandel, P. & Maitre, M. 1985b. Evidence for a role of high Km aldehyde reductase in the degradation of endogenous gamma-hydroxybutyrate from rat brain. *FEBS Lett,* **190,** 55-60.

Vienne, J., Bettler, B., Franken, P. & Tafti, M. 2010. Differential effects of GABAB receptor subtypes, {gamma}-hydroxybutyric Acid, and Baclofen on EEG activity and sleep regulation. *J Neurosci,* **30,** 14194-204.

Villain, M., Cirimele, V., Ludes, B. & Kintz, P. 2003. Ultra-rapid procedure to test for gamma-hydroxybutyric acid in blood and urine by gas chromatography-mass spectrometry. *J Chromatogr B Analyt Technol Biomed Life Sci,* **792,** 83-7.

Villain, M., Tournoud, C., Flesch, F., Cirimele, V. & Kintz, P. 2006. Hair to document exposure to glibenclamide. *J Chromatogr B Analyt Technol Biomed Life Sci,* **842,** 111-5.

Volpi, R., Chiodera, P., Caffarra, P., Scaglioni, A., Malvezzi, L., Saginario, A. & Coiro, V. 2000. Muscarinic cholinergic mediation of the GH response to gamma-hydroxybutyric acid: neuroendocrine evidence in normal and parkinsonian subjects. *Psychoneuroendocrinology,* **25,** 179-85.

Vose, J., Tighe, T., Schwartz, M. & Buel, E. 2001. Detection of gamma-butyrolactone (GBL) as a natural component in wine. *J Forensic Sci,* **46,** 1164-7.

Wang, C., Wang, L. & Geng, X. 2008a. High recovery refolding of rhG-CSF from Escherichia coli, using urea gradient size exclusion chromatography. *Biotechnol Prog,* **24,** 209-13.

Wang, L. 2009. Towards revealing the structure of bacterial inclusion bodies. *Prion,* **3,** 139-45.

Wang, Q. & Morris, M. E. 2007. The role of monocarboxylate transporter 2 and 4 in the transport of gamma-hydroxybutyric acid in mammalian cells. *Drug Metab Dispos,* **35,** 1393-9.

Wang, T., Huang, W. & Chen, F. 2008b. Baclofen, a GABAB receptor agonist, inhibits human hepatocellular carcinoma cell growth in vitro and in vivo. *Life Sci,* **82,** 536-41.

Wermuth, B., Munch, J. D. & von Wartburg, J. P. 1977. Purification and properties of NADPH-dependent aldehyde reductase from human liver. *J Biol Chem,* **252,** 3821-8.

Wermuth, B. & von Wartburg, J. P. 1980. Kinetic studies on NADPH-linked aldehyde reductase from human liver. *Adv Exp Med Biol,* **132,** 189-95.

Werner, M. H., Clore, G. M., Gronenborn, A. M., Kondoh, A. & Fisher, R. J. 1994. Refolding proteins by gel filtration chromatography. *FEBS Lett,* **345,** 125-30.

White, H. L. & Sato, T. L. 1978. GABA-transaminases of human brain and peripheral tissues--kinetic and molecular properties. *J Neurochem,* **31,** 41-7.

Winer, J., Jung, C. K., Shackel, I. & Williams, P. M. 1999. Development and validation of real-time quantitative reverse transcriptase-polymerase chain reaction for monitoring gene expression in cardiac myocytes in vitro. *Anal Biochem,* **270,** 41-9.

Wojtowicz, J. M., Yarema, M. C. & Wax, P. M. 2008. Withdrawal from gamma-hydroxybutyrate, 1,4-butanediol and gamma-butyrolactone: a case report and systematic review. *Cjem,* **10,** 69-74.

Wong, C. G., Gibson, K. M. & Snead, O. C., 3rd 2004. From the street to the brain: neurobiology of the recreational drug gamma-hydroxybutyric acid. *Trends Pharmacol Sci,* **25,** 29-34.

Wood, D. M., Warren-Gash, C., Ashraf, T., Greene, S. L., Shather, Z., Trivedy, C., Clarke, S., Ramsey, J., Holt, D. W. & Dargan, P. I. 2008. Medical and legal confusion surrounding gamma-hydroxybutyrate (GHB) and its precursors gamma-butyrolactone (GBL) and 1,4-butanediol (1,4BD). *QJM,* **101,** 23-9.

Wu, Y., Ali, S., Ahmadian, G., Liu, C. C., Wang, Y. T., Gibson, K. M., Calver, A. R., Francis, J., Pangalos, M. N. & Carter Snead, O., 3rd 2004. Gamma-hydroxybutyric acid (GHB) and gamma-aminobutyric acidB receptor (GABABR) binding sites are distinctive from one another: molecular evidence. *Neuropharmacology,* **47,** 1146-56.

Yates, S. W. & Viera, A. J. 2000. Physostigmine in the treatment of gamma-hydroxybutyric acid overdose. *Mayo Clin Proc,* **75,** 401-2.

Zhuo, Q., Piao, J. H., Wang, R. & Yang, X. G. 2005. Refolding and purification of non-fusion HPT protein expressed in Escherichia coli as inclusion bodies. *Protein Expr Purif,* **41,** 53-60.

Zuo, Y., Yeh, J. Z. & Narahashi, T. 2004. Octanol modulation of neuronal nicotinic acetylcholine receptor single channels. *Alcohol Clin Exp Res,* **28,** 1648-56.

Zvosec, D. L., Smith, S. W., Porrata, T., Strobl, A. Q. & Dyer, J. E. 2011. Case series of 226 gamma-hydroxybutyrate-associated deaths: lethal toxicity and trauma. *Am J Emerg Med,* **29,** 319-32.

RESEARCH OUTPUTS

I. **Alzeer S**, Ellis EM. The role of aldehyde reductase AKR1A1 in the metabolism of gamma-hydroxybutyrate in 1321N1 human astrocytoma cells.

- Published in 2011. *Chem Biol Interact*, **191**(1-3): 303-7.
- Proceedings for the 15th international meeting of Enzymology and molecular biology of Carbonyl metabolism, Lexington, Kentucky, USA. 6-11 July 2010.

II. **Alzeer S**, Panopoulos A, Ellis EM (2011).Production of recombinant Hydroxyacid-oxoacid transhydrogenase and its application to measure gamma hydroxybutyrate by a colorimetric assay. Proceedings for 2011 joint meeting of the Society of Forensic Toxicologists (SOFT) and The International Association of Forensic Toxicologists (TIAFT), San Francisco, USA. 25-30 September 2011.

III. **Alzeer S**, Ellis EM (2011). The Role of AKR1A1 in GHB biosynthesis and breakdown in HEPG2 cells. Proceedings for the joint spring meeting of British Toxicology Society (BTS) and the Dutch Society of Toxicology, University of Durham, UK. 27-30 March 2011.

IV. **Alzeer S**, Ellis EM (2010). Investigation of the factors affecting endogenous GHB concentrations in human hair.

- Proceedings for 48th Annual Meeting of the International Association of Forensic Toxicologists (TIAFT), Joint Meeting with the German society of Toxicological and Forensic Chemistry (GTFCh), Bonn, Germany. 29 August-2 September 2010.
- University of Strathclyde research day, June 2010.

V. Lyon RC, Johnston SM, Panopoulos A, **Alzeer S**, McGarvie G, Ellis EM (2009). Enzymes involved in the metabolism of gamma-hydroxybutyrate in SH-SY5Y cells: identification of an iron-dependent alcohol dehydrogenase ADHFe1. *Chem Biol Interact* **,178**(1-3):283-7.

VI. **Alzeer S**, Panopoulos A, Ellis EM (2008). Cloning, expression and purification of a human hydroxyacid-oxoacid transhydrogenase. Proceedings for the 14th international meeting of Enzymology and molecular biology of Carbonyl metabolism, Kranjska Gora, Slovenia ,8-12 July 2008.